QM/EFP MODELS BEYOND POLARIZABLE EMBEDDING

A Dissertation

Submitted to the Faculty

of

Purdue University

by

Claudia I. Viquez Rojas

In Partial Fulfillment of the

Requirements for the Degree

of

Doctor of Philosophy

May 2020

Purdue University

West Lafayette, Indiana

THE PURDUE UNIVERSITY GRADUATE SCHOOL
STATEMENT OF DISSERTATION APPROVAL

Prof. Lyudmila V. Slipchenko
Department of Chemistry
Prof. Dor Ben-Amotz
Department of Chemistry
Prof. Gaurav Chopra
Department of Chemistry
Prof. Sabre Kais
Department of Chemistry

Approved by:

Prof. Christine A. Hrycyna
Head of the Chemistry Graduate Program

A los 5(+4) en la familia.

ACKNOWLEDGMENTS

Throughout my PhD journey I was lucky enough to be surrounded by extraordinary people, who supported me and guided me every step of the way. My advisor Lyudmila always had the patience to work with me on the biggest challenges. From her I learned about chemistry, math, hard work and persistence. But most importantly, Lyuda provided me with a model for being a leading woman in science. For that I am truly grateful. I also want to thank my committee members, Gaurav Chopra, Dor Ben-Amotz and Sabre Kais for their guidance. And Cindy for all the care and support she shared (and all the chocolate covered pretzels as well).

Other people who made my grad school experience remarkable where the people in my group and office: Carlos, Pradeep, Yongbin, Yen and Victor. Carlos became my mentor the the moment I stepped into the chemistry building. He gave me advice on classes, research and Spanish. He also introduced me to Laura, who soon became a close friend and another of my role models. Pradeep was my TA for CHM673 and between that class and my OP, I must have knocked on his door a thousand times. He always opened it with a smile, ready to help. Yongbin was probably the hardest working of us all, but he also always made time for others. I cannot count how many times I asked him for help yet he never complained (about anything for that matter). Yen kept me sane by accompanying me to the gym every morning or for a coffee after a rough day. She also showed me to be confident and prove people wrong. Last but not least is Victor, my office mate for the last year and a half. He saw me go through a roller coaster of emotions but he always made sure I ended up laughing and with a coke-zero near reach.

Of course, none of this would have been possible without my family. My mom reminded me to let go of unnecessary burden and my dad pushed me to pursue every available opportunity. Jose taught me to laugh at life and Oscar showed me how to find comfort in the little things. But above all, I want to thank Zuhad, the person who got me through the toughest, ugliest times and the one who cheered even my smallest, silliest accomplishments.

PREFACE

This thesis is aimed towards the development and evaluation of the coupling term in the hybrid quantum mechanical/effective fragment potential method (QM/EFP). This is the term from the QM/EFP Hamiltonian that accounts for interactions between the QM region and the effective fragments. While the interaction between effective fragments comprises the sum of four terms, i.e. electrostatics, polarization, dispersion and exchange-repulsion, the interaction between each of these fragments and the QM region has typically been described using only the first two of them. Exchange-repulsion is often excluded due to its high computational cost, however, it is necessary to accurately reproduce interaction energies at short distances between the QM and EFP regions. The dispersion term on the other hand, has been incorporated as an additive correction, but it has only been applied to systems in the ground state. Furthermore, there has also been a charge-penetration correction developed with the purpose of better describing the electrostatics of QM/EFP systems, yet the effect and performance of this correction remain unexplored. This thesis expands on the traditional polarizable embedding by incorporating these three terms and assessing their significance.

Chapter 1 introduces the effective fragment potential method (EFP) as well as the hybrid QM/EFP method. In the latter, a sub-region of the system is modeled with an *ab initio* method while everything else is modeled with EFP. Chapter 2 focuses on the development of a parametrized version of the QM/EFP exchange-repulsion term. Such an implementation provides an accurate yet efficient alternative for computing this term. In addition to explaining how the parameters were identified, Chapter 2 also presents a series of benchmarks that validate the reliability of this parametrization. Chapter 3 applies the exchange-repulsion method proposed in Chapter 2 to complex systems consisting of amino acid dimers. Chapter 4 evaluates the performance of

four different QM/EFP schemes on the singlet excitation energies of 9 biologically relevant chromophores. The use of the four different schemes offers relevant insights on how excitation energies are affected by the parametrized exchange-repulsion and the charge-penetration correction. Chapter 5 looks at the interaction energy of systems in which the QM region is in its lowest triplet state. While all terms are independently analyzed, this chapter centers in particular on the dispersion term. Lastly, Chapter 6 summarizes the main findings discussed throughout the thesis.

TABLE OF CONTENTS

Page

Page

LIST OF TABLES

Table Page

LIST OF FIGURES

Figure Page

Figure Page

ABBREVIATIONS

CCSD(T)	Coupled Cluster Singles Doubles and Perturbative Triples
CBS	Complete Basis Set
CIS	Configuration Interaction Singles
DFT	Density Functional Theory
EFP	Effective Fragment Potential
FMO	Fragment Molecular Orbital
HF	Hartree-Fock
LJ	Lennard-Jones
LMO	Localized Molecular Orbital
LP	Lone Pair(s)
MAE	Mean Absolute Error
MC	Monte Carlo
MD	Molecular Dynamics
MM	Molecular Mechanics
MP2	Second Order Møller-Plesset Perturbation Theory
NTO	Natural Transition Orbital
NVT	Canonical Ensemble
PEC	Potential Energy Curve
PIEDA	Pair Interaction Energy Decomposition Analysis
QM	Quantum Mechanics
SAPT	Symmetry-Adapted Perturbation Theory

ABSTRACT

Viquez Rojas, Claudia I. Ph.D., Purdue University, May 2020. QM/EFP models beyond polarizable embedding. Major Professor: Lyudmila V. Slipchenko.

The Effective Fragment Potential (EFP) is a quantum-mechanical based model used to describe non-covalent interactions of small molecules or fragments. It can be used along with fully *ab initio* methods to study the electronic properties of complex systems, such as solvated chromophores or proteins. For this purpose, the system is divided into two regions: one modeled with quantum mechanics and the other with EFP. The interaction between the QM region and the effective fragments has popularly been described through electrostatics and polarization only. This thesis focuses on the development of the QM/EFP exchange-repulsion term, as well as the evaluation of the dispersion term and a charge-penetration correction. The goal of is to determine how these terms can increase the accuracy of QM/EFP calculations without an increase in their computational cost.

1. INTRODUCTION

1.1 The Effective Fragment Potential Method

The Effective Fragment Potential (EFP) is a quantum mechanics-based model used to compute non-bonded interactions in a system of rigid-body fragments [1–7]. The EFP method falls into the category of general polarizable potentials, along with AMOEBA [8], SIBFA [9,10], and several others [11–15]. In EFP each fragment corresponds to a small molecule or a section of a macromolecule [16]. The full interaction energy of the chemical system is described as the sum of Coulomb, polarization, dispersion and exchange-repulsion terms:

$$E_{EFP} = E^{coul} + E^{pol} + E^{disp} + E^{xr} \tag{1.1}$$

Fig. 1.1 depicts each of the EFP terms. The Coulomb term represents the interaction between fragments due to their static electronic densities, represented with a distributed multipole expansion truncated at octupoles [17]. The Coulomb energy between effective fragments A and B is given by [18]:

$$\begin{aligned} E^{coul,AB} = q^B \Bigg[& T q^A - T_\alpha \hat{\mu}^A_\alpha + \frac{1}{3} T_{\alpha\beta} \hat{\Theta}^A_{\alpha\beta} - \frac{1}{15} T_{\alpha\beta\gamma} \hat{\Omega}^A_{\alpha\beta\gamma} \Bigg] \\ & + \hat{\mu}^B_\alpha \Bigg[T_\alpha q^A - T_{\alpha\beta} \hat{\mu}^A_\beta + \frac{1}{3} T_{\alpha\beta\gamma} \hat{\Theta}^A_{\beta\gamma} \Bigg] \\ & + \hat{\Theta}^B_{\alpha\beta} \Bigg[T_{\alpha\beta} q^A - T_{\alpha\beta\gamma} \hat{\mu}^A_\gamma + \frac{1}{3} T_{\alpha\beta\gamma\delta} \hat{\Theta}^A_{\gamma\delta} \\ & + \hat{\Omega}^B_{\alpha\beta\gamma} \Bigg[- \frac{1}{15} T_{\alpha\beta\gamma} q^A \Bigg] \end{aligned} \tag{1.2}$$

where T refers to the electrostatics tensors of zero, first, second, third and fourth order. The q, μ, Θ and Ω symbols represent the point charges, dipoles, quadrupoles and octupoles. This equation follows the Einstein summation convention such that any given subscript represents a sum over that index. As an example, the term $T_{\alpha\beta}\hat{\Theta}^A_{\alpha\beta}$ is actually a sum over α and β.

This multipole expansion accurately reproduces electrostatic energies at long distances. However, at short distances, when electron densities overlap, the expansion is not attractive enough [17]. Damping corrections based on exponential functions have been developed and evaluated to address this issue [17, 18]. The damped potential for a point charge is given by [18]:

$$Tq(1 + (-\exp(-\alpha \mathrm{R}))) \tag{1.3}$$

From here, the damped potential for higher multipoles can be obtained through a Taylor series [18]. The parameter α in the Gaussian function of Eq. 1.3 is obtained by matching the fully damped electrostatics potential to the quantum mechanical potential [18].

The polarization term in EFP describes energy lowering due to the redistribution of the electronic density on a fragment consequent of the electric field of other fragments. In EFP, polarization is computed as an interaction of induced dipoles, which appear when an electric field acts on distributed anisotropic polarizability tensors ($\alpha_{\alpha\beta}$), with the electric field due to other fragments. The induced dipoles on effective fragment A are found by solving the following equation self-consistently [18, 19]:

$$\mu_a^k = \sum_{l}^{fragments} (D_{ab}^{kl})^{-1} F_b^{mult,l} \tag{1.4}$$

where k and l are distributed points. $F_b^{mult,l}$ corresponds to the x, y, z coordinates of the external field due to static multipoles and nuclei from other fragments. The subscript implies a sum over all Cartesian points. Lastly D_{ab}^{kl} is an operator that acts on dipoles to produce a static external field F. An element in D_{ab}^{kl} can take one of three values [18, 19]:

$$\begin{cases} (\alpha_{ab}^k)^{-1}, & \text{if } l = k,\ l \in A \\ 0 & \text{if } l \neq k,\ k, l \in A \\ -T_{ab}^{kl} & \text{if } k \in A,\ l \in B,\ A \neq B \end{cases}$$

The way Eq. 1.4 is solved allows the polarization term to include many-body effects [3]. With the induced dipoles, and again following the Einstein summation convention, the polarization energy can be computed as [18]:

$$E^{pol} = -\frac{1}{2}\sum_{k} \mu_a^k F_a^{mult,k} \tag{1.5}$$

Like the electrostatics term, the polarization term also fails at short distances and hence requires a damping correction. The recommended damping function for polarization consists of a Gaussian function, which is applied to all T and F_α tensors [18]. Fig. 1.1 depicts the polarization term as the interaction between a fragment in a ground state and a fragment in an excited state since electronic excitations redistribute the charges on a fragment, leading to induced dipoles.

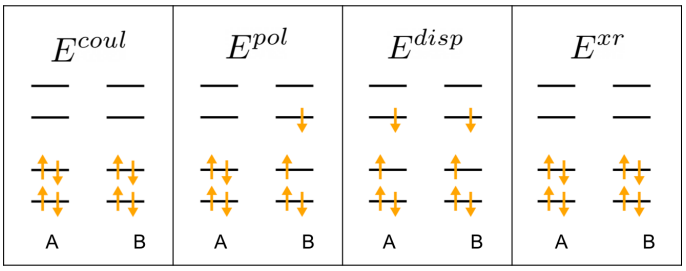

Fig. 1.1. Representation of EFP interaction terms between two fragments: A and B.

Similarly, the dispersion term can be thought of as the excited states of two fragments interacting with each other, as shown in Fig. 1.1. The dispersion terms accounts for London forces between fragments and is modeled as the first R^{-6} term with C6 coefficients computed using distributed dynamic polarizabilities of the fragments [20]. The EFP dispersion energy between fragments A and B is given by [18]:

$$E^{disp} = \sum_{k\in A}\sum_{j\in B} \frac{C_6(j,k) f_S^6(j,k)}{R_{jk}^6} \tag{1.6}$$

with:

$$f_S^6 = 1 - S^2(1 - 2\ln|S| + 2\ln^2|S|) \tag{1.7}$$

f_S^6 is a damping function that improves the behavior of the dispersion function at short range. [18]. In this equation S represents the overlap between a pair of spherical Gaussian functions.

Lastly, exchange-repulsion accounts for the antisymmetry of the wavefunctions of the fragments and is modeled using inter-fragment kinetic and overlap integrals, as well as the Fock matrices from the fragments [21,22]. In EFP, the exchange-repulsion between fragments A and B is approximated as [22]:

$$\begin{aligned} E^{xr} \approx & -2\sum_{i\in A}\sum_{j\in B} 2\sqrt{\frac{-2\ln \mathrm{S_{ij}}}{\pi}}\frac{S_{ij}^2}{R_{ij}} \\ & -2\sum_{i\in A}\sum_{j\in B} S_{ij}\left[\sum_{k\in A} F_{ij}^A S_{kj} + \sum_{l\in B} F_{jl}^B S_{li} - 2T_{ij}\right] \\ & +2\sum_{i\in A}\sum_{j\in B} S_{ij}^2\left[\sum_{J\in B} -Z_j R_{iJ}^{-1} + 2\sum_{l\in B} R_{il}^{-1}\right. \\ & \left.+\sum_{l\in A} -Z_I R_{Ij}^{-1} + 2\sum_{k\in A} R_{kj}^{-1} - R_{ij}^{-1}\right] \end{aligned} \tag{1.8}$$

where i and j are LMOs on fragments A and B respectively. The overlap and kinetic integrals for these LMOs are given by S_{ij} and T_{ij}. R_{ij} indicates the distance between the centroids of charge of the LMOs. Similarly, R_{Ij} gives the distance between the LMO j and the nucleus I, which has a charge of Z_I. Finally, F_{ik}^A comes from the Fock matrix of A, and corresponds to the element containing the i and k LMOs.

For any given fragment, a potential containing all of these terms can be obtained through a `MAKEFP` calculation on the GAMESS [23, 24] electronic structure software. All subsequent energy calculations on systems containing that fragment can be done using this potential. Generally the potential contains distributed atoms and bond midpoints multipoles (up to octupoles) and screening parameters for electrostatics term, distributed at centroids of LMOs static polarizability tensors for polarization term, distributed at centroids of LMOs dynamic polarizability tensors computed at 12 imaginary frequencies for dispersion, and localized wave function, basis set and Fock matrix for exchange-repulsion term. The polarization and dispersion screening

functions can be selected in the input of the subsequent calculations. If desired, some terms can be excluded from the `MAKEFP` calculation. This is generally beneficial for terms that increase the computationally cost of the EFP calculations, such as exchange-repulsion.

1.2 Hybrid Quantum Mechanical Molecular Mechanics Methods

A popular and efficient way to model the electronic properties of solvated systems is to use hybrid quantum mechanical and molecular mechanical methods (QM/MM) [25–29]. In QM/MM the chemically relevant region is modeled with an appropriate *ab initio* method, while its surroundings are modeled with a force field. Applications of QM/MM methods started as early as 1976, with the study of enzymatic reactions done by Warshel [30]. Since then, QM/MM methods have been abundantly researched [31–41]. Some of the developments include multi-layer methods such as ONIOM [42–44], Truhlar MCMM methods [45,46] and polarizable QM/MM for linear response methods by Kongsted and coworkers [11–13].

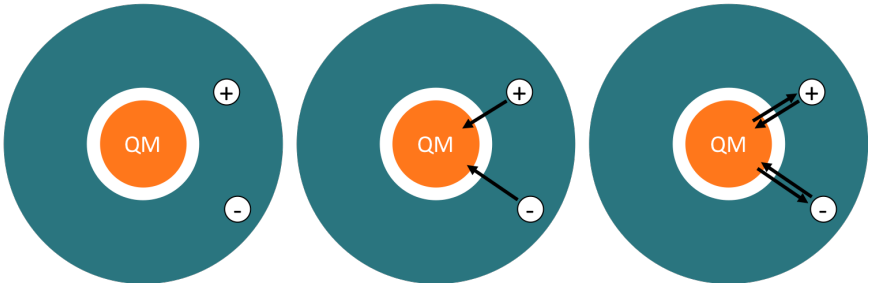

Fig. 1.2. Types of embedding in QM/MM systems. From left to right: mechanistic embedding, electrostatic embedding and polarizable embedding.

The Hamiltonian of a QM/MM system consists of three terms:

$$\hat{H} = \hat{H}_{QM} + \hat{H}_{MM} + \hat{H}_{QM/MM} \tag{1.9}$$

where $\hat{H}_{QM}$ and $\hat{H}_{MM}$ are the Hamiltonians of the QM and MM subsystems, respectively, and $\hat{H}_{QM/MM}$ is the coupling term. Separation of the QM and MM subsystems, in principle, allows one to use any method for each part. Popular methods chosen to describe the QM region include semi-empirical methods, density functional theory (DFT) and post Hartree-Fock alternatives, such as Møller–Plesset perturbation theory (MP2) and coupled cluster methods [29]. The complexity of QM/MM methods varies; ranging from simple mechanistic embedding in which the QM and MM systems do not interact, to electrostatic embedding where the MM system polarizes the QM system, and polarization embedding in which the QM and MM systems polarize each other self-consistently. Fig. 1.2 shows the different types of embedding.

1.3 QM/EFP

EFP can be used in combination with *ab initio* methods as an alternative to classical force fields. This methodology is known as QM/EFP. In previous applications of QM/EFP [19,47,48], the interaction between the fragments and the QM region was typically described by polarizable embedding. This type of embedding includes only the Coulomb and polarization terms and is represented with the following coupling Hamiltonian $\hat{H}_{QM/EFP}$:

$$\hat{H}_{QM/EFP} = \left\langle p \left| \hat{V}^{coul} + \hat{V}^{pol} \right| q \right\rangle p^{\dagger} q \tag{1.10}$$

where p and q represent the atomic orbitals in the QM region. In polarizable embedding, the EFP environment responds to electron density changes in the QM region. This embedding model has been described in detail previously [5, 49, 50] and is defined as:

$$\begin{aligned} E_{PE,0} = &\left\langle \Psi_0 \left| \hat{H}_{QM} + \hat{V}^{coul} + \hat{V}_0^{pol} \right| \Psi_0 \right\rangle \\ &+ E_0^{pol} + E_{QM/EFP,0}^{disp} + E_{EFP}^{coul} + E_{EFP}^{disp} + E_{EFP}^{xr} \end{aligned} \tag{1.11}$$

where Ψ_0 is the ground state electronic wavefunction of the QM region. The last three terms of the sum account for electrostatics, dispersion and exchange-repulsion

interactions between the EFP fragments and are unaffected by the QM wavefunction. Subscript "0" in the polarization energy of the QM/EFP system E_0^{pol} and in the polarization perturbation to the quantum Hamiltonian $\hat{V}_0^{pol}$ indicates that induced dipoles of the fragments are converged to full consistency with the ground state wavefunction Ψ_0 of the QM subsystem [48, 50]. Similarly, the dispersion energy between the QM and EFP subsystems $E_{QM/EFP,0}^{disp}$ is a perturbative energy correction computed based on the ground state wavefunction of the quantum region [51].

The electrostatic contribution to the QM Hamiltonian due to a multipole expansion of a fragment is given by [2, 16]:

$$\begin{aligned}\hat{V}_k^{coul} = q_k T(r_k) &- \sum_a^{x,y,z} \mu_a^k T_a(r_k) \\ &+ \frac{1}{3}\sum_{a,b}^{x,y,z} \Theta_{a,b}^k T_{a,b}(r_k) \\ &- \frac{1}{15}\sum_{a,b}^{x,y,z} \Omega_{a,b,c}^k T_{a,b,c}(r_k)\end{aligned} \tag{1.12}$$

where q, μ, Θ and Ω are net charge, dipole, quadrupole and octupole at point k, T represents the electrostatics tensors of zero, first, second and third order, and r_k is the distance between the expansion point k and the coordinate of an electron in the QM region.

The polarization contribution to the QM Hamiltonian is as follows [48, 50]:

$$\hat{V}_p^{pol} = \frac{1}{2}\sum_a^{x,y,z} \frac{(\mu_a^p + \tilde{\mu}_a^p)a}{r_p^3} \tag{1.13}$$

where μ_a^p and $\tilde{\mu}_a^p$ represent the induced dipole and conjugated induced dipole at the distributed polarizability point p. R refers to the distance between the polarizability point and an electron, and a to the x, y, z component. The induced dipole at a given point depends on the total electric field [48, 50]:

$$\mu_a^p = \sum_a^{x,y,z} \alpha_{ba}^p F_a^{total,p} \tag{1.14}$$

where α_{ba} is the polarizability tensor and F^{total} the total field at the polarizability point p, given as the sum of fields produced by multipoles and induced dipoles on

the fragments in addition to the electronic and nuclear fields due to the quantum region. Since the wave function also depends on the static and induced fields from other fragments, the polarization is computed self-consistently. Convergence for this procedure is reached when the induced dipoles of the fragments are consistent with each other and with the wavefunction [48, 50].

An advantage of using EFP over other force fields is that, as mentioned in Section 1.1, an EFP potential can be computed for any small molecule. Additionally, recent work was able to extend the EFP and QM/EFP methods to biological polymers [16]. Nonetheless, QM/EFP can still be improved on by overcoming its constraint to rigid-bodies and by adding short-range interaction terms without increasing the computational cost of the calculations.

2. PARAMETRIZATION OF THE QM/EFP EXCHANGE-REPULSION TERM

2.1 Motivation

Polarizable embedding allows the effective fragments in QM/EFP to respond to electron density changes in the *ab initio* region [52], which is preferable over electronic embedding in which the classical region is unaffected by changes in the QM region. The electrostatic and polarization terms are considered to be the most important for describing solute-solvent interactions in polar media. However, short-range cavity effects of the environment are essential to account for solvatochromic shifts in non-polar solvents and shifts of diffuse and Rydberg states. In a typical QM/MM scheme, short-range solute-solvent interactions are modeled as Van der Waals terms parameterized within a Lennard-Jones (LJ) potential and included in $\hat{H}_{\mathrm{QM/MM}}$ at the MM level. However, (fixed) LJ parameters of the QM subsystem might become inaccurate during a chemical reaction or electronic redistribution. Additionally, the electronic wave function and electronic density of the QM subsystem are completely unaffected by the LJ interactions with the solvent. To address these issues, a general QM/EFP model, in which short-range interactions are described at the quantum-mechanical level, is under development [5]. Toward this goal, a QM/EFP dispersion energy term based on the second-order perturbation expansion has been recently developed and implemented [51].

With the objective of further improving the description of short-range repulsive interactions between the QM region and the effective fragments, a new formulation of the exchange-repulsion energy is introduced in this chapter. In this formulation the exchange-repulsion contribution due to effective fragments, $\hat{V}^{xr}$, is modeled as a

one-electron term in the QM/EFP coupling Hamiltonian, using a pair of parameters for each localized molecular orbital (LMO) of an effective fragment.

A similar treatment of the exchange-repulsion term is used in the EFP1 water model, developed in 1996 [1]. QM/EFP1 methods were successfully applied to model reactivity, dynamics and photochemistry of aqueous systems [53–56]. The present work extends this approximation of the exchange-repulsion term to molecules other than water, without increasing the cost of QM/EFP simulations. Additionally, a methodologically simple formulation of the QM/EFP exchange-repulsion term allows straightforward implementation in electronic structure packages that incorporate the interface to EFP models through the *libefp* software library [57, 58].

2.2 Methods

2.2.1 Theory

Here we model the QM/EFP exchange-repulsion term as a one-electron contribution to the QM Hamiltonian. $\hat{V}^{xr}$ is described with Gaussian functions containing a pair of parameters for each unique LMO of an effective fragment:

$$\hat{V}^{xr} = \sum_{j}^{J} \beta_j e^{-\alpha_j (r - R_j)^2}. \tag{2.1}$$

where j represents the points of the LMO centroids in effective fragments. The distance between the LMO centroid on an effective fragment and an electron in the QM region is given by $|r - R_j|$, where r corresponds to the electronic coordinate and R_j to the coordinate of the LMO centroid. For each type of LMO, α_j and β_j represent fitted parameters. Values of the parameters for each unique LMO type were optimized by comparing the QM/EFP exchange-repulsion energies to the corresponding EFP and symmetry-adapted perturbation theory (SAPT) energies. Details of the parameterization procedure are described in the following sections.

The QM/EFP exchange-repulsion energy can be computed as an expectation value:

$$E^{xr}_{QM/EFP} = \langle p|\hat{V}^{xr}|q\rangle. \tag{2.2}$$

To determine the optimal α and β parameters, Eq.2.2 was used with different values of parameters in $\hat{V}^{xr}$ without re-optimizing the electronic wave function. That is, during parameter optimization, the computed exchange-repulsion energy was not fully variational. However, this approach was adapted as the most computationally efficient, while pertaining sufficient numerical accuracy, i.e., producing relative errors in values of the exchange-repulsion energies not exceeding a small percentage.

With this implementation of the exchange-repulsion term, the total energy of the QM/EFP system would be given by:

$$\begin{aligned} E_{QM/EFP} = & \left\langle p \left| \hat{H}_{QM} + \hat{V}^{coul} + \hat{V}^{pol} + \hat{V}^{xr} \right| q \right\rangle \\ & + E^{disp}_{QM/EFP} + E^{coul}_{EFP} + E^{pol}_{EFP} \\ & + E^{disp}_{EFP} + E^{xr}_{EFP} \end{aligned} \tag{2.3}$$

where $\hat{V}^{coul}$, $\hat{V}^{pol}$ and $\hat{V}^{xr}$ represent the electrostatic, polarization and repulsion contributions of the effective fragments to the quantum Hamiltonian $\hat{H}_{QM}$. The $E^{disp}_{QM/EFP}$ term describes dispersion energy correction due to interactions between the QM region and effective fragments [51].

2.2.2 Parameterization of the QM/EFP exchange-repulsion

The following molecules were used to determine parameters for the selected LMO types:

- C-H and C-C: methane, ethane, pentane, neopentane, cyclopentane.
- C=C: ethene, trans-2-butene, cis-2-butene, propene, 3-hexene.
- C≡C: ethyne, propyne, hexyne.

- O-H and oxygen lone pair: water.
- C-O: methyl ethyl ether, di-methyl ether, di-ethyl ether.
- C=O: formaldehyde, propanal, acetone, 3-methylbutan-2-one.
- N-H and nitrogen lone pair: ammonia.
- C-N: trimethylamine, triethylamine, N,N-dimethylcyclohexanamine.
- C=N: N-methylmethanimine, N-methylpropan-2-imine, N-methylpentan-3-imine.
- C≡N: hydrogen cyanide.

The C-C and C=C parameters for benzene are not the same as for alkanes and alkenes and were determined by minimizing only the standard deviation of (QM/EFP – SAPT0) total interaction energy differences (see Section 2.2.5) for 12 parallel benzene conformations.

The parameterization of the QM/EFP exchange-repulsion for each unique LMO was done in four steps: molecular dynamics sampling of configurational space of a particular dimer, interaction energy computations (SAPT, EFP and QM/EFP), statistical analysis, and testing of the parameters.

2.2.3 Molecular Dynamics Sampling

For a given LMO type, e.g., C-H bond, C-O bond, a number of associated molecules with diverse connectivity were chosen; for example, methane, ethane, pentane, neopentane and cyclopentane were used in the case of C-H bond; methyl ethyl ether, di-methyl ether, di-ethyl ether were used for parameterizing the C-O bond, etc. The monomers were optimized using Hartree-Fock and a Dunning/Hay double zeta basis set with one p-type and one d-type polarization functions [59]. Homo-trimers of these molecules were constructed. Five rigid-body molecular dynamics (MD) simulations were performed at different temperatures (100, 200, 400, 800, and 1600K),

ensuring a diversity of conformations. A NVT ensemble and periodic boundary conditions were employed. The box size was set to either 20 Å or 30 Å (for molecules with 5 or 6 heteroatoms) and 12 Å or 16 Å for smaller molecules.

The MD trajectories, consisting of 1000 steps, were computed with the EFP-MD module of *libefp* software library [57]. From the five resulting trajectories, a set of dimer geometries was randomly extracted with additional constraints that each dimer had a total interaction energy below 20 kcal/mol and exchange-repulsion energy greater than 0.001 mH according to SAPT. These constraints ensured selection of structures in which interactions are not too strong (at a repulsive part of the potential energy surface (PES)) and not too weak (at a long-range part of the PES).

2.2.4 Energy Calculations

The total interaction energies and the energy components for each dimer were obtained at the SAPT0/jun-cc-pVDZ level of theory in PSI4 quantum chemistry package [60–63]. For further comparison, EFP exchange-repulsion energies were computed in the GAMESS quantum chemistry package [23, 24]. The necessary EFP parameters were calculated in a mixed basis: 6-31+G(d) (or 6-31G(d) in the case of aromatic molecules) for electrostatics and 6-311++G(3df,2p) for all other components [64–70]. The use of the Edmiston-Ruedenberg localization scheme, instead of Boys localization, is the main difference between these parameters and the ones originally employed for the benchmarking of EFP on the S22 dataset [71].

The same EFP potentials were used for the QM/EFP computations (Eq. 2.1), implemented in a local version of GAMESS. For each dimer geometry, the QM/EFP exchange-repulsion energies were calculated using α and β values ranging from 0.0 to 2.0 (Eqs. 2.1 and 2.2). All QM/EFP energies were obtained using a Dunning/Hay double zeta basis set with one p-type and one d-type polarization functions (for hydrogens and heavy atoms, respectively) on a QM subsystem [59]. The Hartree-Fock (HF) method was used for describing the QM region in QM/EFP calculations.

2.2.5 Statistical Analysis

For each selected dimer geometry labeled as n, three errors were calculated for every α and β pair (α,β):

1. $err_{\mathrm{n}}^{\mathrm{EFP\_xr}}(\alpha,\beta) = E_{\mathrm{EFP,n}}^{\mathrm{xr}} - E_{\mathrm{QM/EFP,n}}^{\mathrm{xr}}(\alpha,\beta)$.

2. $err_{\mathrm{n}}^{\mathrm{SAPT\_xr}}(\alpha,\beta) = E_{\mathrm{SAPT,n}}^{\mathrm{xr}} - E_{\mathrm{QM/EFP,n}}^{\mathrm{xr}}(\alpha,\beta)$.

3. $err_{\mathrm{n}}^{\mathrm{SAPT\_rem}}(\alpha,\beta) = E_{\mathrm{SAPT,n}}^{\mathrm{total}} - E_{\mathrm{QM/EFP,n}}^{\mathrm{total}}(\alpha,\beta)$.

The first and second errors compare the exchange-repulsion energy computed by the QM/EFP with the parameterized exchange-repulsion term to the exchange-repulsion energy from the EFP and SAPT calculations, respectively. The last error accounts for the total interaction energy difference between the QM/EFP and SAPT.

The standard deviation associated with a given pair of parameters $S_{\alpha,\beta}$ was estimated for each of the three errors (s):

$$S_{\alpha,\beta}^{s} = \sqrt{\frac{1}{N}\sum_{n=1}^{N}(err_{n}^{s}(\alpha,\beta) - e\bar{r}r^{s}(\alpha,\beta))^{2}}, \tag{2.4}$$

where N is the number of geometries obtained across all molecules used for parameterizing a given LMO type. The (α,β) set was reduced to only those pairs that had a standard deviation for $err^{\mathrm{EFP\_ex-rep}}$ within one unit of the minimum standard deviation:

$$S_{\alpha,\beta}^{\mathrm{EFP\_xr}} < min(S_{\alpha',\beta'}^{\mathrm{EFP\_xr}}) + 1. \tag{2.5}$$

The same step was repeated for $err^{\mathrm{SAPT\_ex-rep}}$:

$$S_{\alpha,\beta}^{\mathrm{SAPT\_xr}} < min(S_{\alpha',\beta'}^{\mathrm{SAPT\_xr}}) + 1. \tag{2.6}$$

From the remaining (α,β) combinations, parameters providing the smallest standard deviation for $err^{\mathrm{SAPT\_rem}}(\alpha,\beta)$ were selected as the final set for a given LMO type.

For each LMO type, mean absolute errors (MAE) and mean relative errors (%) of the optimal parameters are reported in Tables A.4 and A.5 of the Appendix A.

2.2.6 Testing of Parameters

The exchange-repulsion and total interaction QM/EFP energies were tested in four ways.

First, we compared potential energy curves (PEC) for selected dimers (methane, ammonia, water and benzene dimers) obtained with SAPT, EFP and QM/EFP methods. Dimer geometries were adopted from the S22 data set [71,72], with the exception of the parallel (sandwich) benzene dimer, acquired from Ref. [73]. To obtain the PECs, the original geometries of the dimers were displaced along a line connecting centers of the two molecules. In the particular case of the parallel displaced benzene dimer, the effective fragment was shifted along the z-axis only (analogous to the sandwich benzene dimer).

In the second test, local minima of a larger set of dimers (2-aminopyridine, 2-butanol, acetone, benzene, cyclohexanol, di-ethyl ether, di-methyl ether, dimethylamine, ethanol, formaldehyde, methane, methanol, methoxyethane, methyl-siopropyl ketone, methylamine, N-methylmethanimine, piperidine, propan-1-imine, propan-2-imine, tert-butanol and water) were obtained from the EFP-based Monte Carlo simulations [74] and their SAPT, EFP and QM/EFP energies were compared.

In the third test, the QM/EFP, EFP and SAPT energies for all molecules included in the S22 dataset were evaluated [72]. The total interaction energies were compared to the reference energies obtained with the coupled cluster with singles, doubles and perturbative triples (CCSD(T)) method in a complete basis set [75].

Finally, exchange-repulsion and total QM/EFP interaction energies computed with the method developed in this work were compared against QM/EFP exchange-repulsion and total interaction energies from the formulation developed by Kemp and coworkers [5, 76]. For this test, geometries for water, methanol and benzene dimers were extracted from the S66 data set [77].

In all dimer calculations in this work, one monomer represents the QM region and the second is the effective fragment. For this reason, the purely EFP terms in Eq. 2.3 are absent. All QM/EFP and EFP calculations were executed in GAMESS [23, 24].

2.3 Results

Table 2.1 summarizes parameters for describing the QM/EFP exchange-repulsion term (Eq.2.1) positioned at centroids of the localized molecular orbitals corresponding to C-H, C-C, C=C, C≡C, O-H, C-O, N-H, C-N, C=N, C≡N bonds, as well as oxygen and nitrogen lone pairs (LPs). All LMOs in double and triple bonds were treated equally, e.g., in case of the double bond, both LMOs were described with the same set of parameters.

Values of the parameters vary across bonding types. There is no pattern that would help predict which (α,β) combination is optimal for a given LMO. However, it can be noted that LMOs that tend to be surrounded by other orbitals (so called "buried" LMOs) contribute little to exchange-repulsion and prefer parameter values close to zero.

Fig. 2.1 demonstrates the comparison of SAPT, EFP, and QM/EFP exchange-repulsion and total interaction energies at different intermonomer separations in methane, water and ammonia dimers. Exchange-repulsion and total interaction energies of the benzene dimer in parallel, parallel displaced, and T-shaped configurations are shown in Fig. 2.2. In all cases SAPT0/jun-cc-pVDZ is considered as the reference. In ammonia, methane, and water dimers, QM/EFP exchange-repulsion energies are comparable to the EFP exchange-repulsion (Fig. 2.1). The QM/EFP total interaction energies are also close to or better than the EFP energies, even though the latter comparison does not undermine the quality of EFP, in which all energy terms are independent, while fitting of the exchange-repulsion term in QM/EFP specifically favors accurate total energies. In the three benzene dimers, the QM/EFP exchange-repulsion energies are underestimated (Fig. 2.2). Nonetheless, the total interaction

Table 2.1.
QM/EFP exchange-repulsion parameters for LMOs corresponding to different bonding patterns.

LMO	β	α
C-H	0.54	0.41
C-C	0.00	0.00
C=C	0.11	0.21
C≡C	0.18	0.25
LP O	0.70	0.50
O-H	0.40	0.40
O-C	0.00	0.00
O=C	1.02	1.16
LP N (sp3)	0.11	0.23
LP N (sp2 or sp)	0.60	0.40
N-H	1.60	0.62
N-C	0.00	0.00
N=C	0.30	0.80
N≡C	1.90	0.78
Aromatic C-H	0.54	0.41
Aromatic C-C	1.92	0.45
Aromatic C=C	0.00	0.00

energies for these dimers are too positive (repulsive) with respect to SAPT, suggesting that the values of one or several of the attractive QM/EFP components are underestimated in benzene dimers (i.e., less attractive than should be). Overall, the analysis of these PECs shows that the QM/EFP exchange-repulsion energy can be reasonably approximated with the identified parameters and the functional form of the exchange-

repulsion term (Eq. 2.1) is appropriate for describing exchange-repulsion energies at various inter-monomer separations.

The QM/EFP computations utilized for the identification and initial testing of the parameters were performed with the Dunning/Hay polarized double zeta basis for the QM region. Here we examine dependence of the QM/EFP exchange-repulsion energies on the basis set employed for the QM region, using methane, water and parallel benzene dimers as representative examples (see Fig. 2.3). Given that exchange-repulsion depends on the orbital overlap between two molecules, larger bases are expected to produce more repulsive values of the exchange-repulsion energy. This trend is generally true for methane and water dimers. For example, in the case of the water dimer, the magnitude of the exchange-repulsion is significantly increased in diffuse triple-zeta basis sets compared to non-diffuse or double-zeta bases. On the other hand, the basis set has more sporadic effect on the magnitude of the exchange-repulsion in the benzene dimer, with calculations diverging at short distances when diffuse functions are included in the basis set. To summarize, these tests show that while it is possible to use various basis sets for describing the QM region in combination with the EFP model, calculations are expected to be more reliable when double-zeta or non-diffuse triple-zeta bases are employed for the QM region because parameterization is generally basis-set specific and double-zeta basis was used to optimize parameters reported in this chapter.

Exchange-repulsion and total QM/EFP interaction energies of a large set of dimers are shown in Fig. 2.4. Structures of these dimers, obtained from EFP-based Monte Carlo simulations, correspond to local or global minima. All structures and energy values are provided in Appendix A (Table A.1). Energies of the dimers were computed using QM/EFP, SAPT0/aug-cc-pVDZ (for reference) and EFP (for comparison). In agreement with other studies [71], these results show that the EFP exchange-repulsion energies are less repulsive than the corresponding SAPT energies. QM/EFP also underestimates exchange-repulsion, with bigger deviations observed for dimers with larger exchange-repulsion values (Fig. 2.4). The only case in which

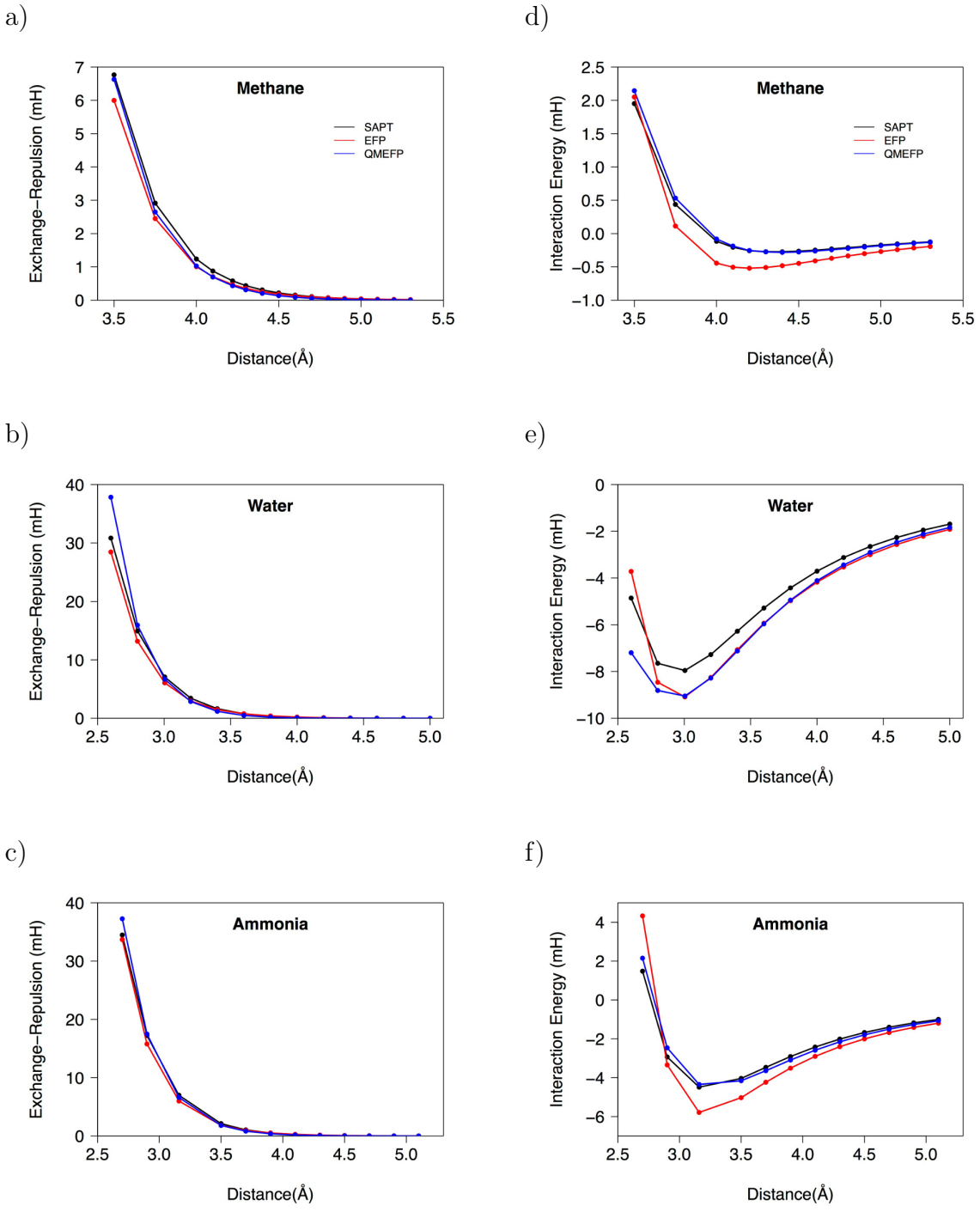

Fig. 2.1. Exchange-repulsion (a,b,c) and total interaction energies (d,e,f) in methane, water, and ammonia dimers (mH).

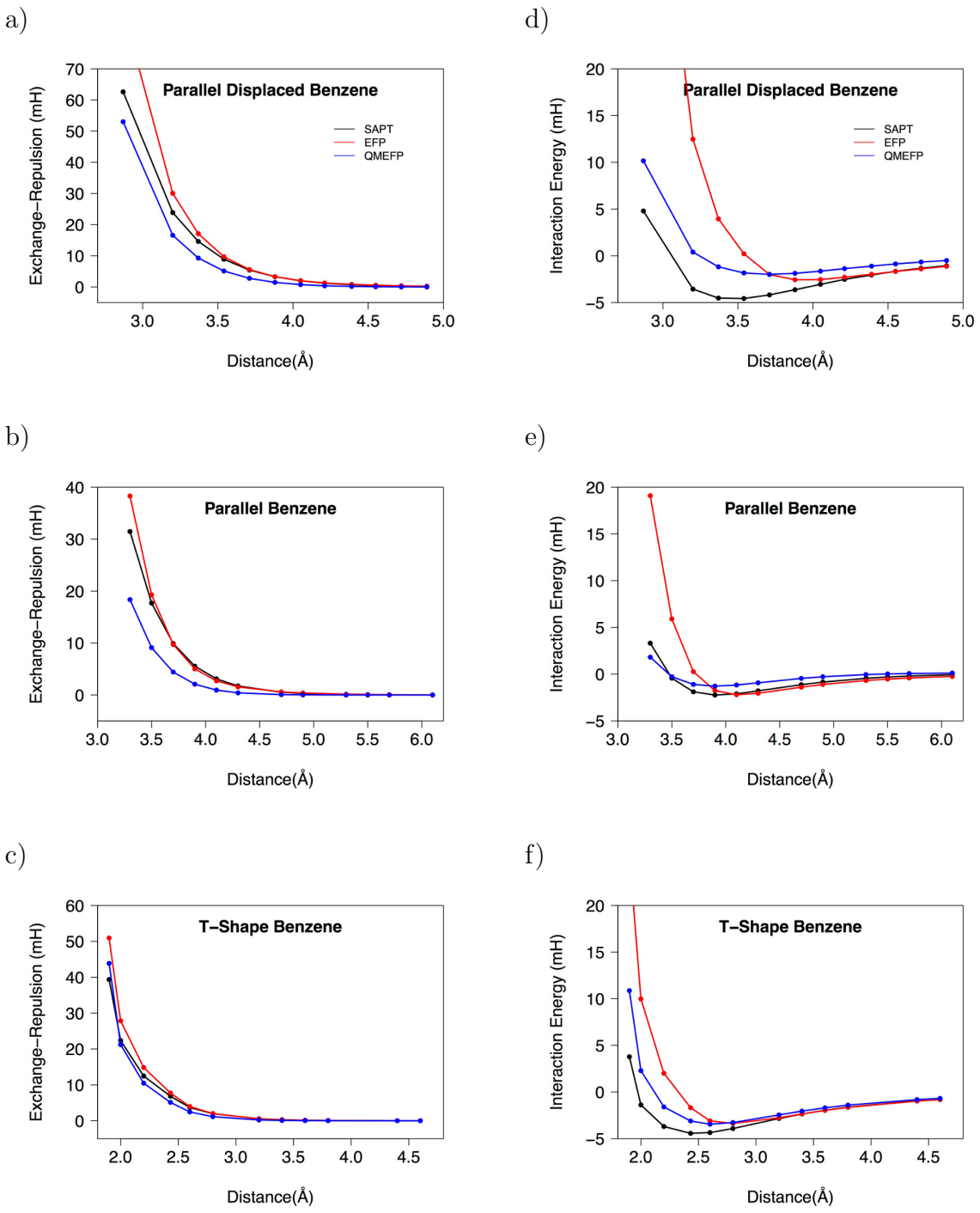

Fig. 2.2. Exchange-repulsion (a,b,c) and total interaction energies (d,e,f) in parallel displaced, parallel (sandwich), and t-shape benzene dimers (mH).

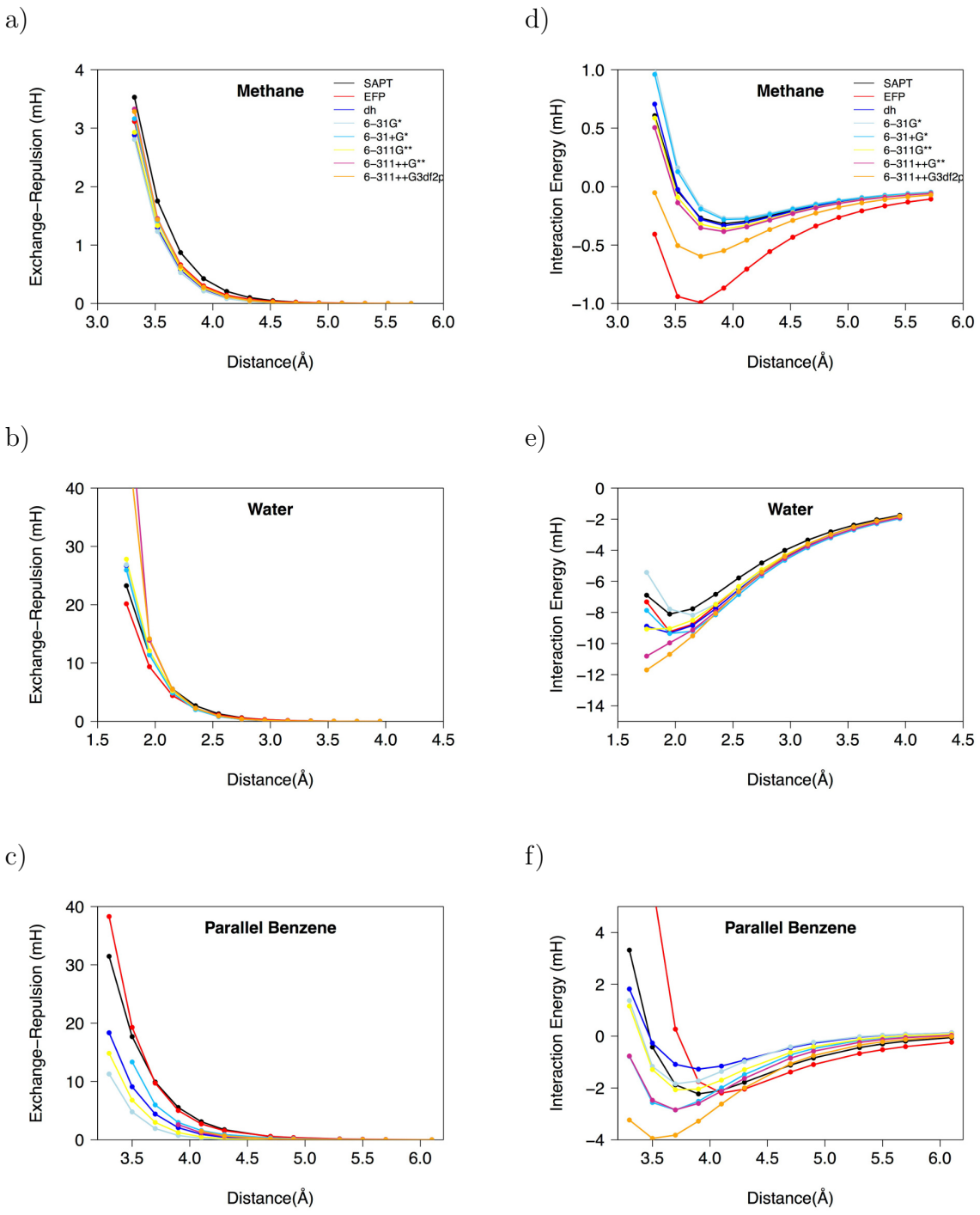

Fig. 2.3. Exchange-repulsion (a,b,c) and total interaction energies (d,e,f) in methane, water and parallel benzene dimers (mH) computed with different basis sets in the QM region.

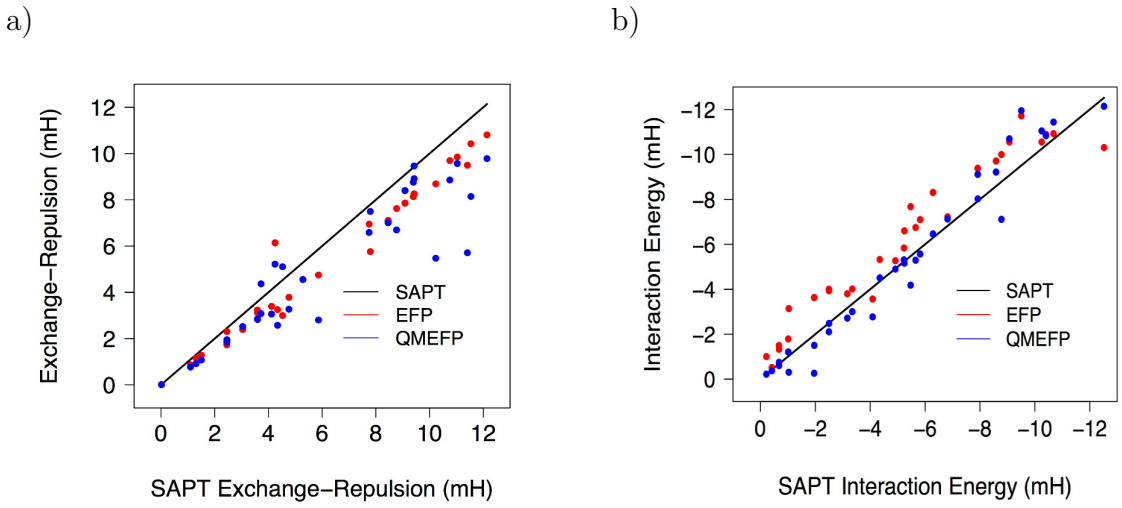

Fig. 2.4. Comparison of (a) exchange-repulsion and (b) total interaction energies by EFP and QM/EFP methods against SAPT0/jun-cc-pVDZ for dimers extracted from the EFP-based Monte Carlo simulations.

the QM/EFP exchange-repulsion energy is considerably lower than the EFP value is methyl isopropyl ketone. On the other hand, the total QM/EFP and EFP interaction energies are within 0.5 mH apart. Indeed, most QM/EFP total interaction energies are more accurate than the EFP total interaction energies, as also seen from Table 2.2. It is clear that while the QM/EFP exchange-repulsion energies are somewhat less accurate than the EFP exchange-repulsion, the total interaction energies are more accurate (balanced) in QM/EFP than in EFP. This is because in optimizing exchange-repulsion parameters, one of the metrics was the deviation from the total interaction SAPT energies, and an error cancellation between different energy components in QM/EFP was explicitly favored. In the pure EFP method, each energy term is independent of other terms and the accuracy of a particular term does not necessarily ensures the accuracy of the total interaction energies.

Fig. 2.5 shows the comparison of the exchange-repulsion and total energies in dimers of the S22 data set. Numerical data are provided in Tables A.3 and A.2

Table 2.2.
Mean absolute errors (MAE) and root mean square errors (RMSE) of the exchange-repulsion and total interaction energies in dimers obtained from the EFP-based Monte Carlo simulations.

	MAE (mH)	RMSE (mH)	MAE (kcal/mol)	RMSE (kcal/mol)
EFP ex-rep	1.00	1.13	0.63	0.71
EFP total	1.16	1.31	0.73	0.82
QM/EFP ex-rep	1.24	1.77	0.78	1.11
QM/EFP total	0.59	0.84	0.37	0.53

of Appendix A. The total QM/EFP and EFP energies are compared against the CCSD(T)/complete basis set (CBS) values. MP2/cc-pVTZ total interaction energies are also provided for comparison. For the exchange-repulsion energies, SAPT0/aug-cc-pVDZ energies are used as a reference.

Since the QM/EFP exchange-repulsion formula provides a different treatment of the QM and EFP parts, it is unsurprising that the exchange-repulsion energy (as well as total interaction energy) in a non-symmetric dimer would differ depending on which monomer is treated as a fragment and which one is treated as a quantum region. This phenomenon can be seen in Fig. 2.5, where two QM/EFP values are provided for all dimers. The QM/EFP values are identical for homo-dimers in a symmetric orientation, e.g., formic acid dimer, parallel benzene dimer, etc. In heterodimers or non-symmetric homodimers, the discrepancies in exchange-repulsion energies rarely exceed 2 mH, with the extreme exceptions being the indole-benzene dimer, in which the difference is 3.4 mH, and the stacked adenine-thymine dimer with the difference of 8.1 mH.

Similarly to previous tests, these results show that for dispersion-dominated complexes, the QM/EFP exchange-repulsion energies are smaller in magnitude (less repulsive) than the SAPT and EFP exchange-repulsion energies. Total QM/EFP in-

teraction energies for aromatic complexes are underestimated (too positive), also in agreement with previous tests. Other noticeable errors in total interaction energies, greater than 1.6 mH, occur in dimers containing amide and ester groups, for which the total interaction energies are overestimated (too negative). It might be possible to improve these results by determining a separate set of parameters for the C-O, C-N and C=O LMOs in highly conjugated systems.

Overall, as shown in Table 2.3, QM/EFP results have higher errors in the exchange-repulsion energies but smaller errors in the total interaction energies than the corresponding EFP data. Note that the EFP statistics for the S22 dataset presented here differs from the one previously reported [71]. One reason for this disagreement is a slight difference in the EFP potentials, originating from a choice of localization methods employed. In the original application of EFP to the S22 data set [71], the Boys localization scheme [78] was used. In this work we opted for the Edmiston-Ruedenberg localization scheme [79]. The localization scheme (and generated localized orbitals) affects polarization, dispersion and exchange-repulsion terms. However, the biggest source of discrepancies occurred because in Ref. [71], EFP total interaction energies were computed at the EFP-optimized geometries. In the present work, S22 geometries were used for the comparison of both the exchange-repulsion and total interaction energies.

In order to place the parameterized QM/EFP exchange-repulsion term in context with a previous implementation of the QM/EFP exchange-repulsion term by Kemp *et al.* [76], we compare exchange-repulsion energies of the parameterized and original QM/EFP implementations on the example of water, methanol and two benzene dimers (see Tables 2.4 and 2.5). Geometries of these dimers are extracted from the S66 data set. For water and methanol dimers, the exchange repulsion-energies of the two methods are within 2 mH from each other, with parameterized implementation being slightly faster. The time difference increases in larger systems such as benzene dimer, where the original implementation is almost three times more expensive than the parameterized form (Table 2.5). For two benzene dimers (parallel displaced and

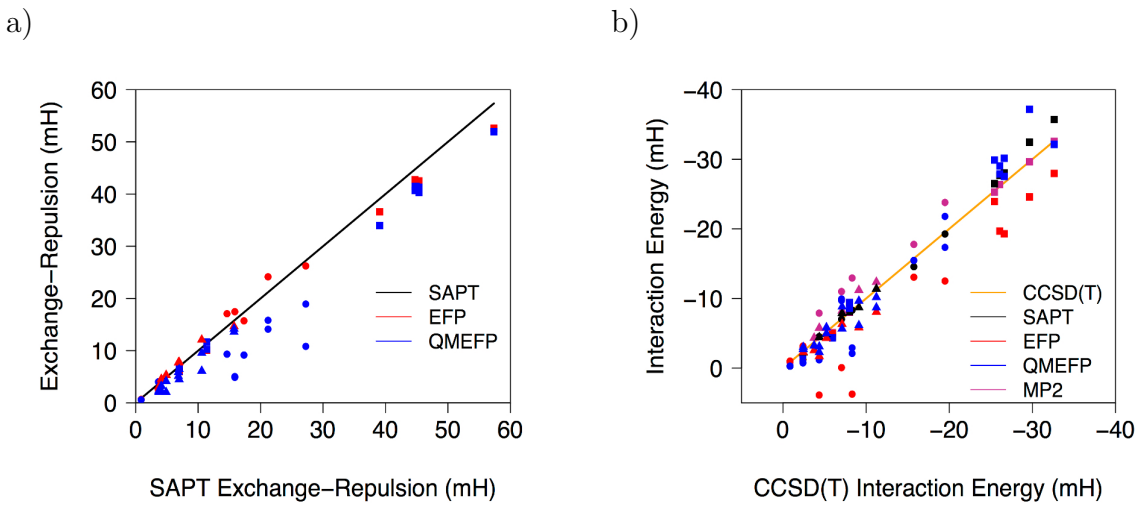

Fig. 2.5. Comparison of (a) exchange-repulsion and (b) total interaction energies of dimers of the S22 dataset by EFP and QM/EFP methods. The dimers are divided into three subgroups based on their predominant interaction type: dispersion-dominated (●), hydrogen bonded (■) and mixed (▲).

Table 2.3.
Mean absolute errors (MAE) and root mean square errors (RMSE) of the exchange-repulsion and total interaction energies of dimers of the S22 dataset. SAPT0/jun-cc-pVDZ is used as a reference for the exchange-repulsion energies; CCSD(T)/CBS is a reference for the total interaction energies.

	MAE (mH)	RMSE (mH)	MAE (kcal/mol)	RMSE (kcal/mol)
EFP ex-rep	1.56	1.90	0.98	1.20
EFP total	3.57	4.76	2.25	3.00
QM/EFP ex-rep	3.64	5.02	2.28	3.15
QM/EFP total	2.07	2.77	1.30	1.74

t-shape), the original implementation (as reported in the GAMESS 2017 R1 version) produces erroneous results and will be corrected in the future releases of GAMESS. The parameterized formula deviates from SAPT for the parallel-displaced benzene dimer, but the energy values are more reasonable and calculations are computationally efficient.

Table 2.4.
Comparison of exchange-repulsion energies (mH) computed using implementation from Ref. [76] ("orig-QM/EFP") and the present parameterized version ("QM/EFP").

Dimer	$E^{ex-rep}_{orig-QM/EFP}$	$E^{ex-rep}_{QM/EFP}$	SAPT0
Water	11.9	10.8	13.4
Methanol	14.8	13.2	10.6
Benzene (parallel disp.)	118.6	5.9	10.1
Benzene (t-shape)	-24.4	5.6	6.4

Table 2.5.
Total time (s) required for QM/EFP calculations by the approach described in Ref. [76] ("orig-QM/EFP") and the present parameterized version ("QM/EFP").

Dimer	orig-QM/EFP	QM/EFP
Water	3.3	3.2
Methanol	4.2	3.5
Benzene (parallel disp.)	23.6	8.2
Benzene (t-shape)	27.3	8.2

2.4 Conclusions

Exchange-repulsion energy for the QM/EFP coupling term has been developed and implemented. The formulation is based on representing each EFP fragment as a set of parameterized Gaussian functions positioned on LMO centroids. Parameters for a number of LMO types have been determined using a fit to a combination of EFP exchange-repulsion and SAPT total interaction and exchange-repulsion energies. By comparing QM/EFP exchange-repulsion and total interaction energies to SAPT, we showed that this parameterization provides accurate results for a variety of molecular dimers, including the dimers from the S22 data set. For example, for the S22 data set, MAEs for the exchange-repulsion term and total interaction energies are 2.25 kcal/mol and 1.30 kcal/mol, respectively. Thus, QM/EFP total interaction energies are on average slightly more accurate than the EFP interaction energies. The present implementation finalizes development of a general QM/EFP model and allows description of electronic structure of solutes embedded in heterogeneous environments.

3. APPLICATION OF PARAMETRIZED EXCHANGE-REPULSION TO AMINO ACIDS

3.1 Motivation

The work done in Chapter 2 and reported in Ref. [80] presents a computationally efficient yet accurate way to incorporate exchange-repulsion in the coupling term of the QM/EFP Hamiltonian. Nonetheless, the method developed and the parameters identified were only applied to simple molecular dimers. While it is important to accurately describe these dimers, they are not representative of the systems typically modeled with hybrid methods. The benefits of QM/MM and QM/EFP methods mainly manifest when modeling complex systems, such as solvated chromophores, polymers or proteins [48,81,82]. These types of systems can be challenging to model, particularly if computationally expensive terms like exchange-repulsion cannot be neglected. Hence, it is in these types of systems where using a parametrized version of exchange-repulsion could have a large impact by producing accurate results at a low computational cost.

In order to determine whether the parametrized version of QM/EFP exchange-repulsion can be successfully applied to these complex systems, it is first necessary to evaluate its performance in amino acid dimers. The main reason for this requirement is that no amino acids were considered during the parametrization of exchange-repulsion; that includes the identification of the parameters as well as their testing. To fill this gap, here we study two types of amino acid dimers, classified as polar-polar and aryl-aryl. Analogous to the evaluations done in Chapter 2, the QM/EFP interaction energies for the dimers were directly compared to the interaction energies computed with SAPT and EFP.

3.2 Methods

3.2.1 Dimers

The amino acid dimers studied in this work fell into one of two categories: polar-polar or aryl-aryl. The first category contained 194 dimers, while the second contained 120. The polar-polar dimers consisted of one or two of the following amino acids: asparagine, glutamine, serine, and threonine. Similarly, the aryl-aryl dimers consisted of one or two of the following amino acids: histidine, phenylalanine, tryptophan, and tyrosine. These amino acids are shown in Fig. 3.1.

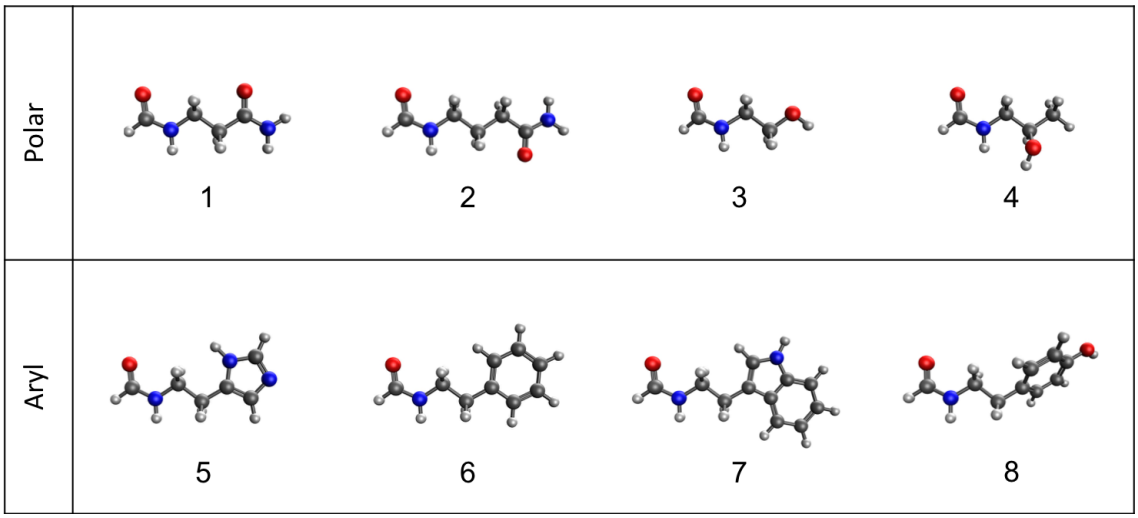

Fig. 3.1. Polar and aryl amino acid fragments considered in this work. Polar: (1) asparagine, (2) glutamine, (3) serine, (4) threonine. Aryl: (5) histidine, (6) phenylalanine, (7) tyrptophan, (8) tyrosine.

3.2.2 Computational Details

The dimers were obtained from 25 snapshots of a molecular dynamics simulation ran on Cry1At protein. From all the amino acid dimers present in the system, we only consider the ones for which the centers of mass were less than 5Å apart. The process of extracting these dimers was done by Yongbin Kim and can be found in

detail in Ref. [83]. Also in his work, Kim describes the procedure followed to compute the EFP potentials used for the EFP and QM/EFP calculations. For a single amino acid fragment, this procedure is as follows: first the molecule was optimized at the wB97XD/6-31G* level of theory. Then, the EFP potential was calculated for the optimized geometry in GAMESS [23, 24]. Each potential was created with a combination of basis sets: 6-31G(d) for electrostatics and 6-311++G(3df,2p) for all other components [64–70]. Unlike the potentials calculated for the parametrization of exhcange-repulsion in Chapter 2, these potentials were computed using the Boys localization scheme [78].

The QM/EFP and EFP/EFP calculations were also run in GAMESS. For the QM/EFP calculations, the QM region was modeled using Hartree Fock with a Dunning/Hay double zeta basis set with one polarization function for hydrogen atoms (p-type) and one polarization function for heavy atoms (d-type) [59]. The number of QM/EFP calculations was doubled for each category so that the QM region could be represented by either amino acid fragment. For the EFP/EFP calculations, damping functions were added to the electrostatics, polarization and dispersion terms. For electrostatics and dispersion an overlap based damping correction was employed, while for polarization the damping consisted of a Tang-Toennis style Gaussian formula. Details on EFP damping functions can be found in Refs. [5,18], as well as the GAMESS manual [23, 24]. Lastly, the reference sSAPT0 [60, 61, 84] energies were obtained by Yonbgin Kim using Psi4 [63,85]. These calculations were done with the jun-cc-pVDZ basis set [62, 86].

The QM/EFP errors were computed as the difference between the QM/EFP interaction energy and the SAPT energy. With this formula a negative error implies the QM/EFP interaction energy is too attractive, while a positive error indicates the interaction is too repulsive. The same formula was used to compute the EFP/EFP erros.

3.2.3 Assignment of Exchange-Repulsion Parameters

With the parameters available from Chapter 2 (or Ref. [80]), the peptide group in amino acids could be described in two ways, differing on how the CN bond is treated: a double bond or a single bond with a lone pair of electrons on the nitrogen atom. An example showing how the LMOs of peptide groups might differ is given in Fig. 1.3. This also applies to the primary amide in asparagine and glutamine.

Table 3.1.
Summary of methods used to assign QM/EFP exchange-repulsion parameters to LMOs in polar amino acids.

Method	Description
Distance	Parameters assigned based on distance cutoff (1.058 Å)
LP	All amides represented with a CN single bond and a lone pair on N
DB	All amides represented with a CN double bond
LP&DB	Peptide bond represented using LP, primary amide using DB
DB&LP	Peptide bond represented using DB, primary amide using LP

In order to identify the best set of QM/EFP exchange-repulsion parameters for the amino acids, three main methods were tested. The first method was fully automated and consisted of assigning parameters to each LMO based on the distance to the nearest two atoms. An LMO was considered to represent a lone pair of electrons if only one atom was found within 1.058 Å, while the LMO was considered to represent a bond if two atoms were within that threshold. If two LMOs shared the nearest two atoms, then they were classified as a double bond. The second method consisted of describing every amide (including the peptide group) as a single CN bond with a lone pair (sp^3) on the nitrogen. The third method consisted of describing every amide as a CN double bond without a lone pair on the nitrogen. Since asparagine and glutamine contain two amides, combinations of the last two methods were also considered for these systems. The final five methods used to assign the parameters for each amino

acid are described in Table 3.1. Note that since serine, threonine and all the aryl amino acids do not have an amide other than the peptide bond, the LP and LP&DB methods result in the same assignment of parameters. This is also true for DB and DB&LP methods.

The aromatic groups in the aryl-aryl dimers were all described with the aromatic parameters from Chapter 2. However, since no aromatic parameters for the C-N bond were identified in that work, the CN bond in the aromatic ring of histidine was described as a regular CN double bond with a lone pair of electrons on the sp^2 hybridized nitrogen.

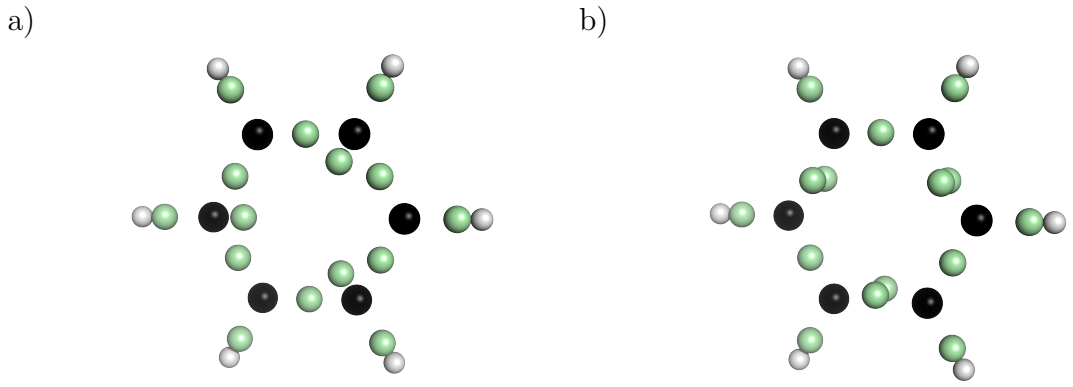

Fig. 3.2. Difference in position of LMOs (shown in green circles) for a) Ruedenberg and b) Boys localization schemes

It is also important to clarify that the use of Boys [78] localization scheme instead of Edmiston-Ruedenberg localization scheme [79] altered the location of the LMOs in the aromatic rings. As shown in Fig. 3.2, the Edmiston-Ruedenberg scheme places a single LMO between each pair of carbon atoms on the ring. In Chapter 2 these six LMOs correspond to aromatic CC single bonds. The remaining three LMOs are located on three alternating carbon atoms and correspond to the aromatic CC double bonds. The LMOs from the Boys scheme resemble more a Lewis structure, with three alternating LMOs representing three single bonds and six LMOs in alternating pairs

representing three double bonds. Since the number of LMOs remains constant and only their location changes, for the present QM/EFP calculations the parameters were switch. In other words, the double bond LMOs were described with the parameters for aromatic CC single bonds and the single bond LMOs were described as aromatic CC double bonds.

3.3 Results

3.3.1 Polar-Polar Dimers

a) b)

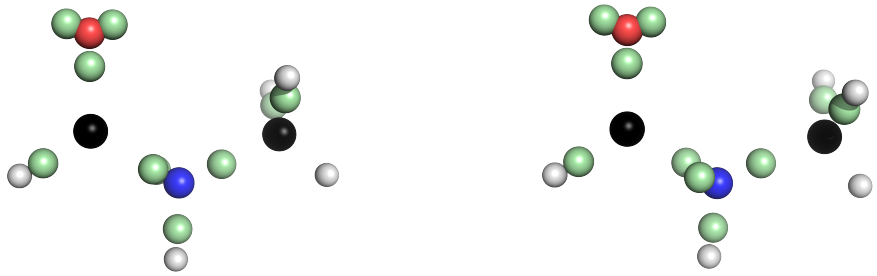

Fig. 3.3. Example of serine peptide bond for two different geometries: a) seems to be best described using a CN double bond b) resembles a single CN bond with a lone pair of electrons on the nitrogen

The reason for testing the methods summarized in Table 3.1 has to do with the conjugation present in amides. Due to this conjugation the best description for the peptide bond is uncertain. Consider for instance the peptide bond depicted in Fig. 3.3a. The QM/EFP energy for the dimer containing this bond in the effective fragment has an error of 4.5805 kcal/mol when calculated using the LP method and an error of 3.2074 kcal/mol when calculated with the DB method instead. Similarly the interaction energy for the dimer containing the segment shown in Fig. 3.3b has an error of -0.6917 kcal/mol for the DB method but shifts to 0.1827 kcal/mol for the LP

method. The reference energies for these dimers can be found in Appendix B. The first dimer corresponds to GLN(057) and SER(060) and was extracted from snapshot number 4. The second dimer corresponds to SER(224) and SER(274) and was extracted from snapshot number 21. These examples raise the question of whether a single set of exchange-repulsion parameters can be applied to all peptide bonds.

Table 3.2 shows the mean absolute errors (MAE), mean signed error (MSE) and standard deviation for the five methods tested. The values seem very similar across methods, although the DB&LP method appears to be the best option when trying to minimize all statistics simultaneously. This method implies the optimal way to describe the peptide bond is using the parameters for a CN double bond. Such representation produces total interaction energies that are less repulsive compared to the LP representation. However, using a double bond to additionally describe the primary amides in asparagine and glutamine (DB method) shifts the mean signed error to the negative side. In other words, the interactions become too attractive. Chemically, it makes sense for primary amides to require more repulsive parameters since their nitrogen is less shielded by other atoms.

Table 3.2.
Mean absolute errors (MAE), mean signed error (MSE) and standard deviations in kcal/mol for total interaction energies of polar-polar dimers.

Method	MAE (kcal/mol)	MSE (kcal/mol)	St. Dev. (kcal/mol)
Distance	0.5727	0.1395	0.9624
LP	0.5833	0.1746	0.9633
DB	0.5360	-0.0774	0.9525
LP&DB	0.5684	0.0526	0.9995
DB&LP	0.5340	0.0446	0.9109

All of the statistics reported in Table 3.2 are lower than the corresponding values for EFP interaction energies. These have an absolute mean error of 0.7933 kcal/mol,

a mean signed error of 0.5314 kcal/mol, and a standard deviation of 1.4663 kcal/mol. For comparison, Fig. 3.4 shows the QM/EFP, EFP and SAPT energies computed for all the polar-polar dimers. The QM/EFP energies were obtained after using the DB&LP method to assign the exchange-repulsion parameters. Unless otherwise specified, this is in fact true for all QM/EFP energies discussed in this section.

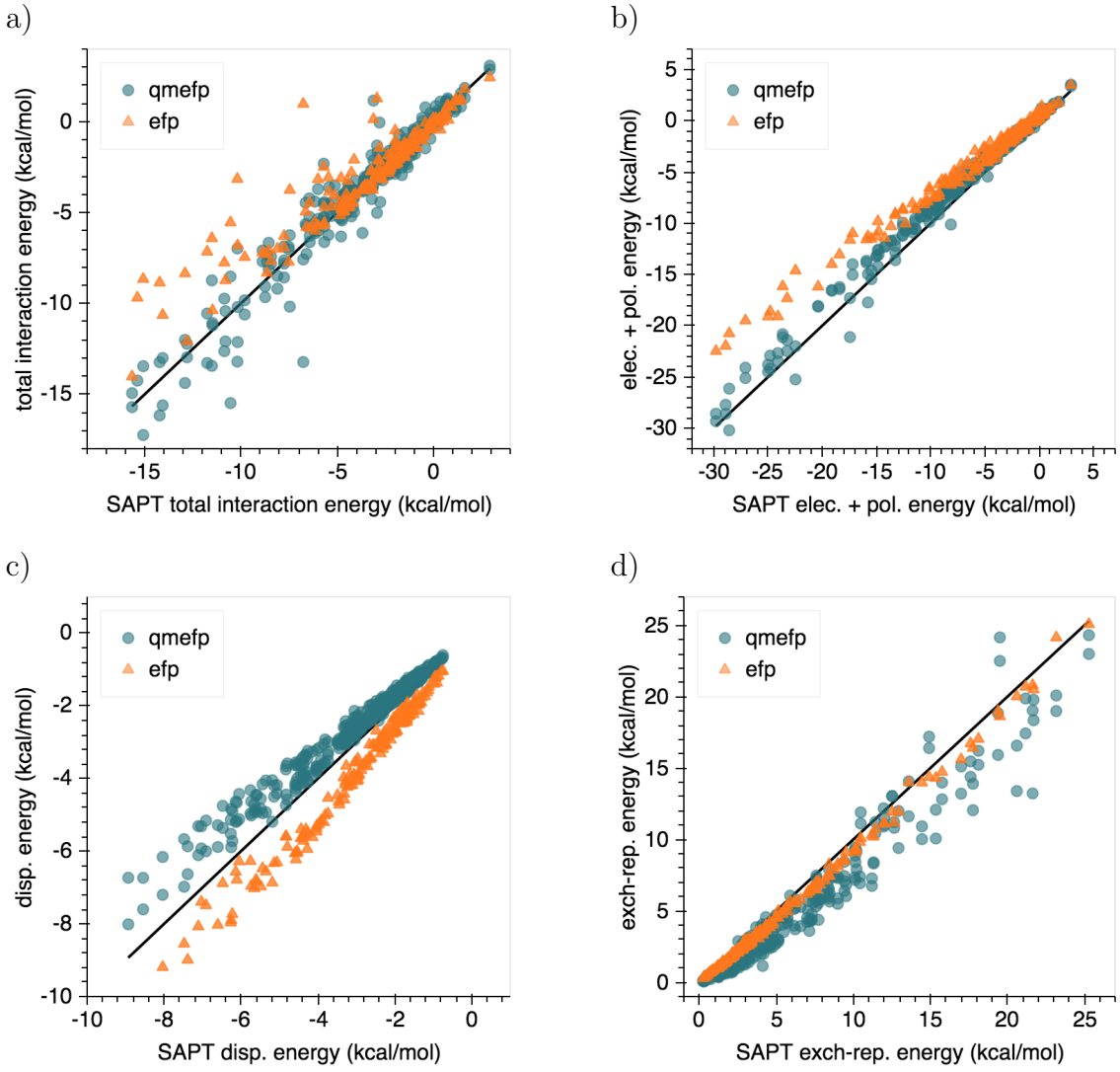

Fig. 3.4. Comparison of interaction energies in polar-polar dimers: a) total interaction energy, b) electrostatics and polarization energy, c) dispersion energy, and d) exchange-repulsion energy. QM/EFP exchange-repulsion parameters were assigned using the DB&LP method.

The plots from Fig. 3.4 show that EFP tends to underestimate the total interaction energies compared to SAPT, that is, the energies are too repulsive. The QM/EFP energies are in good agreement with SAPT, with the exception of a few points in which the total interaction energy is too strong. Looking at the separate components we see that QM/EFP performs very well for electrostatics and polarization, but dispersion and exchange-repulsion energies are both too small in magnitude.

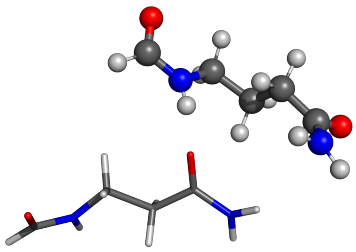

Fig. 3.5. Polar-polar dimer with largest QM/EFP total interaction energy error.

Fig. 3.5 depicts the polar-polar dimer with the largest QM/EFP error for the total interaction energy. The effective fragment in this dimer corresponds to the asparagine amino acid, represented with lines in Fig. 3.5. The figure clearly reveals a hydrogen bond taking place between the peptide bond in the QM region and the primary amide on the EFP fragment. Table 3.3 provides the explicit energy values computed with QM/EFP, EFP, and SAPT. From the table, we see that QM/EFP overestimates the total interaction energy. Most of the error comes from exchange-repulsion not being repulsive enough. Trying to increase the repulsion by modeling the peptide bond in asparagine with a CN single bond and nitrogen lone pair does not improve the error. However, when the QM and EFP regions are flipped and the parameters from the DB&LP method are used, the total interaction energy decreases to -7.5846 kcal/mol.

Interestingly, this shift in the total interaction energy is not solely due to exchange-repulsion. In fact, the value of exchange-repulsion increases only by approximately 1 kcal/mol. Most of the change in the total interaction energy of the flipped system is due to a less attractive electrostatics and polarization energy.

When the energy for the dimer shown in Fig. 3.5 is computed with EFP, we observe that the interaction energy is no longer overestimated. Instead, EFP predicts the total interaction energy to be 0.9768 kcal/mol, which results in an absolute error of 7.7404 kcal/mol. For this method, most of the contribution to the error comes from electrostatics and polarization not being strong enough with a difference of almost 8 kcal/mol when compared to SAPT.

Table 3.3.
QM/EFP, EFP and SAPT energy decomposition for polar-polar dimer with largest total interaction energy error. QM/EFP exchange-repulsion parameters were assigned using the DB&LP method. All energies are given in kcal/mol. *refers to system with exchanged QM and EFP regions.

Interaction Type	QM/EFP	EFP	SAPT	QM/EFP*
Total	-13.2297	0.9768	-6.7636	-7.5846
Elec. and Pol.	-25.2485	-14.6229	-22.4630	-22.0056
Dispersion	-6.9780	-8.5480	-7.4787	-5.6672
Exch.-Rep.	18.9967	24.1477	23.1781	20.0881

The polar-polar dimer with the largest exchange-repulsion energy error is shown in Fig. 3.6 and the energies are given in Table 3.4. The dimer is composed of two glutamine amino acid molecules. The error for the QM/EFP total interaction energy is -4.9455 kcal/mol. As expected, most of the error comes from exchange-repulsion being underestimated. The error for this particular component is -8.4151 kcal/mol. While using the LP method to describe the glutamine fragment would increase the exchange-repulsion, the change would be less than 0.15 kcal/mol and hence negligible. However, sticking to the DB&LP method and flipping the QM and

EFP regions largely reduces the total interaction error, which shifts to a positive value of 2.0218 kcal/mol. The difference is due mainly to a better approximation of exchange-repulsion but also the other terms becoming slightly more repulsive.

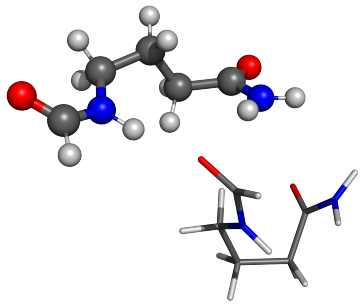

Fig. 3.6. Polar-polar dimer with largest QM/EFP exchange-repulsion energy error.

Table 3.4.
QM/EFP, EFP and SAPT energy decomposition for polar-polar dimer with largest exchange-repulsion energy error. QM/EFP exchange-repulsion parameters were assigned using the DB&LP method. All energies are given in kcal/mol. *refers to system with exchanged QM and EFP regions.

Interaction Type	QM/EFP	EFP	SAPT	QM/EFP*
Total	-15.4899	-5.5476	-10.5444	-8.5226
Elec. and Pol.	-21.1178	-16.1613	-23.6436	-20.8278
Dispersion	-7.6011	-10.2033	-8.5449	-6.7337
Exch.-Rep.	13.2290	20.8169	21.6441	19.0387

The EFP total interaction energy error for the dimer shown in Fig. 3.6 is 4.9968 kcal/mol. While this method better approximates the exchange-repulsion energy,

with an error below 1 kcal/mol, it fails to reproduce the electrostatics and polarization energies. EFP underestimated these combined components by 7.4823 kcal/mol.

3.3.2 Aryl-Aryl Dimers

The QM/EFP exchange-repulsion parameters for the peptide bond in the aryl effective fragments were assigned using the distance, LP and DB methods (not LP&DB or DB&LP since there are no other amides). Table 3.5 summarizes the resulting statistics. Although again we see similar performance across methods, the mean absolute error and mean signed error are minimized with the DB method. This outcome concurs with the results from the polar-polar dimers, suggesting the best way to represent the peptide bond is using a CN double bond. For this reason and unless otherwise specified, the QM/EFP energies discussed in this section were computed after assigning the exchange-repulsion parameters with the DB method. While this method results in highly repulsive energies, the statistics evidence a slight improvement over EFP energies. The EFP total interaction energies have a mean absolute error of 1.8562 kcal/mol, a mean signed error of 1.8455 kcal/mol and a standard deviation of 1.3272 kcal/mol.

Table 3.5.
Mean absolute errors (MAE), mean signed error (MSE) and standard deviations in kcal/mol for total interaction energies of aryl-aryl dimers.

Method	MAE (kcal/mol)	MSE (kcal/mol)	St. Dev. (kcal/mol)
Distance	1.7826	1.6231	1.3691
LP	1.7755	1.7023	1.2284
DB	1.7279	1.5632	1.3588

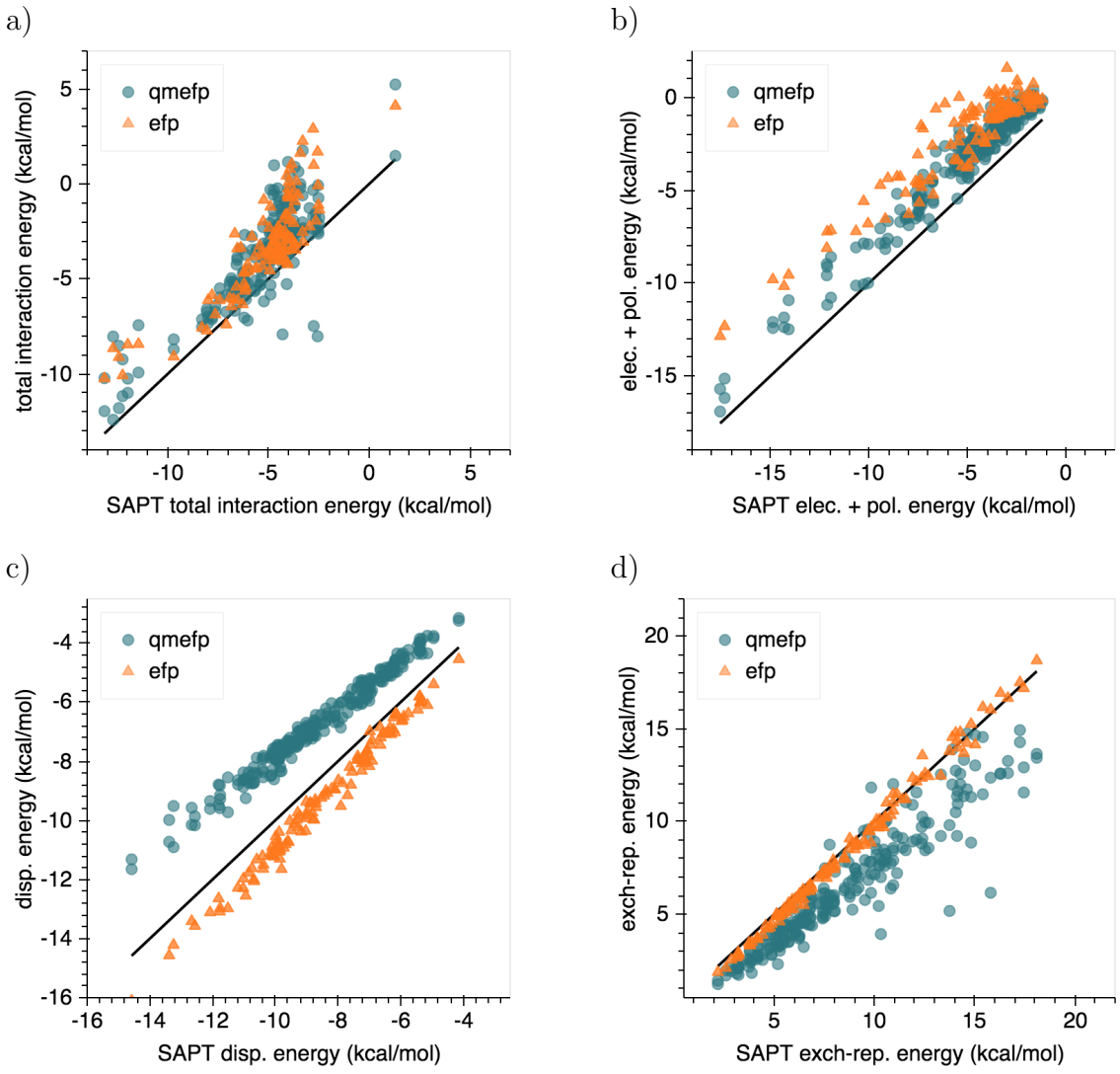

Fig. 3.7. Comparison of interaction energies in aryl-aryl dimers: a) total interaction energy, b) electrostatics and polarization energy, c) dispersion energy, and d) exchange-repulsion energy. QM/EFP exchange-repulsion parameters were assigned using the DB method.

Fig. 3.7 shows the energy decomposition for the aryl-aryl dimers. These results suggest most of the dimers have a total interaction energy between -3.5 and -6.0 kcal/mol according to SAPT. Both QM/EFP and EFP highly underestimate these energies, even resulting in positive values for a few dimers. A possible cause for such weak interaction energies might be the underestimation of the electrostatics

and polarization components, shown in Fig. 3.7a. QM/EFP seems to additionally underestimate the dispersion and the exchange-repulsion energies. Overall, these results agree well with the ones from Chapter 2, which show that for aromatic systems, the QM/EFP total interaction energy remains too repulsive despite the QM/EFP exchange-repulsion being lower than the SAPT exchange-repulsion.

Fig. 3.8 shows the aryl-aryl dimer for which the QM/EFP total interaction energy error is the largest. In this system the QM region corresponds to the phenylalanine amino acid and the effective fragment to the tryptophan. Table 3.6 shows the QM/EFP and SAPT interaction energies for this geometry. Interestingly, this is one of the few cases for which exchange-repulsion is overestimated. This fact, along with weak electrostatics, polarization and dispersion energies leads to a positive total interaction energy. This value is larger than the SAPT interaction energy by 5.705 kcal/mol. Switching the QM and EFP regions reduces the error by more than half. The total interaction energy for the flipped system is -2.511 kcal/mol. Most of the change comes from a decrease in exchange-repulsion, which goes from being overestimated by almost 2 kcal/mol to being underestimated by the same amount, specifically 1.9381 kcal/mol.

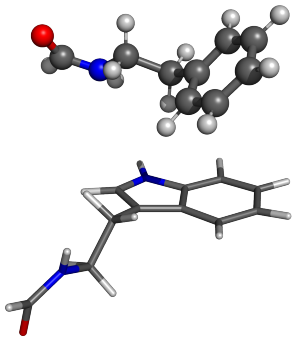

Fig. 3.8. Aryl-aryl dimer with largest QM/EFP total interaction energy error.

Table 3.6.
QM/EFP, EFP and SAPT energy decomposition for aryl-aryl dimer with larges total interaction energy error. QM/EFP exchange-repulsion parameters were assigned using the DB method. All energies are given in kcal/mol. *refers to system with exchanged QM and EFP regions.

Interaction Type	QM/EFP	EFP	SAPT	QM/EFP*
Total	0.9846	-2.9865	-4.7206	-2.5892
Elec. and Pol.	-1.5951	-0.1206	-3.6240	-1.8511
Dispersion	-9.2477	-12.5507	-10.9390	-8.5650
Exch.-Rep.	11.8274	9.6849	9.8424	7.8269

Table 3.6 also indicates that EFP performs better for the system shown in Fig. 3.8. The total interaction energy error for this method is only 1.7341 kcal/mol. The exchange-repulsion term is very well approximated by EFP and does not contribute to the error. Instead, most of the error derives from electrostatics and polarization being underestimated.

The aryl-aryl dimer with the largest exchange-repulsion energy error is depicted in Fig. 3.9. The dimer corresponds to a histidine amino acid in the QM region interacting with a tyrosine amino acid in the EFP region. All the energy components for the complex are provided in Table 3.7. The total interaction energy error for this dimer is -5.4649 kcal/mol and the exchange-repulsion error is -9.6402 kcal/mol. As expected, switching the QM region with the EFP region in this case also reduces the two errors by a significant amount. In the flipped system, the total and exchange-repulsion energy errors become 0.2215 kcal/mol and -3.4355 kcal/mol respectively.

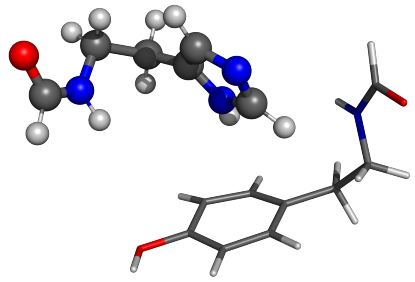

Fig. 3.9. Aryl-aryl dimer with largest QM/EFP exchange-repulsion interaction energy error.

Computing the energy of the original dimer from Fig. 3.9 with EFP results in a positive total interaction energy. However, the magnitude of this error, 4.2532 kcal/mol, is smaller than that of QM/EFP. As expected from the plots shown in Fig. 3.7, while EFP approximates all other components fairly well, it underestimates the electrostatics and polarization energy.

Table 3.7.
QM/EFP and SAPT comparison of interaction energies for aryl-aryl dimer with larges exchange-repulsion energy error. QM/EFP exchange-repulsion parameters were assigned using the DB method. All energies are given in kcal/mol. *refers to system with exchanged QM and EFP regions.

Interaction Type	QM/EFP	EFP	SAPT	QM/EFP*
Total	-8.0248	1.6933	-2.5599	-2.3384
Elec. and Pol.	-6.6701	-4.3613	-9.0470	-7.6155
Dispersion	-7.5082	-9.9718	-9.3066	-7.0810
Exch.-Rep.	6.1535	16.0264	15.7937	12.3582

3.4 Conclusions

This work examined the different ways in which the interaction energy of amino acid dimers can be described using QM/EFP with parametrized exchange-repulsion. In order to identify the optimal exchange-repulsion parameters for the peptide bond, a total of five methods were tested. Although all the methods performed similarly, representing the CN bond in the peptide group as a double bond minimizes the mean absolute error and mean signed error in polar-polar and aryl-aryl dimers. Additionally, the primary amides in glutamine and asparagine seem to be best describe as single CN bond with a lone pair of electrons on the nitrogen.

Overall, QM/EFP tends to underestimate the exchange-repulsion energies. Despite this underestimation, the QM/EFP total interaction energies of polar-polar dimers approach those computed by SAPT. On the other hand, the total interaction energies of aryl-aryl dimers are largely underestimated by QM/EFP. However, due to the low values of exchange-repulsion, the positive errors for these dimers presumably derive from weak electrostatics, polarization and dispersion energies.

4. BENCHMARK STUDY OF QM/EFP SINGLET EXCITATION ENERGIES

4.1 Motivation

It has been extensively shown that polarizable embedding is essential for predicting accurate electronic and redox properties of chromophores in solvents and biological environments [87–90]. However, it is expected that by incorporating short-range terms, the polarizable embedding can be improved. Multiple methodologies have been developed with this aim in mind. Such methodologies include the parametrization of exchange-repulsion discussed in Chapter 2 (and Ref. [80]). Additionally, the dispersion term in QM/EFP was recently developed [51] as well as a charge-penetration correction for the electrostatics term [2, 16]. Despite these developments, the polarizable embedding remains the most popular descriptor of non-covalent interactions between the QM region and the effective fragments in QM/EFP. The reason behind this originates from the limited work dedicated to evaluating the performance of these additional terms. This benchmark study aims to serve as a guide for identifying the best embedding scheme for QM/EFP excitation energy calculations done on common chromophores surrounded by small clusters of solvents. In this benchmark three different QM/EFP embedding schemes are compared to the polariable embedding. All schemes are build from the polarizable embedding with added exchange-repulsion and/or a charge-penetration correction.

4.2 Methods

4.2.1 Theory

The QM/EFP schemes considered in this study are built upon the polarizable embedding by adding two terms: a charge-penetration correction for the electrostatics term and a paramterized version of exchange-repulsion. The charge-penetration correction is an electrostatics screening achieved by Gaussian smearing of the charges on the effective fragments. With this modification, the electrostatics potential of Eq. 1.12 becomes [16]:

$$\begin{aligned}\hat{V}_k^{coul} = [q_k^{nuc} + q_k^{elect}(1 - exp(-\gamma_k r_k^2))]T(r_k) - \sum_a^{x,y,z} \mu_a^k T_a(r_k) \\ + \frac{1}{3}\sum_{a,b}^{x,y,z} \Theta_{a,b}^k T_{a,b}(r_k) - \frac{1}{15}\sum_{a,b}^{x,y,z} \Omega_{a,b,c}^k T_{a,b,c}(r_k)\end{aligned} \tag{4.1}$$

where q_k^{nuc} and q_k^{elec} are the nuclear and electronic components of the net charge q_k on a fragment's expansion point k, and γ_k is the charge-penetration parameter at point k obtained during the parameters-determining step by a fit of the screened multipole potential to the Hartree-Fock potential around the fragment [16–18]. The goal of the charge-penetration screening is to improve the accuracy of the electrostatics interactions at close separations between the QM and EFP regions.

The exchange-repulsion term employed corresponds to the paramterzied version explained in Chapter 2, where the repulsive interaction between the QM region and the effective fragments is modeled using Gaussian functions positioned at the centroids of the localized molecular orbitals of each fragment. This fitted QM/EFP exchange-repulsion term is similar but more simplistic than atomic all-electron pseudopotentials introduced in Ref. [91] and electrostatic repulsive potentials from Ref. [92]. Alternatively, Pauli repulsion can be accounted for using overlap or exchange integrals between solute and solvent densities, which was explored in the context of polarizable density embedding (PDE) and QM/MM models [93–97].

With these two terms, a total of four embedding schemes were built (Table 4.1). These include the basic polarizable embedding scheme (PE), the polarizable embedding with inclusion of charge-penetration screening (PE+S), the scheme with added exchange-repulsion term (PE+XR), and the scheme with both exchange-repulsion and charge-penetration contributions (PE+SXR).

Table 4.1.
QM/EFP embedding schemes.

Label	Description	QM/EFP Hamiltonian
PE	Polarizable Embedding	$\left\langle p \left\vert \hat{V}^{coul} + \hat{V}^{pol} \right\vert q \right\rangle p^{\dagger} q$
PE+S	PE + charge-penetration screen	$\left\langle p \left\vert \hat{V}^{coul}_{chpen} + \hat{V}^{pol} \right\vert q \right\rangle p^{\dagger} q$
PE+XR	PE + exchange-repulsion	$\left\langle p \left\vert \hat{V}^{coul} + \hat{V}^{pol} + \hat{V}^{xr} \right\vert q \right\rangle p^{\dagger} q$
PE+SXR	PE + charge-penetration screen + exchange-repulsion	$\left\langle p \left\vert \hat{V}^{coul}_{chpen} + \hat{V}^{pol} + \hat{V}^{xr} \right\vert q \right\rangle p^{\dagger} q$

4.2.2 Computational Details

A total of 37 neutral molecular systems were considered for this benchmark study. Each system consisted of one of the chromophores shown in Fig. 4.1 surrounded by molecules of water, ammonia, methanol or formic acid. The starting optimized structures were obtained from Ref. [98].

All excitation energies were computed in the GAMESS quantum chemistry package [23,24]. The following six calculations were performed on each system: (i) CIS/cc-pVDZ calculation on the gas-phase chromophore, (ii) CIS/cc-pVDZ calculation on

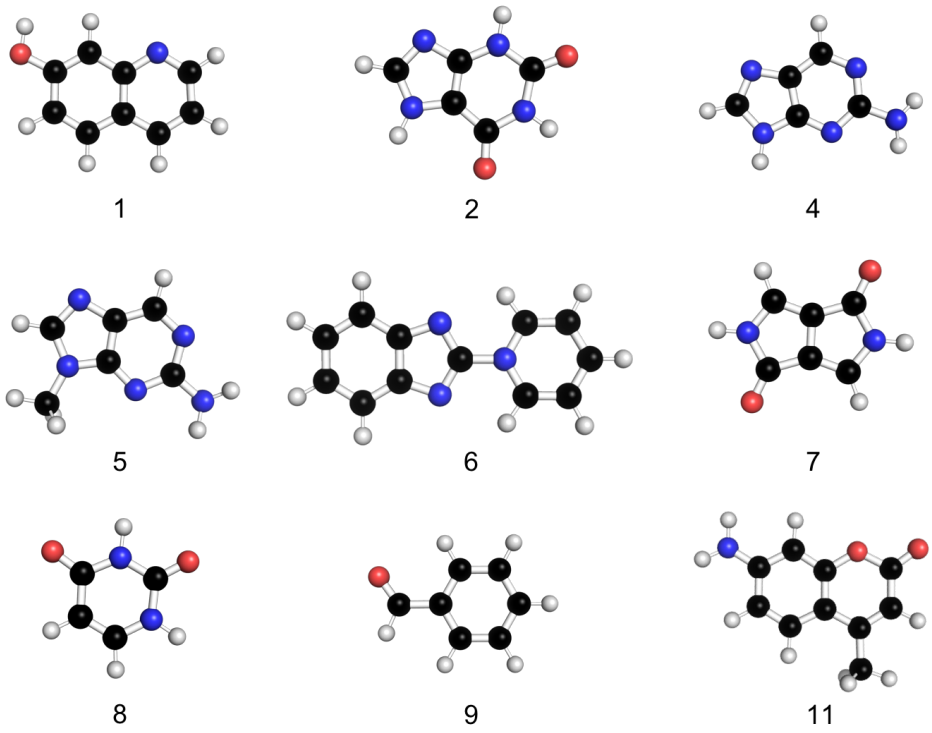

Fig. 4.1. Chromophores studied in this work, borrowed from the work of Zech et al. [98] :(1) 7-hydroxyquinoline, (2) xanthine, (4) 2-aminopurine, (5) 7-methyl-2-aminopurine, (6) pyridiniumyl benzimidazolide, (7) diketopyrrolopyrrole, (8) uracil, (9) benzaldehyde, (11) 7-amino-4-methylcoumarin.

the full system, (iii)-(vi) QM/EFP calculations corresponding to schemes described in Table 4.1. In all QM/EFP calculations, the QM region consisted only of the chromophore and was also modeled at the CIS/cc-pVDZ level of theory. Each solvent molecule was represented by an effective fragment. In this work, the EFP potentials and the parameters for the QM/EFP exchange-repulsion term from Chapter 2 were used. From each single-point energy calculation, we obtained the lowest 15 excitation energies. To match the QM/EFP excitations to the full-system excitations we considered: 1) the molecular orbitals corresponding to the leading transition, 2) the magnitude of the oscillator strength, and 3) the magnitude of the largest transition

dipole component. The first criterion was satisfied if both transitions involved the same orbitals, which were matched visually and based on the scalar product of the orbital expansion coefficients. The second and third criteria were applied only to transitions with oscillator strengths larger than 0.1. The second criterion was satisfied if the difference between the oscillator strengths for the excitations was less than 25%. The same threshold was applied to the third criterion, which looked at the difference between the largest components of the two transition dipole moments.

To evaluate the performance of each scheme, we computed excitation energy errors as:

$$E_{error} = E_{QM/EFP} - E_{full\_QM} \tag{4.2}$$

where, for a particular electronic transition, E_{full_QM} is the corresponding CIS excitation energy for the full system. We then compared the error distribution across schemes. For the best two schemes, we also compared the mean absolute error (MAE) for different transition types and examined the dependence of the errors on solvatochromic shifts E_{shift}, defined as:

$$E_{shift} = E_{full\_QM} - E_{gas} \tag{4.3}$$

where E_{gas} is an excitation energy in the gas-phase (isolated) chromophore. The statistics were also computed considering only the five lowest excited states of each molecular system.

The electronic excitations were classified as $\pi\pi^*$ or $n\pi^*$ based on the molecular orbitals corresponding to the leading transition. Additionally, the excitations were characterized based on whether or not they involved charge transfer to or from the solvent. For this purpose, additional CIS calculations that involved analysis of charge distribution and natural transition orbital [99] (NTO) pairs were performed on each full system in the Q-Chem electronic structure software [100]. A transition was considered to have a charge transfer character if, according to the Mülliken population analysis, over 0.01 of the hole or electron charge was located on the solvent.

For a small subsample consisting of 25 out of the 38 geometries, the lowest five excitations energies were also calculated with the aug-cc-pVDZ basis set in the quantum mechanical region. These calculations were done only with the PE and PE+XR schemes, in addition to CIS. For the QM/EFP calculations, the EFP potential remained unchanged. The analysis followed the steps described for the cc-pVDZ calculations, the only difference concerns the matching of the orbitals, which in this case were matched only visually.

4.3 Results

The error distributions for each QM/EFP scheme with respect to fully quantum calculations are shown in Fig. 4.2. This figure shows data including up to 15 excited states for each system. Positive errors mean that QM/EFP excitation energies are overestimated (shifted toward blue). On average, the basic PE scheme tends to overestimate excitation energies, with a mean absolute error (MAE) of 0.035 eV and a mean signed error of 0.024 eV. Fig. 4.2 shows that adding the charge-penetration correction to the electrostatics term (PE+S) results in a broader error distribution skewed to the blue region. In other words, the excitation energies for this scheme are overestimated by a larger amount when compared to the original PE scheme. However, the main drawback of the PE+S scheme is the number of missing excitations. Out of the considered 387 full-system excitations, 89 could not be matched to any excitation computed with PE+S scheme. This could be consequent of significant changes in the energies and ordering of the QM orbitals upon smearing of the electronic charges on the fragments. Generally speaking, Gaussian smearing results in a more favorable (energetically lowering) interaction of the electronic wave function with fragment charges. That is, the QM density tends to penetrate more into the space of the fragments. In the case of fragment-fragment interactions, charge-penetration correction leads to an increase of electrostatic component (making the Coulomb energy more stabilizing) and a significant improvement of the multipole-based description

of electrostatic energies [17]. This was expected to be the case for the QM/EFP interactions as well [16]. However, as revealed in the present benchmark, in general, the charge-penetration correction does not improve the description of the excitation energies and solvatochromic shifts. On the contrary, the charge smearing produces a destabilizing effect on the electronic excitations and is not recommended for general use.

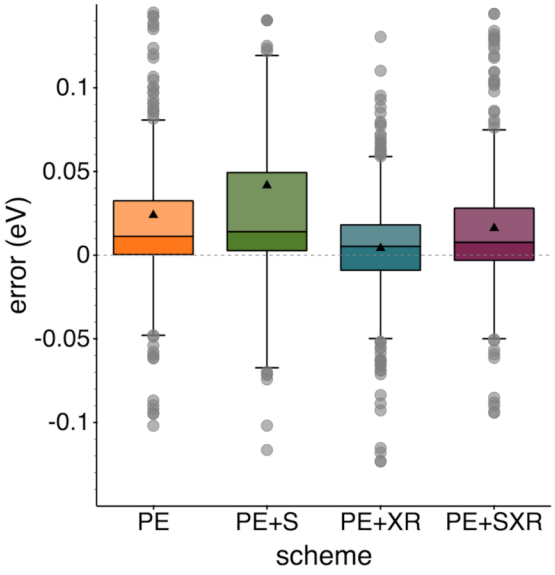

Fig. 4.2. Error distribution for each QM/EFP scheme. Not all outliers are shown. Each box contains 50% of the data, 25% below the median (opaque box) and 25% above it (semi-transparent box). The bottom whisker is computed as q1 – 1.5*IQR and the top as q3 + 1.5 IQR, where q1 is the first quartile, q3 the third quartile and interquartile range (IQR) is their difference. Black triangles represent the means for each scheme

As follows from Fig. 4.2, adding exchange-repulsion to the QM/EFP Hamiltonian clearly improves the description of the excitation energies. In the scheme with exchange-repulsion and charge-penetration correction (PE+SXR), the number of missing excitations is less than 20 and the error distribution is comparable to that of the PE scheme. However, adding only exchange-repulsion to the polarizable embedding (PE+XR) seems to give the best results. This combination noticeably improves

the accuracy of excitation energies, resulting in a narrow error distribution (0.034 eV standard deviation) and a mean near zero (0.004 eV). For comparison, the standard deviation and mean of the PE scheme are 0.052 eV and 0.024 eV respectively.

Table 4.2.
Mean absolute errors (MAE) in eV for all excitations, $\pi\pi^*$ excitation and $n\pi^*$ excitations.

Scheme	QM Basis Set	States	MSE	STD	MAE	$\pi\pi^*$ MAE	$n\pi^*$ MAE
PE	cc-pVDZ	1-15	0.024	0.052	0.035	0.018	0.069
PE+S	cc-pVDZ	1-15	0.042	0.086	0.052	0.020	0.110
PE+XR	cc-pVDZ	1-15	0.004	0.034	0.023	0.018	0.022
PE+SXR	cc-pVDZ	1-15	0.016	0.050	0.031	0.016	0.049
Gas	cc-pVDZ	1-15	-0.094	0.280	0.172	0.136	0.245
PE	cc-pVDZ	1-5	0.026	0.052	0.034	0.018	0.073
PE+S	cc-pVDZ	1-5	0.047	0.087	0.052	0.020	0.124
PE+XR	cc-pVDZ	1-5	0.001	0.025	0.017	0.018	0.016
PE+SXR	cc-pVDZ	1-5	0.016	0.038	0.024	0.015	0.047
Gas	cc-pVDZ	1-5	-0.106	0.268	0.184	0.126	0.298
PE	aug-cc-pVDZ	1-5	0.010	0.104	0.048	0.020	0.065
PE+XR	aug-cc-pVDZ	1-5	-0.024	0.065	0.032	0.021	0.013
Gas	aug-cc-pVDZ	1-5	-0.070	0.242	0.169	0.106	0.261

To better understand the effect of exchange-repulsion on the QM/EFP excitation energies, we separately analyzed errors for the $\pi\pi^*$ and $n\pi^*$ types of excitations. According to Table 4.2, the MAEs for the PE and PE+XR schemes are comparable for $\pi\pi^*$ transitions. However, for $n\pi^*$ transitions, the MAE for the PE scheme is larger than the MAE for PE+XR by approximately a factor of three. Indeed, we observe a significantly better performance of the PE+XR scheme in the case of excitations accompanied by partial charge transfer to or from the solvent. Note that while excita-

tions dominated by a charge transfer between solute and solvent are beyond the reach of most fragmentation and QM/MM models, the excitations with a small to medium amount of charge transfer are still tractable with QM/MM. Here, a transition was considered as possessing charge-transfer character if, in full quantum calculations, over 1% of the electron density corresponding to the hole or electron was located on the solvent, although the value rarely exceeded 10%. We found that less than 20% of the $\pi\pi^*$ excitations involve to/from solvent charge transfer, while the charge-transfer character is present in about 70% of the $n\pi^*$ excitations.

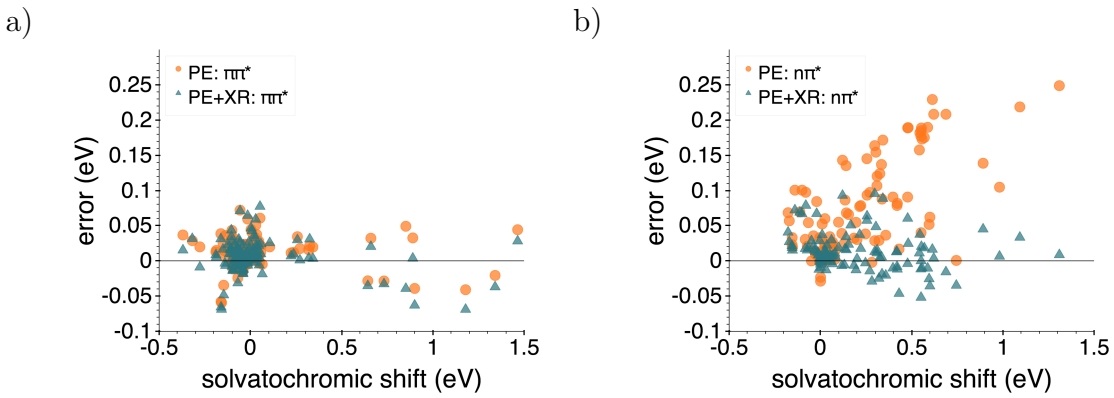

Fig. 4.3. PE and PE+XR errors for (a) $\pi\pi^*$ and (b) $n\pi^*$ excitations as a function of the solvatochromic shift.

Fig. 4.3 shows the overall dependence of PE and PE+XR errors on the values of the solvatochromic shifts for $\pi\pi^*$ and $n\pi^*$ excitations. In the case of $\pi\pi^*$ excitations, errors for both schemes are similar and do not depend on the values of the solvatochromic shifts, which are rather small for the majority of these excitations. On the other hand, PE and PE+XR schemes perform drastically differently for $n\pi^*$ excitations: while the errors of the PE scheme correlate with values of the solvatochromic shifts and become as large as 0.25 eV, the errors of the PE+XR scheme remain relatively constant and do not exceed 0.1 eV. In other words, the exchange-repulsion term significantly improves the description of charge-transfer-to/from-solvent states

with blue solvatochromic shifts. In fact, there is a correlation between the excitation energy errors and the amount of hole density on the solvent, although no such correlation exists for the transfer of the electron density as shown in Fig. 4.4.

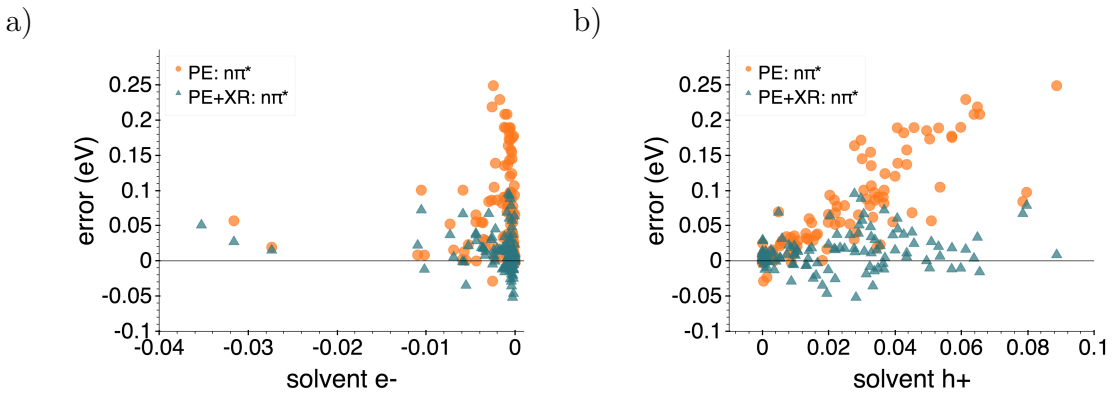

Fig. 4.4. Correlation between errors in solvatochromic shifts (in eV) and amount of electron density (left) and hole density (right) on a solute.

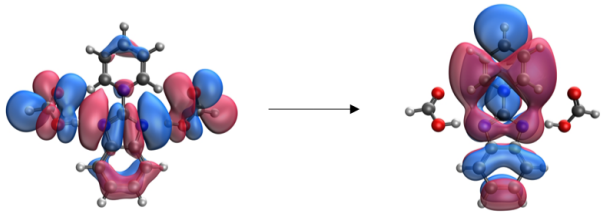

Fig. 4.5. Example of $n\pi^*$ transition involving charge transfer from solvent to solute. This transition is the leading transition in the 11th excited state of pyridiniumyl benzimidazolide (structure 6c in Appendix C).

An example of a solvent-to-solute charge-transfer $n\pi^*$ transition is shown in Fig. 4.5. This excitation corresponds to the data point with the largest error in the PE scheme (0.249 eV). PE+XR decreases the corresponding error to 0.009 eV. Generally, the PE+XR scheme improves the description of such excitations because the exchange-repulsion term destabilizes the electronic density on the solvent. That is, if

an occupied orbital in the fully quantum treatment contains electronic density both on a solute and solvent, it tends to be partially delocalized on the solvent in QM/EFP. However, the exchange-repulsion term prevents such density delocalization into solvent, effectively destabilizing this orbital and ultimately leading to a decrease in the excitation energy. Similar effect of decreasing excitation energies due to mixing of an occupied orbital of a solute with an occupied orbital of a solvent (so-called oo-mixing) was discussed in Ref. [101].

Detailed analysis of several excitations is provided in Table 4.3. Table 4.3 shows $\pi\pi^*$ and $n\pi^*$ transitions with red and blue solvatochromic shifts. As expected, adding the exchange-repulsion term increases the energy of the orbitals when compared to the PE scheme. Despite this shift, both schemes approximate the gap between occupied and virtual orbitals well, although the PE scheme tends to have a slightly larger gap in comparison to the PE+XR scheme. From Table 4.3, it seems that overestimation of the gap by the PE scheme leads to larger excitation energy errors. Additionally, for the PE scheme there is a correlation between the gap and the solvatochromic shift, that is, when the gap estimated by the PE scheme is larger, the corresponding solvatochromic shift is more positive. Unfortunately, no analogous relations can be drawn from comparing the PE+XR scheme and the fully quantum mechanical calculations.

The provided statistics and analysis include a large number of high-energy excited states. Now we switch to discussion of low-lying excited states. These data are shown in Table 4.2. When only the first five excited states are considered for each geometry, the mean absolute errors for the PE and the PE+XR schemes decrease from 0.035 and 0.023 to 0.034 and 0.017 eV respectively. No change was observed in the mean absolute error for the excitations categorized as $\pi\pi^*$, but interestingly, the mean absolute error for the $n\pi^{**}$ transitions increased to 0.073 eV in the PE scheme and decreased to 0.016 in the PE+XR scheme. The increase in the $n\pi^*$ MAE for the PE scheme derives from excluding a large number of high excitations with small absolute errors. However, this increase is not large enough to overcome the contribution of the $\pi\pi^*$ transitions to the overall mean absolute error.

Table 4.3.
Comparison of orbitals and solvatochromic shifts for fully quantum mechanical, PE and PE+XR calculations done using cc-pVDZ basis set. All energies are reported in units of eV. The CIS states are 2, 3, 3 and 2 for the geometries 7a, 1a, 1x and 6c in Appendix C.

Geo.	Scheme	Occupied Energy	Virtual Energy	Gap	Solv. Shift (error)	Occupied Orbital	Virtual Orbital
7a	Full QM	-10.705	0.857	11.562	-0.367		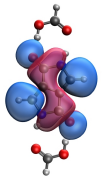
	PE	-10.585	1.009	11.595	-0.333 (0.037)		
	PE+XR	-10.406	1.157	11.562	-0.355 (0.015)		
1a	Full QM	-10.915	2.474	13.388	-0.005	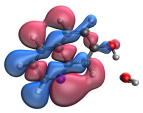	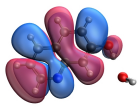
	PE	-10.895	2.493	13.388	-0.006 (-0.001)		
	PE+XR	-10.863	2.533	13.396	-0.001 (0.003)		
1x	Full QM	-11.676	1.733	13.410	0.688	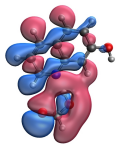	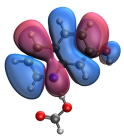
	PE	-12.221	1.772	13.992	0.896 (0.208)		
	PE+XR	-11.965	1.848	13.813	0.672 (-0.016)		
6c	Full QM	-7.823	0.512	8.335	0.900	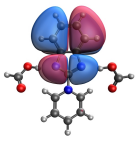	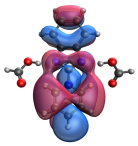
	PE	-7.750	0.539	8.289	0.861 (-0.039)		
	PE+XR	-7.644	0.673	8.280	0.837 (-0.063)		

Utilizing diffuse basis sets is often essential for computing excited state, since many excitations tend to be more delocalized than the ground state. The lowest section of Table 4.2 presents the statistics of calculations with aug-cc-pVDZ basis for the QM region. This data comprises 93 excitation energies (excitations above the fifth state were excluded). The mean absolute errors for the PE and PE+XR schemes with aug-cc-pVDZ basis set are 0.048 and 0.032 eV, respectively, but the values decrease to 0.031 and 0.019 when 30 excitations that involve transitions to Rydberg orbitals are also excluded. The MAEs for the $\pi\pi^*$ transitions are 0.020 and 0.021 eV for the PE and PE+XR schemes while the corresponding values for the $n\pi^*$ transitions are 0.065 and 0.013 eV. Table 4.4 compares PE and PE+XR schemes in cc-pVDZ and aug-cc-pVDZ bases for three characteristic $n\pi^*$ transitions. The same table demonstrates the transferability of the exchange-repulsion parameters to EFP potentials created with a different basis set.

Overall, the performance of QM/EFP models in cc-pVDZ and aug-cc-pVDZ bases is similar. In both basis sets, the PE scheme is reliable for $\pi\pi^*$ transitions but becomes less accurate for $n\pi^*$ transitions, for which the PE+XR scheme is more accurate.

Table 4.4.
Comparison of PE and PE+XR excitation energy errors done using different basis set on the QM region. For all correlated consistent basis set, the EFP parameters were computed using 6-31+G(d) for electrostatics and 6-311++G(3df,2p) for all other components. For the 6-31+G(d) calculations, the EFP parameters were computed with this same basis set. All excitations correspond to $n\pi^*$ dominated transitions.

Structure	cc-pVDZ PE error	cc-pVDZ PE+XR error	aug-cc-pVDZ PE error	aug-cc-pVDZ PE+XR error	6-31+G(d) PE error	6-31+G(d) PE+XR error
1b	0.1239	0.0044	0.1408	-0.0071	0.1305	-0.0157
1d	0.1729	-0.0103	0.2163	-0.0289	0.1807	-0.0472
7a	0.0399	-0.0520	0.1075	-00289	0.0972	-0.0314

The parametrized exchange-repulsion not only improves the accuracy of $n\pi^*$ excited state descriptions but also the speed of these calculations. Table 4.5 shows the average time it took each method to compute 15 CIS excited states on the 37 structures. As expected, modeling the entire system quantum mechanically takes the longest time. The PE QM/EFP scheme reduces the computational cost to about half. The incorporation of parametrized exchange-repulsion further decreases the average time by over two minutes. This decrease in computational time presumably results from exchange-repulsion constraining the electronic density to the QM region. In other words, the electronic wave-function disturbs the effective fragments to a lesser degree, ultimately leading to a faster convergence.

Table 4.5.
Average computational cost required for the Full QM, PE and PE+XR calculations done on 37 structures using the cc-pVDZ basis set. For each geometry, a total of 15 states were requested.

Scheme	Average Time (min)
Full QM	18.12
PE	9.36
PE+XR	7.15

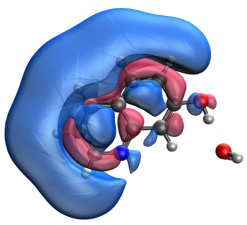

Fig. 4.6. Example of Rydberg orbital (structure 1a in Appendix C).

Out of the original 387 cc-pVDZ excitations considered in this benchmark, 63 could be characterized as transitions to Rydberg orbitals. Despite the initial expectation that the exchange-repulsion term would destabilize Rydberg orbitals and increase the corresponding excitation energy, over half of these energies seem to be underestimated by both PE and PE+XR schemes. By a close examination of such transitions we observed that in most cases the exchange-repulsion term increased the energy of the valence occupied orbital by a larger amount than the energy of the Rydberg orbital. This trend could be attributed to the fact that in most transitions the Rydberg orbitals were located away of the solvent, as shown in Fig. 4.6, and were mainly unaffected by the exchange-repulsion term. Thus, in order to determine whether the exchange-repulsion contribution to the QM/EFP Hamiltonian does in fact destabilize Rydberg orbitals and improves the description of Rydberg states, it is necessary to consider systems in which the chromophore is fully surrounded by solvent molecules.

4.4 Conclusions

Several hybrid QM/MM models in which the solvent is described with the EFP method were introduced and benchmarked for electronic excitations of nine biologically-relevant chromophores embedded in clusters of polar solvent molecules. All considered schemes correspond to polarizable embedding models, augmented with short-range terms introduced as one-electron contributions to the electronic Hamiltonian of the QM subsystem. The original polarizable embedding model performs well for $\pi\pi^*$ excitation energies. This is because most of these transitions do not possess charge transfer to or from solvent. However, in transitions with significant amount of charge transfer which is often the case for $n\pi^*$ excitations, PE scheme becomes less reliable with errors proportional to the values of blue solvatochromic shifts and to the amount of solvent-to-solute charge-transfer. Fortunately, the QM/EFP exchange-repulsion term significantly improves the description of $n\pi^*$ excitations making the

overall QM/EFP description of the excited states more balanced. Interestingly, we found that adding the charge-penetration correction to the electrostatics term does not improve but rather deteriorates the accuracy of the QM/EFP excitation energies. These conclusions remain the same when the calculations are performed with diffuse aug-cc-pVDZ basis on the QM region. The performed benchmarks build a solid base for reliable applications of QM/EFP models in photochemistry and photobiology. Further improvements of accuracy of QM/EFP excitation energies might be achieved by explicitly accounting for interactions between electronic states and solvent polarization.

5. QM/EFP DISPERSION FOR EXCITED AND TRIPLET STATES

5.1 Motivation

QM/EFP is an accurate yet efficient method to describe systems residing in the ground state. Nonetheless, relevant chemistry can also occur in low-lying triplet states. As an example, research has been trying to exploit the use of singlet-triplet fission as a way to improve the efficiency of solar cells [102–105]. There has also been some work dedicated to the study of triplet sensitizers, compounds that act as catalysts when excited to their triplet state [106–108].

To accurately describe these states it is necessary to account for all possible interactions between the QM region and the effective fragments. The work done in previous chapters introduced a parametrized version of exchange-repulsion, such that the QM/EFP energy is given by:

$$\begin{aligned} E_{PE+XR,0} = &\left\langle \Psi_0 \left| \hat{H}_{QM} + \hat{V}^{coul} + \hat{V}_0^{pol} + \hat{V}^{xr} \right| \Psi_0 \right\rangle \\ &+ E_0^{pol} + E_{QM/EFP,0}^{disp} + E_{EFP}^{coul} + E_{EFP}^{disp} + E_{EFP}^{xr} \end{aligned} \tag{5.1}$$

where the last three terms refer to the EFP/EFP interaction energies. The subscript in $\hat{V}_0^{pol}$ and E_0^{polt} specifies the induced dipoles of the fragments are computed until full consistency with the ground state wavefunction of the QM region is achieved [48, 50]. The $E_{QM/EFP,0}^{disp}$ term is a perturbative correction that depends on the ground state wavefunction of the QM region and cannot be directly applied to excited states [51]. In summary, for the purpose of calculating the QM/EFP energy of excited and triplet states, the only coupling term missing in Eq. 5.1 is dispersion. Dispersion can become a significant contributor to the total interaction energy of such states. As an example, Fig. 5.1 illustrates how this component can change between

a QM/EFP system in which the QM region is in the ground state versus an excited state. The dispersion term in QM/EFP accounts for all possible excited states in the QM region interacting with all possible excited states in the effective fragment (blue lines in Fig. 5.1). Excitation of an electron in the QM region might decrease the energy required to reach some of the other QM excited states (red line in Fig. 5.1). Since dispersion is inversely proportionally to this energy, the QM excitation ultimately leads to an increase in the dispersion energy of the system.

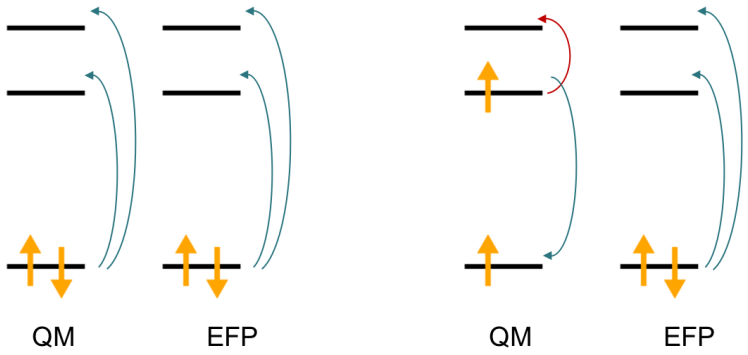

Fig. 5.1. Representation of changes in dispersion due to excitation of the QM region in QM/EFP

5.2 Methods

5.2.1 Theory

A computationally efficient method to estimate the QM/EFP dispersion term was recently developed [51]. This method is based on the following equation:

$$E^{disp}_{QM/EFP} = -\frac{1}{\pi}\sum_{j\in B}\sum_{k}^{occ}\sum_{r}^{vir}\sum_{\alpha\beta}^{x,y,z}\langle k\left|T^j_\alpha\right|r\rangle\langle r\left|T^j_\beta\right|k\rangle \int_0^\infty \frac{\omega^A_{rk}}{(\omega^A_{rk})^2+\omega^2}\alpha^j_{\alpha\beta}(i\omega)d\omega \tag{5.2}$$

where ω_{rk}^{A} is the energy difference between virtual orbital r and occupied orbital k of the QM region. The superscript j points the location of polarizability tensors on the effective fragment B. Lastly, $\langle k\,|T_{\alpha}^{j}|\,r\rangle$ represents the electric field integral in the block of occupied and virtual QM orbitals. This integral is computed as follows [51]:

$$-\int dr' k^{*}(r')\frac{(r'-R^{j})_{\alpha}}{(|r'-R^{j}|)^{3}}r(r') \tag{5.3}$$

where the electrostatic tensor $T_{\alpha}^{j}(r')$ is computed between the electronic coordinate of the QM region r' and the distributed point R^{j} on the effective fragment.

The same formulation was extended to the unrestricted open-shell Hartree-Fock and DFT methods, and can be directly used for computing lowest-energy triplet states. The values and accuracy of this dispersion term were explored for a small series of dimers. We additionally tested the effect of the electrostatic screening discussed in Chapter 4. Electrostatics, polarization and the parametrized version of exchange-repulsion were included in all QM/EFP calculations.

5.2.2 Computational Details

Calculations were performed on seven dimers (Fig. 5.2). For each dimer, a total of 8 geometries were considered in order to explore distance dependence of different energy components. Except for the water-methane dimer, all the geometries were borrowed from the S66x8 data set [77, 109]. In this data set the 8 geometries derive from scaling the closest intermolecular distance of ground state geometry by: 0.80, 0.90, 0.95, 1.00, 1.05, 1.10, 1.25, 1.50 and 2.00. Details on the specifics of the scaling for each dimer can be found in Ref. [77]. For the water-methane dimer the distance between the oxygen atom and the carbon atom was scaled by the same factors specified above, the geometries are given in Appendix D. The initial geometry for this dimer was obtained from a CCSD(T)/jun-cc-pVDZ optimization of the ground state. For each point, the interaction energy of the lowest triplet state was calculated using two reference methods and four QM/EFP schemes. The reference methods included CCSD(T)/jun-cc-pVDZ and HF/6-31+G* [65, 110, 111]. The QM/EFP

schemes were all built from the polarizable embedding scheme with parametrized exchange-repulsion by adding dispersion and/or a charge-penetration correction for the electrostatics term, here referred to as screen. The labels and descriptions for these schemes are given in Table 5.1. In QM/EFP calculations only the monomer corresponding to the QM region resided in the triplet state. For comparison, we also provide interaction energies for the singlet ground state of each dimer. These energies were obtained using QM/EFP and SAPT0 [60, 61]. For the latter we employed the jun-cc-pVDZ basis set.

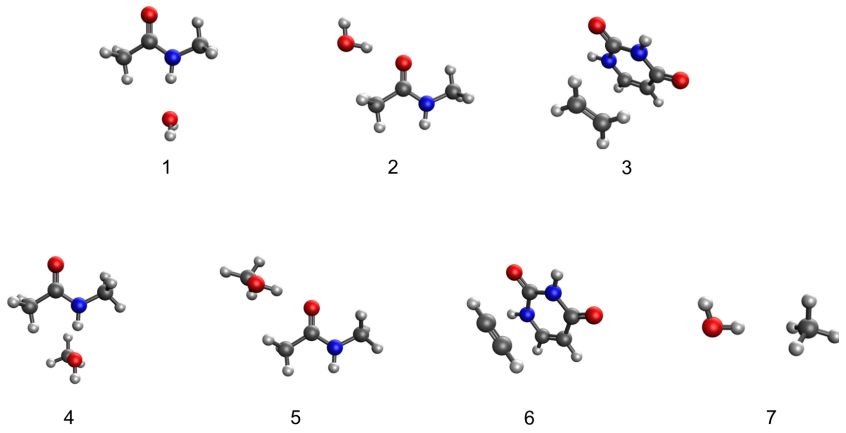

Fig. 5.2. Dimers considered for this study: (1) peptide-water-a, (2) peptide-water-b, (3) uracil-ethene, (4) peptide-methanol-a, (5) peptide-methanol-b, (6) uracil-ethyne, (7) water-methane.

In all the systems from the S66x8 data set, the peptide or uracil molecule represented the QM region. In the case of the water-methane dimer, the water molecule was considered to be the QM region. The dimers are named such that the first monomer specifies the QM region. For all dimers, this region was modeled with HF/6-31+G(d). All the effective fragments remained in their singlet ground state. The potentials for the fragments, as well as the exchange-repulsion parameters, were all taken from the work done in Chapter 2. These potentials were obtained with a combination of basis sets: 6-31+G(d) for electrostatics and 6-311++G(3df,2p) for all other terms [64–70].

An additional pairwise interaction energy decomposition analysis within the Fragment Molecular Orbital method (FMO/PIEDA) [56, 112–115] was performed on the water-methane dimer in the ground state equilibrium geometry. PIEDA can be used as a reference for QM/EFP since it decomposes the energy into electrostatics, dispersion, exchange-repulsion and charge-transfer. The dispersion term comes from using MP2/6-31+G(d) instead of HF/6-31+G(d). All of the calculations were done in GAMESS [23, 24], with the exception of the CCSD(T) [116] and SAPT calculations which were done in Psi4 [63, 85]. Lastly, for all the unscaled geometries, the amount of charge transfer in the ground state and triplet states was estimated from the Mülliken charges of the fully quantum mechanical HF calculations.

Table 5.1.
QM/EFP embedding schemes for study of QM/EFP dispersion in triplet states.

Label	Description
PE+XR	PE + exchange-repulsion
PE+SXR	PE + screen + exchange-repulsion
PE+D+XR	PE + dispersion + exchange-repulsion
PE+D+SXR	PE + dispersion + screen + exchange-repulsion

5.3 Results

For each dimer, the results presented here cover four main aspects. First we introduce the singly occupied orbitals of the lowest triplet state. Then, for that state, we provide the total interaction energies computed with with CCSD(T), HF and several QM/EFP schemes. We also discuss the dispersion energy and in some cases other energy components. Finally, we review the energy decomposition for the ground state of the dimer computed with QM/EFP and SAPT.

The singly occupied orbitals for the lowest triplet state of the peptide-water-a and peptide-water-b dimers are depicted in Figs. 5.3 and 5.4. In both cases, the triplet state involves a transition from a π orbital to a Rydberg orbital. It is not surprising that the transition seems to be the same for both dimers, since they only differ on the location of the water molecule with respect to the peptide.

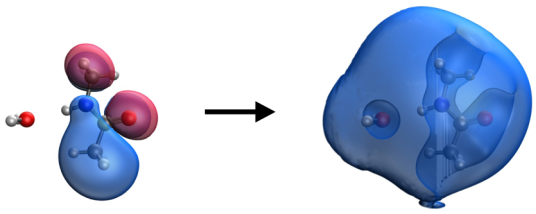

Fig. 5.3. Orbitals involved in the transition from the ground state to the lowest triplet state of the peptide-water-a dimer.

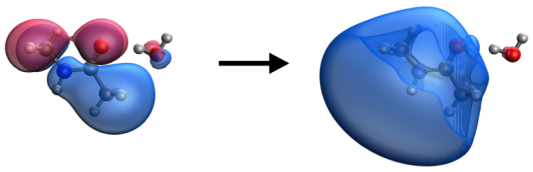

Fig. 5.4. Orbitals involved in the transition from the ground state to the lowest triplet state of the peptide-water-b dimer.

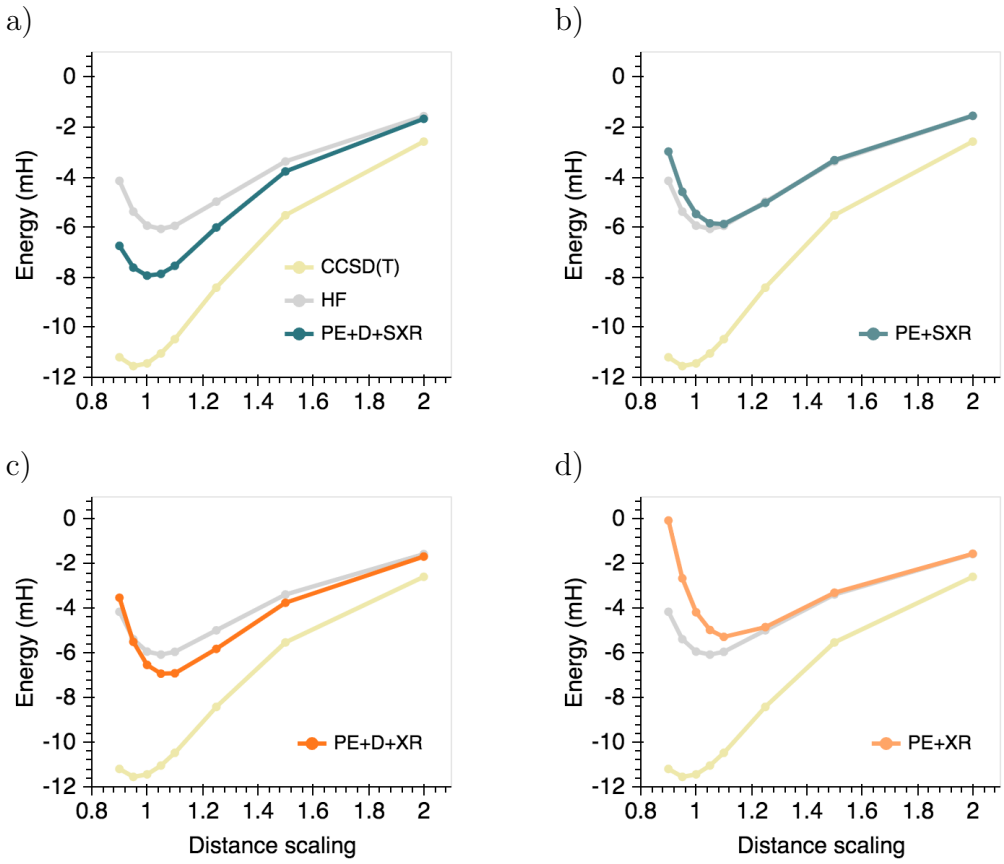

Fig. 5.5. Total interaction energies for the lowest triplet state of the peptide-water-a dimer.

The total interaction energies for the lowest triplet states of these dimers are plotted in Figs. 5.5 and 5.6. From the figures we see that the PE+D+SXR scheme outperforms all others schemes. For the peptide-water-a dimer, the interaction energies predicted by this scheme are between HF and CCSD(T). For the peptide-water-b dimer the error is larger with respect to CCSD(T) but the PE+D+SXR and PE+D+XR curves closely approach the HF curve. Clearly, both schemes provide an improvement over the PE+XR scheme. As an example, comparing Figs. 5.5d and 5.5c reveals a significant decrease in the interaction energy when adding dispersion alone. This shift evidences the importance of accounting for the dispersion term in triplet states.

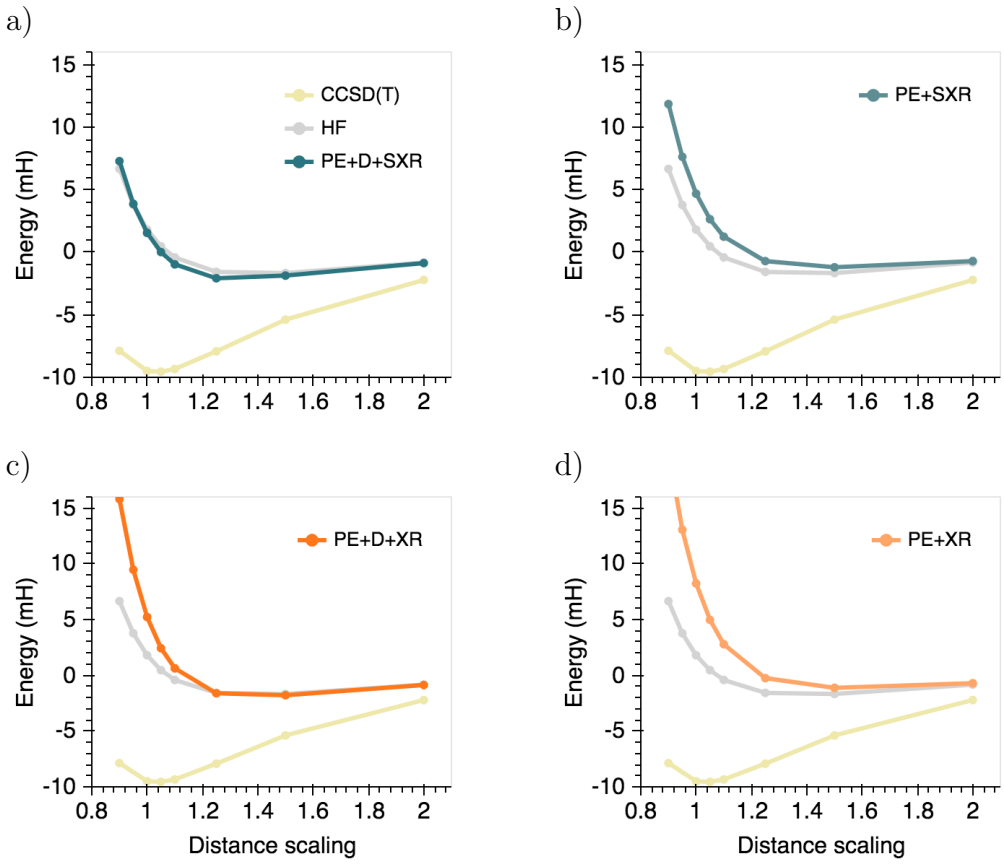

Fig. 5.6. Total interaction energies for the lowest triplet state of the peptide-water-b dimer.

Fig. 5.7 compares the triplet state dispersion energies for these dimers computed with schemes PE+D+SXR and PE+D+XR. From this figure we can see that both QM/EFP schemes result in similar dispersion values. These figures also contain the difference in energy between the CCSD(T) and HF methods. Using this as a rough predictor for dispersion leads to the conclusion that QM/EFP highly underestimates this component, in particular for the peptide-water-b dimer. For this dimer, the maximum difference between the CCSD(T)-HF estimator and the PE+D+XR scheme is 10.22mH. For the peptide-water-a dimer the difference is always below 3.6mH.

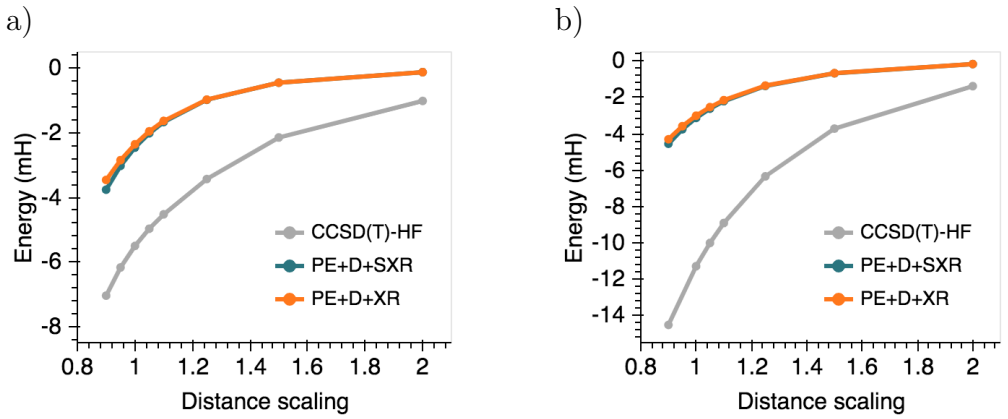

Fig. 5.7. Dispersion interaction energies for the lowest triplet states of the peptide-water-a (left) and peptide-water-b (right) dimers.

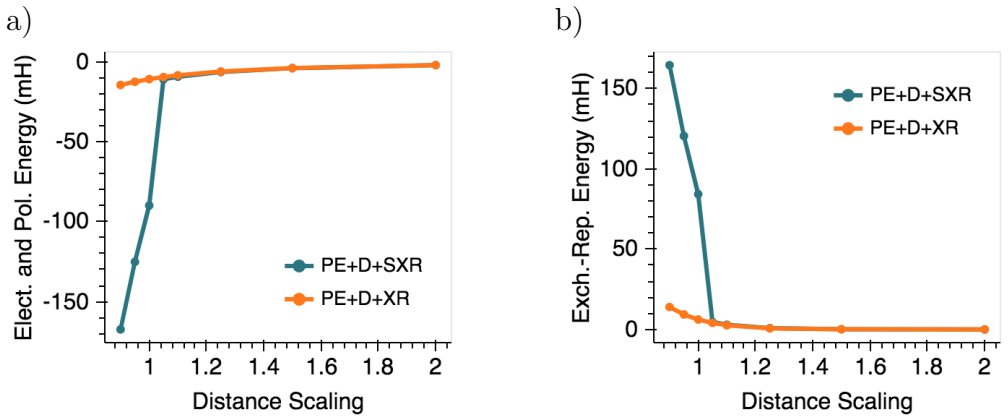

Fig. 5.8. Electrostatics, polarization and exchange-repulsion energies for the lowest triplet state of the peptide-water-a dimer.

The screen correction also seems to stabilize the total interaction energy of the triplet states of the peptide-water dimers. This is particularly true at short distances and can be clearly observed when comparing, for instance, plots c and a in Fig. 5.6. However, when looking at the energy decomposition in Figs. 5.8 and 5.9, it becomes clear that electrostatic screening destabilizes the QM wave-function, such

that QM/EFP calculations without the exchange-repulsion term diverge at short distances. Since these calculations are necessary to evaluate the electrostatics and polarization terms, as well as the exchange-repulsion term, their divergence leads to artificially large values of the individual energy components. Note nevertheless that in the presence of exchange-repulsion the PE+D+SXR scheme is stable.

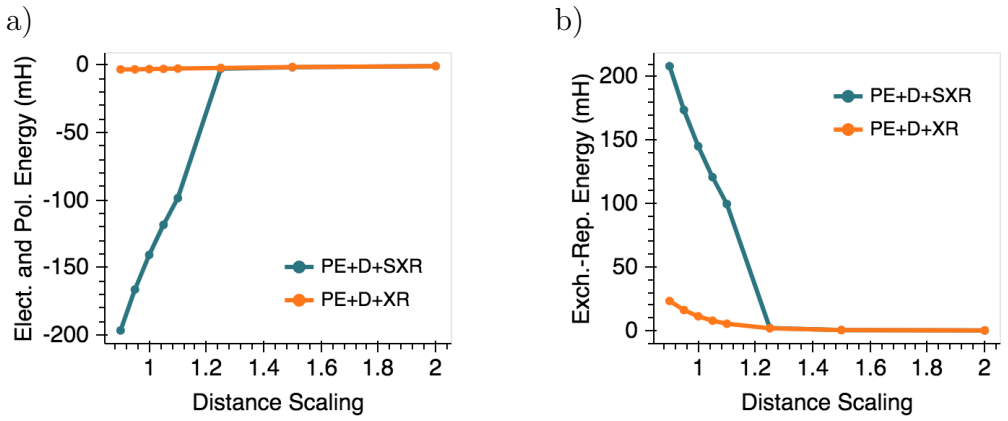

Fig. 5.9. Electrostatics, polarization and exchange-repulsion energies for the lowest triplet state of the peptide-water-b dimer.

The energy decompositions for the ground state of the peptide-water-a and peptide-water-b dimers are shown in Figs. 5.10 and 5.11. Looking at the peptide-water-a first, we see that the PE+D+XR scheme shifts the location of the minimum towards the distance scaled by 1.05. The PE+D+SXR positions the minimum at the correct location but the interaction energy at the point is stronger, mainly due to an over-estimation of the electrostatics and polarization terms. All other components from the PE+D+SXR scheme closely approach the values predicted by SAPT, ultimately resulting in an error smaller than 2mH at the equilibrium geometry.

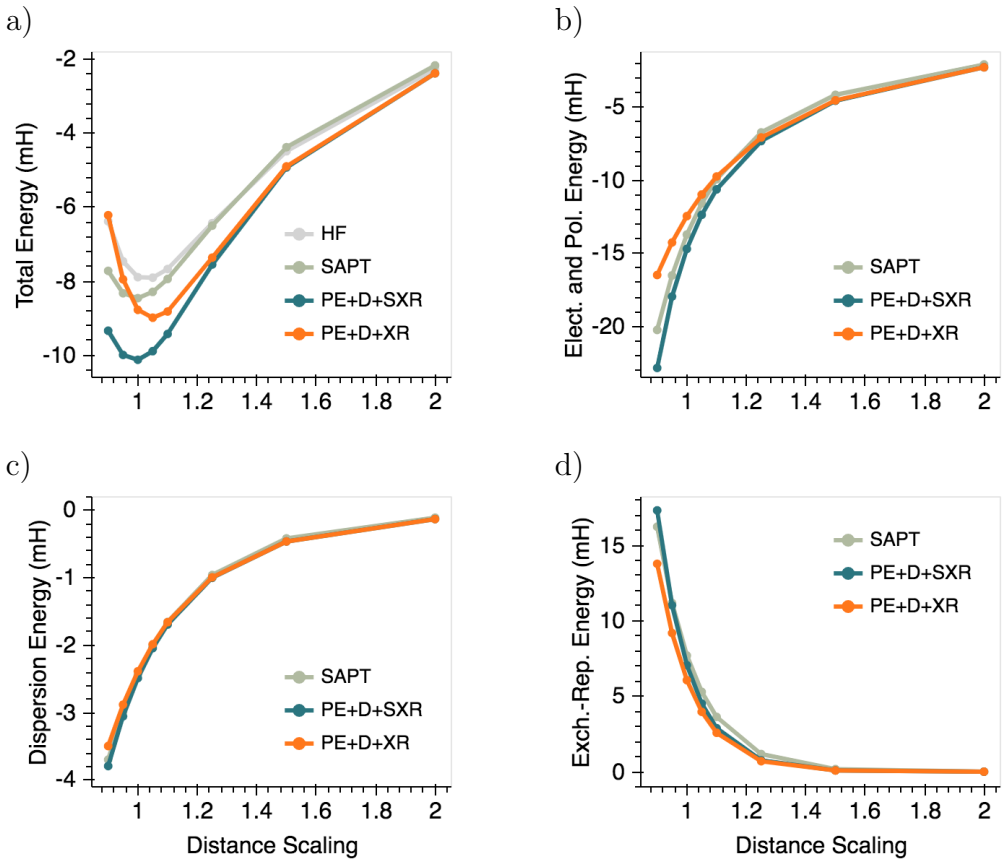

Fig. 5.10. Interaction energies for the ground state of the peptide-water-a dimer.

The difference between the PE+D+SXR and PE+D+XR schemes is more drastic for the ground state of the peptide-water-b dimer. From Fig. 5.11 we first note that the PE+D+SXR scheme performs very well for the total interaction energy. This scheme accurately captures the dispersion term and while electrostatics, polarization and exchange-repulsion are overestimated, the errors cancel in such a way that the total interaction energy remains within 0.5mH from SAPT for all points. However, it is interesting to note that while SAPT shifts the location of the minimum towards the distance scaled by 0.95, the PE+D+SXR scheme does not. The PE+D+XR performs considerably worse than the PE+D+SXR scheme, not only in terms of the location of the minimum but also the magnitude of the interaction energy. With this

scheme the minimum shifts towards the point scaled by 1.10. Furthermore, the error for the shortest distance geometry is over 15mH. For the equilibrium geometry the corresponding error is approximately 7mH. As evidenced from plots b, c and d in the figure, the main contributors to the total interaction error are the electrostatics and polarization terms. For the shortest distance, these terms alone have an error of over 13mH. For the equilibrium distance the error is around 6.73mH.

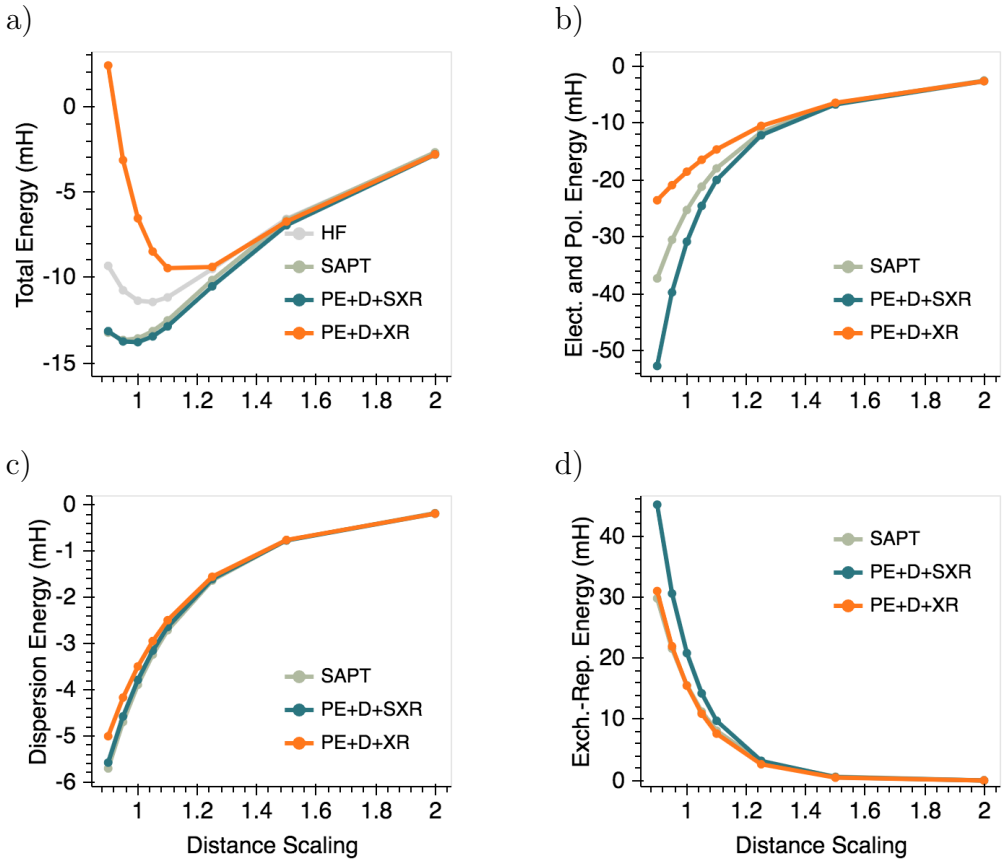

Fig. 5.11. Interaction energies for the ground state of the peptide-water-b dimer.

The peptide-methanol-a and peptide-methanol-b dimers are similar to the previous two dimers in the sense that they differ only on the location of the methanol. The singly occupied orbitals for the lowest triplet states of these dimers are illustrated in Figs. 5.12 and 5.13. To achieve the triplet state, both of these dimers experience a transition from a π orbital to a Rydberg orbital.

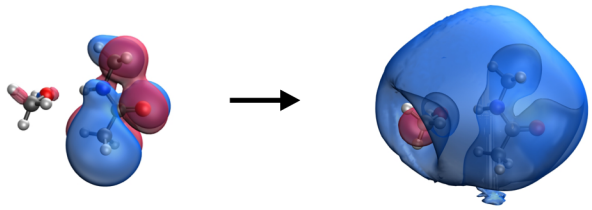

Fig. 5.12. Orbitals involved in the transition from the ground state to the lowest triplet state for the peptide-methanol-a dimer.

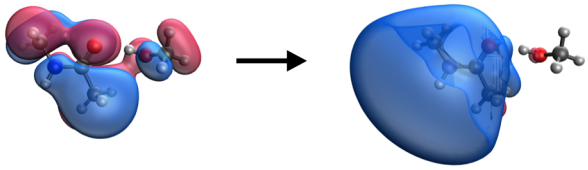

Fig. 5.13. Orbitals involved in the transition from the ground state to the lowest triplet state for the peptide-methanol-b dimer.

The interaction energies for the lowest triplet states of these dimers are plotted in Figs. 5.14 and 5.15. For the peptide-methanol-a the interaction energies predicted by the PE+XR scheme are always weaker than those predicted by HF. Adding dispersion alone, however, shifts the curve below HF and closer to CCSD(T). As an example, for the point with the shortest distance, the shift is over 5mH, moving the interaction energy from positive to negative. These results confirm once again the importance of adding dispersion in order to counteract repulsion. Adding the electrostatics screen

correction along with dispersion seems to further improve the results for long distances. At short distances, however, the effect of the screen correction is such that repulsion becomes negligible.

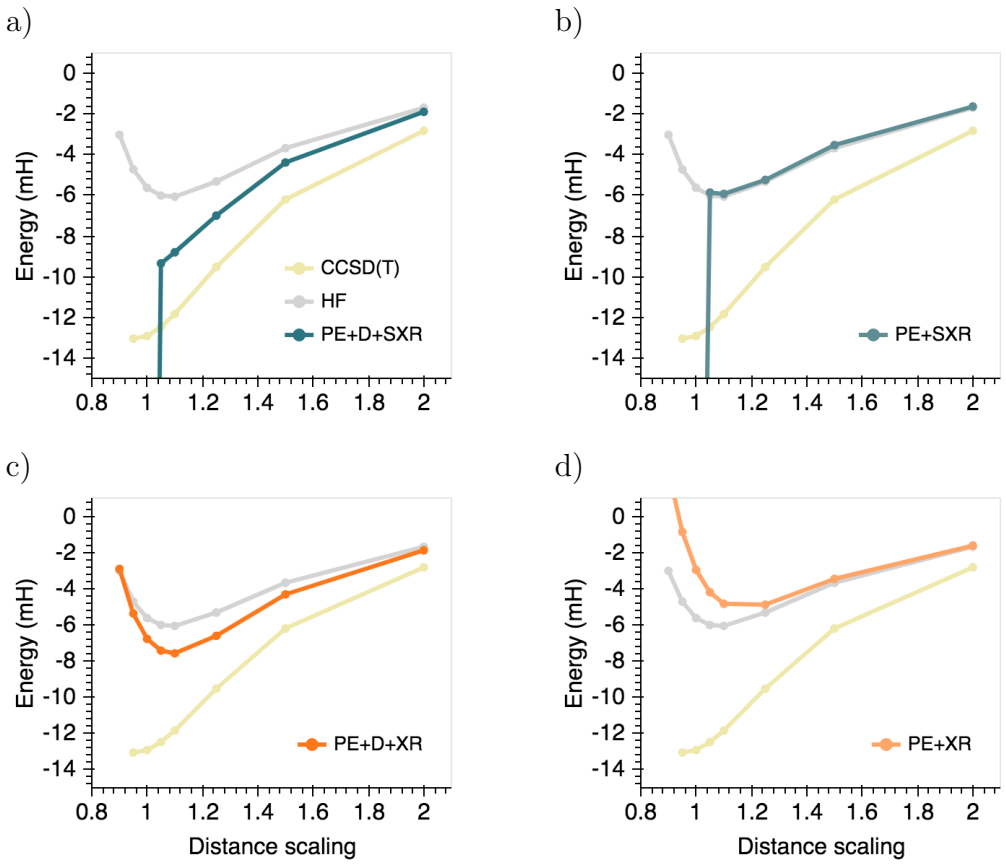

Fig. 5.14. Total interaction energies for the lowest triplet state of the peptide-methanol-a dimer.

Results for the peptide-methanol-b dimer are similar to the ones discussed above. The main difference comes from the fact that the PE+D+XR energies for this dimer remain more repulsive than the HF energies, implying a need for the electrostatics screen correction. Once again, however, this correction results in interaction energies that are too attractive at short distances. Based on how the charge-penetration screen correction was built, its effect is in fact expected to be stronger at short distances.

Unfortunately, these results exhibit cases in which adding this correction can lead to large and inaccurate estimations of the total interaction energy. The inclusion of screen also affects the dispersion term, shown in Fig. 5.16. Fig. 5.16 compares the QM/EFP dispersion energy to the CCSD(T)-HF energy, which serves as rough reference for the term. As expected from previous results, the difference between this reference and both QM/EFP schemes is small for the peptide-methanol-a dimer. For this dimer, the difference is larger at shorter distances but remains below 4mH for the PE+D+XR scheme. For the peptide-methanol-b dimer the corresponding value goes up to 7.16mH for the point with distance scaled by 1.10.

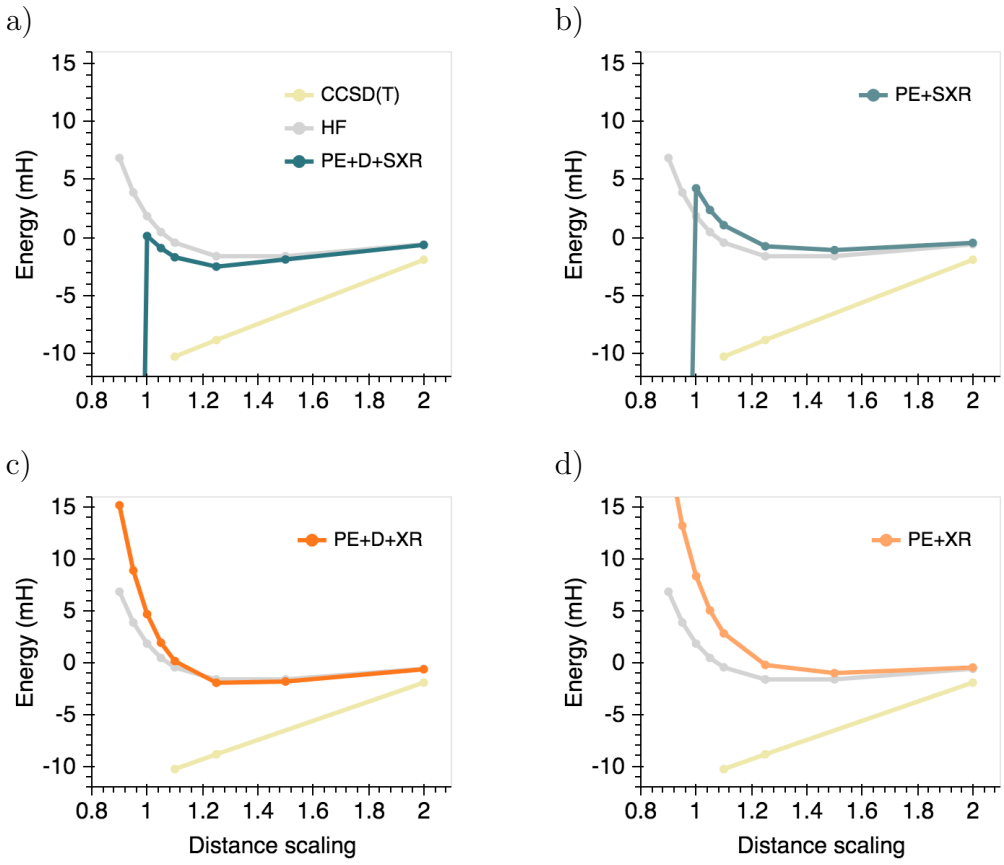

Fig. 5.15. Total interaction energies for the lowest triplet state of the peptide-methanol-b dimer.

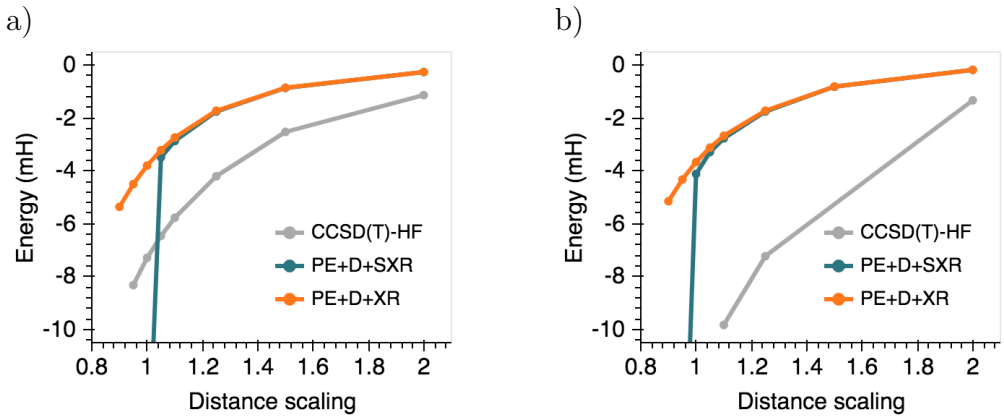

Fig. 5.16. Dispersion interaction energies for the lowest triplet states of the peptide-methanol-a (left) and peptide-methanol-b (right) dimers.

For comparison, Figs. 5.17 and 5.18 provide the energy decomposition for the ground state of the peptide-methanol dimers. For the peptide-methanol-a dimer, the PE+D+XR scheme shifts the minimum of the total interaction energy towards a longer distance, in this case the point scaled by 1.10. The PE+D+SXR scheme does not shift the location of the minimum but it does predict strong interaction energies. The overestimation of the interaction energies comes from electrostatics and polarization. As an example, for the shortest distance point, the electrostatics and polarization energy predicted by this scheme is -57.16mH, resulting in an error of -32.85mH with respect to SAPT. However, exchange-repulsion also has a large error for that point, approximately 31.14mH. Since these values cancel each other out, the total interaction energy error remains below 2mH.

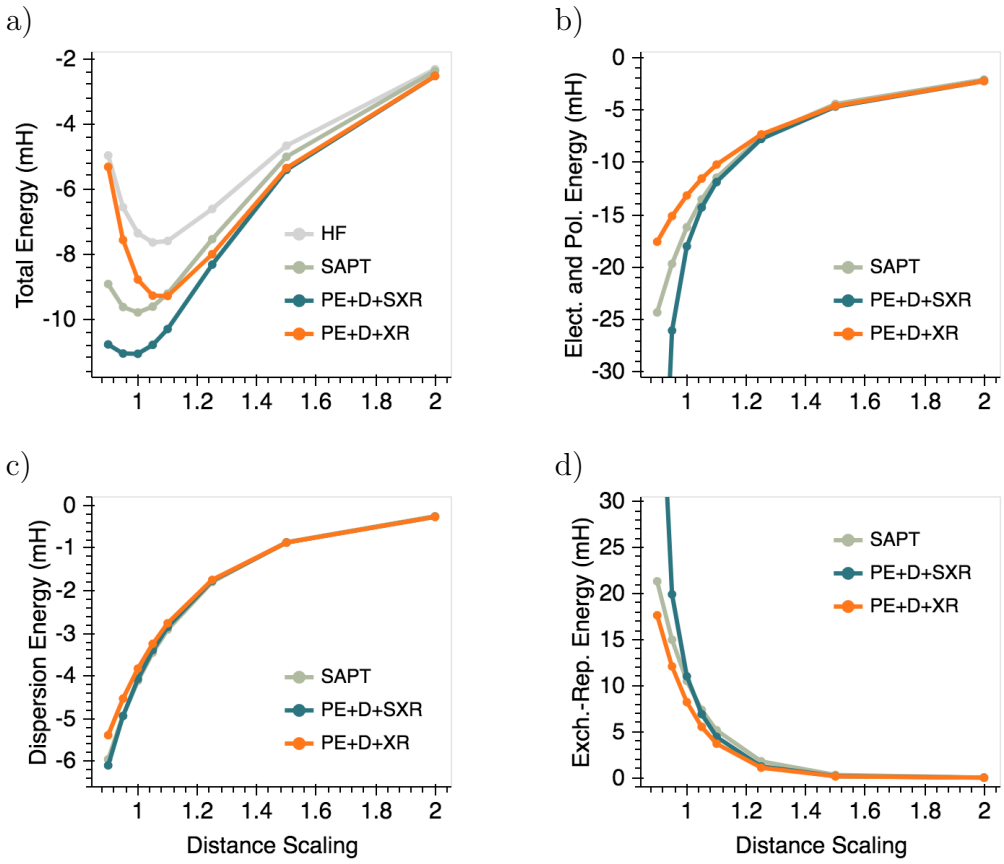

Fig. 5.17. Interaction energies for the ground state of the peptide-methanol-a dimer.

Considering now the peptide-methanol-b dimer, Fig. 5.18 demonstrates that the PE+D+SXR scheme accurately describes the total interaction energy of the dimer, with an error always below 1mH. However, this QM/EFP scheme and SAPT shift the location of the minimum towards the distance scaled by 0.95. On the other hand, the PE+D+XR scheme produces energies that are too repulsive. The use of this scheme shifts the location of the minimum to the point scaled by 1.25. At the equilibrium distance, the error with respect to SAPT is 7.41mH and at the shortest distance the error becomes 15.89mH. The electrostatics and polarization errors for these points are 8.46mH and 16.45mH respectively, making them the largest contributors to the total interaction energy error.

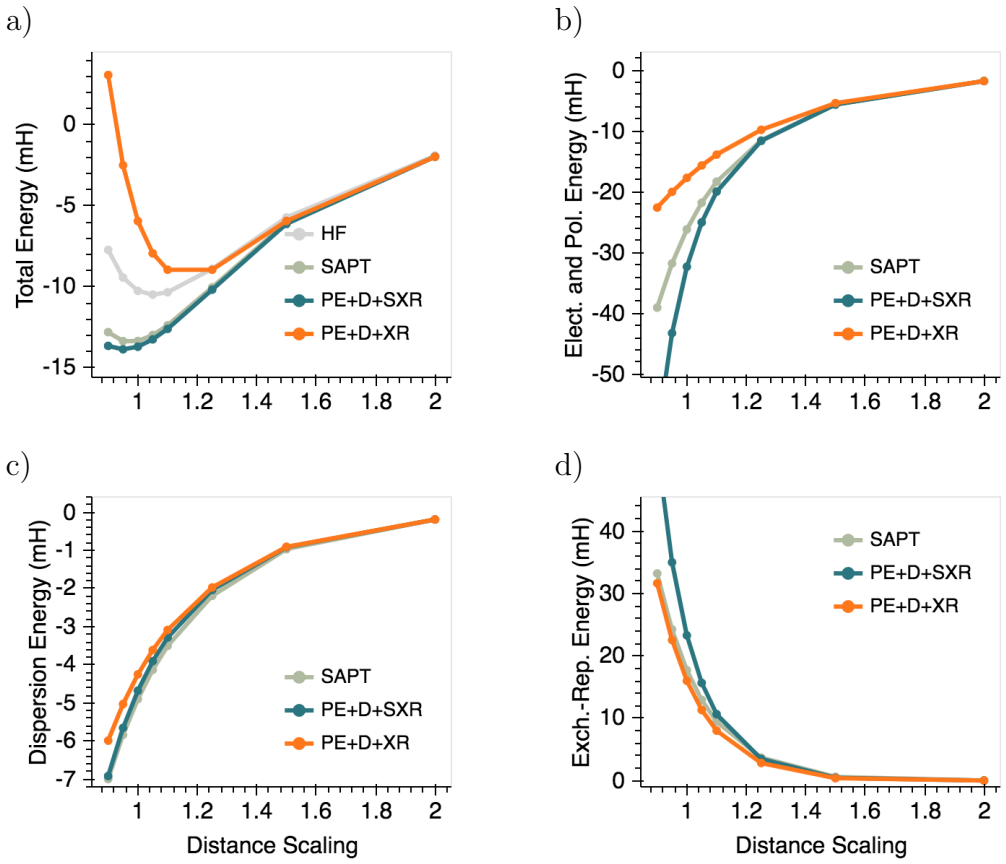

Fig. 5.18. Interaction energies for the ground state of the peptide-methanol-b dimer.

Figs. 5.19 and 5.20 depict the singly occupied orbitals for the triplet states of the uracil-ethene and uracil-ehtyne dimers. As expected for uracil, the orbitals involved in the S0-T1 transition for these dimers are all π orbitals. Nonetheless, unlike other cases, the transitions for these systems seem to involve a mixture of orbitals.

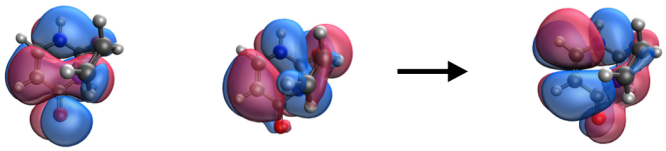

Fig. 5.19. Orbitals involved in the transition from the ground state to the lowest triplet state for the uracil-ethene dimer.

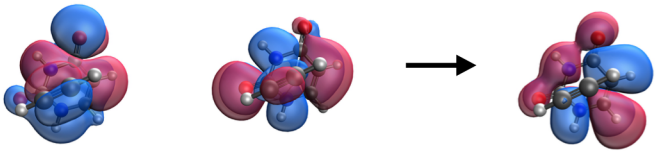

Fig. 5.20. Orbitals involved in the transition from the ground state to the lowest triplet state for the uracil-ethyne dimer.

The total interaction energies for the lowest triplet states of the uracil-ethene and uracil-ethyne dimers are shown in Figs. 5.21 and 5.22. The trends observed are very similar for the two dimers. In both cases, the PE+XR scheme underestimates the total interaction energies, which remain above the HF curve for all points. Adding the dispersion term lowers the energies, in each case shifting the state from unbound to bound. The energies at short distances still remain more repulsive than the HF energies, although the QM/EFP-HF error decreases significantly. For example, for the uracil-ethene dimer the PE+XR error for the shortest distances is around 12.58mH but becomes around 3.35mH upon addition of dispersion.

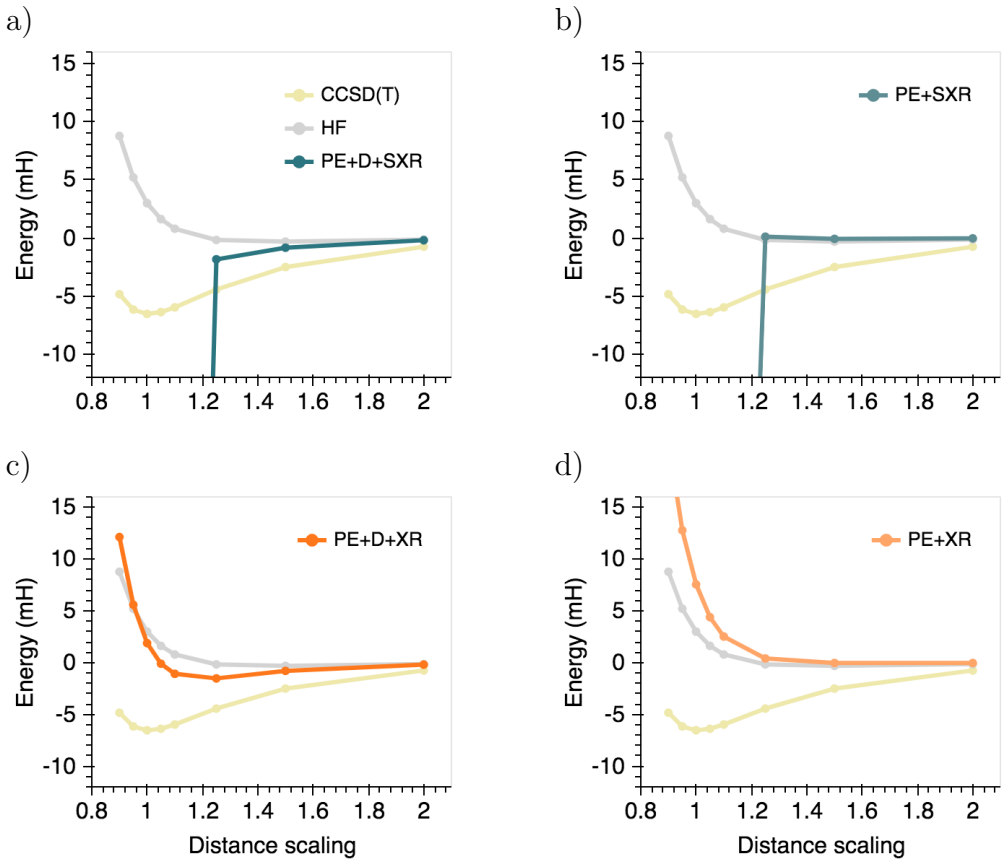

Fig. 5.21. Total interaction energies for the lowest triplet state of the uracil-ethene dimer.

Between the PE+SXR and PE+D+SXR schemes, it seems the PE+D+SXR would perform better, with interaction energies stronger than HF and closer to CCSD(T). However, both of these schemes run into convergence issues. For these dimers, adding the screen correction results in a breakdown of QM/EFP at distances below the 1.25 scaling.

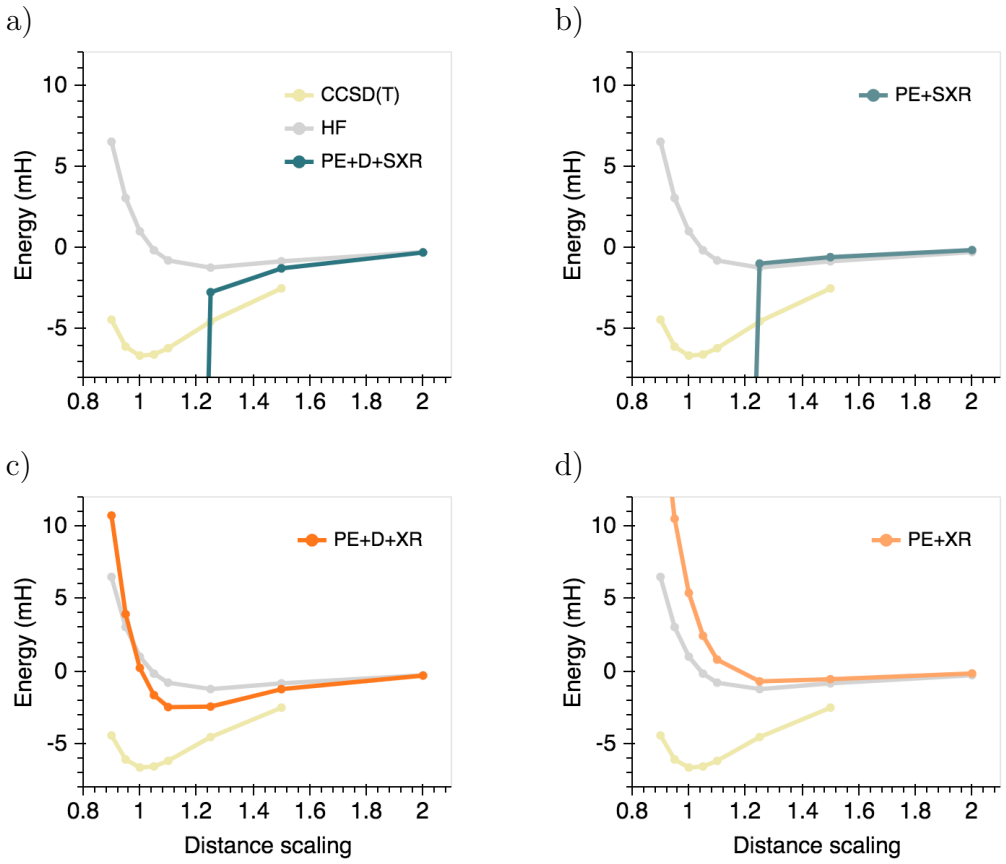

Fig. 5.22. Total interaction energies for the lowest triplet state of the uracil-ethyne dimer.

Fig. 5.23 features the dispersion interaction energies for the lowest triplet states of the uracil-ethene and uracil-ethyne dimers computed with the PE+D+XR and PE+D+SXR schemes. The plots also include the energy difference between CCSD(T) and HF. Considering only the PE+D+XR scheme, the difference between QM/EFP and the CCSD(T)-HF estimator remains below 4.5mH for the uracil-ethene dimer and below 3mH for the uracil-ethyne dimer.

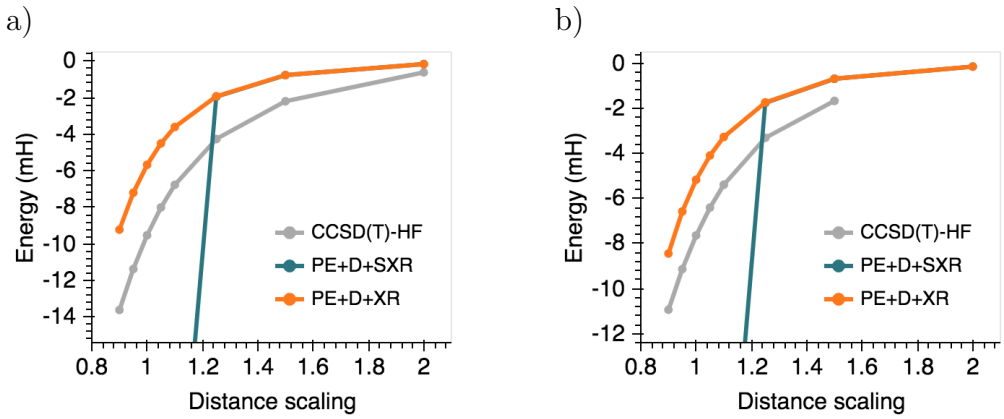

Fig. 5.23. Dispersion interaction energies for uracil-ethene (left) and uracil-ethyne (right) dimers.

Figs. 5.24 and 5.25 provide the energy decomposition for the ground states of the uracil-ethene and uracil-ethyne dimers. For the uracil-ethene dimer, the PE+D+XR scheme shifts the energy of the minimum to the distance scaled by 1.10. With this scheme, the QM/EFP-SAPT total interaction energy error is 11.11mH for the point with the shortest distance and 3.88mH for the equilibrium geometry. Plots c and d in Fig. 5.24 demonstrate a good agreement between this QM/EFP scheme and SAPT, suggesting the error derives from the electrostatics and polarization components. Indeed, for the shortest distance, the error for electrostatics and polarization is 9.84mH. The corresponding value for the equilibrium geometry is 3.95mH. These results match those observed for previous dimers and also agree with the ones for the uracil-ethyne dimer. The total interaction errors for the uracil-ethyne dimer are only slightly larger than the ones reported for the uracil-ethene dimer. Specifically, for the shortest distance the error is 11.82mH and for the equilibrium distance the error is 4.08mH. The respective values for the electrostatics and polarization components are 9.68mH and 3.86mH.

The PE+D+SXR scheme leads to convergence issues for both of these dimers. For long distances, the error for this scheme is below 2.5mH in both cases. However, at shorter distances, the electrostatics term dominates and the interaction energies become too attractive. It is surprising to observe this kind of behaviour in the ground state of the dimers. However, since it is the ground state, a possible solution to this problem might involve tuning the parameters for the electrostatics screening when computing the EFP potential.

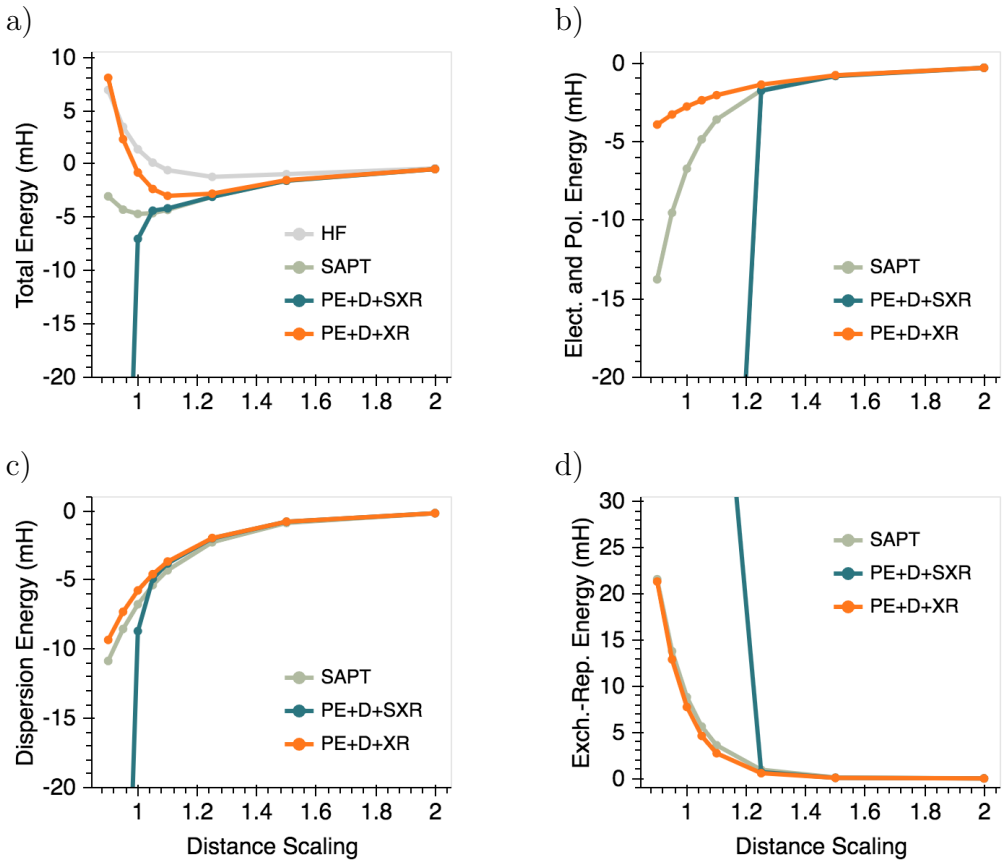

Fig. 5.24. Interaction energies for the ground state of the uracil-ethene dimer.

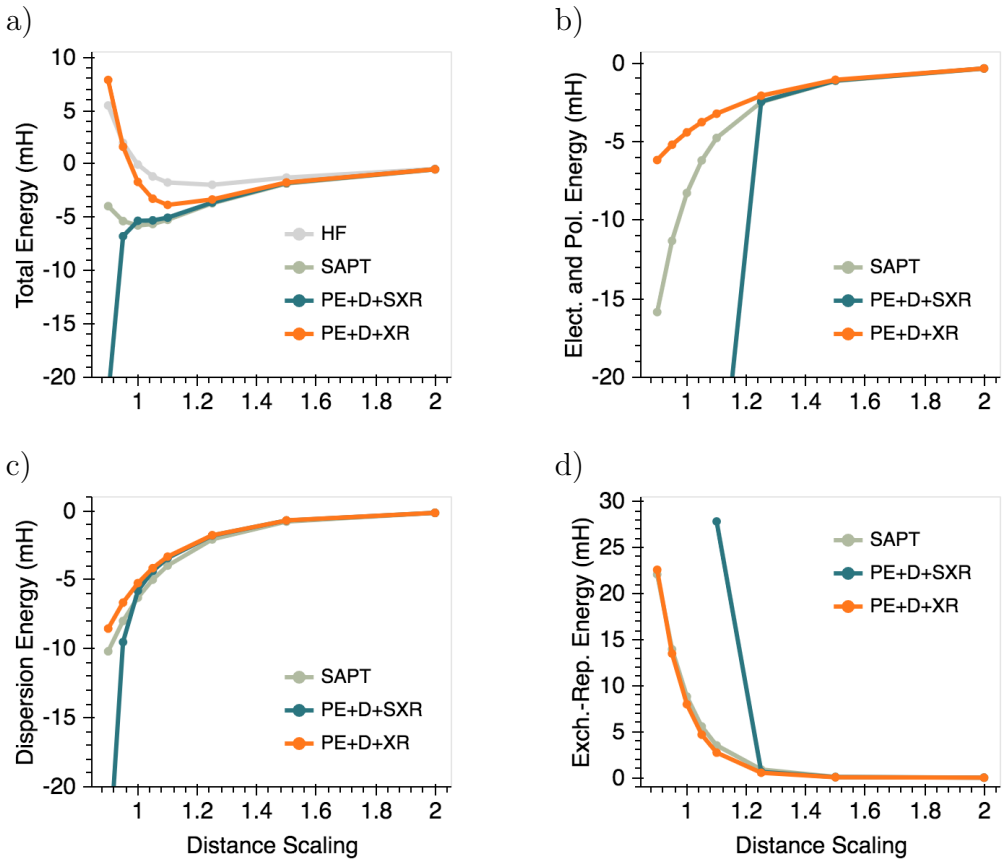

Fig. 5.25. Interaction energies for the ground state of the uracil-ethyne dimer.

The results from the six dimers discussed above show that, while the charge-penetration correction leads to convergence difficulties, adding dispersion can significantly improve the total interaction energy of systems in which the QM region lies on its lowest triplet state. Nonetheless, for most of these systems the dispersion energy of the lowest triplet state resembles that of its singlet ground state. The water-methane dimer is expected to have a larger difference in the dispersion energy between these states. The singly occupied orbitals for the triplet state of this dimer are shown in Fig. 5.26. One of the orbitals corresponds to the lone pair of electrons in the water molecule, while the other resembles a Rydberg orbital. The results for the total interaction energies of the triplet state are given in Fig. 5.27.

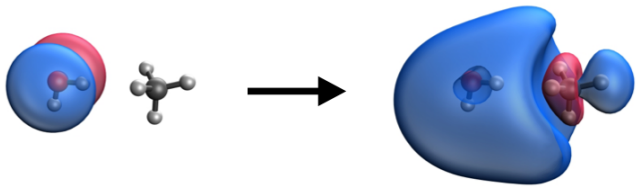

Fig. 5.26. Orbitals involved in the transition from the ground state to the lowest triplet state for the water-methane dimer.

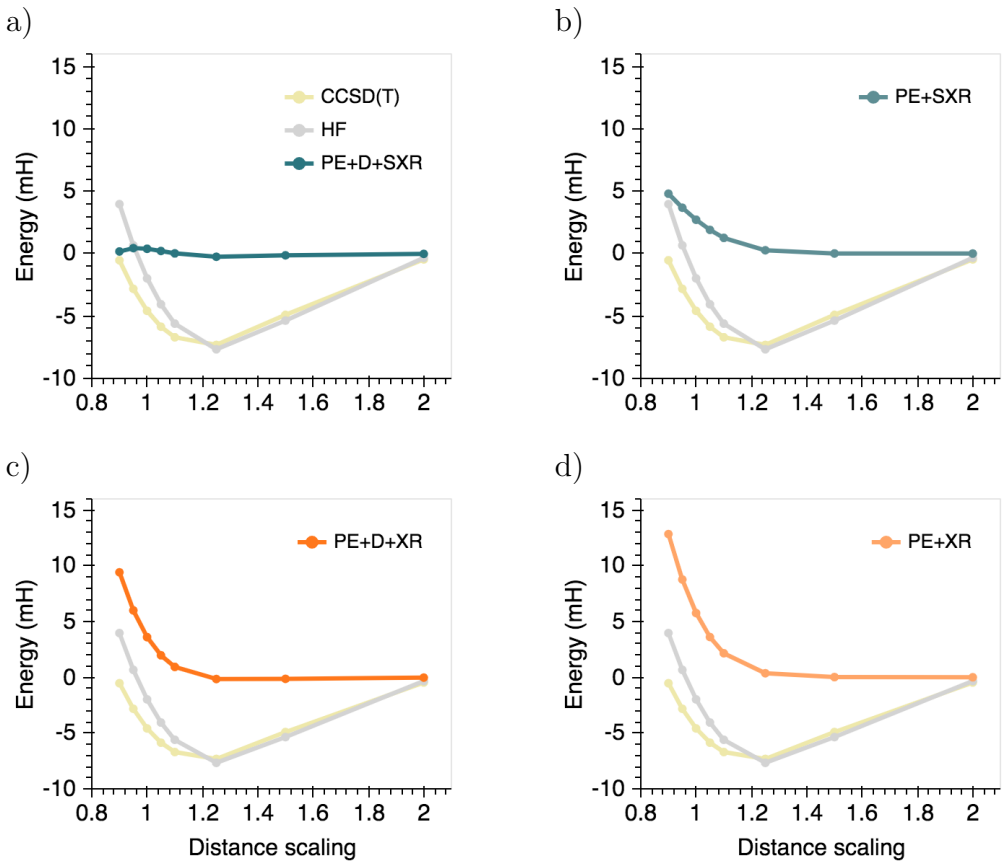

Fig. 5.27. Total interaction energies for the lowest triplet state of the water-methane dimer.

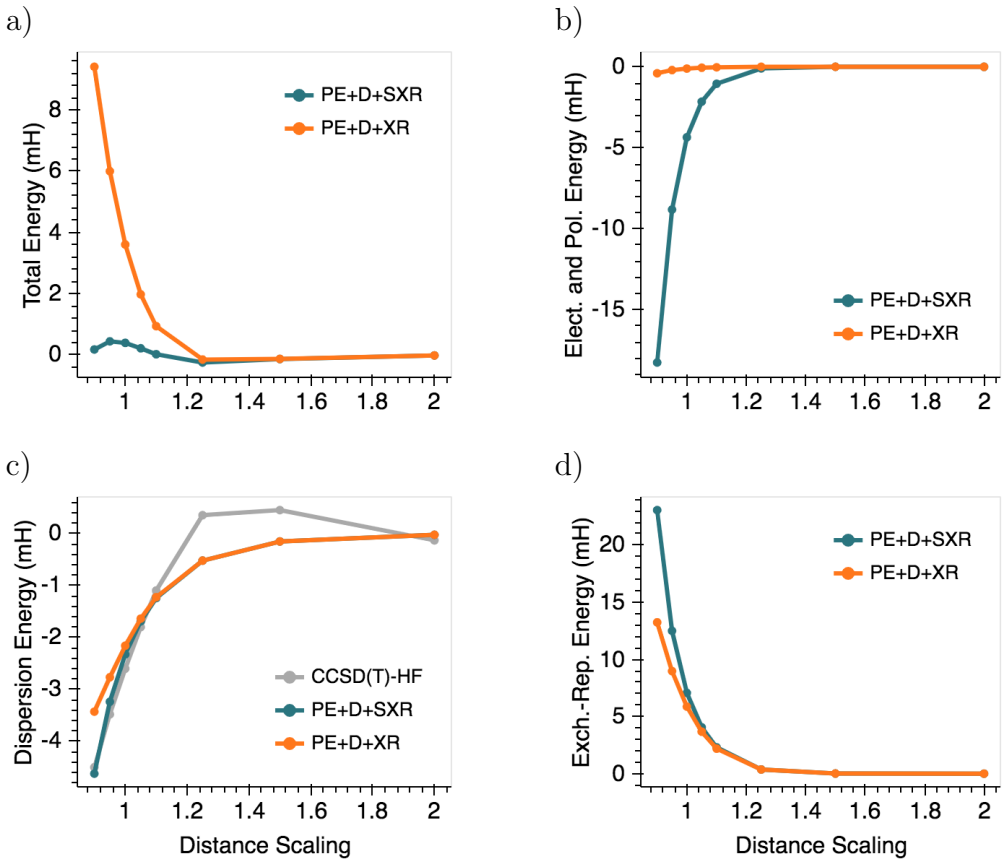

Fig. 5.28. Energy decomposition for the lowest triplet state of the water-methane dimer: (a) total, (b) electrostatics and polarization, (c) dispersion and (d) exchange-repulsion.

These results are particularly interesting for two reasons. The first reason is that the energies computed by HF seem to be lower that those computed by CCSD(T). This was not observed for any of the other cases but a potential explanation could be that most of the binding in this complex originates from charge-transfer, while the dispersion plays a significantly smaller role. The second reason these results are unexpected relates to the QM/EFP energies. The QM/EFP energies are positive for all points and all schemes, suggesting the system is not bound. The disagreement between QM/EFP and the reference methods is large, but can be somewhat understood by looking at the separate QM/EFP components. The energy decomposition

for the PE+D+SXR and PE+D+XR is given in Fig. 5.28. These results show that dispersion and exchange-repulsion seem to behave properly. The electrostatics and polarization terms, on the other hand, follow atypical trends. In particular, by looking at the PE+D+XR results, we see that the contribution from electrostatics and polarization appears to be near zero. Adding the screen correction lowers the electrostatics energy. Nonetheless, the magnitude of exchange-repulsion remains larger, leading to still repulsive total interaction energies.

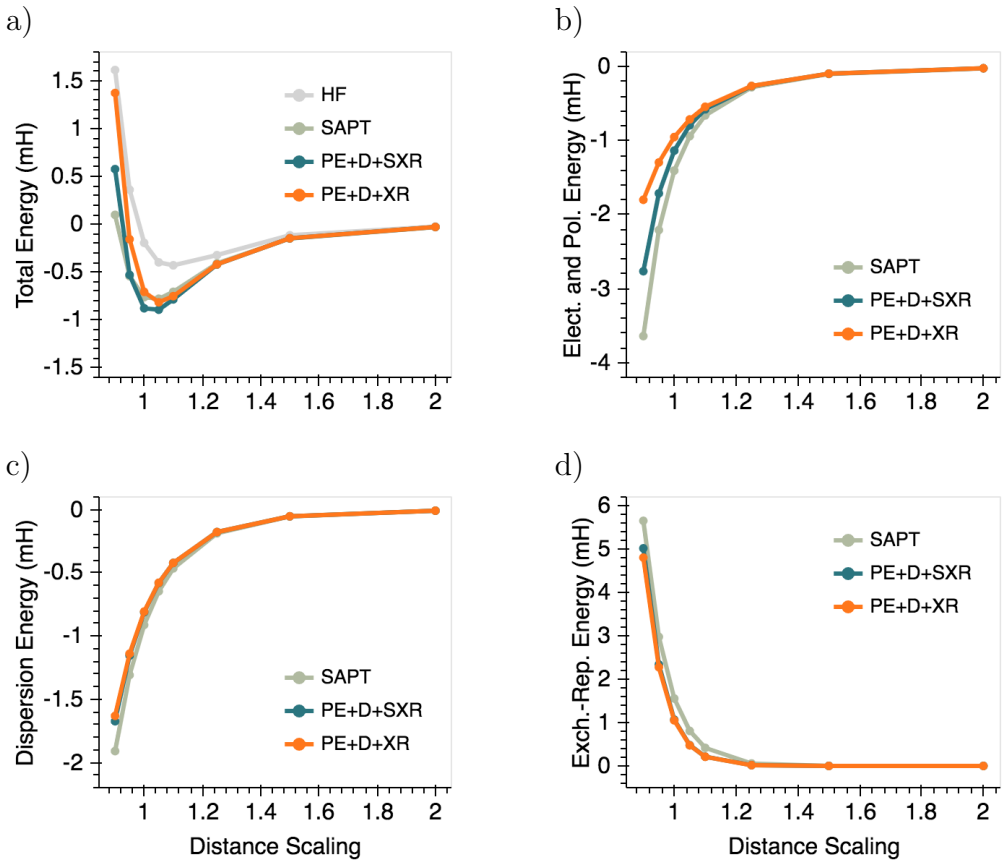

Fig. 5.29. Total interaction energies for the ground state of the water-methane dimer.

Both PE+D+SXR and PE+D+XR produce very accurate values for the ground state energies of this dimer. This energy decomposition is given in Fig. 5.29. These

results show that, as expected, QM/EFP can be used to accurately and efficiently described systems in ground states, but not necessarily systems in excited or triplet states.

In the particular case of the water-methane dimer, a potential reason for the failure of QM/EFP to describe binding in its triplet state might be the presence of charge-transfer. Table 5.2 shows the energy decomposition for the triplet state of the water-methane dimer estimated using FMO/PIEDA. The total interaction energy predicted by PIEDA is close to the CCSD(T) energy (-4.582 mH). Both of the QM/EFP schemes, however, predict positive interaction energies. Table 5.2 confirms that QM/EFP dispersion behaves as expected. Also according to PIEDA, QM/EFP exchange-repulsion is underestimated. Furthermore, while the PE+SXR+D electrostatics and polarization term resembles the PEIDA electrostatics, none of the terms in either QM/EFP scheme account for the -10.586 mH contributed by charge-transfer.

Table 5.2.
Energy decomposition for triplet water-methane dimer at ground state equilibrium geometry. All energies are in units of mH. *only contains electrostatics.

Interaction	PIEDA	PE+SXR+D	PE+XR+D
Elec. + Pol.	-3.799*	-4.351	-0.104
Disp.	-1.914	-2.325	-2.159
Exch.-Rep.	12.052	7.067	5.868
Charge Transfer	-10.586	-	-
Total	-4.247	0.391	3.606

To determine whether charge-transfer is present in other systems, we estimated this value from the Mülliken charges of the fully quantum mechanical HF calculations. This analysis was done for the ground state and lowest triplet state of each dimer at its ground state equilibrium geometry. The results are given in Table 5.3. Taking the water-methane dimer as an example, the positive value of 0.2405 for the triplet state implies the charge transfers from the water molecule to the methane.

Table 5.3.
Charge-transfer estimated from Mülliken charges for each dimer at ground state equilibrium geometry.

Dimer	ground state	triplet state
Peptide-water-a	0.0182	0.0222
Peptide-water-b	-0.0089	-0.0231
Peptide-methanol-a	0.0048	0.0099
Peptide-methanol-a	-0.0120	-0.0284
Uracil-ethene	-0.0229	-0.0252
Uracil-ethyne	-0.0555	-0.0503
Water-methane	0.0053	0.2405

5.4 Conclusions

This chapter explored the possibility of using QM/EFP to compute the energy of low lying triplet states in a small set of dimers. In particular, we were interested in evaluating the performance of the dispersion term. From the results, we see that the PE+D+XR and PE+D+SXR schemes typically achieve triplet state energies that resemble the ones predicted by HF. For some dimers the QM/EFP energies perform better than HF, shifting closer to those estimated by CCSD(T). Overall, QM/EFP dispersion seems to behave normally and there is no significant difference between the values predicted by the PE+D+SXR and PE+D+XR schemes. However, it is

true that adding the screen correction might lead to convergence difficulties at short distances.

For the particular case of the water-methane dimer, the QM/EFP total interaction energies are highly repulsive. It appears most of the error derives from the current inability of QM/EFP to describe energy lowering due to charge-transfer between solute and solvent. While accurately reproducing triplet state dispersion energies is relevant for many applications in catalysis and photovoltaics, the main conclusion of this work is that such states cannot be reliably described with the current implementation of QM/EFP, presumably due to the large contribution of charge-transfer to the total interaction energies and inaccuracies in describing QM/EFP charge-penetration energies.

6. SUMMARY

This thesis focuses on the development and evaluation of QM/EFP models beyond polarizable embedding. Chapter 2 describes the implementation and several benchmarks of the QM/EFP exchange-repulsion term. To reduce the computational cost, this term was constructed as the sum of parametrized Gaussian functions located on the LMO centroids of each effective fragment. Each Gaussian function contains two unique parameters: β which relates to the height of the function and α which relates to the width of the function. The first step in identifying the unique set of parameters for each LMO consisted of selecting various molecules containing such LMO and running molecular dynamic simulations on their corresponding trimers. As a second step, dimers were extracted from the trajectory and their energy was computed using SAPT, EFP and QM/EFP with a specific set of parameters. The last step consisted of finding the set of parameters that, considering all dimers, simultaneously minimized the standard deviation of three different errors: 1) $\mathrm{QM/EFP_{xr}} - \mathrm{EFP_{xr}}$, 2) $\mathrm{QM/EFP_{xr}} - \mathrm{SAPT_{xr}}$, 3) $\mathrm{QM/EFP_{total}} - \mathrm{SAPT_{total}}$. The tests used to evaluate the performance of this parametrization included: 1) reproducing the potential energy curve for water, methane, ammonia and benzene dimers, 2) estimating the interaction energy for dimers obtained from Monte Carlo simulations, and 3) computing total interaction energy for dimers from the S22 dataset. All of these tests lead to similar results, suggesting that while the parametrized QM/EFP exchange-repulsion term was usually underestimated with respect to SAPT, the total QM/EFP and SAPT energies agreed well. The dimers in which QM/EFP tends to have larger errors are those in which there exists some level of conjugation, including aromatic rings, amides or esters. This is a reasonable result, since no specific parameters were identified for such functional groups (except for benzene).

Chapter 3 centers on the evaluation of the parametrized QM/EFP exchange-repulsion term on more complex systems, specifically polar-polar and aryl-aryl amino acid dimers. Since no parameters were previously identified for the peptide-bond, this chapter explores the possible ways in which such group can be described. The options differed in the parameters assigned to the CN bond, which could correspond to a double CN bond or a single CN bond with a lone pair of electrons on the nitrogen. Both of these methods perform similarly, but the first is recommended in order to minimize mean absolute and mean signed errors. However, if the amino acid contains an additional primary amide (as glutamine and asparagine do), the corresponding CN should be described with the second method. Using this assignment of parameters, the results from this chapter support the conclusions from Chapter 2, that is, while the parametrized exchange-repulsion might be too weak, the total QM/EFP interaction energies match those from SAPT. Also as observed in Chapter 2, these results associate larger errors with the aryl-aryl dimers. For QM/EFP these errors derive not only from exchange-repulsion being too weak but also from the other terms being underestimated. Furthermore, for these dimers the EFP total energies have only a slightly larger error than QM/EFP energies. Interestingly, EFP tends to better predict dispersion and exchange-repulsion, but not electrostatics and polarization.

The work done in Chapters 2 and 3 establishes parameterized exchange-repulsion as a way to efficiently incorporate the term in QM/EFP interaction energies of ground state dimers. However, non-covalent interactions can affect many electronic properties of a given system. Chapter 4 explores how different QM/EFP embedding schemes alter the singlet excitation energies of a variety of chromophores surrounded by water, ammonia, methanol and/or formic acid. In particular, this chapter looks at the effect of adding two terms to the traditional polarizable embedding. The first term is the parametrized exchange-repulsion. The second term is a charge-penetration correction known as electrostatics screen, which smears the electronic point charges located on the fragments to closer mimic quantum mechanical electronic distributions. The

excitation energies computed with each QM/EFP scheme were directly compared to fully quantum mechanical excitations, such that a positive error would suggest the QM/EFP excitation energies were too high and a negative error would imply the QM/EFP excitation energies were too low. The results indicate that adding the electrostatics screen leads to larger and more positive energy errors compared to the polarizable embedding. Adding exchange-repulsion has the opposite effect, it lowers the excitation energy errors, bringing the signed mean error close to 0 eV. Most of the shift in this error comes from a better prediction of the excitation energies for n$\pi*$ transitions. These transitions tend to have partial charge transfer from the solvent to the solute. Adding exchange-repulsion destabilizes the density on the solvent, meaning it increases the energy of the occupied orbital and ultimately leads to more accurate excitation energies. Such effect was observed independently of the basis set used in the QM region but did deteriorate if the EFP potential was computed differently. This is expected, since exchange-repulsion was parametrized specifically for EFP potentials done with a hybrid basis set: 6-31+G(d) for electrostatics and 6-311++G(3df,2p) for all other components.

With the objective of further testing the limits of QM/EFP, Chapter 5 focuses on the description of triplet states, that is, dimers in which the QM region is in the lowest lying triplet state while the effective fragment remains in the singlet ground state. Of particular interest in this chapter, was the change in dispersion that occurs when going from the ground state to the lowest triplet state. Despite only looking at a few dimers, the results are conflicting for a number of reasons. First, dispersion behaves as expected but can be affected if convergence issues arise from adding the electrostatics screen. Second, the total QM/EFP interaction energies seem to better match the Hartree-Fock energies when dispersion and electrostatics screening are included, however the latter often leads to convergence issues at short distances. Finally, all QM/EFP schemes failed to describe binding in the lowest triplet state of the water-methane dimer. According to the PIEDA/FMO analysis performed on the system, its total interaction energy is largely impacted by the charge-transfer term.

The studied QM/EFP schemes only account for a small portion of charge-transfer through the electrostatics screening correction, which suggests an important future direction for the development of QM/EFP models.

REFERENCES

REFERENCES

[1] P. N. Day, J. H. Jensen, M. S. Gordon, S. P. Webb, W. J. Stevens, M. Krauss, D. Garmer, H. Basch, and D. Cohen, "An effective fragment method for modeling solvent effects in quantum mechanical calculations," *J. Chem. Phys.*, vol. 105, no. 5, pp. 1968–1986, 1996.

[2] M. S. Gordon, M. A. Freitag, P. Bandyopadhyay, J. H. Jensen, V. Kairys, and W. J. Stevens, "The effective fragment potential method: a qm-based mm approach to modeling environmental effects in chemistry," *J. Phys. Chem. A*, vol. 105, no. 2, pp. 293–307, 2001.

[3] M. S. Gordon, L. Slipchenko, H. Li, and J. H. Jensen, "The effective fragment potential: a general method for predicting intermolecular interactions," *Annu. Rep. Comput. Chem.*, vol. 3, pp. 177–193, 2007.

[4] M. S. Gordon, D. G. Fedorov, S. R. Pruitt, and L. V. Slipchenko, "Fragmentation methods: A route to accurate calculations on large systems," *Chem. Rev.*, vol. 112, no. 1, pp. 632–672, 2012.

[5] M. S. Gordon, Q. A. Smith, P. Xu, and L. V. Slipchenko, "Accurate first principles model potentials for intermolecular interactions," *Annu. Rev. Phys. Chem.*, vol. 64, pp. 553–578, 2013.

[6] L. V. Slipchenko, *Effective Fragment Potential Method.* CRC Press, 2016, p. 147.

[7] L. V. Slipchenko and P. K. Gurunathan, *Effective Fragment Potential Method: Past, Present, and Future.* Wiley-Blackwell, 2017, ch. 6, pp. 183–208.

[8] J. W. Ponder, C. Wu, P. Ren, V. S. Pande, J. D. Chodera, M. J. Schnieders, I. Haque, D. L. Mobley, D. S. Lambrecht, R. A. DiStasio Jr *et al.*, "Current status of the amoeba polarizable force field," *J. Phys. Chem. B*, vol. 114, no. 8, pp. 2549–2564, 2010.

[9] G. Cisneros, T. Darden, N. Gresh, J. Pilmé, P. Reinhardt, O. Parisel, and J.-P. Piquemal, "Design of next generation force fields from ab initio computations: Beyond point charges electrostatics," in *Multi-scale Quantum Models for Biocatalysis.* Springer, 2009, pp. 137–172.

[10] J.-P. Piquemal, G. A. Cisneros, P. Reinhardt, N. Gresh, and T. A. Darden, "Towards a force field based on density fitting," *J. Chem. Phys.*, vol. 124, no. 10, p. 104101, 2006.

[11] T. Schwabe, J. M. H. Olsen, K. Sneskov, J. Kongsted, and O. Christiansen, "Solvation effects on electronic transitions: Exploring the performance of advanced solvent potentials in polarizable embedding calculations," *J. Chem. Theory Comput.*, vol. 7, no. 7, pp. 2209–2217, 2011.

[12] K. Sneskov, T. Schwabe, J. Kongsted, and O. Christiansen, "The polarizable embedding coupled cluster method," *J. Chem. Phys.*, vol. 134, no. 10, p. 03B608, 2011.

[13] A. H. Steindal, K. Ruud, L. Frediani, K. Aidas, and J. Kongsted, "Excitation energies in solution: the fully polarizable qm/mm/pcm method," *J. Phys. Chem. B*, vol. 115, no. 12, pp. 3027–3037, 2011.

[14] S. Grimme, "A general quantum mechanically derived force field (qmdff) for molecules and condensed phase simulations," *J. Chem. Theory Comput.*, vol. 10, no. 10, pp. 4497–4514, 2014.

[15] J. G. McDaniel, K. Yu, and J. Schmidt, "Ab initio, physically motivated force fields for co2 adsorption in zeolitic imidazolate frameworks," *J. Chem. Phys. C*, vol. 116, no. 2, pp. 1892–1903, 2012.

[16] P. K. Gurunathan, A. Acharya, D. Ghosh, D. Kosenkov, I. Kaliman, Y. Shao, A. I. Krylov, and L. V. Slipchenko, "Extension of the effective fragment potential method to macromolecules," *J. Phys. Chem. B*, vol. 120, no. 27, pp. 6562–6574, 2016.

[17] L. V. Slipchenko and M. S. Gordon, "Electrostatic energy in the effective fragment potential method: Theory and application to benzene dimer," *J. Comput. Chem.*, vol. 28, no. 1, pp. 276–291, 2007.

[18] L. V. Slipchenko and M. S. Gordon, "Damping functions in the effective fragment potential method," *Mol. Phys.*, vol. 107, no. 8-12, pp. 999–1016, 2009.

[19] D. Ghosh, D. Kosenkov, V. Vanovschi, C. F. Williams, J. M. Herbert, M. S. Gordon, M. W. Schmidt, L. V. Slipchenko, and A. I. Krylov, "Noncovalent interactions in extended systems described by the effective fragment potential method: Theory and application to nucleobase oligomers," *J. Phys. Chem. A*, vol. 114, no. 48, pp. 12 739–12 754, 2010.

[20] I. Adamovic and M. S. Gordon, "Dynamic polarizability, dispersion coefficient c6 and dispersion energy in the effective fragment potential method," *Mol. Phys.*, vol. 103, no. 2-3, pp. 379–387, 2005.

[21] M. S. Gordon and J. H. Jensen, "An approximate formula for the intermolecular pauli repulsion between closed shell molecules," *Mol. Phys.*, vol. 89, no. 5, pp. 1313–1325, 1996.

[22] J. H. Jensen and M. S. Gordon, "An approximate formula for the intermolecular pauli repulsion between closed shell molecules. ii. application to the effective fragment potential method," *J. Chem. Phys.*, vol. 108, no. 12, p. 4772, 1998.

[23] M. W. Schmidt, K. K. Baldridge, J. A. Boatz, S. T. Elbert, M. S. Gordon, J. H. Jensen, S. Koseki, N. Matsunaga, K. A. Nguyen, S. Su, T. Windus, M. Dupuis, and J. Montgomery, "General atomic and molecular electronic structure system," *J. Comput. Chem.*, vol. 14, no. 11, pp. 1347–1363, 1993.

[24] M. S. Gordon and M. W. Schmidt, "Advances in electronic structure theory: Gamess a decade later," in *Theory and applications of computational chemistry.* Elsevier, 2005, pp. 1167–1189.

[25] P. R. Callis and T. Liu, "Short range photoinduced electron transfer in proteins: Qm-mm simulations of tryptophan and flavin fluorescence quenching in proteins," *J. Chem. Phys.*, vol. 326, no. 1, pp. 230–239, 2006.

[26] S. Hayashi and I. Ohmine, "Proton transfer in bacteriorhodopsin: structure, excitation, ir spectra, and potential energy surface analyses by an ab initio qm/mm method," *J. Phys. Chem. B*, vol. 104, no. 45, pp. 10 678–10 691, 2000.

[27] C. M. Isborn, A. W. Gotz, M. A. Clark, R. C. Walker, and T. J. Martínez, "Electronic absorption spectra from mm and ab initio qm/mm molecular dynamics: Environmental effects on the absorption spectrum of photoactive yellow protein," *J. Chem. Theory Comput.*, vol. 8, no. 12, pp. 5092–5106, 2012.

[28] M. Parac, M. Doerr, C. M. Marian, and W. Thiel, "Qm/mm calculation of solvent effects on absorption spectra of guanine," *J. Comput. Chem.*, vol. 31, no. 1, pp. 90–106, 2010.

[29] H. M. Senn and W. Thiel, "Qm/mm methods for biomolecular systems," *Angew. Chem. Int. Ed.*, vol. 48, no. 7, pp. 1198–1229, 2009.

[30] A. Warshel and M. Levitt, "Theoretical studies of enzymic reactions: dielectric, electrostatic and steric stabilization of the carbonium ion in the reaction of lysozyme," *J. Mol. Biol.*, vol. 103, no. 2, pp. 227–249, 1976.

[31] J. Chen and T. J. Martinez, "Qtpie: Charge transfer with polarization current equalization. a fluctuating charge model with correct asymptotics," *Chem. Phys. Lett.*, vol. 438, no. 4-6, pp. 315–320, 2007.

[32] A. Damjanović, I. Kosztin, U. Kleinekathöfer, and K. Schulten, "Excitons in a photosynthetic light-harvesting system: a combined molecular dynamics, quantum chemistry, and polaron model study," *Phys. Rev. E*, vol. 65, no. 3, p. 031919, 2002.

[33] R. A. Friesner and V. Guallar, "Ab initio quantum chemical and mixed quantum mechanics/molecular mechanics (qm/mm) methods for studying enzymatic catalysis," *Annu. Rev. Phys. Chem.*, vol. 56, pp. 389–427, 2005.

[34] R. D. Froese and K. Morokuma, "The imomo and imonm methods for excited states. a study of the adiabatic $s0 \rightarrow t1$, 2 excitation energies of cyclic alkenes and enones," *Chem. Phys. Lett.*, vol. 263, no. 3-4, pp. 393–400, 1996.

[35] J. Gao, "Hybrid quantum and molecular mechanical simulations: an alternative avenue to solvent effects in organic chemistry," *Acc. Chem. Res.*, vol. 29, no. 6, pp. 298–305, 1996.

[36] v. J. Gao, "Methods and applications of combined quantum mechanical and molecular mechanical potentials," *Rev. Comput. Chem.*, vol. 7, pp. 119–186, 1996.

[37] J. Gao and D. G. Truhlar, "Quantum mechanical methods for enzyme kinetics," *Annu. Rev. Phys. Chem.*, vol. 53, no. 1, pp. 467–505, 2002.

[38] T. Z. Mordasini and W. Thiel, "Combined quantum mechanical and molecular mechanical approaches," *Chimia*, vol. 52, no. 6, pp. 288–291, 1998.

[39] M. J. Field, P. A. Bash, and M. Karplus, "A combined quantum mechanical and molecular mechanical potential for molecular dynamics simulations," *J. Comput. Chem.*, vol. 11, no. 6, pp. 700–733, 1990.

[40] U. C. Singh and P. A. Kollman, "A combined ab initio quantum mechanical and molecular mechanical method for carrying out simulations on complex molecular systems: Applications to the ch3cl+ cl- exchange reaction and gas phase protonation of polyethers," *J. Comput. Chem.*, vol. 7, no. 6, pp. 718–730, 1986.

[41] R. V. Stanton, L. R. Little, and K. M. Merz Jr, "An examination of a hartree-fock/molecular mechanical coupled potential," *J. Phys. Chem.*, vol. 99, no. 48, pp. 17 344–17 348, 1995.

[42] P. Canfield, M. G. Dahlbom, N. S. Hush, and J. R. Reimers, "Density-functional geometry optimization of the 150 000-atom photosystem-i trimer," *J. Chem. Phys.*, vol. 124, no. 2, p. 024301, 2006.

[43] M. Svensson, S. Humbel, R. D. Froese, T. Matsubara, S. Sieber, and K. Morokuma, "Oniom: a multilayered integrated mo+ mm method for geometry optimizations and single point energy predictions. a test for diels- alder reactions and pt (p (t-bu) 3) 2+ h2 oxidative addition," *J. Phys. Chem.*, vol. 100, no. 50, pp. 19 357–19 363, 1996.

[44] T. Vreven, K. Morokuma, Ö. Farkas, H. B. Schlegel, and M. J. Frisch, "Geometry optimization with qm/mm, oniom, and other combined methods. i. microiterations and constraints," *J. Comput. Chem.*, vol. 24, no. 6, pp. 760–769, 2003.

[45] M. Higashi and D. G. Truhlar, "Combined electrostatically embedded multiconfiguration molecular mechanics and molecular mechanical method: application to molecular dynamics simulation of a chemical reaction in aqueous solution with hybrid density functional theory," *J. Chem. Theory Comput.*, vol. 4, no. 7, pp. 1032–1039, 2008.

[46] O. Tishchenko and D. G. Truhlar, "Optimizing the performance of the multiconfiguration molecular mechanics method," *J. Phys. Chem. A*, vol. 110, no. 50, pp. 13 530–13 536, 2006.

[47] D. Ghosh, O. Isayev, L. V. Slipchenko, and A. I. Krylov, "Effect of solvation on the vertical ionization energy of thymine: from microhydration to bulk," *J. Phys. Chem. A*, vol. 115, no. 23, pp. 6028–6038, 2011.

[48] D. Kosenkov and L. V. Slipchenko, "Solvent effects on the electronic transitions of p-nitroaniline: A qm/efp study," *J. Phys. Chem. A*, vol. 115, no. 4, pp. 392–401, 2010.

[49] D. Ghosh, D. Kosenkov, V. Vanovschi, J. Flick, I. Kaliman, Y. Shao, A. T. Gilbert, A. I. Krylov, and L. V. Slipchenko, "Effective fragment potential method in q-chem: A guide for users and developers," *J. Comput. Chem.*, vol. 34, no. 12, pp. 1060–1070, 2013.

[50] L. V. Slipchenko, "Solvation of the excited states of chromophores in polarizable environment: orbital relaxation versus polarization," *J. Phys. Chem. A*, vol. 114, no. 33, pp. 8824–8830, 2010.

[51] L. V. Slipchenko, M. S. Gordon, and K. Ruedenberg, "Dispersion interactions in qm/efp," *J. Phys.Chem. A*, vol. 121, no. 49, pp. 9495–9507, 2017.

[52] A. DeFusco, N. Minezawa, L. V. Slipchenko, F. Zahariev, and M. S. Gordon, "Modeling solvent effects on electronic excited states," *J. Phys. Chem. Lett.*, vol. 2, no. 17, pp. 2184–2192, 2011.

[53] B. M. Rankin, M. D. Hands, D. S. Wilcox, K. R. Fega, L. V. Slipchenko, and D. Ben-Amotz, "Interactions between halide anions and a molecular hydrophobic interface," *Faraday Disc.*, vol. 160, pp. 255–270, 2013.

[54] A. DeFusco, J. Ivanic, M. W. Schmidt, and M. S. Gordon, "Solvent-induced shifts in electronic spectra of uracil," *J. Phys. Chem. A*, vol. 115, no. 18, pp. 4574–4582, 2011.

[55] I. Adamovic and M. S. Gordon, "Solvent effects on the sn2 reaction: application of the density functional theory-based effective fragment potential method," *J. Phys. Chem. A*, vol. 109, no. 8, pp. 1629–1636, 2005.

[56] D. E. Ferreira, B. P. Florentino, W. R. Rocha, and F. Nome, "Quantum mechanical/effective fragment potential (qm/efp) study of phosphate monoester aminolysis in aqueous solution," *J. Phys. Chem. B*, vol. 113, no. 44, pp. 14 831–14 836, 2009.

[57] I. A. Kaliman and L. V. Slipchenko, "Libefp: A new parallel implementation of the effective fragment potential method as a portable software library," *J. Comput. Chem.*, vol. 34, no. 26, pp. 2284–2292, 2013.

[58] I. A. v. Kaliman and L. V. Slipchenko, "Hybrid mpi/openmp parallelization of the effective fragment potential method in the libefp software library," *J. Comput. Chem.*, vol. 36, no. 2, pp. 129–135, 2015.

[59] T. H. Dunning Jr and P. J. Hay, "Gaussian basis sets for molecular calculations," in *Methods of electronic structure theory*. Springer, 1977, pp. 1–27.

[60] E. G. Hohenstein and C. D. Sherrill, "Density fitting of intramonomer correlation effects in symmetry-adapted perturbation theory," *J. Chem. Phys.*, vol. 133, no. 1, p. 014101, 2010.

[61] E. G. Hohenstein, R. M. Parrish, C. D. Sherrill, J. M. Turney, and H. F. Schaefer III, "Large-scale symmetry-adapted perturbation theory computations via density fitting and laplace transformation techniques: Investigating the fundamental forces of dna-intercalator interactions," *J. Chem. Phys.*, vol. 135, no. 17, p. 174107, 2011.

[62] T. H. Dunning Jr, "Gaussian basis sets for use in correlated molecular calculations. i. the atoms boron through neon and hydrogen," *J. Chem. Phys.*, vol. 90, no. 2, pp. 1007–1023, 1989.

[63] J. M. Turney, A. C. Simmonett, R. M. Parrish, E. G. Hohenstein, F. A. Evangelista, J. T. Fermann, B. J. Mintz, L. A. Burns, J. J. Wilke, M. L. Abrams *et al.*, "Psi4: an open-source ab initio electronic structure program," *Wiley Interdiscip. Rev. Comput. Mol. Sci.*, vol. 2, no. 4, pp. 556–565, 2012.

[64] J. D. Dill and J. A. Pople, "Self-consistent molecular orbital methods. xv. extended gaussian-type basis sets for lithium, beryllium, and boron," *J. Chem. Phys.*, vol. 62, no. 7, pp. 2921–2923, 1975.

[65] W. J. Hehre, R. Ditchfield, and J. A. Pople, "Self—consistent molecular orbital methods. xii. further extensions of gaussian—type basis sets for use in molecular orbital studies of organic molecules," *J. Chem. Phys.*, vol. 56, no. 5, pp. 2257–2261, 1972.

[66] W. Hehre and J. Pople, "Self-consistent molecular orbital methods. xiii. an extended gaussian-type basis for boron," *J. Chem. Phys.*, vol. 56, no. 8, pp. 4233–4234, 1972.

[67] W. J. Hehre and W. A. Lathan, "Self-consistent molecular orbital methods. xiv. an extended gaussian-type basis for molecular orbital studies of organic molecules. inclusion of second row elements," *J. Chem. Phys.*, vol. 56, no. 11, pp. 5255–5257, 1972.

[68] J. S. Binkley and J. A. Pople, "Self-consistent molecular orbital methods. xix. split-valence gaussian-type basis sets for beryllium," *J. Chem. Phys.*, vol. 66, no. 2, pp. 879–880, 1977.

[69] M. M. Francl, W. J. Pietro, W. J. Hehre, J. S. Binkley, M. S. Gordon, D. J. DeFrees, and J. A. Pople, "Self-consistent molecular orbital methods. xxiii. a polarization-type basis set for second-row elements," *J. Chem. Phys.*, vol. 77, no. 7, pp. 3654–3665, 1982.

[70] R. Krishnan, J. S. Binkley, R. Seeger, and J. A. Pople, "Self-consistent molecular orbital methods. xx. a basis set for correlated wave functions," *J. Chem. Phys.*, vol. 72, no. 1, pp. 650–654, 1980.

[71] J. C. Flick, D. Kosenkov, E. G. Hohenstein, C. D. Sherrill, and L. V. Slipchenko, "Accurate prediction of noncovalent interaction energies with the effective fragment potential method: Comparison of energy components to symmetry-adapted perturbation theory for the s22 test set," *J. Chem. Theory Comput.*, vol. 8, no. 8, pp. 2835–2843, 2012.

[72] P. Jurečka, J. Šponer, J. Černỳ, and P. Hobza, "Benchmark database of accurate (mp2 and ccsd (t) complete basis set limit) interaction energies of small model complexes, dna base pairs, and amino acid pairs," *Phy. Chem. Chem. Phys.*, vol. 8, no. 17, pp. 1985–1993, 2006.

[73] M. O. Sinnokrot and C. D. Sherrill, "Highly accurate coupled cluster potential energy curves for the benzene dimer: sandwich, t-shaped, and parallel-displaced configurations," *J. Phys. Chem. A*, vol. 108, no. 46, pp. 10 200–10 207, 2004.

[74] P. N. Day, R. Pachter, M. S. Gordon, and G. N. Merrill, "A study of water clusters using the effective fragment potential and monte carlo simulated annealing," *J. Chem. Phys.*, vol. 112, no. 5, pp. 2063–2073, 2000.

[75] T. Takatani, E. G. Hohenstein, M. Malagoli, M. S. Marshall, and C. D. Sherrill, "Basis set consistent revision of the s22 test set of noncovalent interaction energies," *J. Chem. Phys.*, vol. 132, no. 14, p. 144104, 2010.

[76] D. D. Kemp, J. M. Rintelman, M. S. Gordon, and J. H. Jensen, "Exchange repulsion between effective fragment potentials and ab initio molecules," *Theor. Chem. Acc.*, vol. 125, no. 3-6, pp. 481–491, 2010.

[77] J. Rezác, K. E. Riley, and P. Hobza, "S66: A well-balanced database of benchmark interaction energies relevant to biomolecular structures," *J. Chem. Theory Comput.*, vol. 7, no. 8, pp. 2427–2438, 2011.

[78] S. F. Boys, *Quantum theory of atoms, molecules, and the solid state*, P.-O. Löwdin, Ed. Academic Press, 1966.

[79] C. Edmiston and K. Ruedenberg, "Localized atomic and molecular orbitals," *Rev. Mod. Phys.*, vol. 35, no. 3, p. 457, 1963.

[80] C. I. Viquez Rojas, J. Fine, and L. V. Slipchenko, "Exchange-repulsion energy in qm/efp," *J. Chem. Phys.*, vol. 149, no. 9, p. 094103, 2018.

[81] R. Chakraborty, S. Bose, and D. Ghosh, "Effect of solvation on the ionization of guanine nucleotide: A hybrid qm/efp study," *J. Comput. Chem.*, vol. 38, no. 29, pp. 2528–2537, 2017.

[82] Y. Kim, D. Morozov, V. Stadnytskyi, S. Savikhin, and L. Slipchenko, "Predictive first-principles modeling of a photosynthetic antenna protein: The fenna-matthews-olson complex," *J. Phys. Chem. Lett.*, 2020.

[83] Y. Kim and L. V. Slipchenko, "Effective fragment potentials for flexible molecules: Transferable parameters and amino acid database," *manuscript in preparation*.

[84] T. M. Parker, L. A. Burns, R. M. Parrish, A. G. Ryno, and C. D. Sherrill, "Levels of symmetry adapted perturbation theory (sapt). i. efficiency and performance for interaction energies," *J. Chem. Phys.*, vol. 140, no. 9, p. 094106, 2014.

[85] R. M. Parrish, L. A. Burns, D. G. Smith, A. C. Simmonett, A. E. DePrince III, E. G. Hohenstein, U. Bozkaya, A. Y. Sokolov, R. Di Remigio, R. M. Richard *et al.*, "Psi4 1.1: An open-source electronic structure program emphasizing automation, advanced libraries, and interoperability," *J. Chem. Theory Comput.*, vol. 13, no. 7, pp. 3185–3197, 2017.

[86] R. A. Kendall, T. H. Dunning Jr, and R. J. Harrison, "Electron affinities of the first-row atoms revisited. systematic basis sets and wave functions," *J. Chem. Phys.*, vol. 96, no. 9, pp. 6796–6806, 1992.

[87] J. Blumberger, "Free energies for biological electron transfer from qm/mm calculation: method, application and critical assessment," *Phys. Chem. Chem. Phys.*, vol. 10, no. 37, pp. 5651–5667, 2008.

[88] P. Söderhjelm, C. Husberg, A. Strambi, M. Olivucci, and U. Ryde, "Protein influence on electronic spectra modeled by multipoles and polarizabilities," *J. Chem. Theory Comput.*, vol. 5, no. 3, pp. 649–658, 2009.

[89] R. Tazhigulov, P. K. Gurunathan, Y. Kim, L. Slipchenko, and K. B. Bravaya, "Polarizable embedding for simulating redox potentials of biomolecules," *Phys. Chem. Chem. Phys.*, 2019.

[90] M. T. Beerepoot, A. H. Steindal, K. Ruud, J. M. H. Olsen, and J. Kongsted, "Convergence of environment polarization effects in multiscale modeling of excitation energies," *Comput. Theor. Chem.*, vol. 1040, pp. 304–311, 2014.

[91] A. Marefat Khah, P. Reinholdt, J. M. H. Olsen, J. Kongsted, and C. Hattig, "Avoiding electron spill-out in qm/mm calculations on excited states with simple pseudopotentials," *J. Chem. Theory Comput.*, vol. 16, no. 3, pp. 1373–1381, 2020.

[92] J. Dziedzic, T. Head-Gordon, M. Head-Gordon, and C.-K. Skylaris, "Mutually polarizable qm/mm model with in situ optimized localized basis functions," *J. Chem. Phys.*, vol. 150, no. 7, p. 074103, 2019.

[93] P. Reinholdt, J. Kongsted, and J. M. H. Olsen, "Polarizable density embedding: A solution to the electron spill-out problem in multiscale modeling," *J. Phys. Chem. Lett.*, vol. 8, no. 23, pp. 5949–5958, 2017.

[94] T. Giovannini, M. Ambrosetti, and C. Cappelli, "Quantum confinement effects on solvatochromic shifts of molecular solutes," *J. Phys. Chem. Lett.*, vol. 10, no. 19, pp. 5823–5829, 2019.

[95] T. Giovannini, P. Lafiosca, and C. Cappelli, "A general route to include pauli repulsion and quantum dispersion effects in qm/mm approaches," *J. Chem. Theory Comput.*, vol. 13, no. 10, pp. 4854–4870, 2017.

[96] H. Gökcan, E. Kratz, T. A. Darden, J.-P. Piquemal, and G. A. Cisneros, "Qm/mm simulations with the gaussian electrostatic model: a density-based polarizable potential," *J. Phys. Chem. Lett.*, vol. 9, no. 11, pp. 3062–3067, 2018.

[97] N. H. List, J. M. H. Olsen, and J. Kongsted, "Excited states in large molecular systems through polarizable embedding," *Phys. Chem. Chem. Phys.*, vol. 18, no. 30, pp. 20 234–20 250, 2016.

[98] A. Zech, N. Ricardi, S. Prager, A. Dreuw, and T. A. Wesolowski, "Benchmark of excitation energy shifts from frozen-density embedding theory: Introduction of a density-overlap-based applicability threshold," *J. Chem. Theory Comput.*, vol. 14, no. 8, pp. 4028–4040, 2018.

[99] R. L. Martin, "Natural transition orbitals," *J. Chem. Phys.*, vol. 118, no. 11, pp. 4775–4777, 2003.

[100] F. Liu, E. Livshits, R. C. Lochan, A. Luenser, P. Manohar, S. F. Manzer, S.-P. Mao, N. Mardirossian, A. V. Marenich, S. A. Maurer *et al.*, "Advances in molecular quantum chemistry contained in the q-chem 4 program package," 2015.

[101] Y. Mao, M. Head-Gordon, and Y. Shao, "Unraveling substituent effects on frontier orbitals of conjugated molecules using an absolutely localized molecular orbital based analysis," *Chem. Sci.*, vol. 9, no. 45, pp. 8598–8607, 2018.

[102] M. Einzinger, T. Wu, J. F. Kompalla, H. L. Smith, C. F. Perkinson, L. Nienhaus, S. Wieghold, D. N. Congreve, A. Kahn, M. G. Bawendi *et al.*, "Sensitization of silicon by singlet exciton fission in tetracene," *Nature*, vol. 571, no. 7763, pp. 90–94, 2019.

[103] D. N. Congreve, J. Lee, N. J. Thompson, E. Hontz, S. R. Yost, P. D. Reusswig, M. E. Bahlke, S. Reineke, T. Van Voorhis, and M. A. Baldo, "External quantum efficiency above 100% in a singlet-exciton-fission–based organic photovoltaic cell," *Science*, vol. 340, no. 6130, pp. 334–337, 2013.

[104] N. J. Thompson, D. N. Congreve, D. Goldberg, V. M. Menon, and M. A. Baldo, "Slow light enhanced singlet exciton fission solar cells with a 126% yield of electrons per photon," *Appl. Phys. Lett.*, vol. 103, no. 26, p. 244_1, 2013.

[105] L. Yang, M. Tabachnyk, S. L. Bayliss, M. L. Böhm, K. Broch, N. C. Greenham, R. H. Friend, and B. Ehrler, "Solution-processable singlet fission photovoltaic devices," *Nano Lett.*, vol. 15, no. 1, pp. 354–358, 2015.

[106] Y. Lu, N. McGoldrick, F. Murphy, B. Twamley, X. Cui, C. Delaney, G. M. O. Máille, J. Wang, J. Zhao, and S. M. Draper, "Highly efficient triplet photosensitizers: A systematic approach to the application of iriii complexes containing extended phenanthrolines," *Chem. Eur. J.*, vol. 22, no. 32, pp. 11 349–11 356, 2016.

[107] J. Zhao, W. Wu, J. Sun, and S. Guo, "Triplet photosensitizers: from molecular design to applications," *Chem. Soc. Rev*, vol. 42, no. 12, pp. 5323–5351, 2013.

[108] J. D. Williams, M. Nakano, R. Gérardy, J. A. Rincón, O. de Frutos, C. Mateos, J.-C. M. Monbaliu, and C. O. Kappe, "Finding the perfect match: a combined computational and experimental study toward efficient and scalable photosensitized [2+ 2] cycloadditions in flow," *Org. Process Res. Dev.*, vol. 23, no. 1, pp. 78–87, 2018.

[109] J. Rezác, K. E. Riley, and P. Hobza, "Extensions of the s66 data set: more accurate interaction energies and angular-displaced nonequilibrium geometries," *J. Chem. Theory Comput.*, vol. 7, no. 11, pp. 3466–3470, 2011.

[110] P. C. Hariharan and J. A. Pople, "The influence of polarization functions on molecular orbital hydrogenation energies," *Theor. Chim. Acta*, vol. 28, no. 3, pp. 213–222, 1973.

[111] T. Clark, J. Chandrasekhar, G. W. Spitznagel, and P. V. R. Schleyer, "Efficient diffuse function-augmented basis sets for anion calculations. iii. the 3-21+ g basis set for first-row elements, li–f," *J. Comput. Chem.*, vol. 4, no. 3, pp. 294–301, 1983.

[112] M. C. Green, D. G. Fedorov, K. Kitaura, J. S. Francisco, and L. V. Slipchenko, "Open-shell pair interaction energy decomposition analysis (pieda): Formulation and application to the hydrogen abstraction in tripeptides," *J. Chem. Phys.*, vol. 138, no. 7, p. 074111, 2013.

[113] K. Kitaura, E. Ikeo, T. Asada, T. Nakano, and M. Uebayasi, "Fragment molecular orbital method: an approximate computational method for large molecules," *Chem. Phys. Lett.*, vol. 313, no. 3-4, pp. 701–706, 1999.

[114] D. G. Fedorov and K. Kitaura, "Extending the power of quantum chemistry to large systems with the fragment molecular orbital method," *J. Phys. Chem. A*, vol. 111, no. 30, pp. 6904–6914, 2007.

[115] D. G. Fedorov, T. Nagata, and K. Kitaura, "Exploring chemistry with the fragment molecular orbital method," *Phys. Chem. Chem. Phys.*, vol. 14, no. 21, pp. 7562–7577, 2012.

[116] T. D. Crawford and H. F. Schaefer, "An introduction to coupled cluster theory for computational chemists," *Rev. Comput. Chem.*, vol. 14, pp. 33–136, 2000.

APPENDICES

A. SUPPLEMENTARY MATERIAL FOR CHAPTER 2

This appendix contains the supplementary information for Chapter 2, parametrization of the QM/EFP exchange-repulsion term.

A.1 Coordinates (Å) of local and global minima of dimers found with EFP Monte Carlo simulations

2-aminopyridine

N -8.0702736785 -2.7806608567 1.4101812327

C -6.8593647345 -2.9578517062 0.8519149249

C -6.3525381841 -4.2475790025 0.5993574062

C -7.1114170139 -5.3523694181 0.9314515265

C -8.3680915659 -5.1685932517 1.5122344467

C -8.7911911161 -3.8686925078 1.7271325768

H -5.3765653660 -4.3594894733 0.1472391343

H -6.7297476202 -6.3464976169 0.7427739725

H -8.9940577194 -6.0025325990 1.7904737058

H -9.7565428963 -3.6749120169 2.1800074366

N -6.1662869056 -1.8373025519 0.4936625211

H -5.1826334757 -1.9598054628 0.3298471350

H -6.4231492884 -0.9616429614 0.9523784011

N -8.3224933149 2.2523304060 2.3906579724

C -8.3350393312 0.9123250080 2.5072189832

C -7.5347458563 0.2540630971 3.4613031315

C -6.7203621545 0.9968251753 4.2930657942

C -6.7062655308 2.3879727242 4.1713152631

C -7.5218686417 2.9555898215 3.2082271176

H -7.5672053649 -0.8244270454 3.5338511825

H -6.1012063873 0.4999489143 5.0274510734

H -6.0835828148 3.0079518380 4.7978914192

H -7.5417258100 4.0305658596 3.0719084195

N -9.1927853834 0.2226767747 1.6991415779

H -9.0127530932 -0.7608776493 1.6010315194

H -9.5142886579 0.6908593881 0.8502488016

2-butanol

C 7.6388062555 2.0450667635 -1.1132914212

C 6.9854254020 2.6148338769 -2.3737545247

C 5.4657238169 2.7536597969 -2.2636712530

C 4.8562311613 3.4297974237 -3.4892641951

H 8.7123987189 1.9513026906 -1.2443898717

H 7.2379442716 1.0672891959 -0.8738300514

H 7.4638319580 2.6937733605 -0.2595189907

H 7.2194301729 1.9801780219 -3.2283248068

H 7.4077052821 3.5921874105 -2.5928444145

H 5.2333293405 3.3472498027 -1.3864436891

O 4.8487607159 1.5075680898 -2.0210541046

H 5.2594618747 4.4282698860 -3.6246970699

H 3.7801333713 3.5043824787 -3.3797854239

H 5.0673237156 2.8600009552 -4.3920659235

H 4.9682815500 0.9426292248 -2.7687668929

C 3.3448575561 0.5276225297 -7.1232607760

C 2.7383062639 -0.3744491962 -6.0468452104

C 3.1734845457 -0.0071420424 -4.6267785964

C 2.4646081229 -0.8487410845 -3.5685126956

H 3.0199235799 0.2196138577 -8.1122642399

H 4.4275552518 0.4954517555 -7.0947688411

H 3.0395441769 1.5603940061 -6.9799763215

H 3.0100818322 -1.4119848302 -6.2404801839

H 1.6536927178 -0.3264457747 -6.1002281091

H 2.9439394874 1.0381679990 -4.4520775095

O 4.5744675750 -0.0913473022 -4.4770885262

H 1.3889963127 -0.7129061082 -3.6184368670

H 2.8021825381 -0.5667666096 -2.5775188031

H 2.6736392698 -1.9072595270 -3.7103708263

H 4.8507928612 -0.9899265443 -4.5704440118

Acetone

C -0.1434640646 -6.1680196347 -4.0049476201

C -0.8782840274 -7.1011108553 -3.0607989597

C 0.3972202935 -6.7057445111 -5.3166444902

O 0.0075183369 -5.0241421543 -3.7190994296

H -0.9505623192 -8.1150775554 -3.4326680686

H -1.8754638271 -6.7081416135 -2.8918970163

H -0.3628115083 -7.1041847336 -2.1060220864

H 0.1965762187 -7.7595005788 -5.4614870238

H 1.4686073711 -6.5365023078 -5.3450531316

H -0.0440449476 -6.1404591877 -6.1309280615

C -0.7765207167 -1.3913989337 -2.0967623440

C -1.0294269575 -2.6600473973 -1.3039156969

C -0.0637118860 -1.4750530467 -3.4335277897

O -1.1341944033 -0.3396913359 -1.6737478921

H -0.6575592738 -3.5509751693 -1.7934066421

H -2.0974577028 -2.7590043372 -1.1400923303

H -0.5580877876 -2.5606469417 -0.3316610077

H 0.2109669688 -2.4852377472 -3.7086961966

H 0.8285235984 -0.8591858096 -3.3894411569

H -0.7108463169 -1.0575432051 -4.1978724795

Benzene

C 6.8250415078 -5.4261327120 -1.9304013444

C 8.1892065378 -5.6305283573 -1.7349348507

C 8.6892394564 -6.9247596409 -1.6024492472

C 7.8237405898 -8.0156776799 -1.6639229755

C 6.4591722367 -7.8115330371 -1.8620331709

C 5.9605234353 -6.5167513672 -1.9943576606

H 6.4357485338 -4.4212299873 -2.0188948902

H 8.8591382577 -4.7832453697 -1.6796820041

H 9.7485813013 -7.0829535650 -1.4509257548

H 8.2114797639 -9.0204515108 -1.5625211626

H 5.7875245271 -8.6580449959 -1.9120000444

H 4.9008210974 -6.3572474090 -2.1404373977

C 5.0687050113 -7.9817440866 3.3438367786

C 5.6119266044 -7.6519072992 2.1040589947

C 6.6397685891 -6.7143619764 2.0193855478

C 7.1237438798 -6.1048519819 3.1757743058

C 6.5821222186 -6.4365934576 4.4165656035

C 5.5543160129 -7.3743111807 4.4997512127

H 4.2616874887 -8.6985983844 3.4074940433

H 5.2307092480 -8.1195599162 1.2064375798

H 7.0613898823 -6.4587675352 1.0565268886

H 7.9223984193 -5.3781331984 3.1107729037

H 6.9589981050 -5.9653936749 5.3144103350

H 5.1283882887 -7.6265272915 5.4613761160

Cyclohexanol

C 3.4613804799 -4.6808812930 3.2389441526

C 2.1310619028 -5.2439729746 3.7502397399

C 3.8126804943 -3.3639933161 3.9396551751

C 3.8100777253 -3.5195500261 5.4639996915

C 2.4813451788 -4.0725824365 5.9642156296

C 2.1410377938 -5.3940733305 5.2755729782

O 2.5830667330 -4.2218253067 7.3614699694

H 3.4146345429 -4.5319099522 2.1640067804

H 4.2516058247 -5.4068280606 3.4213247608

H 1.9248796119 -6.2038141555 3.2863449973

H 1.3222112297 -4.5768592462 3.4567786568

H 3.0911252287 -2.6012647948 3.6515598700

H 4.7845476555 -3.0108885792 3.6082574576

H 4.0052750989 -2.5684801454 5.9484759749

H 4.5999266738 -4.2009047137 5.7706827116

H 1.6971365336 -3.3496658854 5.7337205291

H 1.1736188798 -5.7531484172 5.6223424879

H 2.8797882273 -6.1350327857 5.5717323556

H 1.7684238748 -4.5475140847 7.7096673256

C -3.2152301638 -2.0690147652 7.9126251736

C -3.4542889446 -3.2606493406 8.8459530227

C -1.7474155690 -1.6291981118 7.9387634182

C -0.8048351170 -2.7954579220 7.6237856166

C -1.0441938627 -3.9725969226 8.5611447666

C -2.5053314607 -4.4196506877 8.5211966611

O -0.1697688267 -5.0073824308 8.1744404768

H -3.8591712695 -1.2405225965 8.1933538253

H -3.4883868177 -2.3488921730 6.8968636020

H -4.4845260742 -3.5957632863 8.7730512926

H -3.3022489933 -2.9454758706 9.8769472429

H -1.5112560529 -1.2274019938 8.9227269671

H -1.5849256094 -0.8237460843 7.2289203187

H 0.2318114362 -2.4841846651 7.7001144133

H -0.9605899417 -3.1355865679 6.6028972850

H -0.8055487892 -3.6585643633 9.5785687741

H -2.6607825990 -5.2379005064 9.2221856366

H -2.7180016868 -4.8075159377 7.5278108263

H -0.2783654332 -5.7500869363 8.7467641264

di-ethyl ether 1

C -2.5867360589 -5.5019078839 -5.7771302588

C -2.1877265839 -4.3787920476 -4.8362508536

O -3.2821961962 -4.0529586823 -4.0287242871

C -3.0392263408 -3.0243047785 -3.1127726099

C -4.3014031128 -2.7744058276 -2.3063533013

H -1.7513161681 -5.7726123198 -6.4154777209

H -3.4161241719 -5.1943409127 -6.4042336880

H -2.8905093935 -6.3776629642 -5.2145317286

H -1.8702892609 -3.5049395634 -5.4059794603

H -1.3449307315 -4.6874963623 -4.2171043898

H -2.7430255286 -2.1168176134 -3.6397545987

H -2.2175073855 -3.2993108273 -2.4508871680

H -5.1179320329 -2.4874969123 -2.9595797138

H -4.1367745213 -1.9780726679 -1.5870162031

H -4.5920903874 -3.6708025103 -1.7699614728

C -4.6132740309 -1.9550399029 -6.4415020584

C -5.0692377908 -0.7190356820 -5.6863580896

O -4.8861806020 0.4033669474 -6.5005034530

C -5.2719573103 1.6127858454 -5.9134660266

C -5.0216498574 2.7406664419 -6.8989016308

H -4.7460543340 -2.8409671508 -5.8281529973

H -3.5653019367 -1.8717848321 -6.7071406808

H -5.1880035812 -2.0757315247 -7.3530182580

H -4.4980422057 -0.6089678833 -4.7640804814

H -6.1197015671 -0.8128488972 -5.4094637382

H -4.7057063067 1.7807559155 -4.9968833795

H -6.3274269115 1.5768581469 -5.6421068038

H -3.9706287871 2.7885074912 -7.1612123107

H -5.3141040025 3.6916759841 -6.4644521413

H -5.5933947898 2.5844394922 -7.8068901608

di-ethyl ether 2

C 2.2285930586 -5.3116150566 -0.1417386525

C 3.5273596734 -4.7560377806 -0.6988660785

O 3.3365934856 -4.4170725456 -2.0423098253

C 4.4687033952 -3.8901343672 -2.6722256834

C 4.1241871067 -3.5677473203 -4.1155644897

H 2.3524257261 -5.5824488778 0.9022964425

H 1.9256593307 -6.1938099944 -0.6946437463

H 1.4377475680 -4.5735626024 -0.2164667649

H 4.3228640744 -5.4964182066 -0.6095079442

H 3.8353036251 -3.8772494605 -0.1315503310

H 5.2875247368 -4.6090816848 -2.6319236053

H 4.8001020122 -2.9899019597 -2.1538635749

H 3.8068545008 -4.4630338867 -4.6385395660

H 4.9895867005 -3.1564723129 -4.6260851520

H 3.3190654380 -2.8428107119 -4.1601549636

C -2.7712429377 -8.3778807206 5.0990447964

C -3.1147582674 -8.0562329449 3.6553025324

O -1.9821587094 -7.5297940982 3.0258498720

C -2.1720275237 -7.1914040226 1.6821338791

C -0.8727664057 -6.6364718895 1.1255167164

H -3.6370298137 -8.7887828901 5.6092087509

H -2.4541596180 -7.4823485260 5.6217503077

H -1.9662323261 -9.1028830037 5.1445630388

H -3.9334535370 -7.3371971101 3.6140614469

H -3.4459355903 -8.9567060741 3.1372144408

H -2.9672575106 -6.4508265754 1.5919551399

H -2.4798986908 -8.0703662292 1.1150505603

H -0.5698867625 -5.7541226823 1.6782053696

H -0.9959069279 -6.3660676025 0.0812883561

H -0.0821894961 -7.3747315934 1.2010353084

di-methyl ether 1

O -2.5462351412 0.7521717371 -6.5436815202

C -1.4126437816 0.0869051639 -6.0791987904

C -3.4410270976 1.1064331547 -5.5351244216

H -0.7902340761 -0.1404143380 -6.9345037726

H -1.6743122607 -0.8440629771 -5.5771407512

H -0.8441936479 0.7047931125 -5.3847103580

H -4.2773484745 1.6123042065 -5.9990646032

H -2.9806534552 1.7785574746 -4.8115444363

H -3.8107092965 0.2298153207 -5.0039574037

O -0.8482438683 4.7283906619 -7.6634839704

C -1.0119299635 5.1090844294 -8.9945107574

C -1.3953503884 3.4812518168 -7.3657250496

H -0.5557504587 6.0824295643 -9.1174502462

H -2.0657185801 5.1779959086 -9.2628670635

H -0.5290677993 4.4060584666 -9.6726212795

H -1.2149561716 3.2838656862 -6.3173567456

H -0.9330256033 2.6914632196 -7.9571240283

H -2.4695638199 3.4633419258 -7.5474030492

di-methyl ether 2

O -8.1805242237 1.6477407561 6.5719707941

C -8.0374914427 0.3092665444 6.9344367906

C -7.7993718075 2.5427775509 7.5704562421

H -8.3578602804 -0.2952596850 6.0962682779

H -8.6508546534 0.0629667923 7.8006679095

H -7.0007002174 0.0676004632 7.1665934499

H -7.9484641496 3.5444907319 7.1897704989

H -6.7499146195 2.4200703494 7.8366244981

H -8.3999454824 2.4154353355 8.4706547632

O -7.7846299103 -2.6876325694 7.5743081240

C -6.9110811708 -3.1248727166 6.5797796710

C -9.0949682581 -3.1321142075 7.4046298816

H -5.9302074471 -2.7274063719 6.8045503388

H -7.2173311574 -2.7704571238 5.5959936776

H -6.8518413379 -4.2124839693 6.5510106004

H -9.6846973276 -2.7399055094 8.2225366125

H -9.1521241692 -4.2201259820 7.4196820474

H -9.5175871712 -2.7782081385 6.4647331295

Dimethylamine

N -1.2302925268 -4.5754754618 4.2633397589

C -2.5049110233 -5.1071493524 4.7051131982

C -0.2208089386 -4.5672408950 5.3041895498

H -1.3548165355 -3.6507898514 3.9047544894

H -2.3899901236 -6.1547793484 4.9650344327

H -3.2261185448 -5.0456305971 3.8976759858

H -2.9187804438 -4.5904566845 5.5753087849

H 0.0088876963 -5.5877406555 5.5942139977

H -0.5217565869 -4.0238563611 6.2040024846

H 0.6912539994 -4.1196548301 4.9251280719

N 0.2393891644 -7.0095624918 2.6598293274

C 0.2388120211 -7.1986082197 1.2222081712

C -0.4401724860 -8.0703122092 3.3778120643

H -0.1744931086 -6.1282321187 2.8858632622

H 0.8087708170 -8.0883337122 0.9735518041

H 0.7210281418 -6.3541341090 0.7424053078

H -0.7609490241 -7.3118132269 0.7942338167

H 0.0956676953 -9.0038405388 3.2374744589

H -1.4735012059 -8.2266128626 3.0564066835

H -0.4434714049 -7.8491588020 4.4393957775

Ethanol 1

C 7.7924446469 7.0556092052 -0.0849868280

C 7.7533949254 8.2929798973 0.8033984742

O 6.4692418191 8.8590938205 0.8880614679

H 8.7882056694 6.6224160827 -0.0901949520

H 7.5312853520 7.3023295130 -1.1112786585

H 7.0921214981 6.3088914574 0.2729054170

H 8.4727255471 9.0295864975 0.4500865232

H 8.0276835904 8.0320220461 1.8174261960

H 6.1882136919 9.1451745373 0.0337776025

C 4.4638390584 8.7136140164 3.9442119554

C 5.9231685698 9.0473918305 4.2284465480

O 6.3700783617 10.1742015637 3.5162152233

H 4.1435264231 7.8669750981 4.5440667526

H 4.3182027300 8.4546959889 2.8982188753

H 3.8283767425 9.5615199370 4.1752313520

H 6.5524069766 8.1856216935 4.0133502443

H 6.0524102086 9.2903100402 5.2752859983

H 6.3187733032 10.0080647764 2.5886451363

Ethanol 2

C 3.6102453011 -3.4437440903 1.1342277470

C 3.7068994873 -3.9418523790 2.5710247601

O 4.9769923656 -4.4589826184 2.8810931282

H 2.6314625526 -3.0126485657 0.9461734996

H 3.7573283697 -4.2568716212 0.4274461696

H 4.3638777283 -2.6877365220 0.9428707824

H 2.9351166342 -4.6854376817 2.7615169817

H 3.5458859978 -3.1231286952 3.2604822847

H 5.1604958913 -5.2067036806 2.3353279987

C 0.6541608920 -3.3851758364 5.1880283248

C 0.1942240829 -3.3335561940 3.7362593694

O 0.8801321869 -2.3633865787 2.9845925635

H 0.1344373166 -4.1738632057 5.7238296486

H 0.4496784485 -2.4462518053 5.6969080778

H 1.7205796419 -3.5748111893 5.2420306340

H -0.8798462725 -3.1629140888 3.6903322009

H 0.3936730652 -4.2791360238 3.2487305173

H 0.7122845385 -1.5052614789 3.3396536674

Ethane 1

C 4.0707268601 4.9821639601 4.9514223001

C 3.1198336917 5.7513425479 5.4623693284

H 4.0022072856 3.9081720758 4.9815789019

H 2.2444480367 5.3304638795 5.9266431439

H 4.9456174541 5.4027254526 4.4859430506

H 3.1869283700 6.8254077731 5.4306132540

C 1.4113299326 2.3995396804 5.6100987503

C 2.0361024138 2.3945792191 6.7790876826

H 0.6749263804 1.6541577499 5.3627558583

H 1.8305210478 1.6448681991 7.5238418451

H 1.6157474556 3.1498499863 4.8656362776

H 2.7710997123 3.1409704042 7.0276946461

Ethane 2

C 1.5073423827 -6.0559046153 -5.5948862923

C 0.3755967783 -5.5228352191 -5.1568345956

H 1.5600360913 -7.0842187870 -5.9093004424

H -0.5322264505 -6.0985868273 -5.0989023490

H 2.4150274240 -5.4800816813 -5.6541506703

H 0.3219234163 -4.4939834537 -4.8442494598

C 0.4778495390 -1.7059920799 -6.3893220450

C 1.6114217266 -2.2373312217 -6.8247450520

H 0.4219404463 -0.6766890150 -6.0787221508

H 2.5178098720 -1.6593897611 -6.8833391824

H -0.4290037087 -2.2833019380 -6.3318158095

H 1.6673420291 -3.2660407371 -7.1374044593

Formaldehyde 1

O -4.8650842640 -0.1039426348 2.3166433579

C -3.9909586643 -0.8603654589 2.5520295957

H -3.3357048073 -1.2514147873 1.7673676476

H -3.7871171764 -1.2127325538 3.5680304054

O -1.7275224592 -2.8319662236 3.1615436357

C -0.8580253791 -3.5927676564 3.3999419188

H -0.6585608178 -3.9450449232 4.4168422007

H -0.2029435295 -3.9882101333 2.6173407528

Formaldehyde 2

O -0.9653012501 -1.5984320225 1.8985929356

C -1.7174460033 -0.8518162914 1.3804028605

H -2.4668948599 -0.2946523053 1.9512498375

H -1.7072090591 -0.6752023178 0.3002758881

O -2.5295268034 -0.6808392327 4.5275387332

C -1.6692424779 -1.4658552630 4.7155239600

H -1.8526230711 -2.5445531962 4.6880668275

H -0.6403698187 -1.1586753101 4.9277339853

Formaldehyde 3

O 8.2074738626 -7.7893366829 -6.5587924210

C 7.1361181033 -7.3092942656 -6.4428879414

H 6.5320835800 -7.0234668377 -7.3097308010

H 6.6872184192 -7.1233334216 -5.4621335352

O 7.9888932167 -7.7397050150 -3.4762309394

C 9.0600345165 -8.2202172665 -3.5921706899

H 9.6642846561 -8.5056156430 -2.7253367365

H 9.5085078124 -8.4070689175 -4.5729508541

Methane

C -7.3103937552 -4.5372586384 2.5848831455

H -7.3015294455 -3.5003580886 2.2494819672

H -6.2860586565 -4.8827895030 2.7230379605

H -7.8487315727 -4.6084722225 3.5297967760

H -7.8052470475 -5.1564370730 1.8368998343

C -7.3441306795 -8.0019927559 3.7292157834

H -6.8084713157 -7.9338298259 2.7825594901

H -6.8470825092 -7.3796486409 4.4731053213

H -8.3686840427 -7.6566671385 3.5921706330

H -7.3517799645 -9.0377610407 4.0681350914

Methanol 1

O -5.9567802349 5.5820030911 -5.1418368448

H -6.0954373940 5.4751488280 -4.1984653076

C -5.1094041574 6.7049183534 -5.3226786068

H -4.9598369325 6.8157962153 -6.3923688658

H -5.5546345995 7.6264578471 -4.9432901874

H -4.1330695765 6.5680557936 -4.8542321195

O -6.5138514374 6.0583496313 -2.2952926427

H -6.5150864507 5.4579424592 -1.5468922145

C -7.7528649140 6.7486339718 -2.2888289144

H -7.7399039977 7.4240712708 -3.1388394878

H -8.6041516721 6.0748497204 -2.4016402427

H -7.8927000925 7.3423229458 -1.3836315819

Methanol 2

O -2.1997600919 2.4080357600 0.3109434629

H -2.9639840091 2.6917353825 -0.1950899619

C -2.2914688655 1.0013184895 0.4672273944

H -1.4226919028 0.6922462197 1.0404659367

H -3.1862376809 0.7019710532 1.0160266629

H -2.2738288838 0.4752823753 -0.4890035000

O -4.3236285483 2.6425803625 -1.7074278813

H -5.0572629394 3.2566081624 -1.7805301354

C -3.6321683239 2.6567049810 -2.9457218282

H -2.8054372968 1.9592286352 -2.8511487816

H -4.2607637240 2.3298634447 -3.7760489871

H -3.2228669860 3.6407102118 -3.1815370234

Methoxyethane

C -6.8415298999 7.9762812300 1.4127762582

O -6.1697915754 9.1896753663 1.2728496420

C -6.3325211523 10.0599426135 2.3558983055

C -5.5571684979 11.3363935958 2.0824082132

H -6.6473629793 7.3877996017 0.5257933718

H -7.9167548200 8.1235465726 1.5081547016

H -6.4914124430 7.4240749434 2.2842087721

H -5.9724519018 9.5883343626 3.2708883951

H -7.3901447878 10.2840628695 2.4989368584

H -4.5029526919 11.1187619200 1.9522868889

H -5.6685745366 12.0288707053 2.9110574909

H -5.9211904196 11.8147442577 1.1800025360

C -11.3898815631 2.7653979815 2.0926800749

O -10.5549138410 3.8751007959 1.9721573335

C -9.2304421589 3.5601253416 1.6505898747

C -8.4295089676 4.8459992578 1.5489533960

H -12.3802924494 3.1234756975 2.3409071606

H -11.0511615980 2.0943106612 2.8812251600

H -11.4431026103 2.2025487611 1.1614030388

H -9.1948900877 3.0176134867 0.7052391413

H -8.8050765576 2.9099984245 2.4158720240

H -8.8420985457 5.4895153021 0.7799780962

H -7.3959429598 4.6264989296 1.2996415599

H -8.4521656421 5.3818735533 2.4912870610

Methyl-isopropyl ketone1

O -0.6980745797 -6.7975914241 4.0451255043

C -1.3635110906 -5.8143401864 3.9756560200

C -1.6993374362 -5.0022266908 5.2069168676

C -1.9271354610 -5.3202815149 2.6470932525

C -0.9771153875 -5.6170165829 1.4875543589

H -1.4260391087 -5.5488702558 6.0990977450

H -2.7543123572 -4.7479488532 5.2325730071

H -1.1424206755 -4.0686530080 5.1730647863

H -2.0680819506 -4.2441140258 2.7267340996

C -3.3055929235 -5.9648633189 2.4254462232

H -0.0116221613 -5.1436590316 1.6375569118

H -1.3947821385 -5.2435629640 0.5570049945

H -0.8113644698 -6.6831874056 1.3888954885

H -3.2112673143 -7.0428144563 2.3392142716

H -3.7511257193 -5.5886448395 1.5100249990

H -3.9917380807 -5.7497783060 3.2395814481

O 1.4408397877 -4.4551831533 3.9817799902

C 1.9891789683 -5.3167010065 4.5913092246

C 1.7371479805 -5.5184924960 6.0691696763

C 2.9857623799 -6.2600479742 3.9251535135

C 2.6020882607 -6.5513150754 2.4749542402

H 1.1831905873 -4.6806205564 6.4699186005

H 2.6688473122 -5.6446647642 6.6116680211

H 1.1583424134 -6.4292999816 6.2043580737

H 2.9873907052 -7.1914645907 4.4880082701

C 4.3909311468 -5.6431134801 4.0233912352

H 1.6180120132 -7.0054362755 2.4108201484

H 3.3186050601 -7.2348830932 2.0286654531

H 2.5844133229 -5.6389872679 1.8907687125

H 4.4346884665 -4.7086260773 3.4728183376

H 5.1266961334 -6.3204976790 3.6016847427

H 4.6771937048 -5.4430226378 5.0519291814

Methyl-isopropyl ketone

O 3.8505215654 -5.0009248549 -4.7536082671

C 3.6445759443 -6.1090909704 -4.3741757733

C 4.7796194117 -7.0683790758 -4.0917689806

C 2.2278805923 -6.6330099535 -4.1612706114

C 1.2873072557 -5.5308875451 -3.6757108503

H 5.7099742437 -6.6648187177 -4.4673709041

H 4.5888527741 -8.0415574182 -4.5331526505

H 4.8581484731 -7.2108135923 -3.0164050152

H 2.2747622084 -7.4190037654 -3.4100310465

C 1.7309222568 -7.2600224707 -5.4745283164

H 1.6302055150 -5.1043838585 -2.7380218313

H 0.2902963138 -5.9323963282 -3.5188825403

H 1.2268495139 -4.7288983013 -4.4017172393

H 1.6680761348 -6.5077433913 -6.2545529802

H 0.7430271100 -7.6871349018 -5.3342643363

H 2.3874008235 -8.0527219230 -5.8217118034

O 4.0850000736 -4.9667878513 -1.5453868933

C 4.6337642593 -3.9331206575 -1.7570582345

C 3.9082142461 -2.7746823058 -2.4050618627

C 6.1010113769 -3.7169186998 -1.4002837416

C 6.4912175604 -4.4810562892 -0.1357865430

H 2.9544468171 -3.1039065361 -2.7942109069

H 4.5038338886 -2.3340401721 -3.1983835450

H 3.7436381419 -2.0023709776 -1.6571902284

H 6.2478285219 -2.6516018985 -1.2332811042

C 6.9674117723 -4.1335099824 -2.6005171112

H 5.8914188920 -4.1699632587 0.7140416696

H 7.5350167112 -4.2995006614 0.1037048492

H 6.3475392039 -5.5465313415 -0.2701241967

H 6.8516482125 -5.1937351985 -2.8025894101

H 8.0145615529 -3.9401985388 -2.3904127162

H 6.7048820844 -3.5871141559 -3.5018509381

Methylamine

C 8.0985926157 -3.9051048458 -0.6729685182

N 7.3824490351 -2.7614209620 -1.2132831286

H 8.8088571713 -4.3611056211 -1.3641282154

H 7.3859464593 -4.6657560122 -0.3729390345

H 8.6417760055 -3.6014359269 0.2154060789

H 6.8522385175 -3.0128596647 -2.0223922929

H 8.0106628217 -2.0310908745 -1.4796806799

C 6.0917474334 -3.1756037885 2.4560542079

N 6.7933971288 -2.0279860663 1.9051680119

H 5.0236559226 -3.2007228521 2.2354556352

H 6.2127019704 -3.1867605996 3.5338844161

H 6.5360916006 -4.0868958746 2.0705967823

H 6.4219008582 -1.1700051990 2.2585256298

H 6.7202075898 -2.0003237584 0.9087341998

N-methylmethanimine 1

N -3.9436832168 -4.8433057481 -3.0947171857

C -3.0063732068 -4.0569967206 -2.8657090561

C -4.8678608878 -4.5123021318 -4.1678496269

H -2.3056098470 -4.2790208552 -2.0741818967

H -2.8403268529 -3.1364805883 -3.4234908307

H -5.6206423403 -5.2854293991 -4.2433040495

H -4.3531014446 -4.4437233038 -5.1228436906

H -5.3688190824 -3.5665131145 -3.9775392914

N -1.7254441622 -5.9257505196 -0.2986162897

C -2.6628788035 -6.7119162980 -0.5276060868

C -0.8012519757 -6.2569334842 0.7744483142

H -3.3636560068 -6.4897571690 -1.3190831108

H -2.8290237622 -7.6324339625 0.0301437961

H -0.0483565555 -5.4839163864 0.8498943834

H -0.3004388319 -7.2027849802 0.5840667392

H -1.3159664337 -6.3254822651 1.7294687815

N-methylmethanimine 2

N 3.9799432771 4.4288151463 1.0141528017

C 2.8210814182 3.9785446172 1.0739215856

C 4.9822799181 3.6468999904 0.3076041870

H 2.0573809656 4.5393447007 1.5927126148

H 2.5167206339 3.0331151646 0.6271895487

H 5.9309548794 4.1654526057 0.3425048968

H 4.7086656319 3.5070877040 -0.7351238449

H 5.1116674999 2.6688993146 0.7641866369

N 0.4909386630 2.2749373021 2.6265483468

C 1.1244602461 2.2915239654 3.6978335337

C -0.8158350937 1.6366035812 2.6141625712

H 2.0974721998 2.7592617985 3.7345527957

H 0.7549994453 1.8552464591 4.6247653024

H -1.2373144406 1.7029031875 1.6201512136

H -1.4978612277 2.1236101268 3.3065201223

H -0.7427885495 0.5860547178 2.8838017556

N-methylmethanimine 3

N 5.5899203593 3.7186169339 -1.6594158811

C 4.7909359282 3.5023238368 -2.5889952699

C 5.4762540310 4.9764401224 -0.9381379943

H 4.8535251667 2.5759169520 -3.1410207384

H 4.0128233912 4.2016320095 -2.8915689119

H 6.2333393751 5.0164352171 -0.1665673683

H 4.5022519469 5.0716546562 -0.4649064080

H 5.6213761608 5.8248713931 -1.6020641559

N 3.3653975109 3.3637653966 -5.5478781543

C 2.3436123264 2.9924013414 -6.1539478206

C 4.5679030357 3.6177820723 -6.3255265253

H 1.4369109655 2.7968558553 -5.6002928270

H 2.3003274543 2.8474218236 -7.2324417746

H 5.3635620221 3.9303913743 -5.6627284729

H 4.4042698538 4.4055163358 -7.0565483536

H 4.8932796144 2.7229277199 -6.8499879364

Piperidine

C -0.4281756800 0.0963699759 -5.6398533126

C 1.0320368848 -0.2383640674 -5.9933623744

C 1.2708322888 -1.7466725828 -5.9366873832

C 0.3842621718 -2.4686835419 -6.9682792330

C -0.9328834284 -1.7071104911 -7.1900478172

N -1.3026408150 -1.0263839430 -5.9623470484

H -0.7229947757 1.0102567690 -6.1616913599

H -0.5146276140 0.2940170232 -4.5752741271

H 1.6993872237 0.2884948760 -5.3181869603

H 1.2628650112 0.1193314943 -6.9946417120

H 1.0357808425 -2.1055205893 -4.9392801711

H 2.3182334515 -1.9726336778 -6.1153588146

H 0.1739001252 -3.4762812697 -6.6227268437

H 0.9078245484 -2.5620986429 -7.9170350440

H -1.7253184752 -2.3967727708 -7.4590747240

H -0.8249591079 -1.0105224877 -8.0272613810

H -2.2570981003 -0.7370562174 -5.9792166585

C -5.7964515398 0.7315616344 -2.2845974826

C -4.4255222771 0.0495465193 -2.1276114628

C -3.6892752040 -0.0006977226 -3.4657615443

C -3.4228407877 1.4245401896 -3.9846042349

C -4.5258175457 2.3921114764 -3.5249354139

N -5.7772699528 1.6662810924 -3.4049543212

H -6.0628664346 1.2216340396 -1.3447706587

H -6.5599398179 -0.0150201040 -2.4835157859

H -4.5600801101 -0.9469280873 -1.7180614547

H -3.8184969226 0.5973184231 -1.4097993628

H -4.2965530509 -0.5426773984 -4.1843113816

H -2.7554334020 -0.5465179067 -3.3655073271

H -3.3723011609 1.4114664319 -5.0691256264

H -2.4602805285 1.7831300927 -3.6270115044

H -4.6526270593 3.1891940096 -4.2491878715

H -4.2366701629 2.8671667342 -2.5823191876

H -6.5562024782 2.2877308176 -3.3596974335

Propan-1-imine

N 8.0308336256 7.5018008078 7.1673165434

C 9.2716015335 7.3358119768 7.1504710489

C 10.2342913901 8.4660802589 6.9256939694

C 11.2011563545 8.6406096851 8.1004993507

H 7.5448341154 6.6389727140 7.3342523708

H 9.7244336914 6.3568906259 7.3067642146

H 9.6645348815 9.3718378781 6.7555047914

H 10.8016900831 8.2549097007 6.0204845073

H 10.6637263493 8.8851324050 9.0116845095

H 11.9049749780 9.4418135861 7.9002151764

H 11.7740406612 7.7345902787 8.2813686960

N 5.0435223655 6.8408166091 7.3330216817

C 3.8019266241 6.9967769972 7.2948452988

C 2.8391119709 5.8649956270 7.5113210679

C 1.9078032545 6.1212001187 8.6997988326

H 5.5295906333 7.7044786015 7.1706609241

H 3.3486485196 7.9702970759 7.1089175056

H 3.4084703244 4.9544137812 7.6550411698

H 2.2444844410 5.7463117875 6.6067379051

H 2.4728262152 6.2109427494 9.6226076313

H 1.2027132637 5.3045937564 8.8155755578

H 1.3356280554 7.0358106792 8.5660663464

Propan-2-imine 1

N 4.5528787061 5.0042335469 -4.4098358880

C 4.5566858562 4.1640162349 -3.4774718209

C 5.0899342781 2.7539326753 -3.5886377786

C 3.9971931554 4.5510864287 -2.1328727845

H 4.9509186410 4.6270012397 -5.2519261572

H 5.4742152553 2.5498014908 -4.5815420743

H 4.3045699650 2.0373480296 -3.3636398555

H 5.8864130013 2.5963456568 -2.8663478788

H 3.6438692821 5.5726711029 -2.1573262264

H 4.7587497522 4.4515709765 -1.3631133371

H 3.1760524905 3.8922714799 -1.8606738609

N 7.4445362542 4.9901812985 -2.4718594682

C 8.4471235201 5.6267342162 -2.0657787661

C 8.6833406517 7.1021821619 -2.2944755542

C 9.5163872083 4.9024622971 -1.2893076860

H 6.8066398658 5.5822622888 -2.9742381335

H 7.8745103597 7.5530939639 -2.8580999468

H 9.6133785629 7.2534171358 -2.8358369773

H 8.7767680396 7.6187523137 -1.3429812948

H 9.2546395960 3.8590299800 -1.1806423098

H 9.6367971758 5.3481347396 -0.3047880590

H 10.4738594847 4.9826022737 -1.7984499120

Propan-2-imine 2

N 4.5989585407 -1.6866501880 -3.8622499202

C 4.6027954850 -0.9786734791 -2.8258925316

C 4.6922712007 -1.5142892088 -1.4151631879

C 4.5131246302 0.5199766701 -2.9555414963

H 4.6631454924 -2.6654974282 -3.6440891072

H 4.7536227844 -2.5965433340 -1.4024218361

H 3.8220500567 -1.2067422175 -0.8415389791

H 5.5676117688 -1.1086535575 -0.9150098789

H 4.4535028709 0.8000315512 -3.9981754140

H 5.3831421096 0.9916305585 -2.5049712163

H 3.6366377610 0.8934889288 -2.4314606409

N 1.4559015855 -1.0999537484 -2.4861273417

C 0.2164081971 -1.0355616392 -2.6726539504

C -0.4577290602 -1.1049204719 -4.0238666299

C -0.7010182206 -0.8774026863 -1.4876997320

H 1.9570917518 -1.2045111495 -3.3508424346

H 0.2641956000 -1.2183745968 -4.8245871160

H -1.0368376883 -0.2025308111 -4.2006173611

H -1.1491132148 -1.9427248163 -4.0552761107

H -0.1245309033 -0.8382685153 -0.5738059380

H -1.4006237748 -1.7083000302 -1.4370731133

H -1.2882876174 0.0328337130 -1.5824928508

Tert-butanol

C 6.2817879171 4.5418354448 9.0739573214

C 6.1559343062 4.0676119620 10.5249996791

C 4.8923463566 4.6397526716 11.1748016051

C 7.3962562764 4.4515444286 11.3274272270

O 6.1091322428 2.6520734103 10.5600221923

H 5.4134420816 4.2413294608 8.4922278037

H 7.1625284456 4.1087127767 8.6127069383

H 6.3589367071 5.6229697532 9.0194969133

H 4.9188991147 5.7244499344 11.1969828050

H 4.7954607951 4.2754267594 12.1916255613

H 4.0043147225 4.3407046982 10.6227955872

H 7.5180632408 5.5293325722 11.3575072278

H 8.2820469914 4.0142986858 10.8803882777

H 7.3141031956 4.0828493586 12.3437769957

H 5.3582701982 2.3427680927 10.0779778101

C 1.8876473995 -0.1058826352 9.6420761444

C 3.2131601275 0.4358877641 10.1859068250

C 4.2488078299 -0.6861920421 10.3067901818

C 3.0030572503 1.1233142374 11.5323816012

O 3.7045460017 1.4450844501 9.3214831023

H 2.0293295452 -0.5678242436 8.6677693712

H 1.1700547723 0.6996860787 9.5317543033

H 1.4677097943 -0.8548162456 10.3057930415

H 3.9149587976 -1.4562286105 10.9947972409

H 5.1925056452 -0.2888827680 10.6640448730

H 4.4238896286 -1.1564151281 9.3419186201

H 2.6233364725 0.4223334548 12.2684570722

H 2.2947209947 1.9379307028 11.4308305501

H 3.9393876687 1.5333879141 11.8940125773

H 3.8583760486 1.0857621613 8.4618004950

Water 1

O -0.2889843910 -6.3951979106 -6.3835440368

H 0.2839591883 -6.0534888797 -5.7184013045

H -0.9762516543 -5.7614896226 -6.4995600423

O 1.5580764686 -5.4197092150 -4.3213189438

H 2.4349305647 -5.3107485320 -4.6479666514

H 1.6148848350 -6.0047441522 -3.5851877525

Water 2

O -1.9651699723 -2.2569873240 -6.9071199727

H -2.3489609164 -1.7566535152 -7.6069877118

H -1.6374610733 -3.0520199159 -7.2917135949

O -3.8639292682 -2.7697994091 -4.7282296434

H -3.5250076779 -2.3909219289 -3.9351166176

H -3.2340644373 -2.5883920750 -5.4047973583

Water 3

O 3.8034972939 4.9464438822 -6.8748554708

H 3.9198932341 4.1810601453 -7.4115900249

H 3.4430020479 4.6501400766 -6.0565465858

O 2.6792242589 4.1265543975 -4.2903778949

H 3.2396873512 4.3523444043 -3.5676440185

H 1.8438330743 4.5269920260 -4.1196340125

A.2 Total interaction and exchange-repulsion energies for different systems

Table A.1.: Total interaction and exchange-repulsion energies (mH) for dimers obtained from EFP Monte Carlo (MC) simulations.

Dimer	SAPT Total	EFP Total	QM/EFP Total	SAPT Ex-rep	EFP Ex-rep	QM/EFP Ex-rep
2-aminopyridine	-12.520	-10.306	-12.141	11.540	10.423	8.144
2-butanol	-10.403	-10.896	-10.833	11.034	9.850	9.566
acetone	-4.916	-5.270	-4.897	4.342	3.249	2.573
benzene	-4.088	-3.563	-2.772	2.455	2.301	1.952
cyclohexanol	-10.247	-10.554	-11.045	10.755	9.699	8.855
di-ethyl ether 1	-2.494	-4.001	-2.106	4.765	3.785	3.270
di-ethyl ether 2	-0.677	-1.328	-0.746	1.306	1.150	0.915
di-methyl ether 1	-1.957	-3.635	-0.261	3.724	3.079	4.367
di-methyl ether 2	-1.959	-3.624	-1.504	3.709	3.066	3.086
dimethylamine	-5.821	-7.099	-5.567	8.773	7.624	6.697
ethanol 1	-8.781	-9.995	-7.109	9.397	8.135	8.760
ethanol 2	-2.498	-3.932	-2.477	4.118	3.395	3.061
ethene 1	-1.033	-3.137	-0.307	4.527	2.996	5.105
ethene 2	-1.014	-1.789	-1.210	2.452	1.729	1.850
formaldehyde 1	-4.348	-5.323	-4.505	3.043	2.389	2.520
formaldehyde 2	-6.818	-7.224	-7.126	5.866	4.748	2.804
formaldehyde 3	-5.472	-7.675	-4.180	7.797	5.759	7.495
methane	-0.216	-1.004	-0.222	1.097	0.868	0.768
methanol 1	-8.585	-9.707	-9.217	9.089	7.858	8.402
methanol 2	-8.585	-9.705	-9.214	9.082	7.852	8.398
methoxyethane	-0.674	-1.496	-0.602	1.506	1.282	1.074

methyl-isopropyl ketone 1	-9.505	-11.715	-11.947	11.409	9.496	5.711
methyl-isopropyl ketone 2	-9.070	-10.554	-10.696	10.232	8.689	5.472
methylamine	-5.245	-6.599	-5.162	7.750	6.949	6.587
N-methylmethanimine 1	-5.655	-6.747	-5.292	8.458	7.112	7.008
N-methylmethanimine 2	-3.347	-4.013	-3.001	3.590	3.234	2.842
N-methylmethanimine 3	-3.167	-3.800	-2.716	3.595	3.104	2.824
piperidine	-0.417	-0.519	-0.371	0.018	0.020	0.003
propan-1-imine	-5.231	-5.836	-5.307	5.286	4.557	4.550
propan-2-imine 1	-6.287	-8.306	-6.458	4.245	6.140	5.216
propan-2-imine 2	-6.288	-8.306	-6.459	4.246	6.141	5.217
tert-butanol	-10.680	-10.923	-11.440	12.139	10.805	9.780
water 1	-7.918	-9.381	-9.113	9.426	8.255	9.463
water 2	-7.918	-9.380	-8.021	9.426	8.254	8.914
water 3	-7.918	-9.380	-9.113	9.426	8.255	9.463

Table A.2.: Total energies (mH) for dimers from the S22 data set. For each dimer, the first molecule refers to the QM region, and the second to the effective fragment.

Dimer	CCSD(T)/CBS	MP2/CBS	SAPT	EFP	QM/EFP
Formic acid	-29.657	-29.641	-32.455	-24.586	-37.179
Formic acid	-29.657	-29.641	-32.455	-24.586	-37.179
ethene-ethyne	-2.438	-2.693	-2.236	-2.308	-2.710
ethyne-ethene	-2.438	-2.693	-2.236	-2.308	-3.016
ethene	-2.406	-2.582	-1.221	-3.159	-0.744
ethene	-2.406	-2.582	-1.221	-3.159	-0.744
benzene-ammonia	-3.745	-4.335	-3.225	-2.561	-3.237
ammonia-benzene	-3.745	-4.335	-3.225	-2.561	-3.229
benzene-water	-5.227	-5.753	-4.891	-4.301	-4.974

water-benzene	-5.227	-5.753	-4.891	-4.301	-5.850
benzene-hcn	-7.107	-8.223	-7.876	-6.320	-5.660
hcn-benzene	-7.107	-8.223	-7.876	-6.320	-8.815
benzene-methane	-2.390	-2.964	-1.706	-1.197	-1.549
methane-benzene	-2.390	-2.964	-1.706	-1.197	-0.925
parallel benzene	-4.351	-7.888	-4.516	3.879	-1.192
parallel benzene	-4.351	-7.888	-4.516	3.879	-1.192
t-shape benzene	-4.366	-5.769	-4.423	-1.693	-3.090
t-shape benzene	-4.366	-5.769	-4.423	-1.693	-2.281
phenol	-11.235	-12.366	-11.375	-8.063	-10.181
phenol	-11.235	-12.366	-11.375	-8.063	-8.700
pyridoxine-aminopyridine	-26.629	-27.681	-28.035	-19.299	-30.137
aminopyridine-pyridoxine	-26.629	-27.681	-28.035	-19.299	-27.527
adenine-thymine stack	-19.490	-23.792	-19.262	-12.509	-17.344
thymine-adenine stack	-19.490	-23.792	-19.262	-12.509	-21.789
adenine-thymine watson	-26.087	-26.358	-27.682	-19.679	-29.030
thymine-adenine watson	-26.087	-26.358	-27.682	-19.679	-27.884
indole-benzene stack	-8.319	-12.940	-8.316	3.742	-2.103
benzene-indole stack	-8.319	-12.940	-8.316	3.742	-2.905
indole-benzene t-shape	-9.131	-11.203	-8.714	-5.837	-6.150
benezene-indole t-shape	-9.131	-11.203	-8.714	-5.837	-9.661
formamide	-25.434	-25.275	-26.492	-23.922	-29.881
formamide	-25.434	-25.275	-26.492	-23.922	-29.881
pyrazine	-7.044	-10.996	-7.022	-0.066	-9.700
pyrazine	-7.044	-10.996	-7.022	-0.066	-9.930
uracil h-bond	-32.621	-32.557	-35.726	-27.963	-32.134
uracil h-bond	-32.621	-32.557	-35.726	-27.963	-32.134
uracil stack	-15.745	-17.769	-14.560	-13.059	-15.464
uracil stack	-15.745	-17.769	-14.560	-13.059	-15.464

water	-8.000	-8.016	-8.102	-9.398	-9.434
water	-8.000	-8.016	-8.102	-9.398	-8.581
methane	-0.845	-0.813	-0.269	-1.006	-0.280
methane	-0.845	-0.813	-0.269	-1.006	-0.280
ammonia	-5.952	-5.100	-4.486	-5.000	-4.346
ammonia	-5.952	-5.100	-4.486	-5.000	-4.346

Table A.3.: Exchange-repulsion energies (mH) for dimers from the S22 data set. For each dimer, the first molecule refers to the QM region, and the second to the effective fragment.

Dimer	SAPT	EFP	QM/EFP
Formic acid	57.362	52.596	51.945
Formic acid	57.362	52.596	51.945
ethene-ethyne	3.704	3.115	2.080
ethyne-ethene	3.704	3.115	2.321
ethene	3.634	2.363	4.027
ethene	3.634	2.363	4.027
benzene-ammonia	4.103	4.559	3.233
ammonia-benzene	4.103	4.559	2.286
benzene-water	4.880	5.331	4.147
water-benzene	4.880	5.331	2.051
benzene-hcn	6.963	7.794	6.443
hcn-benzene	6.963	7.794	4.503
benzene-methane	3.917	4.053	2.836
methane-benzene	3.917	4.053	2.887
parallel benzene	14.624	17.080	9.333
parallel benzene	14.624	17.080	9.333

t-shape benzene	6.839	7.706	5.129
t-shape benzene	6.839	7.706	5.881
phenol	15.757	14.645	13.579
phenol	15.757	14.645	14.180
pyridoxine-aminopyridine	45.378	42.526	40.287
aminopyridine-pyridoxine	45.378	42.526	41.306
adenine-thymine stack	27.240	26.226	18.929
thymine-adenine stack	27.240	26.226	10.820
adenine-thymine watson	44.735	42.765	41.467
thymine-adenine watson	44.735	42.765	40.691
indole-benzene stack	21.197	24.150	15.819
benzene-indole stack	21.197	24.150	14.116
indole-benzene t-shape	10.577	12.082	9.550
benezene-indole t-shape	10.577	12.082	6.127
formamide	39.074	36.605	33.965
formamide	39.074	36.605	33.965
pyrazine	15.876	17.469	4.881
pyrazine	15.876	17.469	5.050
uracil h-bond	44.917	42.099	41.467
uracil h-bond	44.917	42.099	41.467
uracil stack	17.341	15.717	9.162
uracil stack	17.341	15.717	9.162
water	11.387	10.099	11.666
water	11.387	10.099	10.252
methane	0.872	0.662	0.579
methane	0.872	0.662	0.579
ammonia	6.988	5.999	6.607
ammonia	6.988	5.999	6.607

A.3 Details for identified parameters

Table A.4.
Exchange-repulsion parameters for different LMO types with corresponding exchange-repulsion mean absolute errors (MAE, mH) and exchange-repulsion mean relative errors (%). Values were obtained taking into account all test molecules (table A.6).

LMO	β	α	$\mathrm{err}^{\mathrm{EFP\_ex-rep}}$	$\mathrm{err}^{\mathrm{EFP\_ex-rep}}$	$\mathrm{err}^{\mathrm{SAPT\_ex-rep}}$	$\mathrm{err}^{\mathrm{SAPT\_ex-rep}}$
			mH	%	mH	%
C-H	0.54	0.41	1.148	17.9	1.492	23.7
C-C	0.0	0.0	1.148	17.9	1.492	23.7
C=C	0.11	0.21	1.508	15.1	1.813	19.5
C≡C	0.18	0.25	0.551	15.7	0.790	17.3
LP O	0.7	0.5	1.147	25.4	1.474	28.6
O-H	0.4	0.4	1.147	25.4	1.474	28.6
O-C	0.0	0.0	1.158	16.8	1.424	21.3
O=C	1.02	1.16	1.192	16.6	1.431	20.2
LP N (sp3)	0.11	0.23	0.948	16.0	0.982	14.4
LP N (sp2/sp)	0.6	0.4	1.393	14.1	1.740	17.5
N-H	1.6	0.62	0.948	16.0	0.982	14.4
N-C	0.0	0.0	1.793	18.8	2.018	19.9
N=C	0.3	0.8	1.393	14.1	1.740	17.5
N≡C	1.9	0.78	2.202	21.5	2.103	25.9
Aromatic C-H	0.54	0.41	3.396	54.2	2.771	45.1
Aromatic C-C	1.92	0.45	3.396	54.2	2.771	45.1
Aromatic C=C	0.0	0.0	3.396	54.2	2.771	45.1

Table A.5.
Exchange-repulsion parameters for different LMO types with corresponding remainder mean absolute errors (MAE, mH) and remainder mean relative errors (%). Values were obtained taking into account all test molecules (table A.6).

LMO	β	α	err^{SAPT_rem}	err^{SAPT_rem}
			mH	%
C-H	0.54	0.41	1.433	11.6
C-C	0.0	0.0	1.433	11.6
C=C	0.11	0.21	1.036	9.5
C≡C	0.18	0.25	0.418	6.8
LP O	0.7	0.5	1.160	23.7
O-H	0.4	0.4	1.160	23.7
O-C	0.0	0.0	0.682	7.9
O=C	1.02	1.16	1.244	11.8
LP N (sp3)	0.11	0.23	1.093	21.2
LP N (sp2/sp)	0.6	0.4	0.940	7.6
N-H	1.6	0.62	1.093	21.2
N-C	0.0	0.0	1.280	13.3
N=C	0.3	0.8	0.940	7.6
N≡C	1.9	0.78	1.835	16.2
Aromatic C-H	0.54	0.41	0.582	107.1
Aromatic C-C	1.92	0.45	0.582	107.1
Aromatic C=C	0.0	0.0	0.582	107.1

Table A.6.
Molecules used for determining the exchange-repulsion parameters for each LMO type.

LMO	associated molecules	geometries per molecule
C-H	methane, ethane, pentane, neopentane, cyclopentane	35
C-C	methane, ethane, pentane, neopentane, cyclopentane	35
C=C	ethene, trans-butene, cis-butene, propene, hexene	44
C≡C	ethyne, propyne, hexyne, hexyne	50
LP O	water	65
O-H	water	65
O-C	methyl ethyl ether, di-methyl ether, di-ethyl ether	41
O=C	formaldehyde, propanal, acetone, 3-Methylbutan-2-one	35
LP N (sp3)	ammonia	65
LP N (sp2 or sp)	N-methylmethanimine, N-methylpropan-2-imine N-methylpentan-3-imine	25
N-H	ammonia	65
N-C	methylamine, di-methylamine, piperidine	30
N=C	N-methylmethanimine, N-methylpropan-2-imine N-methylpentan-3-imine	25
N≡C	HCN	65
Aromatic C-H	parallel benzene	12
Aromatic C-C	parallel benzene	12
Aromatic C=C	parallel benzene	12

B. SUPPLEMENTARY MATERIAL FOR CHAPTER 3

This appendix contains the supplementary information for Chapter 3, application of parametrized exchange-repulsion to amino acid dimers.

Table B.1.: SAPT, EFP and QM/EFP exchange-repulsion interaction energies computed for polar-polar dimers. All energies are given in units of kcal/mol. For QM/EFP, monA represents the QM region and monB the effective fragment.

snapshot	monA	monB	SAPT	EFP	QMEFP
1	ASN(207)	SER(202)	3.145	2.813	2.019
1	ASN(406)	GLN(408)	9.535	9.106	6.830
1	GLN(057)	SER(060)	17.615	16.732	15.475
1	GLN(092)	SER(002)	5.481	5.043	4.490
1	GLN(389)	THR(394)	2.977	2.515	2.935
1	GLN(408)	ASN(406)	9.535	9.106	6.028
1	GLN(481)	SER(477)	1.216	1.083	0.744
1	SER(002)	GLN(092)	5.481	5.043	3.521
1	SER(060)	GLN(057)	17.615	16.732	14.393
1	SER(074)	SER(080)	4.112	3.621	2.671
1	SER(080)	SER(074)	4.112	3.621	4.068
1	SER(172)	THR(067)	2.757	2.561	2.108
1	SER(202)	ASN(207)	3.145	2.813	2.353
1	SER(224)	SER(274)	10.139	9.339	9.451
1	SER(232)	THR(234)	1.775	1.463	1.010

1	SER(274)	SER(224)	10.139	9.339	8.419
1	SER(288)	SER(383)	4.167	3.670	1.984
1	SER(383)	SER(288)	4.167	3.670	3.175
1	SER(477)	GLN(481)	1.216	1.083	0.447
1	THR(067)	SER(172)	2.757	2.561	1.684
1	THR(234)	SER(232)	1.775	1.463	0.997
1	THR(392)	THR(394)	1.617	1.393	0.810
1	THR(394)	GLN(389)	2.977	2.515	2.001
1	THR(394)	THR(392)	1.617	1.393	1.036
2	ASN(207)	SER(202)	1.225	1.147	0.601
2	ASN(406)	GLN(408)	23.178	24.148	20.088
2	GLN(092)	SER(002)	3.912	3.497	2.658
2	GLN(389)	THR(394)	2.327	2.112	1.626
2	GLN(408)	ASN(406)	23.178	24.148	18.997
2	SER(002)	GLN(092)	3.912	3.497	2.300
2	SER(074)	SER(080)	4.001	3.538	2.625
2	SER(080)	SER(074)	4.001	3.538	3.887
2	SER(202)	ASN(207)	1.225	1.147	0.418
2	SER(224)	SER(274)	6.225	5.525	5.201
2	SER(232)	THR(234)	1.524	1.300	0.805
2	SER(274)	SER(224)	6.225	5.525	3.710
2	SER(288)	SER(383)	1.764	1.442	0.697
2	SER(383)	SER(288)	1.764	1.442	1.016
2	THR(234)	SER(232)	1.524	1.300	0.927
2	THR(392)	THR(394)	7.601	7.023	7.473
2	THR(394)	GLN(389)	2.327	2.112	1.411
2	THR(394)	THR(392)	7.601	7.023	7.294
3	GLN(092)	SER(002)	2.485	2.270	1.519
3	SER(002)	GLN(092)	2.485	2.270	1.286

3	SER(074)	SER(080)	12.522	11.927	13.053
3	SER(080)	SER(074)	12.522	11.927	13.042
3	SER(224)	SER(274)	4.492	3.908	3.051
3	SER(232)	THR(234)	1.266	1.031	0.640
3	SER(274)	SER(224)	4.492	3.908	2.470
3	THR(234)	SER(232)	1.266	1.031	0.699
3	THR(392)	THR(394)	3.938	3.633	3.258
3	THR(394)	THR(392)	3.938	3.633	3.059
4	ASN(015)	ASN(096)	3.235	3.049	2.448
4	ASN(096)	ASN(015)	3.235	3.049	2.034
4	ASN(207)	SER(202)	2.829	2.281	2.133
4	GLN(057)	SER(060)	25.298	25.083	24.315
4	GLN(389)	THR(394)	2.525	2.191	1.643
4	GLN(478)	GLN(481)	11.210	10.312	6.752
4	GLN(481)	GLN(478)	11.210	10.312	7.277
4	GLN(481)	SER(477)	3.865	3.062	3.345
4	SER(060)	GLN(057)	25.298	25.083	22.998
4	SER(074)	SER(080)	0.868	0.783	0.633
4	SER(080)	SER(074)	0.868	0.783	0.442
4	SER(202)	ASN(207)	2.829	2.281	2.253
4	SER(224)	SER(274)	2.698	2.377	1.776
4	SER(274)	SER(224)	2.698	2.377	1.337
4	SER(288)	SER(383)	4.010	3.472	1.987
4	SER(383)	SER(288)	4.010	3.472	2.975
4	SER(477)	GLN(481)	3.865	3.062	3.505
4	THR(392)	THR(394)	4.999	4.500	4.723
4	THR(394)	GLN(389)	2.525	2.191	1.822
4	THR(394)	THR(392)	4.999	4.500	4.565
5	ASN(207)	SER(202)	3.421	2.826	2.858

5	GLN(057)	SER(060)	2.443	2.160	1.252
5	GLN(092)	SER(002)	4.307	3.744	2.964
5	GLN(389)	THR(394)	3.407	3.023	2.676
5	SER(002)	GLN(092)	4.307	3.744	2.459
5	SER(060)	GLN(057)	2.443	2.160	1.528
5	SER(074)	SER(080)	3.865	3.359	2.492
5	SER(080)	SER(074)	3.865	3.359	3.460
5	SER(172)	THR(067)	12.656	11.181	11.216
5	SER(202)	ASN(207)	3.421	2.826	3.274
5	SER(224)	SER(274)	12.937	11.954	12.002
5	SER(274)	SER(224)	12.937	11.954	9.404
5	THR(067)	SER(172)	12.656	11.181	10.817
5	THR(392)	THR(394)	0.847	0.823	0.432
5	THR(394)	GLN(389)	3.407	3.023	2.421
5	THR(394)	THR(392)	0.847	0.823	0.468
6	ASN(207)	SER(202)	3.698	3.479	2.997
6	GLN(389)	THR(394)	3.059	2.633	2.373
6	GLN(478)	GLN(481)	7.148	6.345	3.597
6	GLN(481)	GLN(478)	7.148	6.345	4.272
6	SER(074)	SER(080)	2.224	1.911	1.358
6	SER(080)	SER(074)	2.224	1.911	1.813
6	SER(172)	THR(067)	5.400	4.778	4.568
6	SER(202)	ASN(207)	3.698	3.479	1.847
6	SER(224)	SER(274)	7.591	6.491	5.904
6	SER(232)	THR(234)	1.739	1.472	0.985
6	SER(274)	SER(224)	7.591	6.491	5.853
6	THR(067)	SER(172)	5.400	4.778	4.029
6	THR(234)	SER(232)	1.739	1.472	1.131
6	THR(392)	THR(394)	14.922	14.381	16.403

6	THR(394)	GLN(389)	3.059	2.633	2.311
6	THR(394)	THR(392)	14.922	14.381	17.204
7	ASN(015)	ASN(096)	2.261	2.011	1.553
7	ASN(096)	ASN(015)	2.261	2.011	1.224
7	ASN(207)	SER(202)	0.736	0.735	0.427
7	GLN(389)	THR(394)	2.388	2.108	1.638
7	GLN(478)	GLN(481)	21.644	20.817	19.039
7	GLN(481)	GLN(478)	21.644	20.817	13.229
7	GLN(481)	SER(477)	3.218	2.571	2.478
7	SER(074)	SER(080)	4.315	3.614	2.937
7	SER(080)	SER(074)	4.315	3.614	4.005
7	SER(172)	THR(067)	7.376	6.551	5.992
7	SER(202)	ASN(207)	0.736	0.735	0.643
7	SER(224)	SER(274)	1.524	1.454	0.831
7	SER(274)	SER(224)	1.524	1.454	0.624
7	SER(288)	SER(383)	1.240	1.017	0.466
7	SER(383)	SER(288)	1.240	1.017	0.667
7	SER(477)	GLN(481)	3.218	2.571	3.065
7	THR(067)	SER(172)	7.376	6.551	5.584
7	THR(392)	THR(394)	6.217	5.692	5.819
7	THR(394)	GLN(389)	2.388	2.108	1.789
7	THR(394)	THR(392)	6.217	5.692	5.545
8	ASN(207)	SER(202)	2.976	2.982	2.144
8	GLN(092)	SER(002)	3.171	2.816	2.220
8	GLN(389)	THR(394)	2.059	1.881	1.365
8	GLN(478)	GLN(481)	7.742	7.062	5.547
8	GLN(481)	GLN(478)	7.742	7.062	4.373
8	SER(002)	GLN(092)	3.171	2.816	1.650
8	SER(074)	SER(080)	2.875	2.567	1.781

8	SER(080)	SER(074)	2.875	2.567	2.558
8	SER(172)	THR(067)	11.970	11.089	12.187
8	SER(202)	ASN(207)	2.976	2.982	2.559
8	SER(224)	SER(274)	3.489	3.152	2.435
8	SER(232)	THR(234)	1.986	1.701	1.130
8	SER(274)	SER(224)	3.489	3.152	1.697
8	SER(288)	SER(383)	1.529	1.281	0.617
8	SER(383)	SER(288)	1.529	1.281	0.804
8	THR(067)	SER(172)	11.970	11.089	10.906
8	THR(234)	SER(232)	1.986	1.701	1.262
8	THR(392)	THR(394)	2.800	2.575	2.020
8	THR(394)	GLN(389)	2.059	1.881	1.332
8	THR(394)	THR(392)	2.800	2.575	2.025
9	ASN(207)	SER(202)	3.000	2.809	2.283
9	ASN(406)	GLN(408)	8.998	8.289	5.492
9	GLN(057)	SER(060)	18.126	17.042	16.217
9	GLN(389)	THR(394)	5.730	4.976	4.289
9	GLN(408)	ASN(406)	8.998	8.289	5.879
9	GLN(481)	SER(477)	2.949	2.551	2.319
9	SER(060)	GLN(057)	18.126	17.042	15.236
9	SER(074)	SER(080)	4.328	3.940	2.775
9	SER(080)	SER(074)	4.328	3.940	3.769
9	SER(172)	THR(067)	9.413	8.604	8.431
9	SER(202)	ASN(207)	3.000	2.809	1.255
9	SER(224)	SER(274)	2.776	2.469	1.804
9	SER(274)	SER(224)	2.776	2.469	1.643
9	SER(288)	SER(383)	2.004	1.652	0.784
9	SER(383)	SER(288)	2.004	1.652	1.277
9	SER(477)	GLN(481)	2.949	2.551	2.595

9	THR(067)	SER(172)	9.413	8.604	7.443
9	THR(394)	GLN(389)	5.730	4.976	4.531
10	ASN(015)	ASN(096)	5.135	4.996	4.538
10	ASN(096)	ASN(015)	5.135	4.996	2.984
10	ASN(207)	SER(202)	3.343	2.707	2.637
10	GLN(092)	SER(002)	3.733	3.411	3.048
10	GLN(478)	GLN(481)	7.000	6.182	4.503
10	GLN(481)	GLN(478)	7.000	6.182	4.231
10	SER(002)	GLN(092)	3.733	3.411	2.165
10	SER(074)	SER(080)	0.434	0.385	0.156
10	SER(080)	SER(074)	0.434	0.385	0.266
10	SER(202)	ASN(207)	3.343	2.707	2.810
10	SER(224)	SER(274)	4.128	3.534	2.867
10	SER(274)	SER(224)	4.128	3.534	2.293
10	SER(288)	SER(383)	2.815	2.382	1.212
10	SER(383)	SER(288)	2.815	2.382	1.677
11	ASN(015)	ASN(096)	13.601	14.004	14.074
11	ASN(096)	ASN(015)	13.601	14.004	11.626
11	ASN(207)	SER(202)	1.647	1.335	1.098
11	GLN(389)	THR(394)	7.847	6.836	5.824
11	GLN(478)	GLN(481)	17.769	16.418	13.912
11	GLN(481)	GLN(478)	17.769	16.418	12.052
11	SER(074)	SER(080)	19.516	18.626	24.159
11	SER(080)	SER(074)	19.516	18.626	22.512
11	SER(172)	THR(067)	11.438	10.740	11.229
11	SER(202)	ASN(207)	1.647	1.335	1.182
11	SER(224)	SER(274)	7.063	6.340	5.706
11	SER(232)	THR(234)	1.086	0.952	0.630
11	SER(274)	SER(224)	7.063	6.340	5.027

11	SER(288)	SER(383)	2.168	1.782	0.865
11	SER(383)	SER(288)	2.168	1.782	1.321
11	THR(067)	SER(172)	11.438	10.740	10.438
11	THR(234)	SER(232)	1.086	0.952	0.689
11	THR(394)	GLN(389)	7.847	6.836	5.792
12	ASN(207)	SER(202)	1.711	1.424	1.189
12	SER(074)	SER(080)	4.327	3.956	4.564
12	SER(080)	SER(074)	4.327	3.956	3.498
12	SER(202)	ASN(207)	1.711	1.424	1.480
12	SER(224)	SER(274)	10.134	9.343	8.876
12	SER(274)	SER(224)	10.134	9.343	7.167
12	SER(288)	SER(383)	1.315	1.094	0.446
12	SER(383)	SER(288)	1.315	1.094	0.716
13	ASN(015)	ASN(096)	5.704	5.353	4.924
13	ASN(096)	ASN(015)	5.704	5.353	4.146
13	ASN(207)	SER(202)	1.751	1.524	1.253
13	GLN(057)	SER(060)	19.397	18.975	18.852
13	GLN(389)	THR(394)	10.091	9.105	9.268
13	GLN(478)	GLN(481)	11.318	10.192	8.406
13	GLN(481)	GLN(478)	11.318	10.192	8.319
13	SER(060)	GLN(057)	19.397	18.975	15.925
13	SER(061)	SER(064)	2.163	2.042	1.345
13	SER(064)	SER(061)	2.163	2.042	1.345
13	SER(074)	SER(080)	0.559	0.504	0.377
13	SER(080)	SER(074)	0.559	0.504	0.257
13	SER(172)	THR(067)	2.164	2.047	1.244
13	SER(202)	ASN(207)	1.751	1.524	1.288
13	SER(224)	SER(274)	1.979	1.728	1.346
13	SER(274)	SER(224)	1.979	1.728	0.870

13	SER(288)	SER(383)	1.196	0.955	0.416
13	SER(383)	SER(288)	1.196	0.955	0.614
13	THR(067)	SER(172)	2.164	2.047	0.719
13	THR(394)	GLN(389)	10.091	9.105	7.350
14	ASN(207)	SER(202)	0.325	0.395	0.157
14	GLN(092)	SER(002)	4.973	4.580	3.859
14	GLN(389)	THR(394)	8.135	7.118	6.679
14	SER(002)	GLN(092)	4.973	4.580	2.679
14	SER(061)	SER(064)	2.070	1.723	1.576
14	SER(064)	SER(061)	2.070	1.723	1.093
14	SER(074)	SER(080)	3.202	3.005	3.153
14	SER(080)	SER(074)	3.202	3.005	2.806
14	SER(172)	THR(067)	2.895	2.770	1.679
14	SER(202)	ASN(207)	0.325	0.395	0.059
14	SER(224)	SER(274)	9.425	8.489	7.082
14	SER(274)	SER(224)	9.425	8.489	6.399
14	SER(288)	SER(383)	2.025	1.637	0.666
14	SER(383)	SER(288)	2.025	1.637	1.100
14	THR(067)	SER(172)	2.895	2.770	1.558
14	THR(394)	GLN(389)	8.135	7.118	6.109
15	ASN(207)	SER(202)	1.190	1.111	0.795
15	SER(074)	SER(080)	3.310	2.899	2.852
15	SER(080)	SER(074)	3.310	2.899	2.829
15	SER(172)	THR(067)	2.520	2.268	1.623
15	SER(202)	ASN(207)	1.190	1.111	0.634
15	SER(224)	SER(274)	7.311	6.550	4.787
15	SER(274)	SER(224)	7.311	6.550	4.418
15	SER(288)	SER(383)	1.260	1.091	0.366
15	SER(383)	SER(288)	1.260	1.091	0.707

15	THR(067)	SER(172)	2.520	2.268	1.113
16	ASN(207)	SER(202)	3.687	3.108	2.373
16	GLN(481)	SER(477)	1.448	1.145	1.030
16	SER(074)	SER(080)	1.886	1.703	1.351
16	SER(080)	SER(074)	1.886	1.703	1.491
16	SER(172)	THR(067)	3.988	3.436	3.050
16	SER(202)	ASN(207)	3.687	3.108	3.854
16	SER(224)	SER(274)	8.368	7.484	6.652
16	SER(274)	SER(224)	8.368	7.484	5.885
16	SER(288)	SER(383)	2.568	2.171	1.028
16	SER(383)	SER(288)	2.568	2.171	1.636
16	SER(477)	GLN(481)	1.448	1.145	0.874
16	THR(067)	SER(172)	3.988	3.436	2.507
17	ASN(207)	SER(202)	2.528	2.051	2.032
17	GLN(478)	GLN(481)	20.620	20.027	16.579
17	GLN(481)	GLN(478)	20.620	20.027	13.395
17	GLN(481)	SER(477)	1.549	1.377	0.991
17	SER(074)	SER(080)	1.648	1.402	1.314
17	SER(080)	SER(074)	1.648	1.402	0.836
17	SER(172)	THR(067)	12.010	11.171	11.564
17	SER(202)	ASN(207)	2.528	2.051	2.879
17	SER(224)	SER(274)	8.738	7.881	7.376
17	SER(274)	SER(224)	8.738	7.881	7.450
17	SER(288)	SER(383)	2.099	1.761	0.842
17	SER(383)	SER(288)	2.099	1.761	1.072
17	SER(477)	GLN(481)	1.549	1.377	1.164
17	THR(067)	SER(172)	12.010	11.171	11.029
18	ASN(207)	SER(202)	1.947	1.659	1.419
18	ASN(406)	GLN(408)	14.460	13.980	10.922

18	GLN(057)	SER(060)	15.765	14.733	13.986
18	GLN(389)	THR(394)	8.406	7.462	7.189
18	GLN(408)	ASN(406)	14.460	13.980	10.026
18	GLN(481)	SER(477)	3.324	2.813	2.858
18	SER(060)	GLN(057)	15.765	14.733	12.820
18	SER(074)	SER(080)	3.001	2.513	1.695
18	SER(080)	SER(074)	3.001	2.513	2.358
18	SER(202)	ASN(207)	1.947	1.659	1.334
18	SER(224)	SER(274)	17.002	15.616	15.120
18	SER(274)	SER(224)	17.002	15.616	13.214
18	SER(288)	SER(383)	2.240	1.850	0.851
18	SER(383)	SER(288)	2.240	1.850	1.341
18	SER(477)	GLN(481)	3.324	2.813	2.824
18	THR(394)	GLN(389)	8.406	7.462	5.996
19	ASN(207)	SER(202)	3.213	2.702	2.495
19	ASN(406)	GLN(408)	7.262	6.548	4.312
19	GLN(389)	SER(298)	0.252	0.275	0.087
19	GLN(408)	ASN(406)	7.262	6.548	4.336
19	SER(074)	SER(080)	0.407	0.398	0.168
19	SER(080)	SER(074)	0.407	0.398	0.311
19	SER(172)	THR(067)	10.484	10.099	11.900
19	SER(202)	ASN(207)	3.213	2.702	2.781
19	SER(224)	SER(274)	6.155	5.535	5.133
19	SER(274)	SER(224)	6.155	5.535	3.961
19	SER(288)	SER(383)	0.744	0.663	0.221
19	SER(298)	GLN(389)	0.252	0.275	0.074
19	SER(383)	SER(288)	0.744	0.663	0.381
19	THR(067)	SER(172)	10.484	10.099	11.119
20	ASN(207)	SER(202)	4.229	3.744	3.375

20	SER(074)	SER(080)	1.715	1.422	0.857
20	SER(080)	SER(074)	1.715	1.422	1.065
20	SER(172)	THR(067)	3.338	2.943	3.024
20	SER(202)	ASN(207)	4.229	3.744	3.630
20	SER(224)	SER(274)	9.002	8.116	7.294
20	SER(274)	SER(224)	9.002	8.116	7.387
20	SER(288)	SER(383)	3.220	2.820	1.407
20	SER(383)	SER(288)	3.220	2.820	1.894
20	THR(067)	SER(172)	3.338	2.943	2.330
21	ASN(207)	SER(202)	4.118	3.337	3.630
21	GLN(478)	GLN(481)	4.778	4.179	2.978
21	GLN(481)	GLN(478)	4.778	4.179	3.495
21	SER(074)	SER(080)	1.777	1.573	0.832
21	SER(080)	SER(074)	1.777	1.573	1.457
21	SER(172)	THR(067)	5.902	5.653	6.070
21	SER(202)	ASN(207)	4.118	3.337	1.145
21	SER(224)	SER(274)	8.467	7.438	6.232
21	SER(274)	SER(224)	8.467	7.438	5.655
21	SER(288)	SER(383)	2.930	2.517	1.430
21	SER(383)	SER(288)	2.930	2.517	1.948
21	THR(067)	SER(172)	5.902	5.653	5.409
22	ASN(207)	SER(202)	1.253	1.127	0.819
22	GLN(057)	SER(060)	21.184	20.697	19.876
22	GLN(092)	SER(002)	0.310	0.356	0.145
22	GLN(389)	SER(298)	0.373	0.383	0.156
22	SER(002)	GLN(092)	0.310	0.356	0.072
22	SER(060)	GLN(057)	21.184	20.697	17.434
22	SER(074)	SER(080)	2.771	2.445	1.786
22	SER(080)	SER(074)	2.771	2.445	2.661

22	SER(172)	THR(067)	0.949	0.880	0.480
22	SER(202)	ASN(207)	1.253	1.127	0.363
22	SER(224)	SER(274)	4.766	4.031	3.548
22	SER(274)	SER(224)	4.766	4.031	2.472
22	SER(288)	SER(383)	2.196	1.794	0.837
22	SER(298)	GLN(389)	0.373	0.383	0.159
22	SER(383)	SER(288)	2.196	1.794	1.281
22	THR(067)	SER(172)	0.949	0.880	0.625
23	ASN(207)	SER(202)	0.645	0.652	0.350
23	ASN(406)	GLN(408)	5.128	4.518	2.996
23	GLN(057)	SER(060)	21.702	20.508	19.793
23	GLN(092)	SER(002)	1.466	1.286	1.154
23	GLN(408)	ASN(406)	5.128	4.518	2.835
23	GLN(478)	GLN(481)	4.578	4.204	2.385
23	GLN(481)	GLN(478)	4.578	4.204	2.943
23	SER(002)	GLN(092)	1.466	1.286	0.629
23	SER(060)	GLN(057)	21.702	20.508	18.354
23	SER(074)	SER(080)	2.316	2.095	1.410
23	SER(080)	SER(074)	2.316	2.095	1.802
23	SER(172)	THR(067)	6.579	5.789	3.934
23	SER(202)	ASN(207)	0.645	0.652	0.436
23	SER(224)	SER(274)	4.589	3.843	3.111
23	SER(274)	SER(224)	4.589	3.843	2.618
23	SER(288)	SER(383)	2.063	1.756	1.099
23	SER(383)	SER(288)	2.063	1.756	1.349
23	THR(067)	SER(172)	6.579	5.789	5.276
24	ASN(015)	ASN(096)	8.423	8.247	7.914
24	ASN(096)	ASN(015)	8.423	8.247	6.516
24	ASN(207)	SER(202)	1.368	1.220	0.908

24	GLN(478)	GLN(481)	15.360	14.310	12.083
24	GLN(481)	GLN(478)	15.360	14.310	10.072
24	SER(074)	SER(080)	2.263	1.922	1.288
24	SER(080)	SER(074)	2.263	1.922	1.930
24	SER(172)	THR(067)	10.215	9.260	9.187
24	SER(202)	ASN(207)	1.368	1.220	1.090
24	SER(224)	SER(274)	2.555	2.344	1.464
24	SER(274)	SER(224)	2.555	2.344	1.232
24	SER(288)	SER(383)	1.784	1.523	0.739
24	SER(383)	SER(288)	1.784	1.523	0.983
24	THR(067)	SER(172)	10.215	9.260	7.916
25	ASN(207)	SER(202)	2.808	2.273	2.214
25	ASN(406)	GLN(408)	10.436	9.823	6.934
25	GLN(408)	ASN(406)	10.436	9.823	7.411
25	SER(074)	SER(080)	2.334	2.054	1.202
25	SER(080)	SER(074)	2.334	2.054	1.990
25	SER(172)	THR(067)	7.596	6.484	5.689
25	SER(202)	ASN(207)	2.808	2.273	2.593
25	SER(224)	SER(274)	3.238	2.958	1.746
25	SER(232)	THR(234)	2.922	2.460	1.548
25	SER(274)	SER(224)	3.238	2.958	1.627
25	SER(288)	SER(383)	1.688	1.378	0.587
25	SER(383)	SER(288)	1.688	1.378	0.937
25	THR(067)	SER(172)	7.596	6.484	5.323
25	THR(234)	SER(232)	2.922	2.460	2.111

Table B.2.: SAPT, EFP and QM/EFP total interaction energies computed for aryl-aryl dimers. All energies are given in units of kcal/mol. For QM/EFP, monA represents the QM region and monB the effective fragment.

snapshot	monA	monB	SAPT	EFP	QMEFP
1	PHE(146)	TRP(150)	-6.549	-3.402	-3.858
1	PHE(149)	TYR(290)	-4.798	-3.811	-3.478
1	PHE(278)	TYR(223)	-3.943	-2.837	-2.957
1	PHE(310)	TRP(312)	-3.837	-2.896	-2.539
1	PHE(357)	TRP(322)	-4.214	-1.834	-2.226
1	TRP(150)	PHE(146)	-6.549	-3.402	-3.996
1	TRP(312)	PHE(310)	-3.837	-2.896	-2.323
1	TRP(322)	PHE(357)	-4.214	-1.834	-3.026
1	TYR(223)	PHE(278)	-3.943	-2.837	-3.600
1	TYR(290)	PHE(149)	-4.798	-3.811	-2.565
2	HSD(437)	TYR(412)	-4.309	-2.639	-3.449
2	PHE(149)	TYR(290)	-4.025	-2.790	-2.165
2	PHE(310)	TRP(312)	-4.364	-3.856	-2.252
2	PHE(357)	TRP(322)	-4.332	-3.006	-1.610
2	TRP(312)	PHE(310)	-4.364	-3.856	-2.442
2	TRP(322)	PHE(357)	-4.332	-3.006	-2.835
2	TYR(290)	PHE(149)	-4.025	-2.790	-2.931
2	TYR(412)	HSD(437)	-4.309	-2.639	-4.150
3	PHE(149)	TYR(290)	-4.760	-2.709	-0.569
3	PHE(185)	TRP(033)	-11.452	-8.433	-7.437
3	PHE(310)	TRP(312)	-4.939	-3.666	-2.590
3	PHE(357)	TRP(322)	-4.032	-0.702	1.157
3	TRP(033)	PHE(185)	-11.452	-8.433	-9.932

3	TRP(312)	PHE(310)	-4.939	-3.666	-3.439
3	TRP(322)	PHE(357)	-4.032	-0.702	-2.554
3	TYR(290)	PHE(149)	-4.760	-2.709	-2.387
4	HSD(437)	TYR(412)	-3.623	0.144	-3.187
4	PHE(149)	TYR(290)	-3.872	-1.378	-0.911
4	PHE(185)	TRP(033)	-12.423	-9.120	-8.523
4	PHE(357)	TRP(322)	-4.278	-3.546	-1.962
4	TRP(033)	PHE(185)	-12.423	-9.120	-11.802
4	TRP(322)	PHE(357)	-4.278	-3.546	-2.899
4	TYR(290)	PHE(149)	-3.872	-1.378	-2.422
4	TYR(412)	HSD(437)	-3.623	0.144	-2.973
5	HSD(437)	TYR(412)	-6.207	-5.257	-7.035
5	PHE(146)	TYR(287)	-6.177	-5.634	-5.355
5	PHE(149)	TYR(290)	-4.059	-4.144	-2.979
5	PHE(185)	TRP(033)	-9.704	-9.093	-8.182
5	PHE(357)	TRP(322)	-3.946	-0.733	-0.397
5	TRP(033)	PHE(185)	-9.704	-9.093	-8.711
5	TRP(322)	PHE(357)	-3.946	-0.733	-2.568
5	TYR(287)	PHE(146)	-6.177	-5.634	-5.368
5	TYR(290)	PHE(149)	-4.059	-4.144	-2.631
5	TYR(412)	HSD(437)	-6.207	-5.257	-5.058
6	HSD(295)	TYR(297)	-6.587	-5.416	-4.242
6	HSD(437)	TYR(412)	-4.302	-2.540	-7.921
6	PHE(149)	TYR(290)	-4.103	-2.971	-2.214
6	PHE(185)	TRP(033)	-13.143	-10.241	-10.225
6	PHE(310)	TRP(312)	-3.750	-2.069	-4.142
6	PHE(357)	TRP(322)	-3.717	-0.426	-0.383
6	TRP(033)	PHE(185)	-13.143	-10.241	-11.964
6	TRP(312)	PHE(310)	-3.750	-2.069	-1.180

6	TRP(322)	PHE(357)	-3.717	-0.426	-2.306
6	TYR(290)	PHE(149)	-4.103	-2.971	-2.616
6	TYR(297)	HSD(295)	-6.587	-5.416	-5.296
6	TYR(412)	HSD(437)	-4.302	-2.540	-3.943
7	HSD(295)	TYR(297)	1.300	4.110	5.235
7	HSD(437)	TYR(412)	-4.093	0.428	-2.976
7	PHE(146)	TRP(150)	-6.737	-6.075	-5.213
7	PHE(149)	TYR(290)	-4.319	-4.070	-2.471
7	PHE(185)	TRP(033)	-11.981	-8.459	-10.250
7	PHE(310)	TRP(312)	-5.823	-2.781	-2.766
7	PHE(357)	TRP(322)	-4.010	-0.245	-0.279
7	TRP(033)	PHE(185)	-11.981	-8.459	-11.001
7	TRP(150)	PHE(146)	-6.737	-6.075	-5.127
7	TRP(312)	PHE(310)	-5.823	-2.781	-3.466
7	TRP(322)	PHE(357)	-4.010	-0.245	-3.018
7	TYR(290)	PHE(149)	-4.319	-4.070	-2.844
7	TYR(297)	HSD(295)	1.300	4.110	1.478
7	TYR(412)	HSD(437)	-4.093	0.428	-5.274
8	HSD(437)	TYR(412)	-4.951	-2.316	-3.843
8	PHE(146)	TYR(287)	-6.119	-5.487	-3.729
8	PHE(149)	TYR(290)	-3.693	-3.149	-1.155
8	PHE(185)	TRP(033)	-12.710	-8.653	-8.035
8	PHE(310)	TRP(312)	-3.934	0.775	0.351
8	PHE(357)	TRP(322)	-4.555	-3.461	-3.044
8	TRP(033)	PHE(185)	-12.710	-8.653	-12.420
8	TRP(312)	PHE(310)	-3.934	0.775	-0.827
8	TRP(322)	PHE(357)	-4.555	-3.461	-3.535
8	TYR(287)	PHE(146)	-6.119	-5.487	-6.077
8	TYR(290)	PHE(149)	-3.693	-3.149	-2.496

8	TYR(412)	HSD(437)	-4.951	-2.316	-3.277
9	HSD(437)	TYR(412)	-8.298	-7.569	-7.132
9	PHE(149)	TYR(290)	-4.617	-3.477	-2.767
9	PHE(185)	TRP(033)	-6.838	-6.448	-4.967
9	PHE(310)	TRP(312)	-4.732	-4.029	-2.325
9	PHE(357)	TRP(322)	-4.904	-3.332	-0.300
9	TRP(033)	PHE(185)	-6.838	-6.448	-5.771
9	TRP(312)	PHE(310)	-4.732	-4.029	-3.501
9	TRP(322)	PHE(357)	-4.904	-3.332	-2.529
9	TYR(290)	PHE(149)	-4.617	-3.477	-2.852
9	TYR(412)	HSD(437)	-8.298	-7.569	-7.518
10	HSD(437)	TYR(412)	-7.637	-6.872	-6.723
10	PHE(146)	TYR(287)	-6.281	-6.341	-4.714
10	PHE(149)	TYR(290)	-3.852	-3.438	-2.581
10	PHE(185)	TRP(033)	-8.058	-7.727	-6.594
10	PHE(244)	TRP(050)	-2.786	2.900	-0.323
10	PHE(310)	TRP(312)	-4.171	-1.652	-1.201
10	PHE(357)	TRP(322)	-4.493	-3.335	-2.741
10	TRP(033)	PHE(185)	-8.058	-7.727	-6.750
10	TRP(050)	PHE(244)	-2.786	2.900	-1.723
10	TRP(312)	PHE(310)	-4.171	-1.652	-1.978
10	TRP(322)	PHE(357)	-4.493	-3.335	-3.321
10	TYR(287)	PHE(146)	-6.281	-6.341	-5.449
10	TYR(290)	PHE(149)	-3.852	-3.438	-2.730
10	TYR(412)	HSD(437)	-7.637	-6.872	-6.422
11	HSD(437)	TYR(412)	-7.801	-5.862	-7.118
11	PHE(149)	TYR(290)	-4.740	-3.006	-1.801
11	PHE(319)	TRP(367)	-3.952	-1.930	-3.444
11	PHE(357)	TRP(322)	-3.303	2.253	1.759

11	TRP(322)	PHE(357)	-3.303	2.253	-2.436
11	TRP(367)	PHE(319)	-3.952	-1.930	-2.217
11	TYR(290)	PHE(149)	-4.740	-3.006	-2.943
11	TYR(412)	HSD(437)	-7.801	-5.862	-7.015
12	HSD(437)	TYR(412)	-5.420	-3.255	-5.350
12	PHE(149)	TYR(290)	-3.700	-3.159	-2.302
12	PHE(310)	TRP(312)	-4.087	-1.621	-2.555
12	PHE(357)	TRP(322)	-4.730	-3.089	-1.427
12	TRP(312)	PHE(310)	-4.087	-1.621	-3.805
12	TRP(322)	PHE(357)	-4.730	-3.089	-3.557
12	TYR(290)	PHE(149)	-3.700	-3.159	-2.629
12	TYR(412)	HSD(437)	-5.420	-3.255	-5.280
13	HSD(437)	TYR(412)	-5.682	-3.820	-5.649
13	PHE(146)	TYR(287)	-6.006	-4.598	-4.493
13	PHE(149)	TYR(290)	-3.279	-3.054	-2.505
13	PHE(310)	TRP(312)	-5.318	-4.319	-3.524
13	PHE(357)	TRP(322)	-4.507	-2.287	-1.179
13	TRP(312)	PHE(310)	-5.318	-4.319	-3.381
13	TRP(322)	PHE(357)	-4.507	-2.287	-2.919
13	TYR(287)	PHE(146)	-6.006	-4.598	-4.558
13	TYR(290)	PHE(149)	-3.279	-3.054	-2.326
13	TYR(412)	HSD(437)	-5.682	-3.820	-5.567
14	HSD(437)	TYR(412)	-4.899	-1.198	-5.324
14	PHE(146)	TYR(287)	-7.097	-7.406	-5.853
14	PHE(149)	TYR(290)	-4.123	-3.504	-2.214
14	PHE(185)	TRP(033)	-7.416	-6.125	-5.497
14	PHE(310)	TRP(312)	-5.042	-4.019	-3.301
14	PHE(357)	TRP(322)	-5.247	-3.737	-3.134
14	TRP(033)	PHE(185)	-7.416	-6.125	-5.974

14	TRP(312)	PHE(310)	-5.042	-4.019	-4.024
14	TRP(322)	PHE(357)	-5.247	-3.737	-3.834
14	TYR(287)	PHE(146)	-7.097	-7.406	-6.734
14	TYR(290)	PHE(149)	-4.123	-3.504	-2.977
14	TYR(412)	HSD(437)	-4.899	-1.198	-5.823
15	HSD(437)	TYR(412)	-2.756	0.990	-7.481
15	PHE(149)	TYR(290)	-3.669	-3.475	-2.332
15	PHE(310)	TRP(312)	-4.388	-2.463	-1.315
15	PHE(357)	TRP(322)	-4.483	-2.634	-0.870
15	TRP(312)	PHE(310)	-4.388	-2.463	-2.734
15	TRP(322)	PHE(357)	-4.483	-2.634	-2.316
15	TRP(373)	TYR(041)	-6.921	-6.018	-5.321
15	TYR(041)	TRP(373)	-6.921	-6.018	-5.150
15	TYR(290)	PHE(149)	-3.669	-3.475	-2.546
15	TYR(412)	HSD(437)	-2.756	0.990	-2.374
16	HSD(437)	TYR(412)	-6.035	-4.246	-7.187
16	PHE(149)	TYR(290)	-4.387	-3.664	-2.155
16	PHE(372)	TRP(388)	-4.722	-2.720	-4.692
16	TRP(388)	PHE(372)	-4.722	-2.720	-2.635
16	TYR(290)	PHE(149)	-4.387	-3.664	-2.321
16	TYR(412)	HSD(437)	-6.035	-4.246	-5.235
17	HSD(437)	TYR(412)	-2.560	1.693	-8.025
17	PHE(146)	TYR(287)	-6.186	-4.690	-2.683
17	PHE(149)	TYR(290)	-4.381	-3.642	-2.015
17	PHE(185)	TRP(033)	-5.342	-3.606	-4.620
17	PHE(278)	TYR(223)	-2.480	-1.365	-1.773
17	PHE(310)	TRP(312)	-5.590	-4.430	-3.440
17	PHE(357)	TRP(322)	-4.623	-3.725	-3.021
17	TRP(033)	PHE(185)	-5.342	-3.606	-4.965

17	TRP(312)	PHE(310)	-5.590	-4.430	-3.541
17	TRP(322)	PHE(357)	-4.623	-3.725	-3.658
17	TYR(223)	PHE(278)	-2.480	-1.365	-2.154
17	TYR(287)	PHE(146)	-6.186	-4.690	-5.926
17	TYR(290)	PHE(149)	-4.381	-3.642	-2.932
17	TYR(412)	HSD(437)	-2.560	1.693	-2.338
18	HSD(437)	TYR(412)	-6.535	-6.113	-6.301
18	PHE(146)	TYR(287)	-5.647	-4.472	-3.880
18	PHE(149)	TYR(290)	-4.498	-4.005	-2.773
18	PHE(278)	TYR(223)	-2.522	-1.110	-0.740
18	PHE(310)	TRP(312)	-3.513	-0.584	0.645
18	PHE(357)	TRP(322)	-4.731	-3.028	-0.320
18	TRP(312)	PHE(310)	-3.513	-0.584	-2.479
18	TRP(322)	PHE(357)	-4.731	-3.028	-2.482
18	TYR(223)	PHE(278)	-2.522	-1.110	-2.615
18	TYR(287)	PHE(146)	-5.647	-4.472	-5.097
18	TYR(290)	PHE(149)	-4.498	-4.005	-3.092
18	TYR(412)	HSD(437)	-6.535	-6.113	-5.792
19	HSD(437)	TYR(412)	-6.375	-3.358	-3.415
19	PHE(149)	TYR(290)	-2.656	-1.940	-1.888
19	PHE(310)	TRP(312)	-4.433	-3.431	-2.533
19	TRP(312)	PHE(310)	-4.433	-3.431	-2.872
19	TYR(290)	PHE(149)	-2.656	-1.940	-1.539
19	TYR(412)	HSD(437)	-6.375	-3.358	-5.680
21	HSD(437)	TYR(412)	-5.228	-0.843	-4.486
21	PHE(149)	TYR(290)	-3.754	-3.201	-1.934
21	PHE(278)	TYR(223)	-2.965	-2.243	-1.271
21	PHE(310)	TRP(312)	-4.049	-0.570	-1.260
21	TRP(312)	PHE(310)	-4.049	-0.570	-3.091

21	TYR(223)	PHE(278)	-2.965	-2.243	-2.700
21	TYR(290)	PHE(149)	-3.754	-3.201	-2.488
21	TYR(412)	HSD(437)	-5.228	-0.843	-6.182
22	HSD(437)	TYR(412)	-4.936	-4.557	-4.051
22	PHE(149)	TYR(290)	-4.523	-2.276	-0.655
22	PHE(310)	TRP(312)	-3.851	1.042	-1.308
22	PHE(357)	TRP(322)	-4.721	-2.986	0.985
22	TRP(312)	PHE(310)	-3.851	1.042	-2.744
22	TRP(322)	PHE(357)	-4.721	-2.986	-2.589
22	TYR(290)	PHE(149)	-4.523	-2.276	-2.151
22	TYR(412)	HSD(437)	-4.936	-4.557	-4.157
23	HSD(437)	TYR(412)	-6.218	-4.672	-4.644
23	PHE(149)	TYR(290)	-3.694	-0.916	0.898
23	PHE(185)	TRP(033)	-7.995	-6.121	-6.993
23	PHE(310)	TRP(312)	-4.188	-2.485	-0.871
23	PHE(357)	TRP(322)	-4.997	-3.543	-3.058
23	TRP(033)	PHE(185)	-7.995	-6.121	-7.318
23	TRP(312)	PHE(310)	-4.188	-2.485	-1.650
23	TRP(322)	PHE(357)	-4.997	-3.543	-3.517
23	TYR(290)	PHE(149)	-3.694	-0.916	-2.355
23	TYR(412)	HSD(437)	-6.218	-4.672	-4.935
24	HSD(437)	TYR(412)	-6.673	-2.619	-5.531
24	PHE(149)	TYR(290)	-3.310	-2.533	-0.605
24	PHE(185)	TRP(033)	-12.242	-10.083	-9.239
24	PHE(244)	TRP(050)	-3.418	1.624	-0.200
24	PHE(310)	TRP(312)	-5.265	-1.980	-2.270
24	PHE(357)	TRP(322)	-4.948	-3.511	-2.065
24	TRP(033)	PHE(185)	-12.242	-10.083	-11.169
24	TRP(050)	PHE(244)	-3.418	1.624	-0.005

24	TRP(312)	PHE(310)	-5.265	-1.980	-3.947
24	TRP(322)	PHE(357)	-4.948	-3.511	-3.450
24	TYR(290)	PHE(149)	-3.310	-2.533	-2.024
24	TYR(412)	HSD(437)	-6.673	-2.619	-6.680
25	HSD(437)	TYR(412)	-3.997	0.085	-3.300
25	PHE(149)	TYR(290)	-4.049	-4.240	-2.543
25	PHE(310)	TRP(312)	-4.549	-2.682	-0.231
25	PHE(356)	TYR(329)	-2.539	-0.087	-0.075
25	PHE(357)	TRP(322)	-4.217	-3.513	-2.279
25	TRP(312)	PHE(310)	-4.549	-2.682	-2.568
25	TRP(322)	PHE(357)	-4.217	-3.513	-3.012
25	TYR(290)	PHE(149)	-4.049	-4.240	-2.635
25	TYR(329)	PHE(356)	-2.539	-0.087	-2.501
25	TYR(412)	HSD(437)	-3.997	0.085	-3.635

Table B.3.: SAPT, EFP and QM/EFP exchange-repulsion interaction energies computed for aryl-aryl dimers. All energies are given in units of kcal/mol. For QM/EFP, monA represents the QM region and monB the effective fragment.

snapshot	monA	monB	SAPT	EFP	QMEFP
1	PHE(146)	TRP(150)	10.110	10.093	8.225
1	PHE(149)	TYR(290)	5.581	5.109	4.443
1	PHE(278)	TYR(223)	5.724	5.595	3.528
1	PHE(310)	TRP(312)	7.421	7.089	4.773
1	PHE(357)	TRP(322)	7.948	7.916	5.922
1	TRP(150)	PHE(146)	10.110	10.093	8.517
1	TRP(312)	PHE(310)	7.421	7.089	4.854

1	TRP(322)	PHE(357)	7.948	7.916	5.563
1	TYR(223)	PHE(278)	5.724	5.595	3.498
1	TYR(290)	PHE(149)	5.581	5.109	4.381
2	HSD(437)	TYR(412)	7.432	7.288	5.164
2	PHE(149)	TYR(290)	5.456	5.001	4.080
2	PHE(310)	TRP(312)	7.615	6.946	5.489
2	PHE(357)	TRP(322)	6.794	6.574	6.116
2	TRP(312)	PHE(310)	7.615	6.946	5.627
2	TRP(322)	PHE(357)	6.794	6.574	5.284
2	TYR(290)	PHE(149)	5.456	5.001	3.420
2	TYR(412)	HSD(437)	7.432	7.288	6.118
3	PHE(149)	TYR(290)	9.097	8.698	8.775
3	PHE(185)	TRP(033)	14.463	13.680	13.321
3	PHE(310)	TRP(312)	7.198	6.959	5.563
3	PHE(357)	TRP(322)	10.936	11.483	12.016
3	TRP(033)	PHE(185)	14.463	13.680	11.365
3	TRP(312)	PHE(310)	7.198	6.959	5.632
3	TRP(322)	PHE(357)	10.936	11.483	8.428
3	TYR(290)	PHE(149)	9.097	8.698	7.014
4	HSD(437)	TYR(412)	16.655	16.652	12.609
4	PHE(149)	TYR(290)	10.010	9.772	8.909
4	PHE(185)	TRP(033)	15.025	14.145	14.648
4	PHE(357)	TRP(322)	5.389	5.096	4.797
4	TRP(033)	PHE(185)	15.025	14.145	13.020
4	TRP(322)	PHE(357)	5.389	5.096	3.654
4	TYR(290)	PHE(149)	10.010	9.772	7.148
4	TYR(412)	HSD(437)	16.655	16.652	13.259
5	HSD(437)	TYR(412)	5.188	4.882	2.309
5	PHE(146)	TYR(287)	4.872	4.484	2.798

5	PHE(149)	TYR(290)	2.865	2.542	2.124
5	PHE(185)	TRP(033)	4.181	3.683	2.807
5	PHE(357)	TRP(322)	10.604	11.005	10.052
5	TRP(033)	PHE(185)	4.181	3.683	2.740
5	TRP(322)	PHE(357)	10.604	11.005	7.935
5	TYR(287)	PHE(146)	4.872	4.484	2.846
5	TYR(290)	PHE(149)	2.865	2.542	1.933
5	TYR(412)	HSD(437)	5.188	4.882	3.283
6	HSD(295)	TYR(297)	8.522	7.973	8.154
6	HSD(437)	TYR(412)	10.324	9.816	3.929
6	PHE(149)	TYR(290)	5.809	5.241	4.285
6	PHE(185)	TRP(033)	10.462	9.677	8.486
6	PHE(310)	TRP(312)	10.215	9.666	5.443
6	PHE(357)	TRP(322)	10.936	11.019	9.377
6	TRP(033)	PHE(185)	10.462	9.677	7.851
6	TRP(312)	PHE(310)	10.215	9.666	7.626
6	TRP(322)	PHE(357)	10.936	11.019	8.571
6	TYR(290)	PHE(149)	5.809	5.241	4.361
6	TYR(297)	HSD(295)	8.522	7.973	6.420
6	TYR(412)	HSD(437)	10.324	9.816	6.998
7	HSD(295)	TYR(297)	13.313	12.463	12.533
7	HSD(437)	TYR(412)	16.282	16.920	12.590
7	PHE(146)	TRP(150)	4.678	4.216	3.073
7	PHE(149)	TYR(290)	3.787	3.304	3.014
7	PHE(185)	TRP(033)	12.697	12.437	8.569
7	PHE(310)	TRP(312)	12.355	12.345	9.705
7	PHE(357)	TRP(322)	11.903	12.336	10.897
7	TRP(033)	PHE(185)	12.697	12.437	9.922
7	TRP(150)	PHE(146)	4.678	4.216	3.394

7	TRP(312)	PHE(310)	12.355	12.345	8.805
7	TRP(322)	PHE(357)	11.903	12.336	8.919
7	TYR(290)	PHE(149)	3.787	3.304	2.535
7	TYR(297)	HSD(295)	13.313	12.463	9.216
7	TYR(412)	HSD(437)	16.282	16.920	12.565
8	HSD(437)	TYR(412)	14.154	13.968	10.953
8	PHE(146)	TYR(287)	9.531	8.731	7.920
8	PHE(149)	TYR(290)	6.462	5.817	5.910
8	PHE(185)	TRP(033)	14.612	14.225	14.742
8	PHE(310)	TRP(312)	17.255	17.496	14.920
8	PHE(357)	TRP(322)	5.129	5.018	3.986
8	TRP(033)	PHE(185)	14.612	14.225	11.733
8	TRP(312)	PHE(310)	17.255	17.496	14.270
8	TRP(322)	PHE(357)	5.129	5.018	3.552
8	TYR(287)	PHE(146)	9.531	8.731	5.767
8	TYR(290)	PHE(149)	6.462	5.817	4.945
8	TYR(412)	HSD(437)	14.154	13.968	11.633
9	HSD(437)	TYR(412)	6.702	6.463	5.002
9	PHE(149)	TYR(290)	6.174	5.549	4.654
9	PHE(185)	TRP(033)	3.224	2.859	2.622
9	PHE(310)	TRP(312)	5.282	4.915	4.252
9	PHE(357)	TRP(322)	7.766	7.459	8.747
9	TRP(033)	PHE(185)	3.224	2.859	2.201
9	TRP(312)	PHE(310)	5.282	4.915	3.351
9	TRP(322)	PHE(357)	7.766	7.459	6.025
9	TYR(290)	PHE(149)	6.174	5.549	4.459
9	TYR(412)	HSD(437)	6.702	6.463	4.435
10	HSD(437)	TYR(412)	6.443	6.321	4.802
10	PHE(146)	TYR(287)	4.803	4.282	3.923

10	PHE(149)	TYR(290)	3.217	2.943	2.348
10	PHE(185)	TRP(033)	3.221	2.769	2.149
10	PHE(244)	TRP(050)	14.054	14.773	12.741
10	PHE(310)	TRP(312)	11.403	11.188	8.591
10	PHE(357)	TRP(322)	5.139	4.975	4.177
10	TRP(033)	PHE(185)	3.221	2.769	2.135
10	TRP(050)	PHE(244)	14.054	14.773	10.493
10	TRP(312)	PHE(310)	11.403	11.188	9.097
10	TRP(322)	PHE(357)	5.139	4.975	3.399
10	TYR(287)	PHE(146)	4.803	4.282	3.199
10	TYR(290)	PHE(149)	3.217	2.943	2.066
10	TYR(412)	HSD(437)	6.443	6.321	4.575
11	HSD(437)	TYR(412)	10.262	10.100	7.604
11	PHE(149)	TYR(290)	6.894	6.406	5.892
11	PHE(319)	TRP(367)	7.982	7.555	5.159
11	PHE(357)	TRP(322)	15.405	16.160	14.551
11	TRP(322)	PHE(357)	15.405	16.160	11.466
11	TRP(367)	PHE(319)	7.982	7.555	6.027
11	TYR(290)	PHE(149)	6.894	6.406	4.395
11	TYR(412)	HSD(437)	10.262	10.100	7.985
12	HSD(437)	TYR(412)	10.941	10.576	6.568
12	PHE(149)	TYR(290)	3.226	2.826	2.267
12	PHE(310)	TRP(312)	8.768	9.077	5.935
12	PHE(357)	TRP(322)	7.532	7.270	7.480
12	TRP(312)	PHE(310)	8.768	9.077	6.106
12	TRP(322)	PHE(357)	7.532	7.270	5.738
12	TYR(290)	PHE(149)	3.226	2.826	1.729
12	TYR(412)	HSD(437)	10.941	10.576	7.894
13	HSD(437)	TYR(412)	8.903	8.851	5.247

13	PHE(146)	TYR(287)	9.208	8.696	6.975
13	PHE(149)	TYR(290)	2.195	1.877	1.230
13	PHE(310)	TRP(312)	7.619	7.229	5.560
13	PHE(357)	TRP(322)	8.708	8.521	7.793
13	TRP(312)	PHE(310)	7.619	7.229	5.283
13	TRP(322)	PHE(357)	8.708	8.521	6.685
13	TYR(287)	PHE(146)	9.208	8.696	6.432
13	TYR(290)	PHE(149)	2.195	1.877	1.418
13	TYR(412)	HSD(437)	8.903	8.851	6.834
14	HSD(437)	TYR(412)	17.448	17.178	11.561
14	PHE(146)	TYR(287)	6.478	5.486	4.756
14	PHE(149)	TYR(290)	5.272	4.607	4.129
14	PHE(185)	TRP(033)	5.510	5.302	3.635
14	PHE(310)	TRP(312)	5.910	5.784	4.396
14	PHE(357)	TRP(322)	7.668	7.391	5.538
14	TRP(033)	PHE(185)	5.510	5.302	3.713
14	TRP(312)	PHE(310)	5.910	5.784	3.931
14	TRP(322)	PHE(357)	7.668	7.391	5.536
14	TYR(287)	PHE(146)	6.478	5.486	3.238
14	TYR(290)	PHE(149)	5.272	4.607	3.257
14	TYR(412)	HSD(437)	17.448	17.178	12.914
15	HSD(437)	TYR(412)	13.746	13.780	5.175
15	PHE(149)	TYR(290)	3.133	2.661	2.172
15	PHE(310)	TRP(312)	9.090	8.912	7.215
15	PHE(357)	TRP(322)	8.503	8.072	7.832
15	TRP(312)	PHE(310)	9.090	8.912	6.275
15	TRP(322)	PHE(357)	8.503	8.072	6.279
15	TRP(373)	TYR(041)	4.580	4.384	3.569
15	TYR(041)	TRP(373)	4.580	4.384	3.865

15	TYR(290)	PHE(149)	3.133	2.661	1.812
15	TYR(412)	HSD(437)	13.746	13.780	9.803
16	HSD(437)	TYR(412)	10.816	10.328	6.382
16	PHE(149)	TYR(290)	6.771	6.243	5.559
16	PHE(372)	TRP(388)	9.035	8.494	7.480
16	TRP(388)	PHE(372)	9.035	8.494	7.434
16	TYR(290)	PHE(149)	6.771	6.243	5.306
16	TYR(412)	HSD(437)	10.816	10.328	7.746
17	HSD(437)	TYR(412)	15.794	16.026	6.153
17	PHE(146)	TYR(287)	8.035	7.663	7.290
17	PHE(149)	TYR(290)	5.789	5.360	5.221
17	PHE(185)	TRP(033)	6.266	6.092	3.849
17	PHE(278)	TYR(223)	6.071	5.854	4.006
17	PHE(310)	TRP(312)	7.986	7.428	5.643
17	PHE(357)	TRP(322)	5.106	4.877	3.871
17	TRP(033)	PHE(185)	6.266	6.092	4.581
17	TRP(312)	PHE(310)	7.986	7.428	5.748
17	TRP(322)	PHE(357)	5.106	4.877	3.421
17	TYR(223)	PHE(278)	6.071	5.854	4.037
17	TYR(287)	PHE(146)	8.035	7.663	5.167
17	TYR(290)	PHE(149)	5.789	5.360	3.836
17	TYR(412)	HSD(437)	15.794	16.026	12.358
18	HSD(437)	TYR(412)	3.887	3.497	1.838
18	PHE(146)	TYR(287)	6.785	6.344	4.784
18	PHE(149)	TYR(290)	3.794	3.350	3.023
18	PHE(278)	TYR(223)	7.476	7.184	6.394
18	PHE(310)	TRP(312)	12.098	12.148	11.563
18	PHE(357)	TRP(322)	9.481	8.966	9.504
18	TRP(312)	PHE(310)	12.098	12.148	9.023

18	TRP(322)	PHE(357)	9.481	8.966	7.448
18	TYR(223)	PHE(278)	7.476	7.184	5.040
18	TYR(287)	PHE(146)	6.785	6.344	4.440
18	TYR(290)	PHE(149)	3.794	3.350	2.401
18	TYR(412)	HSD(437)	3.887	3.497	2.469
19	HSD(437)	TYR(412)	14.281	14.809	12.569
19	PHE(149)	TYR(290)	3.749	3.452	2.161
19	PHE(310)	TRP(312)	6.506	6.191	4.524
19	TRP(312)	PHE(310)	6.506	6.191	4.813
19	TYR(290)	PHE(149)	3.749	3.452	2.603
19	TYR(412)	HSD(437)	14.281	14.809	11.999
21	HSD(437)	TYR(412)	18.093	18.679	13.430
21	PHE(149)	TYR(290)	4.160	3.651	3.224
21	PHE(278)	TYR(223)	5.287	4.947	4.150
21	PHE(310)	TRP(312)	12.529	12.583	9.949
21	TRP(312)	PHE(310)	12.529	12.583	8.450
21	TYR(223)	PHE(278)	5.287	4.947	3.032
21	TYR(290)	PHE(149)	4.160	3.651	2.576
21	TYR(412)	HSD(437)	18.093	18.679	13.642
22	HSD(437)	TYR(412)	4.425	3.886	2.539
22	PHE(149)	TYR(290)	9.764	9.456	9.237
22	PHE(310)	TRP(312)	14.819	15.248	11.322
22	PHE(357)	TRP(322)	9.842	9.685	11.827
22	TRP(312)	PHE(310)	14.819	15.248	8.858
22	TRP(322)	PHE(357)	9.842	9.685	7.827
22	TYR(290)	PHE(149)	9.764	9.456	7.816
22	TYR(412)	HSD(437)	4.425	3.886	2.832
23	HSD(437)	TYR(412)	10.567	10.229	8.264
23	PHE(149)	TYR(290)	11.561	11.201	11.031

23	PHE(185)	TRP(033)	6.247	6.021	3.790
23	PHE(310)	TRP(312)	10.509	10.199	9.944
23	PHE(357)	TRP(322)	6.298	6.088	5.083
23	TRP(033)	PHE(185)	6.247	6.021	3.694
23	TRP(312)	PHE(310)	10.509	10.199	7.605
23	TRP(322)	PHE(357)	6.298	6.088	4.491
23	TYR(290)	PHE(149)	11.561	11.201	8.450
23	TYR(412)	HSD(437)	10.567	10.229	8.239
24	HSD(437)	TYR(412)	12.391	13.554	9.077
24	PHE(149)	TYR(290)	5.964	5.276	5.451
24	PHE(185)	TRP(033)	9.832	8.853	7.182
24	PHE(244)	TRP(050)	13.885	14.542	13.884
24	PHE(310)	TRP(312)	11.129	11.466	9.178
24	PHE(357)	TRP(322)	6.822	6.599	6.028
24	TRP(033)	PHE(185)	9.832	8.853	6.151
24	TRP(050)	PHE(244)	13.885	14.542	11.996
24	TRP(312)	PHE(310)	11.129	11.466	7.212
24	TRP(322)	PHE(357)	6.822	6.599	4.852
24	TYR(290)	PHE(149)	5.964	5.276	4.604
24	TYR(412)	HSD(437)	12.391	13.554	10.249
25	HSD(437)	TYR(412)	14.120	14.381	9.219
25	PHE(149)	TYR(290)	2.598	2.102	1.969
25	PHE(310)	TRP(312)	9.697	9.518	9.577
25	PHE(356)	TYR(329)	7.546	7.389	6.131
25	PHE(357)	TRP(322)	4.162	3.729	3.299
25	TRP(312)	PHE(310)	9.697	9.518	6.850
25	TRP(322)	PHE(357)	4.162	3.729	2.678
25	TYR(290)	PHE(149)	2.598	2.102	1.698
25	TYR(329)	PHE(356)	7.546	7.389	4.891

25	TYR(412)	HSD(437)	14.120	14.381	11.359

Table B.4.: SAPT, EFP and QM/EFP electrostatics and polarization interaction energies computed for polar-polar dimers. All energies are given in units of kcal/mol. For QM/EFP, monA represents the QM region and monB the effective fragment.

snapshot	monA	monB	SAPT	EFP	QMEFP
1	ASN(207)	SER(202)	-0.289	0.475	0.284
1	ASN(406)	GLN(408)	-14.994	-11.276	-13.204
1	GLN(057)	SER(060)	-23.238	-17.325	-21.402
1	GLN(092)	SER(002)	-10.279	-7.888	-9.091
1	GLN(389)	THR(394)	-4.853	-3.986	-4.261
1	GLN(408)	ASN(406)	-14.994	-11.276	-13.196
1	GLN(481)	SER(477)	-3.305	-2.872	-2.966
1	SER(002)	GLN(092)	-10.279	-7.888	-8.731
1	SER(060)	GLN(057)	-23.238	-17.325	-22.481
1	SER(074)	SER(080)	-2.834	-1.479	-1.922
1	SER(080)	SER(074)	-2.834	-1.479	-2.585
1	SER(172)	THR(067)	-3.379	-2.281	-2.597
1	SER(202)	ASN(207)	-0.289	0.475	0.302
1	SER(224)	SER(274)	-8.628	-5.733	-8.124
1	SER(232)	THR(234)	0.395	0.825	0.686
1	SER(274)	SER(224)	-8.628	-5.733	-7.281
1	SER(288)	SER(383)	-3.827	-2.354	-3.099
1	SER(383)	SER(288)	-3.827	-2.354	-2.899
1	SER(477)	GLN(481)	-3.305	-2.872	-2.830
1	THR(067)	SER(172)	-3.379	-2.281	-2.333

1	THR(234)	SER(232)	0.395	0.825	0.716
1	THR(392)	THR(394)	1.349	1.552	1.676
1	THR(394)	GLN(389)	-4.853	-3.986	-4.076
1	THR(394)	THR(392)	1.349	1.552	1.562
2	ASN(207)	SER(202)	0.866	1.116	1.079
2	ASN(406)	GLN(408)	-22.463	-14.623	-22.006
2	GLN(092)	SER(002)	-2.521	-1.134	-1.367
2	GLN(389)	THR(394)	-2.245	-1.382	-1.539
2	GLN(408)	ASN(406)	-22.463	-14.623	-25.248
2	SER(002)	GLN(092)	-2.521	-1.134	-1.515
2	SER(074)	SER(080)	-1.865	-0.652	-0.990
2	SER(080)	SER(074)	-1.865	-0.652	-1.684
2	SER(202)	ASN(207)	0.866	1.116	1.100
2	SER(224)	SER(274)	-6.396	-4.372	-5.508
2	SER(232)	THR(234)	0.459	0.777	0.695
2	SER(274)	SER(224)	-6.396	-4.372	-4.929
2	SER(288)	SER(383)	-2.067	-1.384	-1.531
2	SER(383)	SER(288)	-2.067	-1.384	-1.549
2	THR(234)	SER(232)	0.459	0.777	0.654
2	THR(392)	THR(394)	-9.725	-7.552	-8.686
2	THR(394)	GLN(389)	-2.245	-1.382	-1.709
2	THR(394)	THR(392)	-9.725	-7.552	-9.288
3	GLN(092)	SER(002)	-1.306	-0.415	-0.528
3	SER(002)	GLN(092)	-1.306	-0.415	-0.611
3	SER(074)	SER(080)	-15.469	-11.534	-15.454
3	SER(080)	SER(074)	-15.469	-11.534	-14.615
3	SER(224)	SER(274)	-4.996	-3.530	-4.078
3	SER(232)	THR(234)	-0.027	0.207	0.133
3	SER(274)	SER(224)	-4.996	-3.530	-3.723

3	THR(234)	SER(232)	-0.027	0.207	0.150
3	THR(392)	THR(394)	-6.856	-5.431	-5.873
3	THR(394)	THR(392)	-6.856	-5.431	-6.067
4	ASN(015)	ASN(096)	-4.292	-3.058	-3.541
4	ASN(096)	ASN(015)	-4.292	-3.058	-3.495
4	ASN(207)	SER(202)	-3.767	-2.949	-3.169
4	GLN(057)	SER(060)	-28.577	-20.747	-26.140
4	GLN(389)	THR(394)	-1.880	-0.980	-1.095
4	GLN(478)	GLN(481)	-12.568	-8.618	-9.952
4	GLN(481)	GLN(478)	-12.568	-8.618	-10.305
4	GLN(481)	SER(477)	-3.639	-2.356	-2.830
4	SER(060)	GLN(057)	-28.577	-20.747	-30.206
4	SER(074)	SER(080)	-2.675	-2.190	-2.358
4	SER(080)	SER(074)	-2.675	-2.190	-2.193
4	SER(202)	ASN(207)	-3.767	-2.949	-2.961
4	SER(224)	SER(274)	-3.875	-3.048	-3.265
4	SER(274)	SER(224)	-3.875	-3.048	-3.067
4	SER(288)	SER(383)	-3.230	-1.823	-2.524
4	SER(383)	SER(288)	-3.230	-1.823	-2.198
4	SER(477)	GLN(481)	-3.639	-2.356	-2.609
4	THR(392)	THR(394)	-7.401	-6.054	-6.637
4	THR(394)	GLN(389)	-1.880	-0.980	-1.269
4	THR(394)	THR(392)	-7.401	-6.054	-6.745
5	ASN(207)	SER(202)	-1.990	-1.276	-1.802
5	GLN(057)	SER(060)	-4.443	-3.388	-3.648
5	GLN(092)	SER(002)	-2.872	-1.272	-1.738
5	GLN(389)	THR(394)	-3.352	-2.085	-2.308
5	SER(002)	GLN(092)	-2.872	-1.272	-1.952
5	SER(060)	GLN(057)	-4.443	-3.388	-3.741

5	SER(074)	SER(080)	-1.747	-0.502	-0.822
5	SER(080)	SER(074)	-1.747	-0.502	-1.399
5	SER(172)	THR(067)	-15.925	-11.590	-13.845
5	SER(202)	ASN(207)	-1.990	-1.276	-1.589
5	SER(224)	SER(274)	-10.126	-6.558	-9.887
5	SER(274)	SER(224)	-10.126	-6.558	-8.685
5	THR(067)	SER(172)	-15.925	-11.590	-13.666
5	THR(392)	THR(394)	0.434	0.809	0.894
5	THR(394)	GLN(389)	-3.352	-2.085	-2.651
5	THR(394)	THR(392)	0.434	0.809	0.811
6	ASN(207)	SER(202)	0.222	1.413	0.994
6	GLN(389)	THR(394)	-4.785	-3.751	-3.926
6	GLN(478)	GLN(481)	-6.608	-4.036	-4.342
6	GLN(481)	GLN(478)	-6.608	-4.036	-4.846
6	SER(074)	SER(080)	-1.578	-0.907	-1.137
6	SER(080)	SER(074)	-1.578	-0.907	-1.284
6	SER(172)	THR(067)	-9.602	-7.454	-8.386
6	SER(202)	ASN(207)	0.222	1.413	1.252
6	SER(224)	SER(274)	-5.609	-3.547	-4.480
6	SER(232)	THR(234)	0.864	1.224	1.193
6	SER(274)	SER(224)	-5.609	-3.547	-4.156
6	THR(067)	SER(172)	-9.602	-7.454	-7.777
6	THR(234)	SER(232)	0.864	1.224	1.140
6	THR(392)	THR(394)	-15.785	-11.279	-14.964
6	THR(394)	GLN(389)	-4.785	-3.751	-4.187
6	THR(394)	THR(392)	-15.785	-11.279	-17.734
7	ASN(015)	ASN(096)	-2.274	-1.341	-1.599
7	ASN(096)	ASN(015)	-2.274	-1.341	-1.499
7	ASN(207)	SER(202)	0.418	0.643	0.655

7	GLN(389)	THR(394)	-3.252	-2.382	-2.493
7	GLN(478)	GLN(481)	-23.644	-16.161	-20.828
7	GLN(481)	GLN(478)	-23.644	-16.161	-21.118
7	GLN(481)	SER(477)	-5.653	-4.612	-5.061
7	SER(074)	SER(080)	-3.786	-2.189	-2.451
7	SER(080)	SER(074)	-3.786	-2.189	-3.142
7	SER(172)	THR(067)	-11.435	-8.623	-9.840
7	SER(202)	ASN(207)	0.418	0.643	0.743
7	SER(224)	SER(274)	-2.017	-1.625	-1.642
7	SER(274)	SER(224)	-2.017	-1.625	-1.559
7	SER(288)	SER(383)	-1.586	-1.083	-1.160
7	SER(383)	SER(288)	-1.586	-1.083	-1.193
7	SER(477)	GLN(481)	-5.653	-4.612	-4.940
7	THR(067)	SER(172)	-11.435	-8.623	-9.564
7	THR(392)	THR(394)	-9.230	-7.335	-8.258
7	THR(394)	GLN(389)	-3.252	-2.382	-2.733
7	THR(394)	THR(392)	-9.230	-7.335	-8.578
8	ASN(207)	SER(202)	-2.501	-1.955	-2.204
8	GLN(092)	SER(002)	-2.575	-1.520	-1.630
8	GLN(389)	THR(394)	-2.583	-1.787	-1.857
8	GLN(478)	GLN(481)	-8.677	-5.853	-6.570
8	GLN(481)	GLN(478)	-8.677	-5.853	-6.739
8	SER(002)	GLN(092)	-2.575	-1.520	-1.711
8	SER(074)	SER(080)	-1.657	-0.888	-1.109
8	SER(080)	SER(074)	-1.657	-0.888	-1.511
8	SER(172)	THR(067)	-13.273	-9.218	-12.216
8	SER(202)	ASN(207)	-2.501	-1.955	-2.130
8	SER(224)	SER(274)	-4.528	-3.424	-3.882
8	SER(232)	THR(234)	-1.305	-0.654	-0.756

8	SER(274)	SER(224)	-4.528	-3.424	-3.481
8	SER(288)	SER(383)	-1.312	-0.729	-0.826
8	SER(383)	SER(288)	-1.312	-0.729	-0.849
8	THR(067)	SER(172)	-13.273	-9.218	-11.641
8	THR(234)	SER(232)	-1.305	-0.654	-0.809
8	THR(392)	THR(394)	-6.360	-5.505	-5.602
8	THR(394)	GLN(389)	-2.583	-1.787	-2.086
8	THR(394)	THR(392)	-6.360	-5.505	-5.809
9	ASN(207)	SER(202)	-2.072	-0.913	-1.218
9	ASN(406)	GLN(408)	-8.971	-5.786	-7.198
9	GLN(057)	SER(060)	-24.989	-19.110	-23.800
9	GLN(389)	THR(394)	-4.752	-2.934	-3.554
9	GLN(408)	ASN(406)	-8.971	-5.786	-7.755
9	GLN(481)	SER(477)	-5.878	-4.939	-5.317
9	SER(060)	GLN(057)	-24.989	-19.110	-24.500
9	SER(074)	SER(080)	-0.818	0.304	-0.197
9	SER(080)	SER(074)	-0.818	0.304	-0.612
9	SER(172)	THR(067)	-13.659	-10.301	-11.721
9	SER(202)	ASN(207)	-2.072	-0.913	-0.904
9	SER(224)	SER(274)	-2.888	-2.112	-2.206
9	SER(274)	SER(224)	-2.888	-2.112	-2.118
9	SER(288)	SER(383)	-2.332	-1.601	-1.771
9	SER(383)	SER(288)	-2.332	-1.601	-1.815
9	SER(477)	GLN(481)	-5.878	-4.939	-5.207
9	THR(067)	SER(172)	-13.659	-10.301	-11.736
9	THR(394)	GLN(389)	-4.752	-2.934	-5.447
10	ASN(015)	ASN(096)	-7.393	-5.479	-6.693
10	ASN(096)	ASN(015)	-7.393	-5.479	-6.455
10	ASN(207)	SER(202)	-4.888	-4.014	-4.345

10	GLN(092)	SER(002)	-3.433	-1.867	-2.334
10	GLN(478)	GLN(481)	-14.222	-11.438	-12.286
10	GLN(481)	GLN(478)	-14.222	-11.438	-12.273
10	SER(002)	GLN(092)	-3.433	-1.867	-2.686
10	SER(074)	SER(080)	0.461	0.513	0.534
10	SER(080)	SER(074)	0.461	0.513	0.500
10	SER(202)	ASN(207)	-4.888	-4.014	-4.193
10	SER(224)	SER(274)	-5.902	-4.703	-5.167
10	SER(274)	SER(224)	-5.902	-4.703	-4.835
10	SER(288)	SER(383)	-2.400	-1.442	-1.847
10	SER(383)	SER(288)	-2.400	-1.442	-1.696
11	ASN(015)	ASN(096)	-13.266	-9.075	-12.853
11	ASN(096)	ASN(015)	-13.266	-9.075	-13.601
11	ASN(207)	SER(202)	-2.281	-1.859	-1.997
11	GLN(389)	THR(394)	-5.058	-2.601	-3.460
11	GLN(478)	GLN(481)	-17.197	-10.989	-14.005
11	GLN(481)	GLN(478)	-17.197	-10.989	-15.032
11	SER(074)	SER(080)	-17.442	-11.629	-21.112
11	SER(080)	SER(074)	-17.442	-11.629	-17.304
11	SER(172)	THR(067)	-12.595	-8.723	-11.138
11	SER(202)	ASN(207)	-2.281	-1.859	-1.822
11	SER(224)	SER(274)	-9.236	-7.056	-8.150
11	SER(232)	THR(234)	0.441	0.676	0.638
11	SER(274)	SER(224)	-9.236	-7.056	-7.710
11	SER(288)	SER(383)	-1.962	-1.282	-1.487
11	SER(383)	SER(288)	-1.962	-1.282	-1.459
11	THR(067)	SER(172)	-12.595	-8.723	-11.243
11	THR(234)	SER(232)	0.441	0.676	0.631
11	THR(394)	GLN(389)	-5.058	-2.601	-4.011

12	ASN(207)	SER(202)	-1.436	-0.916	-1.067
12	SER(074)	SER(080)	-1.642	-0.369	-1.561
12	SER(080)	SER(074)	-1.642	-0.369	-0.636
12	SER(202)	ASN(207)	-1.436	-0.916	-0.916
12	SER(224)	SER(274)	-7.842	-4.907	-7.032
12	SER(274)	SER(224)	-7.842	-4.907	-6.072
12	SER(288)	SER(383)	-0.620	-0.279	-0.337
12	SER(383)	SER(288)	-0.620	-0.279	-0.364
13	ASN(015)	ASN(096)	-8.138	-6.268	-7.135
13	ASN(096)	ASN(015)	-8.138	-6.268	-7.284
13	ASN(207)	SER(202)	-0.542	0.006	-0.139
13	GLN(057)	SER(060)	-24.802	-18.607	-22.924
13	GLN(389)	THR(394)	-5.933	-2.938	-4.117
13	GLN(478)	GLN(481)	-20.380	-16.190	-18.065
13	GLN(481)	GLN(478)	-20.380	-16.190	-18.144
13	SER(060)	GLN(057)	-24.802	-18.607	-24.189
13	SER(061)	SER(064)	-4.689	-4.084	-4.321
13	SER(064)	SER(061)	-4.689	-4.084	-4.230
13	SER(074)	SER(080)	-0.265	-0.065	-0.066
13	SER(080)	SER(074)	-0.265	-0.065	-0.032
13	SER(172)	THR(067)	-2.425	-1.548	-1.628
13	SER(202)	ASN(207)	-0.542	0.006	0.025
13	SER(224)	SER(274)	-4.418	-3.783	-3.984
13	SER(274)	SER(224)	-4.418	-3.783	-3.779
13	SER(288)	SER(383)	-1.672	-1.251	-1.283
13	SER(383)	SER(288)	-1.672	-1.251	-1.348
13	THR(067)	SER(172)	-2.425	-1.548	-1.597
13	THR(394)	GLN(389)	-5.933	-2.938	-4.725
14	ASN(207)	SER(202)	1.818	1.777	1.843

14	GLN(092)	SER(002)	-3.506	-1.586	-2.244
14	GLN(389)	THR(394)	-5.119	-2.679	-3.356
14	SER(002)	GLN(092)	-3.506	-1.586	-2.388
14	SER(061)	SER(064)	2.926	3.481	3.371
14	SER(064)	SER(061)	2.926	3.481	3.520
14	SER(074)	SER(080)	-1.383	-0.378	-1.078
14	SER(080)	SER(074)	-1.383	-0.378	-0.522
14	SER(172)	THR(067)	-2.677	-1.498	-1.770
14	SER(202)	ASN(207)	1.818	1.777	1.853
14	SER(224)	SER(274)	-7.197	-4.267	-5.661
14	SER(274)	SER(224)	-7.197	-4.267	-4.975
14	SER(288)	SER(383)	-1.222	-0.671	-0.775
14	SER(383)	SER(288)	-1.222	-0.671	-0.821
14	THR(067)	SER(172)	-2.677	-1.498	-1.585
14	THR(394)	GLN(389)	-5.119	-2.679	-3.999
15	ASN(207)	SER(202)	0.564	0.929	0.867
15	SER(074)	SER(080)	-0.348	0.614	0.251
15	SER(080)	SER(074)	-0.348	0.614	0.281
15	SER(172)	THR(067)	-1.415	-0.497	-0.518
15	SER(202)	ASN(207)	0.564	0.929	0.940
15	SER(224)	SER(274)	-8.387	-6.068	-7.234
15	SER(274)	SER(224)	-8.387	-6.068	-6.549
15	SER(288)	SER(383)	-1.236	-0.828	-0.767
15	SER(383)	SER(288)	-1.236	-0.828	-0.905
15	THR(067)	SER(172)	-1.415	-0.497	-0.498
16	ASN(207)	SER(202)	-0.447	0.251	-0.048
16	GLN(481)	SER(477)	-3.361	-2.653	-2.859
16	SER(074)	SER(080)	-2.414	-1.838	-1.932
16	SER(080)	SER(074)	-2.414	-1.838	-2.033

16	SER(172)	THR(067)	-3.004	-1.692	-2.079
16	SER(202)	ASN(207)	-0.447	0.251	-0.661
16	SER(224)	SER(274)	-10.473	-7.805	-9.342
16	SER(274)	SER(224)	-10.473	-7.805	-8.824
16	SER(288)	SER(383)	-2.922	-1.844	-2.160
16	SER(383)	SER(288)	-2.922	-1.844	-2.158
16	SER(477)	GLN(481)	-3.361	-2.653	-2.674
16	THR(067)	SER(172)	-3.004	-1.692	-1.762
17	ASN(207)	SER(202)	-0.383	-0.017	-0.061
17	GLN(478)	GLN(481)	-27.079	-19.501	-24.100
17	GLN(481)	GLN(478)	-27.079	-19.501	-25.111
17	GLN(481)	SER(477)	-0.700	-0.071	-0.161
17	SER(074)	SER(080)	-2.492	-1.834	-2.056
17	SER(080)	SER(074)	-2.492	-1.834	-1.858
17	SER(172)	THR(067)	-11.694	-8.072	-10.532
17	SER(202)	ASN(207)	-0.383	-0.017	-0.215
17	SER(224)	SER(274)	-8.143	-5.580	-6.982
17	SER(274)	SER(224)	-8.143	-5.580	-10.124
17	SER(288)	SER(383)	-2.364	-1.572	-1.816
17	SER(383)	SER(288)	-2.364	-1.572	-1.761
17	SER(477)	GLN(481)	-0.700	-0.071	-0.122
17	THR(067)	SER(172)	-11.694	-8.072	-10.875
18	ASN(207)	SER(202)	-2.652	-2.134	-2.334
18	ASN(406)	GLN(408)	-18.410	-13.062	-16.230
18	GLN(057)	SER(060)	-24.083	-19.103	-22.675
18	GLN(389)	THR(394)	-4.522	-2.088	-2.955
18	GLN(408)	ASN(406)	-18.410	-13.062	-16.433
18	GLN(481)	SER(477)	-5.567	-4.397	-4.917
18	SER(060)	GLN(057)	-24.083	-19.103	-23.473

18	SER(074)	SER(080)	0.029	0.858	0.509
18	SER(080)	SER(074)	0.029	0.858	0.372
18	SER(202)	ASN(207)	-2.652	-2.134	-2.227
18	SER(224)	SER(274)	-14.867	-9.813	-14.204
18	SER(274)	SER(224)	-14.867	-9.813	-12.603
18	SER(288)	SER(383)	-2.108	-1.312	-1.525
18	SER(383)	SER(288)	-2.108	-1.312	-1.432
18	SER(477)	GLN(481)	-5.567	-4.397	-4.625
18	THR(394)	GLN(389)	-4.522	-2.088	-3.275
19	ASN(207)	SER(202)	-2.090	-1.069	-1.411
19	ASN(406)	GLN(408)	-10.932	-8.153	-9.327
19	GLN(389)	SER(298)	-1.068	-0.950	-0.974
19	GLN(408)	ASN(406)	-10.932	-8.153	-9.378
19	SER(074)	SER(080)	1.039	1.124	1.155
19	SER(080)	SER(074)	1.039	1.124	1.109
19	SER(172)	THR(067)	-9.246	-6.232	-8.730
19	SER(202)	ASN(207)	-2.090	-1.069	-1.225
19	SER(224)	SER(274)	-7.750	-5.952	-7.172
19	SER(274)	SER(224)	-7.750	-5.952	-6.819
19	SER(288)	SER(383)	-0.244	-0.095	-0.085
19	SER(298)	GLN(389)	-1.068	-0.950	-0.905
19	SER(383)	SER(288)	-0.244	-0.095	-0.098
19	THR(067)	SER(172)	-9.246	-6.232	-9.108
20	ASN(207)	SER(202)	-3.478	-2.037	-2.637
20	SER(074)	SER(080)	0.399	0.927	0.863
20	SER(080)	SER(074)	0.399	0.927	0.784
20	SER(172)	THR(067)	-4.530	-3.146	-3.809
20	SER(202)	ASN(207)	-3.478	-2.037	-2.374
20	SER(224)	SER(274)	-7.754	-5.187	-6.597

20	SER(274)	SER(224)	-7.754	-5.187	-5.811
20	SER(288)	SER(383)	-2.852	-1.526	-2.028
20	SER(383)	SER(288)	-2.852	-1.526	-1.922
20	THR(067)	SER(172)	-4.530	-3.146	-3.478
21	ASN(207)	SER(202)	-4.947	-3.383	-4.021
21	GLN(478)	GLN(481)	-4.664	-3.111	-3.275
21	GLN(481)	GLN(478)	-4.664	-3.111	-3.649
21	SER(074)	SER(080)	-0.390	0.132	0.036
21	SER(080)	SER(074)	-0.390	0.132	-0.151
21	SER(172)	THR(067)	-5.970	-4.349	-5.424
21	SER(202)	ASN(207)	-4.947	-3.383	-3.490
21	SER(224)	SER(274)	-8.676	-6.140	-7.488
21	SER(274)	SER(224)	-8.676	-6.140	-6.922
21	SER(288)	SER(383)	-3.570	-2.310	-2.799
21	SER(383)	SER(288)	-3.570	-2.310	-2.690
21	THR(067)	SER(172)	-5.970	-4.349	-5.697
22	ASN(207)	SER(202)	-2.625	-2.089	-2.138
22	GLN(057)	SER(060)	-29.794	-22.475	-28.582
22	GLN(092)	SER(002)	-3.908	-3.682	-3.728
22	GLN(389)	SER(298)	-0.961	-0.807	-0.868
22	SER(002)	GLN(092)	-3.908	-3.682	-3.689
22	SER(060)	GLN(057)	-29.794	-22.475	-29.319
22	SER(074)	SER(080)	-0.111	0.680	0.353
22	SER(080)	SER(074)	-0.111	0.680	0.055
22	SER(172)	THR(067)	-1.386	-0.938	-1.017
22	SER(202)	ASN(207)	-2.625	-2.089	-2.062
22	SER(224)	SER(274)	-4.296	-3.030	-3.523
22	SER(274)	SER(224)	-4.296	-3.030	-3.201
22	SER(288)	SER(383)	-2.900	-1.937	-2.198

22	SER(298)	GLN(389)	-0.961	-0.807	-0.788
22	SER(383)	SER(288)	-2.900	-1.937	-2.195
22	THR(067)	SER(172)	-1.386	-0.938	-1.034
23	ASN(207)	SER(202)	0.083	0.147	0.161
23	ASN(406)	GLN(408)	-9.559	-7.483	-8.045
23	GLN(057)	SER(060)	-28.902	-21.972	-27.718
23	GLN(092)	SER(002)	-3.953	-3.201	-3.478
23	GLN(408)	ASN(406)	-9.559	-7.483	-8.354
23	GLN(478)	GLN(481)	-12.322	-10.050	-10.601
23	GLN(481)	GLN(478)	-12.322	-10.050	-10.761
23	SER(002)	GLN(092)	-3.953	-3.201	-3.180
23	SER(060)	GLN(057)	-28.902	-21.972	-28.599
23	SER(074)	SER(080)	-0.723	0.056	-0.066
23	SER(080)	SER(074)	-0.723	0.056	-0.271
23	SER(172)	THR(067)	-7.234	-4.937	-5.466
23	SER(202)	ASN(207)	0.083	0.147	0.210
23	SER(224)	SER(274)	-4.582	-3.414	-3.836
23	SER(274)	SER(224)	-4.582	-3.414	-3.641
23	SER(288)	SER(383)	-2.760	-1.872	-2.210
23	SER(383)	SER(288)	-2.760	-1.872	-2.065
23	THR(067)	SER(172)	-7.234	-4.937	-5.670
24	ASN(015)	ASN(096)	-11.397	-8.635	-10.572
24	ASN(096)	ASN(015)	-11.397	-8.635	-10.571
24	ASN(207)	SER(202)	-1.629	-1.166	-1.324
24	GLN(478)	GLN(481)	-19.117	-13.994	-16.513
24	GLN(481)	GLN(478)	-19.117	-13.994	-16.595
24	SER(074)	SER(080)	-1.669	-0.948	-1.083
24	SER(080)	SER(074)	-1.669	-0.948	-1.285
24	SER(172)	THR(067)	-10.107	-6.848	-8.449

24	SER(202)	ASN(207)	-1.629	-1.166	-1.112
24	SER(224)	SER(274)	-4.671	-3.838	-4.010
24	SER(274)	SER(224)	-4.671	-3.838	-3.867
24	SER(288)	SER(383)	-1.715	-1.044	-1.179
24	SER(383)	SER(288)	-1.715	-1.044	-1.181
24	THR(067)	SER(172)	-10.107	-6.848	-8.433
25	ASN(207)	SER(202)	-3.350	-2.574	-2.903
25	ASN(406)	GLN(408)	-14.804	-10.805	-12.607
25	GLN(408)	ASN(406)	-14.804	-10.805	-13.071
25	SER(074)	SER(080)	-0.239	0.400	0.244
25	SER(080)	SER(074)	-0.239	0.400	0.021
25	SER(172)	THR(067)	-10.581	-8.161	-8.717
25	SER(202)	ASN(207)	-3.350	-2.574	-2.778
25	SER(224)	SER(274)	-4.441	-3.438	-3.765
25	SER(232)	THR(234)	-0.407	0.224	0.092
25	SER(274)	SER(224)	-4.441	-3.438	-3.515
25	SER(288)	SER(383)	-1.306	-0.776	-0.894
25	SER(383)	SER(288)	-1.306	-0.776	-0.883
25	THR(067)	SER(172)	-10.581	-8.161	-8.577
25	THR(234)	SER(232)	-0.407	0.224	-0.034

Table B.5.: SAPT, EFP and QM/EFP electrostatics and polarization interaction energies computed for aryl-aryl dimers. All energies are given in units of kcal/mol. For QM/EFP, monA represents the QM region and monB the effective fragment.

snapshot	monA	monB	SAPT	EFP	QMEFP
1	PHE(146)	TRP(150)	-6.785	-2.612	-4.474

1	PHE(149)	TYR(290)	-3.214	-0.932	-2.212
1	PHE(278)	TYR(223)	-2.633	-0.608	-0.872
1	PHE(310)	TRP(312)	-1.651	0.734	0.377
1	PHE(357)	TRP(322)	-3.306	-0.310	-1.051
1	TRP(150)	PHE(146)	-6.785	-2.612	-4.568
1	TRP(312)	PHE(310)	-1.651	0.734	0.117
1	TRP(322)	PHE(357)	-3.306	-0.310	-1.712
1	TYR(223)	PHE(278)	-2.633	-0.608	-1.686
1	TYR(290)	PHE(149)	-3.214	-0.932	-1.631
2	HSD(437)	TYR(412)	-5.516	-3.408	-3.728
2	PHE(149)	TYR(290)	-2.846	-0.596	-0.943
2	PHE(310)	TRP(312)	-2.250	0.123	-0.071
2	PHE(357)	TRP(322)	-3.024	-0.622	-1.053
2	TRP(312)	PHE(310)	-2.250	0.123	-0.650
2	TRP(322)	PHE(357)	-3.024	-0.622	-1.825
2	TYR(290)	PHE(149)	-2.846	-0.596	-1.435
2	TYR(412)	HSD(437)	-5.516	-3.408	-5.458
3	PHE(149)	TYR(290)	-4.691	-1.023	-2.114
3	PHE(185)	TRP(033)	-14.894	-9.817	-12.109
3	PHE(310)	TRP(312)	-3.435	-1.071	-1.297
3	PHE(357)	TRP(322)	-4.853	-1.032	-2.390
3	TRP(033)	PHE(185)	-14.894	-9.817	-12.430
3	TRP(312)	PHE(310)	-3.435	-1.071	-2.362
3	TRP(322)	PHE(357)	-4.853	-1.032	-3.119
3	TYR(290)	PHE(149)	-4.691	-1.023	-2.448
4	HSD(437)	TYR(412)	-9.434	-4.732	-7.063
4	PHE(149)	TYR(290)	-5.123	-1.169	-2.717
4	PHE(185)	TRP(033)	-17.573	-12.871	-15.720
4	PHE(357)	TRP(322)	-1.813	0.097	-0.243

4	TRP(033)	PHE(185)	-17.573	-12.871	-16.936
4	TRP(322)	PHE(357)	-1.813	0.097	-0.562
4	TYR(290)	PHE(149)	-5.123	-1.169	-2.963
4	TYR(412)	HSD(437)	-9.434	-4.732	-7.866
5	HSD(437)	TYR(412)	-5.289	-3.707	-4.381
5	PHE(146)	TYR(287)	-3.923	-2.072	-2.372
5	PHE(149)	TYR(290)	-1.783	-0.590	-0.762
5	PHE(185)	TRP(033)	-7.985	-6.290	-6.497
5	PHE(357)	TRP(322)	-4.400	-0.636	-1.948
5	TRP(033)	PHE(185)	-7.985	-6.290	-6.892
5	TRP(322)	PHE(357)	-4.400	-0.636	-2.620
5	TYR(287)	PHE(146)	-3.923	-2.072	-2.830
5	TYR(290)	PHE(149)	-1.783	-0.590	-0.814
5	TYR(412)	HSD(437)	-5.289	-3.707	-3.991
6	HSD(295)	TYR(297)	-7.530	-4.593	-6.328
6	HSD(437)	TYR(412)	-7.394	-4.434	-5.793
6	PHE(149)	TYR(290)	-3.440	-1.149	-1.388
6	PHE(185)	TRP(033)	-14.325	-10.182	-11.869
6	PHE(310)	TRP(312)	-3.581	-0.092	-1.047
6	PHE(357)	TRP(322)	-4.722	-0.761	-1.770
6	TRP(033)	PHE(185)	-14.325	-10.182	-12.388
6	TRP(312)	PHE(310)	-3.581	-0.092	-0.923
6	TRP(322)	PHE(357)	-4.722	-0.761	-3.029
6	TYR(290)	PHE(149)	-3.440	-1.149	-2.147
6	TYR(297)	HSD(295)	-7.530	-4.593	-5.723
6	TYR(412)	HSD(437)	-7.394	-4.434	-5.688
7	HSD(295)	TYR(297)	-2.998	1.574	-0.230
7	HSD(437)	TYR(412)	-10.279	-5.601	-7.870
7	PHE(146)	TRP(150)	-4.176	-2.221	-2.781

7	PHE(149)	TYR(290)	-1.924	-0.349	-0.501
7	PHE(185)	TRP(033)	-14.090	-9.571	-10.937
7	PHE(310)	TRP(312)	-4.794	-0.555	-1.746
7	PHE(357)	TRP(322)	-5.174	-0.959	-2.422
7	TRP(033)	PHE(185)	-14.090	-9.571	-12.502
7	TRP(150)	PHE(146)	-4.176	-2.221	-2.663
7	TRP(312)	PHE(310)	-4.794	-0.555	-2.287
7	TRP(322)	PHE(357)	-5.174	-0.959	-3.466
7	TYR(290)	PHE(149)	-1.924	-0.349	-0.787
7	TYR(297)	HSD(295)	-2.998	1.574	-0.605
7	TYR(412)	HSD(437)	-10.279	-5.601	-10.082
8	HSD(437)	TYR(412)	-8.420	-4.287	-6.061
8	PHE(146)	TYR(287)	-5.853	-2.569	-3.316
8	PHE(149)	TYR(290)	-3.248	-0.980	-1.462
8	PHE(185)	TRP(033)	-17.346	-12.341	-15.160
8	PHE(310)	TRP(312)	-6.608	-0.617	-2.918
8	PHE(357)	TRP(322)	-2.612	-0.854	-1.225
8	TRP(033)	PHE(185)	-17.346	-12.341	-16.198
8	TRP(312)	PHE(310)	-6.608	-0.617	-3.778
8	TRP(322)	PHE(357)	-2.612	-0.854	-1.572
8	TYR(287)	PHE(146)	-5.853	-2.569	-4.093
8	TYR(290)	PHE(149)	-3.248	-0.980	-2.181
8	TYR(412)	HSD(437)	-8.420	-4.287	-6.714
9	HSD(437)	TYR(412)	-7.451	-5.673	-6.075
9	PHE(149)	TYR(290)	-3.662	-1.197	-1.699
9	PHE(185)	TRP(033)	-4.693	-3.310	-3.355
9	PHE(310)	TRP(312)	-1.634	0.053	0.053
9	PHE(357)	TRP(322)	-2.832	0.218	-0.855
9	TRP(033)	PHE(185)	-4.693	-3.310	-3.914

9	TRP(312)	PHE(310)	-1.634	0.053	-0.642
9	TRP(322)	PHE(357)	-2.832	0.218	-1.052
9	TYR(290)	PHE(149)	-3.662	-1.197	-2.021
9	TYR(412)	HSD(437)	-7.451	-5.673	-6.397
10	HSD(437)	TYR(412)	-6.742	-5.245	-5.573
10	PHE(146)	TYR(287)	-4.086	-2.458	-2.689
10	PHE(149)	TYR(290)	-1.759	-0.430	-0.562
10	PHE(185)	TRP(033)	-4.943	-3.637	-3.725
10	PHE(244)	TRP(050)	-7.362	-1.531	-5.172
10	PHE(310)	TRP(312)	-3.817	0.128	-0.516
10	PHE(357)	TRP(322)	-2.567	-0.672	-1.040
10	TRP(033)	PHE(185)	-4.943	-3.637	-4.088
10	TRP(050)	PHE(244)	-7.362	-1.531	-4.693
10	TRP(312)	PHE(310)	-3.817	0.128	-1.933
10	TRP(322)	PHE(357)	-2.567	-0.672	-1.339
10	TYR(287)	PHE(146)	-4.086	-2.458	-3.178
10	TYR(290)	PHE(149)	-1.759	-0.430	-0.938
10	TYR(412)	HSD(437)	-6.742	-5.245	-5.691
11	HSD(437)	TYR(412)	-9.177	-6.553	-7.840
11	PHE(149)	TYR(290)	-3.434	-0.480	-1.185
11	PHE(319)	TRP(367)	-4.569	-1.653	-3.105
11	PHE(357)	TRP(322)	-6.147	-0.334	-2.629
11	TRP(322)	PHE(357)	-6.147	-0.334	-4.038
11	TRP(367)	PHE(319)	-4.569	-1.653	-2.237
11	TYR(290)	PHE(149)	-3.434	-0.480	-1.307
11	TYR(412)	HSD(437)	-9.177	-6.553	-8.175
12	HSD(437)	TYR(412)	-7.641	-4.526	-5.147
12	PHE(149)	TYR(290)	-1.545	-0.188	-0.279
12	PHE(310)	TRP(312)	-3.645	-0.845	-1.540

12	PHE(357)	TRP(322)	-3.824	-1.198	-1.932
12	TRP(312)	PHE(310)	-3.645	-0.845	-2.746
12	TRP(322)	PHE(357)	-3.824	-1.198	-2.583
12	TYR(290)	PHE(149)	-1.545	-0.188	-0.508
12	TYR(412)	HSD(437)	-7.641	-4.526	-6.531
13	HSD(437)	TYR(412)	-6.965	-4.473	-5.052
13	PHE(146)	TYR(287)	-5.364	-1.995	-3.129
13	PHE(149)	TYR(290)	-1.333	-0.385	-0.494
13	PHE(310)	TRP(312)	-2.867	-0.356	-0.816
13	PHE(357)	TRP(322)	-3.828	-0.679	-1.446
13	TRP(312)	PHE(310)	-2.867	-0.356	-1.095
13	TRP(322)	PHE(357)	-3.828	-0.679	-2.249
13	TYR(287)	PHE(146)	-5.364	-1.995	-3.428
13	TYR(290)	PHE(149)	-1.333	-0.385	-0.592
13	TYR(412)	HSD(437)	-6.965	-4.473	-6.561
14	HSD(437)	TYR(412)	-11.942	-7.170	-8.607
14	PHE(146)	TYR(287)	-5.668	-3.376	-3.752
14	PHE(149)	TYR(290)	-2.753	-0.664	-1.071
14	PHE(185)	TRP(033)	-4.588	-2.352	-2.763
14	PHE(310)	TRP(312)	-2.421	-0.564	-0.964
14	PHE(357)	TRP(322)	-3.245	-0.318	-1.058
14	TRP(033)	PHE(185)	-4.588	-2.352	-3.218
14	TRP(312)	PHE(310)	-2.421	-0.564	-1.534
14	TRP(322)	PHE(357)	-3.245	-0.318	-1.680
14	TYR(287)	PHE(146)	-5.668	-3.376	-3.955
14	TYR(290)	PHE(149)	-2.753	-0.664	-1.357
14	TYR(412)	HSD(437)	-11.942	-7.170	-10.796
15	HSD(437)	TYR(412)	-7.524	-3.086	-5.405
15	PHE(149)	TYR(290)	-1.423	-0.120	-0.250

15	PHE(310)	TRP(312)	-2.465	0.595	0.105
15	PHE(357)	TRP(322)	-3.120	0.353	-0.795
15	TRP(312)	PHE(310)	-2.465	0.595	-0.633
15	TRP(322)	PHE(357)	-3.120	0.353	-0.882
15	TRP(373)	TYR(041)	-4.110	-2.449	-3.339
15	TYR(041)	TRP(373)	-4.110	-2.449	-2.909
15	TYR(290)	PHE(149)	-1.423	-0.120	-0.396
15	TYR(412)	HSD(437)	-7.524	-3.086	-5.390
16	HSD(437)	TYR(412)	-8.147	-5.152	-6.430
16	PHE(149)	TYR(290)	-3.469	-0.758	-1.361
16	PHE(372)	TRP(388)	-6.779	-4.226	-6.980
16	TRP(388)	PHE(372)	-6.779	-4.226	-4.506
16	TYR(290)	PHE(149)	-3.469	-0.758	-1.830
16	TYR(412)	HSD(437)	-8.147	-5.152	-6.552
17	HSD(437)	TYR(412)	-9.047	-4.361	-6.670
17	PHE(146)	TYR(287)	-5.438	-2.385	-2.927
17	PHE(149)	TYR(290)	-2.929	-0.683	-1.221
17	PHE(185)	TRP(033)	-4.958	-2.851	-3.333
17	PHE(278)	TYR(223)	-2.173	-0.198	-0.678
17	PHE(310)	TRP(312)	-3.201	-0.359	-0.722
17	PHE(357)	TRP(322)	-2.581	-0.741	-1.036
17	TRP(033)	PHE(185)	-4.958	-2.851	-4.365
17	TRP(312)	PHE(310)	-3.201	-0.359	-1.476
17	TRP(322)	PHE(357)	-2.581	-0.741	-1.605
17	TYR(223)	PHE(278)	-2.173	-0.198	-1.203
17	TYR(287)	PHE(146)	-5.438	-2.385	-3.969
17	TYR(290)	PHE(149)	-2.929	-0.683	-1.473
17	TYR(412)	HSD(437)	-9.047	-4.361	-7.616
18	HSD(437)	TYR(412)	-5.022	-3.791	-3.906

18	PHE(146)	TYR(287)	-4.344	-1.863	-2.182
18	PHE(149)	TYR(290)	-2.359	-0.751	-0.992
18	PHE(278)	TYR(223)	-3.050	-0.852	-1.438
18	PHE(310)	TRP(312)	-3.533	0.383	-1.310
18	PHE(357)	TRP(322)	-3.537	0.065	-1.107
18	TRP(312)	PHE(310)	-3.533	0.383	-2.158
18	TRP(322)	PHE(357)	-3.537	0.065	-1.540
18	TYR(223)	PHE(278)	-3.050	-0.852	-2.317
18	TYR(287)	PHE(146)	-4.344	-1.863	-3.083
18	TYR(290)	PHE(149)	-2.359	-0.751	-1.154
18	TYR(412)	HSD(437)	-5.022	-3.791	-4.292
19	HSD(437)	TYR(412)	-10.668	-7.217	-8.091
19	PHE(149)	TYR(290)	-1.461	0.003	-0.218
19	PHE(310)	TRP(312)	-1.942	0.201	0.109
19	TRP(312)	PHE(310)	-1.942	0.201	-0.825
19	TYR(290)	PHE(149)	-1.461	0.003	-0.382
19	TYR(412)	HSD(437)	-10.668	-7.217	-10.147
21	HSD(437)	TYR(412)	-12.132	-7.238	-9.132
21	PHE(149)	TYR(290)	-1.945	-0.209	-0.447
21	PHE(278)	TYR(223)	-1.952	-0.104	-0.314
21	PHE(310)	TRP(312)	-3.914	0.258	-1.058
21	TRP(312)	PHE(310)	-3.914	0.258	-1.971
21	TYR(223)	PHE(278)	-1.952	-0.104	-0.899
21	TYR(290)	PHE(149)	-1.945	-0.209	-0.665
21	TYR(412)	HSD(437)	-12.132	-7.238	-11.188
22	HSD(437)	TYR(412)	-3.610	-2.062	-2.099
22	PHE(149)	TYR(290)	-5.261	-1.377	-2.571
22	PHE(310)	TRP(312)	-5.428	0.011	-1.725
22	PHE(357)	TRP(322)	-3.624	-0.121	-1.595

22	TRP(312)	PHE(310)	-5.428	0.011	-2.091
22	TRP(322)	PHE(357)	-3.624	-0.121	-1.851
22	TYR(290)	PHE(149)	-5.261	-1.377	-3.092
22	TYR(412)	HSD(437)	-3.610	-2.062	-2.761
23	HSD(437)	TYR(412)	-7.522	-4.673	-5.475
23	PHE(149)	TYR(290)	-5.684	-1.385	-2.608
23	PHE(185)	TRP(033)	-7.332	-4.845	-5.536
23	PHE(310)	TRP(312)	-3.188	0.294	-1.091
23	PHE(357)	TRP(322)	-3.311	-0.989	-1.473
23	TRP(033)	PHE(185)	-7.332	-4.845	-5.811
23	TRP(312)	PHE(310)	-3.188	0.294	-0.711
23	TRP(322)	PHE(357)	-3.311	-0.989	-1.881
23	TYR(290)	PHE(149)	-5.684	-1.385	-3.488
23	TYR(412)	HSD(437)	-7.522	-4.673	-6.191
24	HSD(437)	TYR(412)	-10.054	-6.804	-7.913
24	PHE(149)	TYR(290)	-3.048	-0.891	-1.099
24	PHE(185)	TRP(033)	-12.154	-8.129	-8.982
24	PHE(244)	TRP(050)	-7.264	-1.689	-5.475
24	PHE(310)	TRP(312)	-4.590	-0.804	-1.960
24	PHE(357)	TRP(322)	-2.956	-0.373	-0.862
24	TRP(033)	PHE(185)	-12.154	-8.129	-9.592
24	TRP(050)	PHE(244)	-7.264	-1.689	-4.167
24	TRP(312)	PHE(310)	-4.590	-0.804	-2.376
24	TRP(322)	PHE(357)	-2.956	-0.373	-1.531
24	TYR(290)	PHE(149)	-3.048	-0.891	-1.900
24	TYR(412)	HSD(437)	-10.054	-6.804	-10.011
25	HSD(437)	TYR(412)	-8.584	-4.274	-5.200
25	PHE(149)	TYR(290)	-1.197	-0.087	-0.153
25	PHE(310)	TRP(312)	-2.479	0.889	-0.222

25	PHE(356)	TYR(329)	-3.923	-1.094	-1.610
25	PHE(357)	TRP(322)	-1.812	-0.180	-0.278
25	TRP(312)	PHE(310)	-2.479	0.889	-0.599
25	TRP(322)	PHE(357)	-1.812	-0.180	-0.775
25	TYR(290)	PHE(149)	-1.197	-0.087	-0.259
25	TYR(329)	PHE(356)	-3.923	-1.094	-2.842
25	TYR(412)	HSD(437)	-8.584	-4.274	-7.790

Table B.6.: SAPT, EFP and QM/EFP dispersion interaction energies computed for polar-polar dimers. All energies are given in units of kcal/mol. For QM/EFP, monA represents the QM region and monB the effective fragment.

snapshot	monA	monB	SAPT	EFP	QMEFP
1	ASN(207)	SER(202)	-1.878	-2.474	-1.532
1	ASN(406)	GLN(408)	-5.352	-6.561	-4.055
1	GLN(057)	SER(060)	-6.138	-6.567	-4.632
1	GLN(092)	SER(002)	-2.961	-3.452	-2.263
1	GLN(389)	THR(394)	-2.476	-3.165	-2.247
1	GLN(408)	ASN(406)	-5.352	-6.561	-4.926
1	GLN(481)	SER(477)	-1.495	-1.962	-1.417
1	SER(002)	GLN(092)	-2.961	-3.452	-2.602
1	SER(060)	GLN(057)	-6.138	-6.567	-5.195
1	SER(074)	SER(080)	-2.261	-2.773	-1.797
1	SER(080)	SER(074)	-2.261	-2.773	-2.063
1	SER(172)	THR(067)	-2.932	-3.902	-2.666
1	SER(202)	ASN(207)	-1.878	-2.474	-1.699
1	SER(224)	SER(274)	-4.378	-5.717	-4.109

1	SER(232)	THR(234)	-1.944	-2.243	-1.595
1	SER(274)	SER(224)	-4.378	-5.717	-3.401
1	SER(288)	SER(383)	-1.973	-2.709	-1.823
1	SER(383)	SER(288)	-1.973	-2.709	-1.707
1	SER(477)	GLN(481)	-1.495	-1.962	-1.162
1	THR(067)	SER(172)	-2.932	-3.902	-2.373
1	THR(234)	SER(232)	-1.944	-2.243	-1.608
1	THR(392)	THR(394)	-2.180	-2.845	-1.805
1	THR(394)	GLN(389)	-2.476	-3.165	-2.112
1	THR(394)	THR(392)	-2.180	-2.845	-2.010
2	ASN(207)	SER(202)	-1.419	-1.702	-1.160
2	ASN(406)	GLN(408)	-7.479	-8.548	-5.667
2	GLN(092)	SER(002)	-3.457	-4.632	-3.078
2	GLN(389)	THR(394)	-2.658	-3.471	-2.329
2	GLN(408)	ASN(406)	-7.479	-8.548	-6.978
2	SER(002)	GLN(092)	-3.457	-4.632	-2.999
2	SER(074)	SER(080)	-2.144	-2.693	-1.720
2	SER(080)	SER(074)	-2.144	-2.693	-1.963
2	SER(202)	ASN(207)	-1.419	-1.702	-1.183
2	SER(224)	SER(274)	-3.064	-3.900	-2.823
2	SER(232)	THR(234)	-1.708	-2.035	-1.390
2	SER(274)	SER(224)	-3.064	-3.900	-2.317
2	SER(288)	SER(383)	-1.534	-2.119	-1.441
2	SER(383)	SER(288)	-1.534	-2.119	-1.324
2	THR(234)	SER(232)	-1.708	-2.035	-1.467
2	THR(392)	THR(394)	-2.998	-3.530	-2.300
2	THR(394)	GLN(389)	-2.658	-3.471	-2.370
2	THR(394)	THR(392)	-2.998	-3.530	-2.817
3	GLN(092)	SER(002)	-2.659	-3.412	-2.271

3	SER(002)	GLN(092)	-2.659	-3.412	-2.270
3	SER(074)	SER(080)	-3.051	-3.569	-2.949
3	SER(080)	SER(074)	-3.051	-3.569	-2.138
3	SER(224)	SER(274)	-3.061	-3.900	-2.727
3	SER(232)	THR(234)	-1.673	-1.917	-1.351
3	SER(274)	SER(224)	-3.061	-3.900	-2.374
3	THR(234)	SER(232)	-1.673	-1.917	-1.366
3	THR(392)	THR(394)	-2.369	-2.874	-1.818
3	THR(394)	THR(392)	-2.369	-2.874	-2.182
4	ASN(015)	ASN(096)	-1.739	-2.153	-1.433
4	ASN(096)	ASN(015)	-1.739	-2.153	-1.476
4	ASN(207)	SER(202)	-1.378	-1.969	-1.327
4	GLN(057)	SER(060)	-6.910	-7.490	-5.157
4	GLN(389)	THR(394)	-2.821	-3.621	-2.454
4	GLN(478)	GLN(481)	-7.387	-8.991	-5.865
4	GLN(481)	GLN(478)	-7.387	-8.991	-6.633
4	GLN(481)	SER(477)	-2.013	-2.636	-1.882
4	SER(060)	GLN(057)	-6.910	-7.490	-6.000
4	SER(074)	SER(080)	-1.131	-1.567	-1.077
4	SER(080)	SER(074)	-1.131	-1.567	-0.914
4	SER(202)	ASN(207)	-1.378	-1.969	-1.054
4	SER(224)	SER(274)	-2.306	-2.941	-2.068
4	SER(274)	SER(224)	-2.306	-2.941	-1.745
4	SER(288)	SER(383)	-2.109	-2.929	-1.968
4	SER(383)	SER(288)	-2.109	-2.929	-1.867
4	SER(477)	GLN(481)	-2.013	-2.636	-1.608
4	THR(392)	THR(394)	-3.294	-4.162	-2.596
4	THR(394)	GLN(389)	-2.821	-3.621	-2.556
4	THR(394)	THR(392)	-3.294	-4.162	-3.068

5	ASN(207)	SER(202)	-1.992	-2.594	-1.827
5	GLN(057)	SER(060)	-2.537	-3.080	-2.089
5	GLN(092)	SER(002)	-3.176	-3.896	-2.703
5	GLN(389)	THR(394)	-2.809	-3.615	-2.444
5	SER(002)	GLN(092)	-3.176	-3.896	-2.634
5	SER(060)	GLN(057)	-2.537	-3.080	-2.150
5	SER(074)	SER(080)	-2.302	-3.022	-1.888
5	SER(080)	SER(074)	-2.302	-3.022	-2.220
5	SER(172)	THR(067)	-5.611	-6.791	-4.462
5	SER(202)	ASN(207)	-1.992	-2.594	-1.658
5	SER(224)	SER(274)	-4.795	-5.885	-4.580
5	SER(274)	SER(224)	-4.795	-5.885	-3.586
5	THR(067)	SER(172)	-5.611	-6.791	-4.841
5	THR(392)	THR(394)	-1.725	-2.402	-1.512
5	THR(394)	GLN(389)	-2.809	-3.615	-2.539
5	THR(394)	THR(392)	-1.725	-2.402	-1.533
6	ASN(207)	SER(202)	-2.285	-3.099	-2.132
6	GLN(389)	THR(394)	-2.946	-3.852	-2.604
6	GLN(478)	GLN(481)	-5.063	-6.307	-4.179
6	GLN(481)	GLN(478)	-5.063	-6.307	-4.410
6	SER(074)	SER(080)	-1.864	-2.393	-1.564
6	SER(080)	SER(074)	-1.864	-2.393	-1.674
6	SER(172)	THR(067)	-4.446	-5.645	-3.880
6	SER(202)	ASN(207)	-2.285	-3.099	-1.797
6	SER(224)	SER(274)	-3.848	-5.201	-3.585
6	SER(232)	THR(234)	-2.110	-2.697	-1.759
6	SER(274)	SER(224)	-3.848	-5.201	-3.050
6	THR(067)	SER(172)	-4.446	-5.645	-3.597
6	THR(234)	SER(232)	-2.110	-2.697	-1.851

6	THR(392)	THR(394)	-4.834	-5.592	-3.751
6	THR(394)	GLN(389)	-2.946	-3.852	-2.702
6	THR(394)	THR(392)	-4.834	-5.592	-4.737
7	ASN(015)	ASN(096)	-1.482	-1.850	-1.177
7	ASN(096)	ASN(015)	-1.482	-1.850	-1.338
7	ASN(207)	SER(202)	-0.906	-1.361	-0.861
7	GLN(389)	THR(394)	-2.751	-3.521	-2.404
7	GLN(478)	GLN(481)	-8.545	-10.203	-6.734
7	GLN(481)	GLN(478)	-8.545	-10.203	-7.601
7	GLN(481)	SER(477)	-1.975	-2.704	-1.865
7	SER(074)	SER(080)	-2.423	-3.145	-1.934
7	SER(080)	SER(074)	-2.423	-3.145	-2.409
7	SER(172)	THR(067)	-4.379	-5.600	-3.573
7	SER(202)	ASN(207)	-0.906	-1.361	-0.782
7	SER(224)	SER(274)	-1.843	-2.488	-1.665
7	SER(274)	SER(224)	-1.843	-2.488	-1.455
7	SER(288)	SER(383)	-1.215	-1.734	-1.139
7	SER(383)	SER(288)	-1.215	-1.734	-1.065
7	SER(477)	GLN(481)	-1.975	-2.704	-1.603
7	THR(067)	SER(172)	-4.379	-5.600	-3.838
7	THR(392)	THR(394)	-2.660	-3.068	-1.992
7	THR(394)	GLN(389)	-2.751	-3.521	-2.500
7	THR(394)	THR(392)	-2.660	-3.068	-2.432
8	ASN(207)	SER(202)	-2.092	-2.445	-1.630
8	GLN(092)	SER(002)	-3.318	-4.419	-3.002
8	GLN(389)	THR(394)	-2.326	-3.083	-2.043
8	GLN(478)	GLN(481)	-5.657	-7.023	-4.711
8	GLN(481)	GLN(478)	-5.657	-7.023	-4.911
8	SER(002)	GLN(092)	-3.318	-4.419	-2.819

8	SER(074)	SER(080)	-1.888	-2.461	-1.541
8	SER(080)	SER(074)	-1.888	-2.461	-1.820
8	SER(172)	THR(067)	-5.141	-6.329	-4.192
8	SER(202)	ASN(207)	-2.092	-2.445	-1.749
8	SER(224)	SER(274)	-2.614	-3.435	-2.400
8	SER(232)	THR(234)	-2.350	-2.882	-1.944
8	SER(274)	SER(224)	-2.614	-3.435	-1.972
8	SER(288)	SER(383)	-1.543	-2.136	-1.459
8	SER(383)	SER(288)	-1.543	-2.136	-1.340
8	THR(067)	SER(172)	-5.141	-6.329	-4.498
8	THR(234)	SER(232)	-2.350	-2.882	-2.029
8	THR(392)	THR(394)	-2.568	-3.074	-1.963
8	THR(394)	GLN(389)	-2.326	-3.083	-2.092
8	THR(394)	THR(392)	-2.568	-3.074	-2.352
9	ASN(207)	SER(202)	-1.732	-2.418	-1.653
9	ASN(406)	GLN(408)	-4.826	-5.603	-3.656
9	GLN(057)	SER(060)	-6.050	-6.283	-4.425
9	GLN(389)	THR(394)	-3.739	-4.965	-3.342
9	GLN(408)	ASN(406)	-4.826	-5.603	-4.442
9	GLN(481)	SER(477)	-1.857	-2.436	-1.753
9	SER(060)	GLN(057)	-6.050	-6.283	-5.119
9	SER(074)	SER(080)	-2.402	-3.125	-2.021
9	SER(080)	SER(074)	-2.402	-3.125	-2.225
9	SER(172)	THR(067)	-4.313	-5.399	-3.377
9	SER(202)	ASN(207)	-1.732	-2.418	-1.321
9	SER(224)	SER(274)	-2.237	-3.058	-2.048
9	SER(274)	SER(224)	-2.237	-3.058	-1.783
9	SER(288)	SER(383)	-1.517	-2.132	-1.398
9	SER(383)	SER(288)	-1.517	-2.132	-1.331

9	SER(477)	GLN(481)	-1.857	-2.436	-1.464
9	THR(067)	SER(172)	-4.313	-5.399	-3.814
9	THR(394)	GLN(389)	-3.739	-4.965	-3.506
10	ASN(015)	ASN(096)	-2.000	-2.321	-1.578
10	ASN(096)	ASN(015)	-2.000	-2.321	-1.741
10	ASN(207)	SER(202)	-1.708	-2.337	-1.661
10	GLN(092)	SER(002)	-2.244	-2.879	-1.957
10	GLN(478)	GLN(481)	-5.587	-6.830	-4.444
10	GLN(481)	GLN(478)	-5.587	-6.830	-4.929
10	SER(002)	GLN(092)	-2.244	-2.879	-1.893
10	SER(074)	SER(080)	-0.925	-1.200	-0.767
10	SER(080)	SER(074)	-0.925	-1.200	-0.822
10	SER(202)	ASN(207)	-1.708	-2.337	-1.316
10	SER(224)	SER(274)	-2.875	-3.766	-2.659
10	SER(274)	SER(224)	-2.875	-3.766	-2.169
10	SER(288)	SER(383)	-1.788	-2.438	-1.694
10	SER(383)	SER(288)	-1.788	-2.438	-1.499
11	ASN(015)	ASN(096)	-3.264	-3.651	-2.531
11	ASN(096)	ASN(015)	-3.264	-3.651	-3.044
11	ASN(207)	SER(202)	-1.355	-1.861	-1.271
11	GLN(389)	THR(394)	-3.924	-5.167	-3.504
11	GLN(478)	GLN(481)	-8.036	-9.191	-6.159
11	GLN(481)	GLN(478)	-8.036	-9.191	-7.200
11	SER(074)	SER(080)	-5.186	-6.866	-5.189
11	SER(080)	SER(074)	-5.186	-6.866	-4.046
11	SER(172)	THR(067)	-5.485	-6.973	-4.554
11	SER(202)	ASN(207)	-1.355	-1.861	-1.066
11	SER(224)	SER(274)	-3.813	-5.015	-3.565
11	SER(232)	THR(234)	-1.681	-2.085	-1.404

11	SER(274)	SER(224)	-3.813	-5.015	-2.926
11	SER(288)	SER(383)	-1.682	-2.372	-1.581
11	SER(383)	SER(288)	-1.682	-2.372	-1.455
11	THR(067)	SER(172)	-5.485	-6.973	-4.833
11	THR(234)	SER(232)	-1.681	-2.085	-1.437
11	THR(394)	GLN(389)	-3.924	-5.167	-3.650
12	ASN(207)	SER(202)	-1.315	-1.906	-1.253
12	SER(074)	SER(080)	-1.941	-2.688	-1.812
12	SER(080)	SER(074)	-1.941	-2.688	-1.582
12	SER(202)	ASN(207)	-1.315	-1.906	-1.075
12	SER(224)	SER(274)	-4.265	-5.495	-4.097
12	SER(274)	SER(224)	-4.265	-5.495	-3.236
12	SER(288)	SER(383)	-1.637	-2.267	-1.550
12	SER(383)	SER(288)	-1.637	-2.267	-1.413
13	ASN(015)	ASN(096)	-2.035	-2.344	-1.556
13	ASN(096)	ASN(015)	-2.035	-2.344	-1.884
13	ASN(207)	SER(202)	-1.417	-1.923	-1.270
13	GLN(057)	SER(060)	-6.109	-6.787	-4.663
13	GLN(389)	THR(394)	-4.572	-6.230	-4.362
13	GLN(478)	GLN(481)	-6.603	-8.029	-5.285
13	GLN(481)	GLN(478)	-6.603	-8.029	-5.885
13	SER(060)	GLN(057)	-6.109	-6.787	-5.176
13	SER(061)	SER(064)	-2.226	-2.675	-1.794
13	SER(064)	SER(061)	-2.226	-2.675	-1.935
13	SER(074)	SER(080)	-0.979	-1.396	-0.887
13	SER(080)	SER(074)	-0.979	-1.396	-0.833
13	SER(172)	THR(067)	-2.956	-4.034	-2.504
13	SER(202)	ASN(207)	-1.417	-1.923	-1.124
13	SER(224)	SER(274)	-1.947	-2.418	-1.774

13	SER(274)	SER(224)	-1.947	-2.418	-1.437
13	SER(288)	SER(383)	-1.297	-1.769	-1.251
13	SER(383)	SER(288)	-1.297	-1.769	-1.088
13	THR(067)	SER(172)	-2.956	-4.034	-2.580
13	THR(394)	GLN(389)	-4.572	-6.230	-4.096
14	ASN(207)	SER(202)	-0.750	-1.037	-0.674
14	GLN(092)	SER(002)	-3.490	-4.460	-3.036
14	GLN(389)	THR(394)	-4.043	-5.373	-3.750
14	SER(002)	GLN(092)	-3.490	-4.460	-2.966
14	SER(061)	SER(064)	-2.060	-2.773	-1.868
14	SER(064)	SER(061)	-2.060	-2.773	-1.741
14	SER(074)	SER(080)	-1.692	-2.446	-1.626
14	SER(080)	SER(074)	-1.692	-2.446	-1.426
14	SER(172)	THR(067)	-3.232	-4.231	-2.672
14	SER(202)	ASN(207)	-0.750	-1.037	-0.604
14	SER(224)	SER(274)	-4.579	-6.053	-4.277
14	SER(274)	SER(224)	-4.579	-6.053	-3.558
14	SER(288)	SER(383)	-1.748	-2.426	-1.665
14	SER(383)	SER(288)	-1.748	-2.426	-1.490
14	THR(067)	SER(172)	-3.232	-4.231	-2.778
14	THR(394)	GLN(389)	-4.043	-5.373	-3.684
15	ASN(207)	SER(202)	-1.267	-1.640	-1.100
15	SER(074)	SER(080)	-2.312	-3.193	-2.001
15	SER(080)	SER(074)	-2.312	-3.193	-2.003
15	SER(172)	THR(067)	-2.982	-4.073	-2.665
15	SER(202)	ASN(207)	-1.267	-1.640	-1.005
15	SER(224)	SER(274)	-4.594	-6.059	-4.179
15	SER(274)	SER(224)	-4.594	-6.059	-3.636
15	SER(288)	SER(383)	-1.519	-2.228	-1.387

15	SER(383)	SER(288)	-1.519	-2.228	-1.342
15	THR(067)	SER(172)	-2.982	-4.073	-2.522
16	ASN(207)	SER(202)	-1.806	-2.092	-1.503
16	GLN(481)	SER(477)	-1.519	-1.970	-1.413
16	SER(074)	SER(080)	-1.703	-2.433	-1.443
16	SER(080)	SER(074)	-1.703	-2.433	-1.633
16	SER(172)	THR(067)	-3.316	-4.582	-2.893
16	SER(202)	ASN(207)	-1.806	-2.092	-1.635
16	SER(224)	SER(274)	-4.321	-5.543	-3.936
16	SER(274)	SER(224)	-4.321	-5.543	-3.340
16	SER(288)	SER(383)	-1.716	-2.377	-1.605
16	SER(383)	SER(288)	-1.716	-2.377	-1.483
16	SER(477)	GLN(481)	-1.519	-1.970	-1.188
16	THR(067)	SER(172)	-3.316	-4.582	-2.841
17	ASN(207)	SER(202)	-1.775	-2.476	-1.648
17	GLN(478)	GLN(481)	-8.931	-10.215	-6.731
17	GLN(481)	GLN(478)	-8.931	-10.215	-8.012
17	GLN(481)	SER(477)	-1.637	-2.174	-1.508
17	SER(074)	SER(080)	-1.617	-2.251	-1.516
17	SER(080)	SER(074)	-1.617	-2.251	-1.349
17	SER(172)	THR(067)	-5.734	-6.957	-4.632
17	SER(202)	ASN(207)	-1.775	-2.476	-1.556
17	SER(224)	SER(274)	-4.277	-5.943	-4.033
17	SER(274)	SER(224)	-4.277	-5.943	-3.453
17	SER(288)	SER(383)	-1.700	-2.295	-1.578
17	SER(383)	SER(288)	-1.700	-2.295	-1.450
17	SER(477)	GLN(481)	-1.637	-2.174	-1.330
17	THR(067)	SER(172)	-5.734	-6.957	-5.017
18	ASN(207)	SER(202)	-1.545	-2.028	-1.379

18	ASN(406)	GLN(408)	-6.226	-7.730	-4.895
18	GLN(057)	SER(060)	-5.754	-6.274	-4.320
18	GLN(389)	THR(394)	-4.035	-5.463	-3.762
18	GLN(408)	ASN(406)	-6.226	-7.730	-5.723
18	GLN(481)	SER(477)	-1.803	-2.397	-1.731
18	SER(060)	GLN(057)	-5.754	-6.274	-4.961
18	SER(074)	SER(080)	-1.851	-2.132	-1.499
18	SER(080)	SER(074)	-1.851	-2.132	-1.648
18	SER(202)	ASN(207)	-1.545	-2.028	-1.251
18	SER(224)	SER(274)	-6.254	-7.899	-5.891
18	SER(274)	SER(224)	-6.254	-7.899	-4.836
18	SER(288)	SER(383)	-1.637	-2.285	-1.562
18	SER(383)	SER(288)	-1.637	-2.285	-1.399
18	SER(477)	GLN(481)	-1.803	-2.397	-1.437
18	THR(394)	GLN(389)	-4.035	-5.463	-3.659
19	ASN(207)	SER(202)	-1.700	-2.358	-1.589
19	ASN(406)	GLN(408)	-4.437	-5.395	-3.477
19	GLN(389)	SER(298)	-0.791	-1.055	-0.674
19	GLN(408)	ASN(406)	-4.437	-5.395	-4.154
19	SER(074)	SER(080)	-0.866	-1.174	-0.737
19	SER(080)	SER(074)	-0.866	-1.174	-0.802
19	SER(172)	THR(067)	-4.034	-5.304	-3.219
19	SER(202)	ASN(207)	-1.700	-2.358	-1.336
19	SER(224)	SER(274)	-3.284	-4.091	-3.043
19	SER(274)	SER(224)	-3.284	-4.091	-2.422
19	SER(288)	SER(383)	-1.364	-1.931	-1.306
19	SER(298)	GLN(389)	-0.791	-1.055	-0.719
19	SER(383)	SER(288)	-1.364	-1.931	-1.163
19	THR(067)	SER(172)	-4.034	-5.304	-3.822

20	ASN(207)	SER(202)	-2.223	-3.073	-1.960
20	SER(074)	SER(080)	-1.573	-2.048	-1.307
20	SER(080)	SER(074)	-1.573	-2.048	-1.404
20	SER(172)	THR(067)	-3.445	-4.720	-3.170
20	SER(202)	ASN(207)	-2.223	-3.073	-1.847
20	SER(224)	SER(274)	-4.142	-5.615	-3.905
20	SER(274)	SER(224)	-4.142	-5.615	-3.264
20	SER(288)	SER(383)	-1.999	-2.743	-1.900
20	SER(383)	SER(288)	-1.999	-2.743	-1.724
20	THR(067)	SER(172)	-3.445	-4.720	-2.905
21	ASN(207)	SER(202)	-2.371	-3.308	-2.269
21	GLN(478)	GLN(481)	-4.373	-5.544	-3.611
21	GLN(481)	GLN(478)	-4.373	-5.544	-3.902
21	SER(074)	SER(080)	-1.620	-2.061	-1.277
21	SER(080)	SER(074)	-1.620	-2.061	-1.522
21	SER(172)	THR(067)	-3.150	-4.013	-2.487
21	SER(202)	ASN(207)	-2.371	-3.308	-1.916
21	SER(224)	SER(274)	-4.539	-6.010	-4.184
21	SER(274)	SER(224)	-4.539	-6.010	-3.593
21	SER(288)	SER(383)	-1.572	-2.101	-1.453
21	SER(383)	SER(288)	-1.572	-2.101	-1.334
21	THR(067)	SER(172)	-3.150	-4.013	-2.867
22	ASN(207)	SER(202)	-1.384	-2.143	-1.341
22	GLN(057)	SER(060)	-6.475	-6.882	-4.752
22	GLN(092)	SER(002)	-1.116	-1.472	-1.058
22	GLN(389)	SER(298)	-0.958	-1.208	-0.814
22	SER(002)	GLN(092)	-1.116	-1.472	-0.871
22	SER(060)	GLN(057)	-6.475	-6.882	-5.361
22	SER(074)	SER(080)	-1.864	-2.316	-1.540

22	SER(080)	SER(074)	-1.864	-2.316	-1.696
22	SER(172)	THR(067)	-1.602	-2.046	-1.286
22	SER(202)	ASN(207)	-1.384	-2.143	-1.178
22	SER(224)	SER(274)	-3.105	-4.175	-2.843
22	SER(274)	SER(224)	-3.105	-4.175	-2.497
22	SER(288)	SER(383)	-1.627	-2.267	-1.556
22	SER(298)	GLN(389)	-0.958	-1.208	-0.878
22	SER(383)	SER(288)	-1.627	-2.267	-1.395
22	THR(067)	SER(172)	-1.602	-2.046	-1.400
23	ASN(207)	SER(202)	-0.951	-1.234	-0.822
23	ASN(406)	GLN(408)	-3.331	-3.970	-2.587
23	GLN(057)	SER(060)	-7.032	-7.394	-5.315
23	GLN(092)	SER(002)	-1.656	-2.127	-1.612
23	GLN(408)	ASN(406)	-3.331	-3.970	-3.056
23	GLN(478)	GLN(481)	-3.737	-4.535	-2.992
23	GLN(481)	GLN(478)	-3.737	-4.535	-3.265
23	SER(002)	GLN(092)	-1.656	-2.127	-1.229
23	SER(060)	GLN(057)	-7.032	-7.394	-5.926
23	SER(074)	SER(080)	-1.774	-2.462	-1.476
23	SER(080)	SER(074)	-1.774	-2.462	-1.663
23	SER(172)	THR(067)	-3.980	-5.257	-3.161
23	SER(202)	ASN(207)	-0.951	-1.234	-0.793
23	SER(224)	SER(274)	-3.155	-4.195	-2.855
23	SER(274)	SER(224)	-3.155	-4.195	-2.609
23	SER(288)	SER(383)	-1.468	-1.975	-1.322
23	SER(383)	SER(288)	-1.468	-1.975	-1.280
23	THR(067)	SER(172)	-3.980	-5.257	-3.694
24	ASN(015)	ASN(096)	-2.482	-2.686	-1.867
24	ASN(096)	ASN(015)	-2.482	-2.686	-2.181

24	ASN(207)	SER(202)	-1.167	-1.631	-1.097
24	GLN(478)	GLN(481)	-7.110	-8.072	-5.311
24	GLN(481)	GLN(478)	-7.110	-8.072	-6.109
24	SER(074)	SER(080)	-1.790	-2.356	-1.453
24	SER(080)	SER(074)	-1.790	-2.356	-1.712
24	SER(172)	THR(067)	-6.266	-7.967	-5.134
24	SER(202)	ASN(207)	-1.167	-1.631	-0.937
24	SER(224)	SER(274)	-2.714	-3.665	-2.491
24	SER(274)	SER(224)	-2.714	-3.665	-2.126
24	SER(288)	SER(383)	-1.630	-2.279	-1.562
24	SER(383)	SER(288)	-1.630	-2.279	-1.378
24	THR(067)	SER(172)	-6.266	-7.967	-5.519
25	ASN(207)	SER(202)	-1.743	-2.395	-1.633
25	ASN(406)	GLN(408)	-5.440	-6.474	-4.158
25	GLN(408)	ASN(406)	-5.440	-6.474	-4.953
25	SER(074)	SER(080)	-1.788	-2.283	-1.434
25	SER(080)	SER(074)	-1.788	-2.283	-1.667
25	SER(172)	THR(067)	-4.534	-6.043	-3.992
25	SER(202)	ASN(207)	-1.743	-2.395	-1.410
25	SER(224)	SER(274)	-2.969	-3.933	-2.693
25	SER(232)	THR(234)	-2.277	-2.731	-1.858
25	SER(274)	SER(224)	-2.969	-3.933	-2.332
25	SER(288)	SER(383)	-1.637	-2.239	-1.549
25	SER(383)	SER(288)	-1.637	-2.239	-1.398
25	THR(067)	SER(172)	-4.534	-6.043	-3.628
25	THR(234)	SER(232)	-2.277	-2.731	-1.965

Table B.7.: SAPT, EFP and QM/EFP total interaction energies computed for polar-polar dimers. All energies are given in units of kcal/mol. For QM/EFP, monA represents the QM region and monB the effective fragment.

snapshot	monA	monB	SAPT	EFP	QMEFP
1	ASN(207)	SER(202)	0.978	0.813	0.771
1	ASN(406)	GLN(408)	-10.810	-8.731	-10.429
1	GLN(057)	SER(060)	-11.760	-7.159	-10.559
1	GLN(092)	SER(002)	-7.759	-6.297	-6.864
1	GLN(389)	THR(394)	-4.351	-4.636	-3.574
1	GLN(408)	ASN(406)	-10.810	-8.731	-12.094
1	GLN(481)	SER(477)	-3.583	-3.751	-3.639
1	SER(002)	GLN(092)	-7.759	-6.297	-7.812
1	SER(060)	GLN(057)	-11.760	-7.159	-13.283
1	SER(074)	SER(080)	-0.983	-0.631	-1.048
1	SER(080)	SER(074)	-0.983	-0.631	-0.579
1	SER(172)	THR(067)	-3.555	-3.622	-3.155
1	SER(202)	ASN(207)	0.978	0.813	0.956
1	SER(224)	SER(274)	-2.868	-2.110	-2.782
1	SER(232)	THR(234)	0.225	0.046	0.101
1	SER(274)	SER(224)	-2.868	-2.110	-2.263
1	SER(288)	SER(383)	-1.632	-1.393	-2.938
1	SER(383)	SER(288)	-1.632	-1.393	-1.431
1	SER(477)	GLN(481)	-3.583	-3.751	-3.545
1	THR(067)	SER(172)	-3.555	-3.622	-3.021
1	THR(234)	SER(232)	0.225	0.046	0.104
1	THR(392)	THR(394)	0.786	0.100	0.681
1	THR(394)	GLN(389)	-4.351	-4.636	-4.188

1	THR(394)	THR(392)	0.786	0.100	0.589
2	ASN(207)	SER(202)	0.672	0.562	0.520
2	ASN(406)	GLN(408)	-6.764	0.977	-7.585
2	GLN(092)	SER(002)	-2.066	-2.269	-1.788
2	GLN(389)	THR(394)	-2.577	-2.741	-2.242
2	GLN(408)	ASN(406)	-6.764	0.977	-13.230
2	SER(002)	GLN(092)	-2.066	-2.269	-2.213
2	SER(074)	SER(080)	-0.008	0.192	-0.085
2	SER(080)	SER(074)	-0.008	0.192	0.240
2	SER(202)	ASN(207)	0.672	0.562	0.335
2	SER(224)	SER(274)	-3.235	-2.747	-3.130
2	SER(232)	THR(234)	0.276	0.042	0.110
2	SER(274)	SER(224)	-3.235	-2.747	-3.536
2	SER(288)	SER(383)	-1.836	-2.061	-2.275
2	SER(383)	SER(288)	-1.836	-2.061	-1.856
2	THR(234)	SER(232)	0.276	0.042	0.114
2	THR(392)	THR(394)	-5.122	-4.058	-3.512
2	THR(394)	GLN(389)	-2.577	-2.741	-2.668
2	THR(394)	THR(392)	-5.122	-4.058	-4.811
3	GLN(092)	SER(002)	-1.481	-1.558	-1.279
3	SER(002)	GLN(092)	-1.481	-1.558	-1.596
3	SER(074)	SER(080)	-5.997	-3.177	-5.349
3	SER(080)	SER(074)	-5.997	-3.177	-3.710
3	SER(224)	SER(274)	-3.564	-3.522	-3.755
3	SER(232)	THR(234)	-0.434	-0.679	-0.578
3	SER(274)	SER(224)	-3.564	-3.522	-3.626
3	THR(234)	SER(232)	-0.434	-0.679	-0.518
3	THR(392)	THR(394)	-5.288	-4.672	-4.433
3	THR(394)	THR(392)	-5.288	-4.672	-5.190

4	ASN(015)	ASN(096)	-2.796	-2.162	-2.526
4	ASN(096)	ASN(015)	-2.796	-2.162	-2.937
4	ASN(207)	SER(202)	-2.316	-2.637	-2.362
4	GLN(057)	SER(060)	-10.189	-3.154	-6.982
4	GLN(389)	THR(394)	-2.176	-2.410	-1.906
4	GLN(478)	GLN(481)	-8.744	-7.298	-9.065
4	GLN(481)	GLN(478)	-8.744	-7.298	-9.660
4	GLN(481)	SER(477)	-1.787	-1.931	-1.367
4	SER(060)	GLN(057)	-10.189	-3.154	-13.209
4	SER(074)	SER(080)	-2.938	-2.974	-2.802
4	SER(080)	SER(074)	-2.938	-2.974	-2.666
4	SER(202)	ASN(207)	-2.316	-2.637	-1.761
4	SER(224)	SER(274)	-3.483	-3.612	-3.556
4	SER(274)	SER(224)	-3.483	-3.612	-3.475
4	SER(288)	SER(383)	-1.329	-1.280	-2.505
4	SER(383)	SER(288)	-1.329	-1.280	-1.090
4	SER(477)	GLN(481)	-1.787	-1.931	-0.712
4	THR(392)	THR(394)	-5.696	-5.715	-4.510
4	THR(394)	GLN(389)	-2.176	-2.410	-2.002
4	THR(394)	THR(392)	-5.696	-5.715	-5.248
5	ASN(207)	SER(202)	-0.560	-1.044	-0.771
5	GLN(057)	SER(060)	-4.537	-4.308	-4.485
5	GLN(092)	SER(002)	-1.741	-1.425	-1.477
5	GLN(389)	THR(394)	-2.754	-2.676	-2.076
5	SER(002)	GLN(092)	-1.741	-1.425	-2.127
5	SER(060)	GLN(057)	-4.537	-4.308	-4.363
5	SER(074)	SER(080)	-0.184	-0.165	-0.218
5	SER(080)	SER(074)	-0.184	-0.165	-0.159
5	SER(172)	THR(067)	-8.880	-7.200	-7.092

5	SER(202)	ASN(207)	-0.560	-1.044	0.027
5	SER(224)	SER(274)	-1.984	-0.488	-2.464
5	SER(274)	SER(224)	-1.984	-0.488	-2.866
5	THR(067)	SER(172)	-8.880	-7.200	-7.690
5	THR(392)	THR(394)	-0.445	-0.769	-0.186
5	THR(394)	GLN(389)	-2.754	-2.676	-2.769
5	THR(394)	THR(392)	-0.445	-0.769	-0.254
6	ASN(207)	SER(202)	1.635	1.792	1.859
6	GLN(389)	THR(394)	-4.672	-4.970	-4.157
6	GLN(478)	GLN(481)	-4.523	-3.998	-4.924
6	GLN(481)	GLN(478)	-4.523	-3.998	-4.984
6	SER(074)	SER(080)	-1.218	-1.389	-1.343
6	SER(080)	SER(074)	-1.218	-1.389	-1.146
6	SER(172)	THR(067)	-8.648	-8.321	-7.698
6	SER(202)	ASN(207)	1.635	1.792	1.302
6	SER(224)	SER(274)	-1.866	-2.257	-2.161
6	SER(232)	THR(234)	0.492	-0.000	0.418
6	SER(274)	SER(224)	-1.866	-2.257	-1.353
6	THR(067)	SER(172)	-8.648	-8.321	-7.345
6	THR(234)	SER(232)	0.492	-0.000	0.420
6	THR(392)	THR(394)	-5.697	-2.490	-2.312
6	THR(394)	GLN(389)	-4.672	-4.970	-4.578
6	THR(394)	THR(392)	-5.697	-2.490	-5.267
7	ASN(015)	ASN(096)	-1.494	-1.181	-1.223
7	ASN(096)	ASN(015)	-1.494	-1.181	-1.613
7	ASN(207)	SER(202)	0.249	0.017	0.222
7	GLN(389)	THR(394)	-3.615	-3.795	-3.260
7	GLN(478)	GLN(481)	-10.544	-5.548	-8.523
7	GLN(481)	GLN(478)	-10.544	-5.548	-15.490

7	GLN(481)	SER(477)	-4.411	-4.745	-4.448
7	SER(074)	SER(080)	-1.894	-1.719	-1.449
7	SER(080)	SER(074)	-1.894	-1.719	-1.546
7	SER(172)	THR(067)	-8.438	-7.672	-7.421
7	SER(202)	ASN(207)	0.249	0.017	0.604
7	SER(224)	SER(274)	-2.336	-2.659	-2.476
7	SER(274)	SER(224)	-2.336	-2.659	-2.391
7	SER(288)	SER(383)	-1.562	-1.800	-1.833
7	SER(383)	SER(288)	-1.562	-1.800	-1.591
7	SER(477)	GLN(481)	-4.411	-4.745	-3.478
7	THR(067)	SER(172)	-8.438	-7.672	-7.818
7	THR(392)	THR(394)	-5.673	-4.711	-4.430
7	THR(394)	GLN(389)	-3.615	-3.795	-3.444
7	THR(394)	THR(392)	-5.673	-4.711	-5.464
8	ASN(207)	SER(202)	-1.616	-1.418	-1.690
8	GLN(092)	SER(002)	-2.722	-3.123	-2.412
8	GLN(389)	THR(394)	-2.850	-2.989	-2.536
8	GLN(478)	GLN(481)	-6.592	-5.814	-5.734
8	GLN(481)	GLN(478)	-6.592	-5.814	-7.277
8	SER(002)	GLN(092)	-2.722	-3.123	-2.880
8	SER(074)	SER(080)	-0.671	-0.781	-0.869
8	SER(080)	SER(074)	-0.671	-0.781	-0.773
8	SER(172)	THR(067)	-6.444	-4.458	-4.221
8	SER(202)	ASN(207)	-1.616	-1.418	-1.320
8	SER(224)	SER(274)	-3.653	-3.707	-3.846
8	SER(232)	THR(234)	-1.670	-1.835	-1.571
8	SER(274)	SER(224)	-3.653	-3.707	-3.756
8	SER(288)	SER(383)	-1.326	-1.584	-1.668
8	SER(383)	SER(288)	-1.326	-1.584	-1.384

8	THR(067)	SER(172)	-6.444	-4.458	-5.233
8	THR(234)	SER(232)	-1.670	-1.835	-1.576
8	THR(392)	THR(394)	-6.128	-6.004	-5.545
8	THR(394)	GLN(389)	-2.850	-2.989	-2.845
8	THR(394)	THR(392)	-6.128	-6.004	-6.136
9	ASN(207)	SER(202)	-0.804	-0.523	-0.588
9	ASN(406)	GLN(408)	-4.798	-3.099	-5.362
9	GLN(057)	SER(060)	-12.913	-8.351	-12.008
9	GLN(389)	THR(394)	-2.761	-2.924	-2.607
9	GLN(408)	ASN(406)	-4.798	-3.099	-6.318
9	GLN(481)	SER(477)	-4.787	-4.825	-4.751
9	SER(060)	GLN(057)	-12.913	-8.351	-14.383
9	SER(074)	SER(080)	1.108	1.119	0.557
9	SER(080)	SER(074)	1.108	1.119	0.933
9	SER(172)	THR(067)	-8.559	-7.095	-6.668
9	SER(202)	ASN(207)	-0.804	-0.523	-0.970
9	SER(224)	SER(274)	-2.349	-2.701	-2.450
9	SER(274)	SER(224)	-2.349	-2.701	-2.259
9	SER(288)	SER(383)	-1.845	-2.080	-2.385
9	SER(383)	SER(288)	-1.845	-2.080	-1.869
9	SER(477)	GLN(481)	-4.787	-4.825	-4.077
9	THR(067)	SER(172)	-8.559	-7.095	-8.106
9	THR(394)	GLN(389)	-2.761	-2.924	-4.423
10	ASN(015)	ASN(096)	-4.258	-2.804	-3.733
10	ASN(096)	ASN(015)	-4.258	-2.804	-5.211
10	ASN(207)	SER(202)	-3.253	-3.644	-3.369
10	GLN(092)	SER(002)	-1.944	-1.336	-1.242
10	GLN(478)	GLN(481)	-12.809	-12.087	-12.226
10	GLN(481)	GLN(478)	-12.809	-12.087	-12.971

10	SER(002)	GLN(092)	-1.944	-1.336	-2.414
10	SER(074)	SER(080)	-0.029	-0.302	-0.077
10	SER(080)	SER(074)	-0.029	-0.302	-0.056
10	SER(202)	ASN(207)	-3.253	-3.644	-2.699
10	SER(224)	SER(274)	-4.650	-4.935	-4.959
10	SER(274)	SER(224)	-4.650	-4.935	-4.711
10	SER(288)	SER(383)	-1.372	-1.498	-2.329
10	SER(383)	SER(288)	-1.372	-1.498	-1.519
11	ASN(015)	ASN(096)	-2.928	1.278	-1.310
11	ASN(096)	ASN(015)	-2.928	1.278	-5.019
11	ASN(207)	SER(202)	-1.990	-2.385	-2.170
11	GLN(389)	THR(394)	-1.135	-0.932	-1.139
11	GLN(478)	GLN(481)	-7.464	-3.762	-6.252
11	GLN(481)	GLN(478)	-7.464	-3.762	-10.180
11	SER(074)	SER(080)	-3.112	0.130	-2.141
11	SER(080)	SER(074)	-3.112	0.130	1.163
11	SER(172)	THR(067)	-6.642	-4.956	-4.463
11	SER(202)	ASN(207)	-1.990	-2.385	-1.706
11	SER(224)	SER(274)	-5.986	-5.732	-6.009
11	SER(232)	THR(234)	-0.154	-0.457	-0.137
11	SER(274)	SER(224)	-5.986	-5.732	-5.609
11	SER(288)	SER(383)	-1.476	-1.872	-2.203
11	SER(383)	SER(288)	-1.476	-1.872	-1.594
11	THR(067)	SER(172)	-6.642	-4.956	-5.637
11	THR(234)	SER(232)	-0.154	-0.457	-0.117
11	THR(394)	GLN(389)	-1.135	-0.932	-1.869
12	ASN(207)	SER(202)	-1.040	-1.398	-1.131
12	SER(074)	SER(080)	0.743	0.899	1.191
12	SER(080)	SER(074)	0.743	0.899	1.280

12	SER(202)	ASN(207)	-1.040	-1.398	-0.511
12	SER(224)	SER(274)	-1.973	-1.059	-2.253
12	SER(274)	SER(224)	-1.973	-1.059	-2.141
12	SER(288)	SER(383)	-0.941	-1.452	-1.441
12	SER(383)	SER(288)	-0.941	-1.452	-1.062
13	ASN(015)	ASN(096)	-4.469	-3.259	-3.767
13	ASN(096)	ASN(015)	-4.469	-3.259	-5.023
13	ASN(207)	SER(202)	-0.208	-0.393	-0.157
13	GLN(057)	SER(060)	-11.514	-6.419	-8.735
13	GLN(389)	THR(394)	-0.414	-0.063	0.789
13	GLN(478)	GLN(481)	-15.665	-14.027	-14.944
13	GLN(481)	GLN(478)	-15.665	-14.027	-15.711
13	SER(060)	GLN(057)	-11.514	-6.419	-13.440
13	SER(061)	SER(064)	-4.752	-4.717	-4.770
13	SER(064)	SER(061)	-4.752	-4.717	-4.820
13	SER(074)	SER(080)	-0.685	-0.957	-0.577
13	SER(080)	SER(074)	-0.685	-0.957	-0.609
13	SER(172)	THR(067)	-3.216	-3.535	-2.888
13	SER(202)	ASN(207)	-0.208	-0.393	0.189
13	SER(224)	SER(274)	-4.386	-4.473	-4.412
13	SER(274)	SER(224)	-4.386	-4.473	-4.346
13	SER(288)	SER(383)	-1.773	-2.066	-2.118
13	SER(383)	SER(288)	-1.773	-2.066	-1.822
13	THR(067)	SER(172)	-3.216	-3.535	-3.458
13	THR(394)	GLN(389)	-0.414	-0.063	-1.470
14	ASN(207)	SER(202)	1.393	1.134	1.326
14	GLN(092)	SER(002)	-2.024	-1.466	-1.420
14	GLN(389)	THR(394)	-1.027	-0.935	-0.427
14	SER(002)	GLN(092)	-2.024	-1.466	-2.675

14	SER(061)	SER(064)	2.936	2.431	3.080
14	SER(064)	SER(061)	2.936	2.431	2.872
14	SER(074)	SER(080)	0.127	0.181	0.449
14	SER(080)	SER(074)	0.127	0.181	0.858
14	SER(172)	THR(067)	-3.014	-2.959	-2.764
14	SER(202)	ASN(207)	1.393	1.134	1.308
14	SER(224)	SER(274)	-2.351	-1.830	-2.856
14	SER(274)	SER(224)	-2.351	-1.830	-2.134
14	SER(288)	SER(383)	-0.945	-1.460	-1.774
14	SER(383)	SER(288)	-0.945	-1.460	-1.211
14	THR(067)	SER(172)	-3.014	-2.959	-2.805
14	THR(394)	GLN(389)	-1.027	-0.935	-1.575
15	ASN(207)	SER(202)	0.488	0.400	0.562
15	SER(074)	SER(080)	0.651	0.320	1.102
15	SER(080)	SER(074)	0.651	0.320	1.107
15	SER(172)	THR(067)	-1.877	-2.302	-1.560
15	SER(202)	ASN(207)	0.488	0.400	0.569
15	SER(224)	SER(274)	-5.670	-5.578	-6.626
15	SER(274)	SER(224)	-5.670	-5.578	-5.767
15	SER(288)	SER(383)	-1.495	-1.964	-1.789
15	SER(383)	SER(288)	-1.495	-1.964	-1.539
15	THR(067)	SER(172)	-1.877	-2.302	-1.906
16	ASN(207)	SER(202)	1.434	1.267	0.822
16	GLN(481)	SER(477)	-3.433	-3.478	-3.242
16	SER(074)	SER(080)	-2.231	-2.568	-2.024
16	SER(080)	SER(074)	-2.231	-2.568	-2.176
16	SER(172)	THR(067)	-2.331	-2.838	-1.922
16	SER(202)	ASN(207)	1.434	1.267	1.558
16	SER(224)	SER(274)	-6.426	-5.864	-6.626

16	SER(274)	SER(224)	-6.426	-5.864	-6.279
16	SER(288)	SER(383)	-2.070	-2.051	-2.738
16	SER(383)	SER(288)	-2.070	-2.051	-2.005
16	SER(477)	GLN(481)	-3.433	-3.478	-2.988
16	THR(067)	SER(172)	-2.331	-2.838	-2.096
17	ASN(207)	SER(202)	0.370	-0.443	0.324
17	GLN(478)	GLN(481)	-15.389	-9.689	-14.252
17	GLN(481)	GLN(478)	-15.389	-9.689	-19.728
17	GLN(481)	SER(477)	-0.787	-0.867	-0.678
17	SER(074)	SER(080)	-2.461	-2.683	-2.258
17	SER(080)	SER(074)	-2.461	-2.683	-2.371
17	SER(172)	THR(067)	-5.418	-3.859	-3.600
17	SER(202)	ASN(207)	0.370	-0.443	1.108
17	SER(224)	SER(274)	-3.682	-3.642	-3.638
17	SER(274)	SER(224)	-3.682	-3.642	-6.127
17	SER(288)	SER(383)	-1.966	-2.106	-2.552
17	SER(383)	SER(288)	-1.966	-2.106	-2.139
17	SER(477)	GLN(481)	-0.787	-0.867	-0.287
17	THR(067)	SER(172)	-5.418	-3.859	-4.863
18	ASN(207)	SER(202)	-2.250	-2.503	-2.294
18	ASN(406)	GLN(408)	-10.175	-6.813	-10.202
18	GLN(057)	SER(060)	-14.072	-10.643	-13.009
18	GLN(389)	THR(394)	-0.152	-0.089	0.473
18	GLN(408)	ASN(406)	-10.175	-6.813	-12.130
18	GLN(481)	SER(477)	-4.046	-3.981	-3.789
18	SER(060)	GLN(057)	-14.072	-10.643	-15.614
18	SER(074)	SER(080)	1.178	1.238	0.706
18	SER(080)	SER(074)	1.178	1.238	1.082
18	SER(202)	ASN(207)	-2.250	-2.503	-2.144

18	SER(224)	SER(274)	-4.120	-2.095	-4.975
18	SER(274)	SER(224)	-4.120	-2.095	-4.225
18	SER(288)	SER(383)	-1.505	-1.747	-2.235
18	SER(383)	SER(288)	-1.505	-1.747	-1.490
18	SER(477)	GLN(481)	-4.046	-3.981	-3.238
18	THR(394)	GLN(389)	-0.152	-0.089	-0.938
19	ASN(207)	SER(202)	-0.577	-0.725	-0.505
19	ASN(406)	GLN(408)	-8.108	-7.000	-8.492
19	GLN(389)	SER(298)	-1.608	-1.731	-1.562
19	GLN(408)	ASN(406)	-8.108	-7.000	-9.196
19	SER(074)	SER(080)	0.579	0.348	0.586
19	SER(080)	SER(074)	0.579	0.348	0.618
19	SER(172)	THR(067)	-2.796	-1.436	-0.049
19	SER(202)	ASN(207)	-0.577	-0.725	0.219
19	SER(224)	SER(274)	-4.879	-4.508	-5.082
19	SER(274)	SER(224)	-4.879	-4.508	-5.280
19	SER(288)	SER(383)	-0.865	-1.363	-1.170
19	SER(298)	GLN(389)	-1.608	-1.731	-1.550
19	SER(383)	SER(288)	-0.865	-1.363	-0.880
19	THR(067)	SER(172)	-2.796	-1.436	-1.811
20	ASN(207)	SER(202)	-1.472	-1.366	-1.222
20	SER(074)	SER(080)	0.540	0.301	0.413
20	SER(080)	SER(074)	0.540	0.301	0.445
20	SER(172)	THR(067)	-4.636	-4.922	-3.955
20	SER(202)	ASN(207)	-1.472	-1.366	-0.591
20	SER(224)	SER(274)	-2.894	-2.687	-3.208
20	SER(274)	SER(224)	-2.894	-2.687	-1.688
20	SER(288)	SER(383)	-1.632	-1.449	-2.521
20	SER(383)	SER(288)	-1.632	-1.449	-1.752

20	THR(067)	SER(172)	-4.636	-4.922	-4.053
21	ASN(207)	SER(202)	-3.200	-3.355	-2.660
21	GLN(478)	GLN(481)	-4.260	-4.476	-3.908
21	GLN(481)	GLN(478)	-4.260	-4.476	-4.056
21	SER(074)	SER(080)	-0.233	-0.357	-0.409
21	SER(080)	SER(074)	-0.233	-0.357	-0.216
21	SER(172)	THR(067)	-3.218	-2.709	-1.841
21	SER(202)	ASN(207)	-3.200	-3.355	-4.261
21	SER(224)	SER(274)	-4.748	-4.712	-5.439
21	SER(274)	SER(224)	-4.748	-4.712	-4.860
21	SER(288)	SER(383)	-2.211	-1.895	-2.822
21	SER(383)	SER(288)	-2.211	-1.895	-2.076
21	THR(067)	SER(172)	-3.218	-2.709	-3.156
22	ASN(207)	SER(202)	-2.757	-3.105	-2.660
22	GLN(057)	SER(060)	-15.085	-8.660	-13.458
22	GLN(092)	SER(002)	-4.714	-4.798	-4.642
22	GLN(389)	SER(298)	-1.546	-1.632	-1.526
22	SER(002)	GLN(092)	-4.714	-4.798	-4.488
22	SER(060)	GLN(057)	-15.085	-8.660	-17.246
22	SER(074)	SER(080)	0.796	0.809	0.599
22	SER(080)	SER(074)	0.796	0.809	1.020
22	SER(172)	THR(067)	-2.039	-2.105	-1.822
22	SER(202)	ASN(207)	-2.757	-3.105	-2.877
22	SER(224)	SER(274)	-2.635	-3.173	-2.818
22	SER(274)	SER(224)	-2.635	-3.173	-3.226
22	SER(288)	SER(383)	-2.331	-2.410	-2.917
22	SER(298)	GLN(389)	-1.546	-1.632	-1.507
22	SER(383)	SER(288)	-2.331	-2.410	-2.309
22	THR(067)	SER(172)	-2.039	-2.105	-1.809

23	ASN(207)	SER(202)	-0.222	-0.434	-0.311
23	ASN(406)	GLN(408)	-7.761	-6.936	-7.636
23	GLN(057)	SER(060)	-14.231	-8.858	-13.240
23	GLN(092)	SER(002)	-4.143	-4.042	-3.937
23	GLN(408)	ASN(406)	-7.761	-6.936	-8.574
23	GLN(478)	GLN(481)	-11.481	-10.381	-11.208
23	GLN(481)	GLN(478)	-11.481	-10.381	-11.084
23	SER(002)	GLN(092)	-4.143	-4.042	-3.781
23	SER(060)	GLN(057)	-14.231	-8.858	-16.171
23	SER(074)	SER(080)	-0.180	-0.311	-0.133
23	SER(080)	SER(074)	-0.180	-0.311	-0.131
23	SER(172)	THR(067)	-4.636	-4.406	-4.692
23	SER(202)	ASN(207)	-0.222	-0.434	-0.147
23	SER(224)	SER(274)	-3.148	-3.765	-3.580
23	SER(274)	SER(224)	-3.148	-3.765	-3.632
23	SER(288)	SER(383)	-2.166	-2.091	-2.432
23	SER(383)	SER(288)	-2.166	-2.091	-1.996
23	THR(067)	SER(172)	-4.636	-4.406	-4.088
24	ASN(015)	ASN(096)	-5.456	-3.074	-4.525
24	ASN(096)	ASN(015)	-5.456	-3.074	-6.236
24	ASN(207)	SER(202)	-1.428	-1.577	-1.513
24	GLN(478)	GLN(481)	-10.867	-7.756	-9.741
24	GLN(481)	GLN(478)	-10.867	-7.756	-12.632
24	SER(074)	SER(080)	-1.197	-1.382	-1.247
24	SER(080)	SER(074)	-1.197	-1.382	-1.068
24	SER(172)	THR(067)	-6.158	-5.554	-4.397
24	SER(202)	ASN(207)	-1.428	-1.577	-0.959
24	SER(224)	SER(274)	-4.830	-5.159	-5.036
24	SER(274)	SER(224)	-4.830	-5.159	-4.761

24	SER(288)	SER(383)	-1.562	-1.799	-2.002
24	SER(383)	SER(288)	-1.562	-1.799	-1.576
24	THR(067)	SER(172)	-6.158	-5.554	-6.036
25	ASN(207)	SER(202)	-2.285	-2.695	-2.322
25	ASN(406)	GLN(408)	-9.808	-7.456	-9.831
25	GLN(408)	ASN(406)	-9.808	-7.456	-10.613
25	SER(074)	SER(080)	0.307	0.171	0.012
25	SER(080)	SER(074)	0.307	0.171	0.344
25	SER(172)	THR(067)	-7.520	-7.720	-7.020
25	SER(202)	ASN(207)	-2.285	-2.695	-1.595
25	SER(224)	SER(274)	-4.172	-4.413	-4.713
25	SER(232)	THR(234)	0.238	-0.047	-0.218
25	SER(274)	SER(224)	-4.172	-4.413	-4.220
25	SER(288)	SER(383)	-1.256	-1.637	-1.856
25	SER(383)	SER(288)	-1.256	-1.637	-1.343
25	THR(067)	SER(172)	-7.520	-7.720	-6.883
25	THR(234)	SER(232)	0.238	-0.047	0.112

Table B.8.: SAPT, EFP and QM/EFP dispersion interaction energies computed for aryl-aryl dimers. All energies are given in units of kcal/mol. For QM/EFP, monA represents the QM region and monB the effective fragment.

snapshot	monA	monB	SAPT	EFP	QMEFP
1	PHE(146)	TRP(150)	-9.874	-10.883	-7.609
1	PHE(149)	TYR(290)	-7.165	-7.988	-5.710
1	PHE(278)	TYR(223)	-7.033	-7.823	-5.613
1	PHE(310)	TRP(312)	-9.607	-10.719	-7.689

1	PHE(357)	TRP(322)	-8.856	-9.439	-7.097
1	TRP(150)	PHE(146)	-9.874	-10.883	-7.944
1	TRP(312)	PHE(310)	-9.607	-10.719	-7.294
1	TRP(322)	PHE(357)	-8.856	-9.439	-6.877
1	TYR(223)	PHE(278)	-7.033	-7.823	-5.413
1	TYR(290)	PHE(149)	-7.165	-7.988	-5.316
2	HSD(437)	TYR(412)	-6.225	-6.519	-4.886
2	PHE(149)	TYR(290)	-6.635	-7.196	-5.301
2	PHE(310)	TRP(312)	-9.729	-10.926	-7.670
2	PHE(357)	TRP(322)	-8.103	-8.958	-6.673
2	TRP(312)	PHE(310)	-9.729	-10.926	-7.419
2	TRP(322)	PHE(357)	-8.103	-8.958	-6.294
2	TYR(290)	PHE(149)	-6.635	-7.196	-4.915
2	TYR(412)	HSD(437)	-6.225	-6.519	-4.810
3	PHE(149)	TYR(290)	-9.165	-10.384	-7.230
3	PHE(185)	TRP(033)	-11.021	-12.297	-8.648
3	PHE(310)	TRP(312)	-8.702	-9.554	-6.855
3	PHE(357)	TRP(322)	-10.115	-11.153	-8.469
3	TRP(033)	PHE(185)	-11.021	-12.297	-8.867
3	TRP(312)	PHE(310)	-8.702	-9.554	-6.709
3	TRP(322)	PHE(357)	-10.115	-11.153	-7.863
3	TYR(290)	PHE(149)	-9.165	-10.384	-6.953
4	HSD(437)	TYR(412)	-10.844	-11.775	-8.734
4	PHE(149)	TYR(290)	-8.758	-9.981	-7.103
4	PHE(185)	TRP(033)	-9.874	-10.394	-7.452
4	PHE(357)	TRP(322)	-7.854	-8.739	-6.516
4	TRP(033)	PHE(185)	-9.874	-10.394	-7.886
4	TRP(322)	PHE(357)	-7.854	-8.739	-5.991
4	TYR(290)	PHE(149)	-8.758	-9.981	-6.607

4	TYR(412)	HSD(437)	-10.844	-11.775	-8.365
5	HSD(437)	TYR(412)	-6.106	-6.432	-4.964
5	PHE(146)	TYR(287)	-7.126	-8.045	-5.780
5	PHE(149)	TYR(290)	-5.142	-6.097	-4.342
5	PHE(185)	TRP(033)	-5.899	-6.486	-4.492
5	PHE(357)	TRP(322)	-10.150	-11.103	-8.501
5	TRP(033)	PHE(185)	-5.899	-6.486	-4.559
5	TRP(322)	PHE(357)	-10.150	-11.103	-7.883
5	TYR(287)	PHE(146)	-7.126	-8.045	-5.385
5	TYR(290)	PHE(149)	-5.142	-6.097	-3.750
5	TYR(412)	HSD(437)	-6.106	-6.432	-4.350
6	HSD(295)	TYR(297)	-7.578	-8.797	-6.068
6	HSD(437)	TYR(412)	-7.232	-7.922	-6.058
6	PHE(149)	TYR(290)	-6.473	-7.063	-5.111
6	PHE(185)	TRP(033)	-9.280	-9.736	-6.842
6	PHE(310)	TRP(312)	-10.384	-11.643	-8.538
6	PHE(357)	TRP(322)	-9.930	-10.685	-7.990
6	TRP(033)	PHE(185)	-9.280	-9.736	-7.428
6	TRP(312)	PHE(310)	-10.384	-11.643	-7.884
6	TRP(322)	PHE(357)	-9.930	-10.685	-7.848
6	TYR(290)	PHE(149)	-6.473	-7.063	-4.831
6	TYR(297)	HSD(295)	-7.578	-8.797	-5.993
6	TYR(412)	HSD(437)	-7.232	-7.922	-5.253
7	HSD(295)	TYR(297)	-9.015	-9.927	-7.068
7	HSD(437)	TYR(412)	-10.096	-10.891	-7.696
7	PHE(146)	TRP(150)	-7.239	-8.070	-5.505
7	PHE(149)	TYR(290)	-6.181	-7.025	-4.984
7	PHE(185)	TRP(033)	-10.587	-11.325	-7.882
7	PHE(310)	TRP(312)	-13.384	-14.572	-10.724

7	PHE(357)	TRP(322)	-10.738	-11.622	-8.753
7	TRP(033)	PHE(185)	-10.587	-11.325	-8.420
7	TRP(150)	PHE(146)	-7.239	-8.070	-5.858
7	TRP(312)	PHE(310)	-13.384	-14.572	-9.985
7	TRP(322)	PHE(357)	-10.738	-11.622	-8.471
7	TYR(290)	PHE(149)	-6.181	-7.025	-4.592
7	TYR(297)	HSD(295)	-9.015	-9.927	-7.134
7	TYR(412)	HSD(437)	-10.096	-10.891	-7.757
8	HSD(437)	TYR(412)	-10.685	-11.998	-8.735
8	PHE(146)	TYR(287)	-9.796	-11.649	-8.332
8	PHE(149)	TYR(290)	-6.908	-7.985	-5.603
8	PHE(185)	TRP(033)	-9.976	-10.537	-7.616
8	PHE(310)	TRP(312)	-14.581	-16.104	-11.650
8	PHE(357)	TRP(322)	-7.071	-7.624	-5.805
8	TRP(033)	PHE(185)	-9.976	-10.537	-7.955
8	TRP(312)	PHE(310)	-14.581	-16.104	-11.319
8	TRP(322)	PHE(357)	-7.071	-7.624	-5.515
8	TYR(287)	PHE(146)	-9.796	-11.649	-7.750
8	TYR(290)	PHE(149)	-6.908	-7.985	-5.259
8	TYR(412)	HSD(437)	-10.685	-11.998	-8.197
9	HSD(437)	TYR(412)	-7.549	-8.359	-6.059
9	PHE(149)	TYR(290)	-7.129	-7.829	-5.722
9	PHE(185)	TRP(033)	-5.369	-5.996	-4.234
9	PHE(310)	TRP(312)	-8.380	-8.997	-6.630
9	PHE(357)	TRP(322)	-9.837	-11.009	-8.192
9	TRP(033)	PHE(185)	-5.369	-5.996	-4.058
9	TRP(312)	PHE(310)	-8.380	-8.997	-6.210
9	TRP(322)	PHE(357)	-9.837	-11.009	-7.502
9	TYR(290)	PHE(149)	-7.129	-7.829	-5.290

9	TYR(412)	HSD(437)	-7.549	-8.359	-5.557
10	HSD(437)	TYR(412)	-7.338	-7.948	-5.952
10	PHE(146)	TYR(287)	-6.998	-8.164	-5.948
10	PHE(149)	TYR(290)	-5.310	-5.952	-4.367
10	PHE(185)	TRP(033)	-6.337	-6.859	-5.018
10	PHE(244)	TRP(050)	-9.479	-10.342	-7.892
10	PHE(310)	TRP(312)	-11.757	-12.968	-9.276
10	PHE(357)	TRP(322)	-7.065	-7.637	-5.877
10	TRP(033)	PHE(185)	-6.337	-6.859	-4.796
10	TRP(050)	PHE(244)	-9.479	-10.342	-7.523
10	TRP(312)	PHE(310)	-11.757	-12.968	-9.142
10	TRP(322)	PHE(357)	-7.065	-7.637	-5.381
10	TYR(287)	PHE(146)	-6.998	-8.164	-5.470
10	TYR(290)	PHE(149)	-5.310	-5.952	-3.857
10	TYR(412)	HSD(437)	-7.338	-7.948	-5.306
11	HSD(437)	TYR(412)	-8.885	-9.409	-6.882
11	PHE(149)	TYR(290)	-8.200	-8.931	-6.508
11	PHE(319)	TRP(367)	-7.366	-7.832	-5.499
11	PHE(357)	TRP(322)	-12.561	-13.573	-10.164
11	TRP(322)	PHE(357)	-12.561	-13.573	-9.864
11	TRP(367)	PHE(319)	-7.366	-7.832	-6.008
11	TYR(290)	PHE(149)	-8.200	-8.931	-6.032
11	TYR(412)	HSD(437)	-8.885	-9.409	-6.826
12	HSD(437)	TYR(412)	-8.721	-9.305	-6.771
12	PHE(149)	TYR(290)	-5.382	-5.797	-4.291
12	PHE(310)	TRP(312)	-9.210	-9.852	-6.951
12	PHE(357)	TRP(322)	-8.438	-9.160	-6.975
12	TRP(312)	PHE(310)	-9.210	-9.852	-7.166
12	TRP(322)	PHE(357)	-8.438	-9.160	-6.712

12	TYR(290)	PHE(149)	-5.382	-5.797	-3.849
12	TYR(412)	HSD(437)	-8.721	-9.305	-6.643
13	HSD(437)	TYR(412)	-7.620	-8.198	-5.843
13	PHE(146)	TYR(287)	-9.850	-11.299	-8.339
13	PHE(149)	TYR(290)	-4.141	-4.546	-3.240
13	PHE(310)	TRP(312)	-10.070	-11.192	-8.268
13	PHE(357)	TRP(322)	-9.387	-10.129	-7.526
13	TRP(312)	PHE(310)	-10.070	-11.192	-7.569
13	TRP(322)	PHE(357)	-9.387	-10.129	-7.354
13	TYR(287)	PHE(146)	-9.850	-11.299	-7.561
13	TYR(290)	PHE(149)	-4.141	-4.546	-3.152
13	TYR(412)	HSD(437)	-7.620	-8.198	-5.840
14	HSD(437)	TYR(412)	-10.404	-11.207	-8.278
14	PHE(146)	TYR(287)	-7.907	-9.516	-6.857
14	PHE(149)	TYR(290)	-6.642	-7.447	-5.273
14	PHE(185)	TRP(033)	-8.338	-9.074	-6.368
14	PHE(310)	TRP(312)	-8.531	-9.239	-6.733
14	PHE(357)	TRP(322)	-9.670	-10.810	-7.614
14	TRP(033)	PHE(185)	-8.338	-9.074	-6.470
14	TRP(312)	PHE(310)	-8.531	-9.239	-6.420
14	TRP(322)	PHE(357)	-9.670	-10.810	-7.689
14	TYR(287)	PHE(146)	-7.907	-9.516	-6.018
14	TYR(290)	PHE(149)	-6.642	-7.447	-4.877
14	TYR(412)	HSD(437)	-10.404	-11.207	-7.941
15	HSD(437)	TYR(412)	-8.978	-9.705	-7.251
15	PHE(149)	TYR(290)	-5.379	-6.017	-4.254
15	PHE(310)	TRP(312)	-11.013	-11.969	-8.635
15	PHE(357)	TRP(322)	-9.866	-11.059	-7.907
15	TRP(312)	PHE(310)	-11.013	-11.969	-8.377

15	TRP(322)	PHE(357)	-9.866	-11.059	-7.713
15	TRP(373)	TYR(041)	-7.390	-7.953	-5.551
15	TYR(041)	TRP(373)	-7.390	-7.953	-6.106
15	TYR(290)	PHE(149)	-5.379	-6.017	-3.962
15	TYR(412)	HSD(437)	-8.978	-9.705	-6.787
16	HSD(437)	TYR(412)	-8.705	-9.422	-7.140
16	PHE(149)	TYR(290)	-7.690	-9.149	-6.353
16	PHE(372)	TRP(388)	-6.978	-6.987	-5.192
16	TRP(388)	PHE(372)	-6.978	-6.987	-5.563
16	TYR(290)	PHE(149)	-7.690	-9.149	-5.797
16	TYR(412)	HSD(437)	-8.705	-9.422	-6.429
17	HSD(437)	TYR(412)	-9.307	-9.972	-7.508
17	PHE(146)	TYR(287)	-8.783	-9.969	-7.046
17	PHE(149)	TYR(290)	-7.240	-8.319	-6.015
17	PHE(185)	TRP(033)	-6.650	-6.847	-5.137
17	PHE(278)	TYR(223)	-6.378	-7.021	-5.100
17	PHE(310)	TRP(312)	-10.375	-11.500	-8.361
17	PHE(357)	TRP(322)	-7.148	-7.861	-5.857
17	TRP(033)	PHE(185)	-6.650	-6.847	-5.182
17	TRP(312)	PHE(310)	-10.375	-11.500	-7.813
17	TRP(322)	PHE(357)	-7.148	-7.861	-5.474
17	TYR(223)	PHE(278)	-6.378	-7.021	-4.987
17	TYR(287)	PHE(146)	-8.783	-9.969	-7.124
17	TYR(290)	PHE(149)	-7.240	-8.319	-5.295
17	TYR(412)	HSD(437)	-9.307	-9.972	-7.081
18	HSD(437)	TYR(412)	-5.400	-5.818	-4.234
18	PHE(146)	TYR(287)	-8.088	-8.953	-6.482
18	PHE(149)	TYR(290)	-5.933	-6.604	-4.804
18	PHE(278)	TYR(223)	-6.949	-7.442	-5.696

18	PHE(310)	TRP(312)	-12.078	-13.114	-9.609
18	PHE(357)	TRP(322)	-10.675	-12.060	-8.717
18	TRP(312)	PHE(310)	-12.078	-13.114	-9.343
18	TRP(322)	PHE(357)	-10.675	-12.060	-8.390
18	TYR(223)	PHE(278)	-6.949	-7.442	-5.338
18	TYR(287)	PHE(146)	-8.088	-8.953	-6.454
18	TYR(290)	PHE(149)	-5.933	-6.604	-4.339
18	TYR(412)	HSD(437)	-5.400	-5.818	-3.969
19	HSD(437)	TYR(412)	-9.987	-10.950	-7.894
19	PHE(149)	TYR(290)	-4.945	-5.395	-3.831
19	PHE(310)	TRP(312)	-8.997	-9.823	-7.166
19	TRP(312)	PHE(310)	-8.997	-9.823	-6.859
19	TYR(290)	PHE(149)	-4.945	-5.395	-3.760
19	TYR(412)	HSD(437)	-9.987	-10.950	-7.532
21	HSD(437)	TYR(412)	-11.189	-12.284	-8.783
21	PHE(149)	TYR(290)	-5.969	-6.643	-4.711
21	PHE(278)	TYR(223)	-6.301	-7.086	-5.107
21	PHE(310)	TRP(312)	-12.664	-13.412	-10.151
21	TRP(312)	PHE(310)	-12.664	-13.412	-9.570
21	TYR(223)	PHE(278)	-6.301	-7.086	-4.833
21	TYR(290)	PHE(149)	-5.969	-6.643	-4.399
21	TYR(412)	HSD(437)	-11.189	-12.284	-8.637
22	HSD(437)	TYR(412)	-5.751	-6.381	-4.491
22	PHE(149)	TYR(290)	-9.026	-10.354	-7.322
22	PHE(310)	TRP(312)	-13.243	-14.217	-10.904
22	PHE(357)	TRP(322)	-10.939	-12.551	-9.248
22	TRP(312)	PHE(310)	-13.243	-14.217	-9.512
22	TRP(322)	PHE(357)	-10.939	-12.551	-8.565
22	TYR(290)	PHE(149)	-9.026	-10.354	-6.875

22	TYR(412)	HSD(437)	-5.751	-6.381	-4.229
23	HSD(437)	TYR(412)	-9.263	-10.228	-7.433
23	PHE(149)	TYR(290)	-9.570	-10.732	-7.525
23	PHE(185)	TRP(033)	-6.910	-7.297	-5.248
23	PHE(310)	TRP(312)	-11.509	-12.977	-9.724
23	PHE(357)	TRP(322)	-7.984	-8.642	-6.668
23	TRP(033)	PHE(185)	-6.910	-7.297	-5.201
23	TRP(312)	PHE(310)	-11.509	-12.977	-8.544
23	TRP(322)	PHE(357)	-7.984	-8.642	-6.126
23	TYR(290)	PHE(149)	-9.570	-10.732	-7.317
23	TYR(412)	HSD(437)	-9.263	-10.228	-6.984
24	HSD(437)	TYR(412)	-9.010	-9.369	-6.695
24	PHE(149)	TYR(290)	-6.226	-6.918	-4.957
24	PHE(185)	TRP(033)	-9.920	-10.808	-7.439
24	PHE(244)	TRP(050)	-10.039	-11.229	-8.608
24	PHE(310)	TRP(312)	-11.804	-12.642	-9.488
24	PHE(357)	TRP(322)	-8.814	-9.736	-7.231
24	TRP(033)	PHE(185)	-9.920	-10.808	-7.728
24	TRP(050)	PHE(244)	-10.039	-11.229	-7.834
24	TRP(312)	PHE(310)	-11.804	-12.642	-8.783
24	TRP(322)	PHE(357)	-8.814	-9.736	-6.772
24	TYR(290)	PHE(149)	-6.226	-6.918	-4.729
24	TYR(412)	HSD(437)	-9.010	-9.369	-6.918
25	HSD(437)	TYR(412)	-9.533	-10.022	-7.319
25	PHE(149)	TYR(290)	-5.449	-6.255	-4.359
25	PHE(310)	TRP(312)	-11.767	-13.089	-9.587
25	PHE(356)	TYR(329)	-6.161	-6.382	-4.596
25	PHE(357)	TRP(322)	-6.567	-7.061	-5.300
25	TRP(312)	PHE(310)	-11.767	-13.089	-8.819

25	TRP(322)	PHE(357)	-6.567	-7.061	-4.915
25	TYR(290)	PHE(149)	-5.449	-6.255	-4.074
25	TYR(329)	PHE(356)	-6.161	-6.382	-4.551
25	TYR(412)	HSD(437)	-9.533	-10.022	-7.204

C. SUPPLEMENTARY MATERIAL FOR CHAPTER 4

This appendix contains the supplementary information for Chapter 4, benchmark study of QM/EFP singlet excitation energies.

Table C.1.: cc-pVDZ Excitation energies for full quantum mechanical (CIS), QM/EFP (PE, PE+S, PE+XR, PE+SXR) and gas-phase (CIS Gas) calculations, as well as charge-transfer character (chtr) and transition types (np, pp and pr for n→π^*, $\pi\rightarrow\pi^*$ and $\pi\rightarrow$Ryd respectively). All energies are given in units of eV. N/A indicates the transitions for which full quantum CIS states could not be matches to QM/EFP or gas-phase transitions.

Geo.	CIS	CIS	PE	PE+S	PE+XR	PE+SXR	gas	chtr	Type
1a	1	5.176	5.172	5.176	5.165	5.168	5.232	0	pp
1a	2	5.400	5.400	5.401	5.398	5.399	5.418	0	pp
1a	3	6.004	6.003	5.997	6.007	6.005	6.008	0	np
1a	6	7.395	7.394	7.395	7.390	7.391	7.437	0	pp
1a	7	7.680	7.687	7.670	7.686	7.685	7.664	0	pp
1a	8	7.961	7.966	7.958	7.971	7.969	7.927	0	np
1a	9	8.422	8.415	8.436	8.403	8.416	8.550	0	pr
1a	10	8.482	8.482	8.482	8.481	8.481	8.502	0	pp
1a	12	8.728	8.719	8.738	8.709	8.714	8.823	0	pr
1a	13	9.066	9.037	N/A	9.061	9.065	9.065	0	np
1a	14	9.180	9.225	N/A	9.160	9.146	N/A	0	pr
1b	1	5.186	5.196	5.194	5.196	5.195	5.242	0	pp

1b	2	5.403	5.407	5.408	5.406	5.407	5.422	0	pp
1b	3	6.284	6.408	6.485	6.288	6.355	5.958	1	np
1b	6	7.386	7.393	7.392	7.394	7.393	7.455	0	pp
1b	7	7.701	7.707	7.704	7.708	7.708	7.664	0	pp
1b	9	8.193	8.300	8.364	8.204	8.258	7.883	1	np
1b	10	8.484	8.493	8.494	8.492	8.493	N/A	0	pp
1b	11	8.616	8.616	8.544	8.610	8.608	N/A	0	pr
1b	12	8.876	8.877	8.876	8.871	8.874	N/A	0	pr
1b	13	9.066	9.074	9.075	9.074	9.074	9.077	0	np
1b	14	9.306	9.313	9.313	9.313	9.313	N/A	0	pp
1b	15	9.314	9.366	N/A	9.351	9.350	9.304	1	np
1c	1	5.054	5.060	5.074	5.048	5.051	5.190	0	pp
1c	2	5.359	5.364	5.365	5.357	5.360	5.400	0	pp
1c	3	6.383	6.462	6.524	6.375	6.426	5.963	1	np
1c	6	7.338	7.348	7.349	7.340	7.341	7.442	0	pp
1c	7	7.696	7.721	7.690	7.733	7.724	N/A	0	pp
1c	8	8.355	N/A	8.472	8.367	8.407	7.938	1	np
1c	13	9.174	9.210	N/A	9.193	9.199	N/A	0	pp
1d	1	5.059	5.052	5.057	5.047	5.047	N/A	0	pp
1d	2	5.368	5.366	5.372	5.364	5.365	5.405	0	pp
1d	3	6.470	6.643	6.755	6.459	6.572	5.913	1	np
1d	6	7.349	7.348	7.364	7.348	7.344	7.441	0	pp
1d	8	8.390	8.547	N/A	8.401	8.494	7.847	1	np
1d	9	8.451	8.458	N/A	8.460	8.460	N/A	0	pp
1d	10	8.501	8.470	N/A	8.439	8.455	8.537	0	pr
1d	11	8.833	8.815	N/A	8.794	8.802	8.821	0	pr
1d	14	9.211	9.217	N/A	9.203	9.208	N/A	0	pp
1e	1	5.154	5.129	5.136	5.122	5.127	5.222	0	pp
1e	2	5.399	5.394	5.396	5.392	5.393	5.413	0	pp

1e	3	6.037	6.044	6.037	6.047	6.043	6.008	0	np
1e	6	7.391	7.383	7.381	7.380	7.381	7.430	0	pp
1e	7	7.663	7.678	7.661	7.678	7.677	7.668	0	pp
1e	8	7.991	8.016	8.007	8.021	8.017	7.931	0	np
1e	11	8.481	8.479	8.480	8.478	8.478	8.497	0	pp
1e	13	9.042	9.045	N/A	9.041	9.045	9.045	0	np
1e	14	9.199	9.204	N/A	9.260	8.989	N/A	1	pr
1f	1	5.182	5.186	5.188	5.183	5.185	5.240	0	pp
1f	2	5.398	5.400	5.402	5.397	5.399	5.422	0	pp
1f	3	6.128	6.196	6.229	6.144	6.170	5.986	1	np
1f	6	7.381	7.384	7.386	7.381	7.383	7.450	0	pp
1f	7	7.700	7.711	7.705	7.715	7.713	7.662	0	pp
1f	8	8.070	8.135	8.163	8.093	8.114	7.915	1	np
1f	10	8.476	8.484	8.486	8.482	8.483	N/A	0	pp
1f	11	8.534	8.536	8.463	8.531	8.526	N/A	0	pr
1f	13	8.810	8.811	8.813	8.805	8.808	N/A	0	pr
1f	14	9.066	9.077	9.078	9.075	9.076	9.075	0	np
1f	15	9.231	9.329	N/A	9.310	N/A	9.311	1	np
1g	1	5.053	5.019	5.033	5.005	5.013	5.200	0	pp
1g	2	5.363	5.355	5.364	5.349	5.353	5.407	0	pp
1g	3	6.197	6.274	6.298	6.235	6.254	5.982	1	np
1g	6	7.340	7.334	7.330	7.327	7.329	7.436	0	pp
1g	7	7.694	7.724	7.681	7.730	7.725	7.672	0	pp
1g	8	8.188	8.281	8.302	8.252	8.267	7.932	1	np
1g	9	8.353	8.299	8.387	8.269	8.296	8.528	0	pr
1g	10	8.441	8.441	8.449	8.437	8.439	N/A	0	pp
1g	11	8.722	8.695	N/A	8.675	8.687	8.818	0	pr
1g	12	8.957	8.988	N/A	8.975	8.986	9.040	1	np
1g	14	9.156	9.069	N/A	9.068	9.066	N/A	0	pr

1g	15	9.172	9.272	N/A	9.244	N/A	9.312	1	np
1h	1	5.050	4.991	5.003	4.981	4.989	5.208	0	pp
1h	2	5.363	5.349	5.355	5.345	5.348	5.404	0	pp
1h	3	6.215	6.360	6.403	6.272	6.318	5.960	1	np
1h	6	7.332	7.324	7.348	7.320	7.319	7.426	0	pp
1h	7	7.664	7.708	7.717	7.710	7.710	7.660	0	pp
1h	8	8.178	8.341	8.372	8.273	8.309	7.880	1	np
1h	9	8.348	8.257	8.314	8.231	8.260	8.530	0	pr
1h	10	8.440	8.448	N/A	8.446	8.447	N/A	0	pp
1h	11	8.728	8.693	N/A	8.676	8.687	8.806	0	pr
1h	13	8.889	8.957	N/A	8.929	8.946	9.066	1	np
1i	1	5.134	5.135	5.142	5.127	5.130	5.189	0	pp
1i	2	5.354	5.357	5.364	5.355	5.356	5.371	0	pp
1i	3	5.997	5.996	5.990	6.000	5.998	5.998	0	np
1i	4	6.991	7.022	N/A	7.014	7.026	7.077	1	pp
1i	6	7.339	7.341	7.388	7.335	7.338	7.378	0	pp
1i	7	7.593	7.617	7.648	7.620	7.616	7.601	0	pp
1i	8	7.943	7.948	7.952	7.957	7.952	7.916	0	np
1i	9	8.400	8.424	8.426	8.423	8.423	8.439	1	pp
1i	10	8.415	8.405	N/A	8.390	8.402	8.520	0	pr
1i	11	8.702	8.697	N/A	8.686	N/A	8.786	0	pr
1i	13	9.011	8.988	N/A	9.002	9.006	9.011	1	np
1i	14	9.172	9.202	N/A	9.135	9.158	N/A	1	pr
1i	15	9.193	9.208	N/A	9.198	N/A	9.245	0	pp
1j	1	5.183	5.196	5.195	5.197	5.196	5.241	0	pp
1j	2	5.401	5.408	5.409	5.406	5.407	5.421	0	pp
1j	3	6.288	6.425	6.519	6.293	6.374	5.953	1	np
1j	6	7.381	7.395	7.394	7.396	7.394	7.456	0	pp
1j	9	8.190	8.311	8.389	8.206	8.271	7.880	1	np

1j	10	8.464	8.493	N/A	8.492	8.493	N/A	0	pp
1j	11	8.628	8.627	8.475	8.619	8.614	N/A	0	pr
1j	12	8.885	8.885	8.869	8.878	8.882	N/A	0	pr
1j	13	9.061	9.072	9.072	9.073	9.072	9.075	0	np
1j	14	9.282	9.366	N/A	9.349	N/A	9.302	1	np
1j	15	9.295	9.313	N/A	9.314	9.314	N/A	0	pp
1k	1	5.045	5.060	5.089	5.042	5.047	5.185	0	pp
1k	2	5.350	5.359	5.335	5.352	5.355	5.392	0	pp
1k	3	6.377	6.459	6.526	6.365	6.425	5.955	1	np
1k	6	7.323	7.342	7.341	7.333	7.328	7.438	0	pp
1k	7	7.683	7.710	N/A	7.729	7.717	N/A	0	pp
1k	8	8.350	N/A	8.433	8.363	N/A	7.931	1	np
1k	10	8.485	8.485	8.539	N/A	8.465	8.538	0	pr
1k	11	8.827	8.827	N/A	8.803	8.816	8.835	0	pr
1k	12	8.957	8.978	N/A	8.973	8.978	9.029	0	np
1k	15	9.307	N/A	N/A	9.252	N/A	N/A	0	pr
1l	1	5.037	5.044	5.145	5.033	5.036	N/A	0	pp
1l	2	5.360	5.367	5.374	5.362	5.364	5.401	0	pp
1l	3	6.491	6.681	6.816	6.481	6.617	5.903	1	np
1l	6	7.332	7.352	N/A	7.348	7.343	7.440	0	pp
1l	7	7.649	7.708	N/A	7.713	7.709	7.664	0	pp
1l	9	8.401	8.460	N/A	8.459	8.459	N/A	0	pp
1l	10	8.514	8.485	N/A	8.443	8.468	8.532	0	pr
1l	11	8.854	8.841	N/A	8.812	8.837	8.818	0	pr
1l	12	8.948	9.002	N/A	8.966	8.978	9.013	0	np
1l	13	9.172	9.205	N/A	9.191	9.201	N/A	0	pp
1l	14	9.205	9.305	N/A	9.272	N/A	9.306	1	np
1l	15	9.290	N/A	N/A	9.259	N/A	N/A	1	pr
1m	1	5.036	4.988	4.997	4.981	4.986	N/A	0	pp

1m	2	5.363	5.354	5.359	5.350	5.352	5.402	0	pp
1m	3	6.402	6.591	6.687	6.427	6.520	5.921	1	np
1m	6	7.336	7.334	7.356	7.331	7.329	7.433	0	pp
1m	7	7.671	7.711	7.720	7.713	7.713	7.662	0	pp
1m	8	8.329	8.517	N/A	8.389	8.463	7.850	1	np
1m	9	8.433	8.339	8.359	8.310	8.339	8.530	0	pr
1m	10	8.439	8.450	8.450	8.448	8.449	N/A	0	pp
1m	11	8.778	8.740	N/A	8.720	8.733	8.810	0	pr
1m	12	8.894	8.951	N/A	8.921	8.938	9.065	1	np
1n	1	5.048	4.990	5.003	4.982	4.989	5.209	0	pp
1n	2	5.360	5.345	5.354	5.342	5.344	5.402	0	pp
1n	3	6.255	6.409	6.461	6.304	6.357	5.951	1	np
1n	4	6.953	6.925	N/A	6.922	6.928	N/A	0	pp
1n	5	7.180	7.147	N/A	7.143	7.143	N/A	0	pp
1n	6	7.330	7.318	7.345	7.316	7.313	7.426	0	pp
1n	7	7.672	7.712	7.722	7.713	7.712	N/A	0	pp
1n	8	8.215	8.386	8.423	8.303	8.345	7.872	1	np
1n	9	8.366	8.276	8.330	8.251	8.281	8.533	0	pr
1n	10	8.445	8.442	N/A	8.441	8.442	N/A	0	pp
1n	11	8.746	8.712	N/A	8.694	8.705	8.809	0	pr
1n	12	8.909	8.928	N/A	8.924	8.941	9.061	1	np
1o	1	5.030	4.986	4.995	4.981	4.985	N/A	0	pp
1o	2	5.359	5.349	5.354	5.346	5.348	5.401	0	pp
1o	3	6.462	6.647	6.760	6.462	6.572	5.910	1	np
1o	6	7.335	7.329	7.350	7.327	7.324	7.434	0	pp
1o	7	7.686	7.719	7.729	7.718	7.719	7.661	0	pp
1o	8	8.385	8.567	N/A	8.423	8.509	7.840	1	np
1o	9	8.445	8.445	8.445	8.445	8.445	N/A	0	pp
1o	10	8.449	8.354	8.379	8.326	8.355	8.531	0	pr

1o	11	8.793	8.750	N/A	8.729	8.742	8.812	0	pr
1o	12	8.908	8.931	N/A	8.930	8.945	9.063	1	np
1o	15	9.198	9.166	N/A	9.156	9.167	N/A	0	pp
1t	1	5.127	5.146	5.147	5.144	5.144	5.233	0	pp
1t	2	5.379	5.388	5.391	5.385	5.386	5.416	0	pp
1t	3	6.534	6.742	6.923	6.538	6.702	5.913	1	np
1t	5	7.025	7.060	7.040	N/A	N/A	7.161	0	pp
1t	6	7.249	7.275	7.274	7.277	7.274	N/A	0	pp
1t	7	7.360	7.369	7.371	7.365	7.366	N/A	0	pp
1t	8	7.733	7.743	7.736	7.744	7.744	N/A	0	pp
1t	10	8.422	8.597	8.739	8.440	8.566	7.852	1	np
1t	11	8.466	8.479	8.482	8.475	8.477	N/A	0	pp
1t	12	8.653	8.642	8.551	8.626	8.609	8.555	0	pr
1t	13	8.895	8.887	8.928	8.875	8.883	8.840	0	pr
1t	14	9.040	9.053	9.054	9.055	9.054	9.071	0	np
1t	15	9.295	9.304	N/A	9.303	9.304	N/A	1	pp
1u	1	5.161	5.161	5.166	5.154	5.157	5.233	0	pp
1u	2	5.394	5.395	5.397	5.392	5.393	5.418	0	pp
1u	3	6.019	6.016	6.014	6.019	6.018	6.009	0	np
1u	7	7.378	7.381	7.384	7.376	7.378	7.435	0	pp
1u	8	7.684	7.690	7.682	7.692	7.689	7.664	0	pp
1u	9	7.986	7.988	7.983	7.993	7.990	7.928	0	np
1u	10	8.402	8.397	8.450	8.385	8.401	8.549	0	pr
1u	11	8.480	8.482	8.482	8.480	8.481	N/A	0	pp
1u	13	8.717	8.716	8.731	8.707	8.711	8.821	0	pr
1u	15	9.065	9.078	9.073	9.063	9.064	9.064	0	np
1v	1	5.167	5.179	5.173	5.185	5.180	5.239	0	pp
1v	2	5.401	5.406	5.405	5.407	5.406	5.419	0	pp
1v	4	6.528	6.757	6.929	6.544	6.699	5.914	1	np

1v	5	7.055	7.084	7.069	7.098	7.087	7.159	0	pp
1v	7	7.385	7.392	7.389	7.395	7.392	7.460	0	pp
1v	8	7.696	7.715	7.719	7.711	7.715	N/A	0	pp
1v	9	8.241	8.245	8.125	8.252	8.223	N/A	0	pr
1v	10	8.402	8.590	8.730	8.422	8.546	7.848	1	np
1v	11	8.475	8.495	8.495	8.496	8.496	N/A	0	pp
1v	12	8.741	8.732	8.690	8.728	8.726	N/A	0	pr
1v	13	8.981	8.980	8.981	8.974	8.978	N/A	0	pr
1v	14	9.049	9.058	9.058	9.062	9.060	9.076	0	np
1v	15	9.293	9.306	9.305	9.307	9.307	N/A	0	pp
1w	1	5.153	5.155	5.166	5.147	5.150	5.228	0	pp
1w	2	5.392	5.394	5.394	5.393	5.394	5.414	0	pp
1w	3	6.036	6.037	6.034	6.040	6.039	6.007	0	np
1w	7	7.382	7.386	7.387	7.382	7.383	7.433	0	pp
1w	8	7.677	7.687	7.681	7.692	7.689	7.664	0	pp
1w	9	8.011	8.013	8.005	8.021	8.018	7.931	0	np
1w	11	8.424	8.416	8.429	8.402	8.411	8.549	1	pr
1w	12	8.474	8.480	8.470	8.479	8.480	8.497	1	pp
1w	15	9.057	9.065	N/A	9.045	9.046	9.064	0	np
1x	1	5.229	5.234	5.228	5.241	5.236	N/A	0	pp
1x	2	5.433	5.435	5.434	5.437	5.436	5.417	0	pp
1x	3	6.571	6.779	6.980	6.555	6.742	5.883	1	np
1x	5	7.104	7.120	7.108	7.135	7.124	7.167	0	pp
1x	6	7.349	7.365	7.357	N/A	7.367	N/A	0	pp
1x	7	7.427	7.432	7.425	7.441	7.434	7.463	0	pp
1x	8	7.687	7.696	7.703	7.688	7.695	N/A	0	pp
1x	9	8.074	8.062	8.071	8.049	8.060	7.898	0	pr
1x	10	8.378	8.555	8.728	8.367	8.524	7.828	1	np
1x	11	8.521	8.525	8.524	8.526	8.526	N/A	0	pp

1x	12	8.756	8.732	8.700	8.726	8.727	8.561	0	pr
1x	13	8.967	9.036	9.034	9.036	9.035	9.079	0	np
1x	15	9.270	9.209	N/A	9.263	9.232	N/A	0	pr
1y	1	5.295	5.292	5.295	5.289	5.291	5.247	0	pp
1y	2	5.414	5.418	5.419	5.415	5.416	5.428	0	pp
1y	3	6.022	6.023	6.022	6.023	6.023	6.021	0	np
1y	7	7.445	7.454	7.456	7.450	7.452	7.455	0	pp
1y	8	7.666	7.675	7.674	7.674	7.674	7.675	0	pp
1y	10	7.942	7.942	7.938	7.947	7.944	7.940	0	np
1y	11	8.518	8.520	8.520	8.519	8.520	8.504	0	pp
1y	12	8.693	8.680	8.683	8.681	8.670	8.561	0	pr
1y	13	9.042	9.077	9.087	9.063	9.069	9.079	0	np
1z	5	6.957	7.029	7.052	7.028	N/A	7.013	1	pp
1z	6	7.234	7.271	N/A	7.254	7.261	7.200	0	pp
1z	7	7.354	7.381	7.416	7.363	7.377	7.328	0	pp
1z	8	7.466	7.490	N/A	N/A	7.490	N/A	1	pp
1z	9	7.786	7.786	7.756	7.814	7.794	7.835	0	np
1z	11	8.531	8.538	8.568	8.509	8.535	8.449	0	pr
1z	12	8.768	8.770	8.784	8.759	8.765	8.707	0	pr
2c	1	6.154	6.177	6.165	6.180	6.177	6.212	0	pp
2c	2	6.992	7.009	7.045	6.946	6.979	6.561	1	np
2c	3	7.661	7.680	7.671	7.673	7.673	7.744	0	pp
2c	6	8.495	8.523	8.518	8.526	8.524	N/A	0	np
2c	8	8.895	8.881	8.911	8.865	8.887	8.922	0	pr
2c	9	8.966	8.985	N/A	8.991	8.983	8.859	0	pp
2c	11	9.515	9.495	N/A	9.626	9.748	9.725	1	pr
2c	12	9.890	9.878	N/A	9.970	N/A	N/A	1	pr
2c	14	10.258	N/A	N/A	10.439	10.097	N/A	1	pr
4a	1	5.632	5.638	5.636	5.638	5.637	5.668	0	pp

4a	2	6.416	6.441	6.462	6.410	6.429	6.285	0	np
4a	3	6.621	6.622	6.627	6.616	6.619	N/A	0	pp
4a	4	7.533	7.539	7.540	7.534	7.535	7.501	0	np
4a	5	7.959	7.967	7.967	7.960	7.962	N/A	0	pp
4a	7	8.111	8.150	8.183	8.104	8.131	7.994	0	np
4a	9	8.744	8.775	8.792	8.747	8.763	8.543	0	np
4a	14	9.719	9.733	N/A	9.733	9.731	N/A	1	pp
4b	1	5.577	5.589	5.585	5.583	5.583	5.652	0	pp
4b	2	6.483	6.538	6.582	6.470	6.509	6.288	1	np
4b	3	6.624	6.629	N/A	6.630	6.627	6.604	0	pp
4b	4	7.533	7.555	7.566	7.538	7.547	7.509	0	np
4b	5	7.969	7.973	7.985	7.964	7.966	N/A	0	pp
4b	6	8.057	8.070	8.078	8.076	8.064	8.065	0	pp
4b	7	8.242	8.280	8.300	8.239	8.264	7.995	0	np
4b	8	8.525	8.525	8.554	8.499	8.510	8.481	0	pr
4b	9	8.604	8.664	8.695	8.619	8.642	8.580	1	np
4b	11	9.180	9.192	9.185	9.190	9.186	9.123	0	pp
4b	13	9.372	9.363	N/A	N/A	9.326	N/A	1	pp
4b	14	9.433	9.420	9.448	9.401	N/A	9.344	0	pr
4b	15	9.634	9.650	N/A	9.642	9.631	N/A	1	pp
4c	1	5.539	5.556	5.552	5.550	5.550	5.644	0	pp
4c	2	6.583	6.671	6.724	6.565	6.622	6.245	1	np
4c	3	6.640	6.644	N/A	6.642	6.643	N/A	0	pp
4c	4	7.554	7.589	7.601	7.563	7.575	7.503	0	np
4c	5	7.927	7.944	7.946	7.950	7.933	8.050	0	pp
4c	7	8.387	8.478	8.543	8.377	8.434	7.989	1	np
4c	9	8.767	8.846	8.884	8.785	8.816	8.546	0	np
4c	10	9.169	9.197	9.163	9.191	9.185	9.123	0	pp
4c	14	9.601	9.629	9.358	9.623	9.614	N/A	1	pp

4d	1	5.467	5.492	5.490	5.484	5.484	5.617	0	pp
4d	2	6.526	6.623	6.708	6.511	6.575	6.255	1	np
4d	3	6.655	6.665	N/A	6.658	6.659	6.617	0	pp
4d	4	7.524	7.549	7.564	7.528	7.539	7.501	0	np
4d	5	7.910	7.934	7.926	7.918	7.921	7.932	0	pp
4d	6	8.040	8.073	8.065	8.075	8.069	8.144	0	pp
4d	7	8.401	8.432	8.491	8.365	8.401	8.410	1	pr
4d	8	8.500	8.590	8.657	8.496	8.554	8.022	1	np
4d	9	8.710	8.845	8.906	8.744	8.796	8.569	1	np
4d	10	9.220	9.241	N/A	9.226	9.232	N/A	0	pp
4d	12	9.337	9.373	9.378	9.345	9.344	N/A	0	pp
4d	13	9.398	9.414	N/A	9.356	N/A	9.315	1	pr
5a	1	5.563	5.573	5.562	5.577	5.572	5.618	0	pp
5a	2	6.359	6.386	6.406	6.355	6.373	6.293	0	np
5a	3	6.554	6.555	6.549	6.551	6.553	6.524	0	pp
5a	4	7.494	7.501	7.507	7.493	7.498	7.487	0	np
5a	5	7.894	7.906	7.918	7.917	7.906	N/A	0	pp
5a	7	8.170	8.202	8.225	8.163	8.187	7.985	0	np
5a	8	8.684	8.827	8.839	8.741	8.813	8.782	1	pr
5a	9	8.700	8.787	8.824	8.717	8.755	8.565	1	np
5a	11	8.876	N/A	8.876	8.879	N/A	N/A	0	pp
5a	12	9.283	9.291	9.296	9.290	9.286	N/A	0	pp
5a	13	9.535	9.556	9.554	9.566	9.530	9.210	1	pp
6a	1	4.045	4.057	4.061	4.054	4.058	3.808	0	pp
6a	2	4.564	4.579	4.589	4.568	4.576	4.244	0	pp
6a	3	5.535	5.546	5.551	5.542	5.546	5.312	0	pp
6a	4	6.065	6.073	6.076	6.070	6.072	6.016	0	pp
6a	5	6.111	6.125	6.126	6.122	6.124	6.075	0	pp
6a	7	6.491	6.511	6.523	6.494	6.506	6.148	0	pp

6a	8	6.796	6.861	6.878	6.835	6.851	N/A	0	np
6a	10	7.292	7.326	7.331	7.322	7.327	7.034	0	pp
6a	11	7.572	7.628	7.641	7.609	7.621	N/A	1	np
6b	1	4.506	4.538	4.560	4.526	4.546	3.846	0	pp
6b	2	5.072	5.105	5.139	5.076	5.107	4.182	0	pp
6b	3	5.750	5.762	5.764	5.760	5.762	N/A	0	pp
6b	4	6.124	6.128	6.139	6.115	6.125	N/A	0	pp
6b	5	6.272	6.287	6.308	6.265	6.284	N/A	0	pp
6b	6	6.805	6.849	6.875	6.833	6.858	5.340	0	pp
6b	7	6.949	6.961	6.964	6.959	6.963	N/A	0	pp
6b	8	7.276	7.324	7.371	7.286	7.328	N/A	0	pp
6b	9	7.413	7.631	7.726	7.446	7.567	6.320	1	np
6b	12	8.140	8.279	N/A	8.185	8.249	7.248	1	np
6c	1	4.502	4.473	4.489	4.466	4.489	3.858	0	pp
6c	2	5.064	5.025	5.056	5.001	5.037	4.164	0	pp
6c	3	5.748	5.752	5.751	5.749	5.755	N/A	0	pp
6c	4	6.135	6.130	6.144	6.116	6.129	6.070	0	pp
6c	5	6.271	6.259	N/A	6.238	6.260	N/A	0	pp
6c	6	6.684	6.663	6.686	6.647	6.674	5.343	0	pp
6c	7	6.960	N/A	6.963	N/A	6.958	N/A	1	pp
6c	10	7.140	7.099	7.146	7.071	7.110	5.960	0	pp
6c	11	7.603	7.852	8.052	7.612	7.811	6.294	1	np
6c	12	7.697	7.668	7.683	7.664	7.681	6.965	0	pp
6c	13	7.974	7.982	7.981	7.980	7.980	N/A	0	pp
6c	14	8.196	8.192	N/A	8.161	8.188	N/A	0	pp
6c	15	8.240	8.344	N/A	8.246	8.338	7.258	1	np
7a	1	4.494	4.516	4.527	4.503	4.511	4.503	0	pp
7a	2	5.121	5.157	5.188	5.136	5.147	5.490	0	pp
7a	3	6.068	6.108	6.178	6.016	6.085	5.516	0	np

7a	4	6.495	6.556	6.635	6.459	6.533	5.894	0	np
7a	5	6.933	6.954	6.934	6.957	6.955	6.875	0	pp
7a	8	8.477	8.477	8.513	8.464	8.498	8.446	0	np
7a	9	8.677	8.615	8.843	8.611	8.933	N/A	0	pr
7a	10	8.807	8.864	8.842	8.859	8.854	N/A	0	pp
7a	11	8.985	8.883	9.137	8.892	9.164	9.027	0	pr
7a	13	9.239	9.257	N/A	9.241	9.249	8.968	1	pp
7a	14	9.347	9.299	N/A	9.368	9.521	N/A	1	pr
7a	15	9.665	9.808	N/A	9.758	9.793	9.544	1	np
7b	1	4.507	4.529	4.537	4.516	4.521	4.533	0	pp
7b	2	5.254	5.273	5.305	5.245	5.257	5.531	0	pp
7b	3	5.885	5.914	5.937	5.861	5.885	5.565	0	np
7b	4	6.303	6.340	6.367	6.283	6.309	5.945	0	np
7b	5	6.915	6.933	6.918	6.937	6.935	6.883	0	pp
7b	6	8.401	8.384	8.692	8.401	8.192	N/A	1	pr
7b	7	8.539	8.540	8.509	8.537	8.518	8.481	0	np
7b	9	8.858	8.896	8.881	8.889	8.887	9.020	0	pp
7b	11	9.234	N/A	N/A	9.260	9.263	N/A	0	pp
7b	12	9.250	N/A	N/A	9.243	9.245	N/A	0	pp
7b	13	9.678	9.733	N/A	9.696	9.712	9.578	0	np
7c	1	4.527	4.577	4.574	4.586	4.581	4.497	0	pp
7c	2	5.168	5.196	5.213	5.199	5.197	5.486	0	pp
7c	3	5.826	5.854	5.856	5.839	5.843	5.528	0	np
7c	4	6.635	6.636	6.650	6.600	6.616	5.890	0	np
7c	5	6.892	6.952	6.933	6.969	6.959	6.839	0	pp
7c	6	8.492	8.501	8.523	8.514	8.543	8.457	0	np
7c	8	8.759	8.827	N/A	8.844	8.835	N/A	0	pp
7c	10	9.052	9.170	N/A	9.182	9.171	N/A	1	pp
7c	14	9.700	N/A	N/A	9.751	N/A	9.534	0	np

8a	1	6.400	6.444	6.566	6.428	6.432	6.502	0	pp
8a	2	6.957	7.006	7.017	6.918	6.956	6.105	1	pp
8a	4	8.263	8.342	N/A	8.323	8.321	N/A	0	pp
8a	5	8.790	8.839	N/A	8.819	8.815	N/A	0	pp
8a	8	9.656	9.679	N/A	9.645	N/A	N/A	1	pp
8a	9	9.698	9.784	N/A	9.728	9.759	N/A	1	np
9a	1	4.946	4.944	4.955	4.917	4.928	4.664	0	np
9a	2	5.664	5.681	5.680	5.680	5.680	5.774	0	pp
9a	3	5.774	5.786	5.779	5.790	5.787	5.838	0	pp
9a	4	7.539	7.568	7.562	7.570	7.568	N/A	0	pp
9a	5	7.845	7.858	7.848	7.862	7.859	N/A	0	pp
9a	6	8.575	8.608	8.614	8.593	8.595	8.730	0	np
9a	7	8.894	8.897	9.016	8.903	8.890	8.840	0	pr
9a	9	9.219	9.237	9.206	N/A	9.238	9.256	0	pp
9a	10	9.234	9.214	9.440	9.249	9.209	9.021	0	pr
9a	11	9.430	9.447	N/A	9.438	9.441	9.362	0	np
9a	12	9.525	9.558	9.586	9.554	9.545	9.528	1	np
11a	1	4.828	4.843	4.846	4.833	4.835	5.014	0	pp
11a	3	6.634	6.675	6.690	6.670	6.671	N/A	1	pp
11a	4	6.873	6.925	6.960	6.848	6.885	6.277	1	np
11a	5	7.170	7.178	7.189	7.172	7.173	N/A	0	pp
11a	6	7.718	7.730	7.731	7.726	7.726	7.907	0	pp
11a	8	8.079	8.098	8.204	8.103	8.053	8.411	1	pr
11a	10	8.660	N/A	8.707	8.722	8.724	N/A	1	pp
11a	11	8.717	N/A	8.729	8.654	8.694	8.798	1	pr
11a	12	8.820	8.835	8.828	8.825	8.831	8.737	0	np
11a	14	9.172	9.193	N/A	9.187	9.184	N/A	0	pp

Table C.2.: Aug-cc-pVDZ Excitation energies for full quantum mechanical (CIS), QM/EFP (PE, PE+S, PE+XR, PE+SXR) and gas-phase (CIS Gas) calculations, as well corresponding transition types (np, pp and pr for n→π^*, $\pi\rightarrow\pi^*$ and $\pi\rightarrow$Ryd respectively). All energies are given in units of eV. N/A indicates the transitions for which full quantum CIS states could not be matched to QM/EFP or gas-phase transitions.

Geo.	CIS	CIS	PE	PE+XR	gas	Type
1a	1	5.051	5.042	5.037	5.107	pp
1a	2	5.280	5.277	5.276	5.300	pp
1a	3	5.809	5.943	5.797	6.210	pr
1a	4	5.997	5.996	6.000	6.002	np
1b	1	5.069	5.072	5.076	5.117	pp
1b	2	5.292	5.294	5.293	5.305	pp
1b	3	6.124	6.139	6.108	6.237	pr
1b	4	6.276	6.417	6.269	5.953	np
1b	5	6.415	6.432	6.390	5.969	pr
1d	1	4.945	4.923	4.928	5.085	pp
1d	2	5.256	5.249	5.249	5.287	pp
1d	3	5.954	5.910	5.857	N/A	pr
1d	5	6.453	6.669	6.424	5.909	np
1e	1	5.028	4.999	4.994	5.096	pp
1e	2	5.277	5.269	5.268	5.295	pp
1e	4	6.028	6.037	6.045	6.002	np
1e	5	6.067	5.823	5.685	N/A	pr
1f	1	5.062	5.057	5.059	5.116	pp
1f	2	5.283	5.282	5.281	5.305	pp

1f	3	6.015	6.011	5.998	6.239	pr
1f	4	6.116	6.201	6.127	5.981	np
1g	1	4.934	4.994	4.965	5.073	pp
1g	2	5.245	5.265	5.254	5.289	pp
1g	5	6.176	6.249	6.207	5.976	np
1i	1	5.015	5.005	5.003	5.065	pp
1i	2	5.239	5.235	5.237	5.254	pp
1i	3	5.874	5.977	5.835	N/A	pr
1i	4	5.993	5.992	5.995	5.993	np
1j	1	5.068	5.073	5.078	5.116	pp
1j	2	5.290	5.295	5.294	5.304	pp
1j	3	6.160	6.151	6.138	6.237	pr
1j	5	6.440	6.447	6.410	5.968	pr
1k	1	4.933	4.929	4.922	5.059	pp
1k	2	5.241	5.243	5.238	5.276	pp
1k	4	6.350	6.484	6.348	5.951	np
1m	1	4.924	4.912	4.915	5.078	pp
1m	2	5.250	5.251	5.250	5.284	pp
1m	3	5.830	5.932	5.761	N/A	pr
1m	5	6.359	6.422	6.352	6.606	pr
1n	1	4.931	4.854	4.857	5.082	pp
1n	2	5.243	5.219	5.218	5.284	pp
1n	5	6.231	N/A	N/A	5.946	np
1o	1	4.915	4.967	4.941	5.079	pp
1o	2	5.245	5.260	5.251	5.283	pp
1o	3	5.851	6.035	5.880	N/A	pr
1t	1	5.013	5.021	5.027	5.108	pp
1t	2	5.271	5.277	5.275	5.299	pp
1t	3	6.168	6.178	6.127	6.229	pr

1t	4	6.515	N/A	N/A	5.909	np
1u	1	5.033	5.031	5.024	5.108	pp
1u	2	5.273	5.272	5.270	5.300	pp
1u	3	5.818	5.867	5.786	N/A	pr
1u	4	6.014	6.009	6.012	6.002	np
1v	1	5.057	5.057	5.071	5.114	pp
1v	2	5.295	5.298	5.299	5.302	pp
1v	3	6.331	6.311	6.299	6.230	pr
1v	5	6.508	N/A	N/A	5.910	np
1x	1	5.121	5.121	5.131	N/A	pp
1x	2	5.328	5.330	5.330	5.300	pp
1x	3	6.211	6.219	6.159	6.237	pr
1x	4	6.491	N/A	6.431	5.962	pr
2c	1	5.931	N/A	5.947	5.978	pp
2c	2	6.357	6.319	6.341	6.234	pr
2c	3	7.014	N/A	6.997	N/A	np
4a	1	5.398	5.401	5.401	5.427	pp
4a	3	6.356	6.365	6.321	N/A	pr
4a	4	6.384	6.420	6.381	6.258	np
4a	5	6.454	6.462	N/A	N/A	pr
4d	2	5.798	5.825	5.742	5.671	pr
4d	3	6.327	6.355	6.271	N/A	pr
5a	1	5.335	5.336	5.345	5.372	pp
5a	2	5.868	5.880	5.848	5.754	pr
5a	3	6.264	6.809	6.250	N/A	pr
5a	4	6.335	6.367	6.331	6.258	np
5a	5	6.434	6.450	6.401	6.166	pr
6a	3	5.367	4.975	5.178	5.085	pr
6a	4	5.418	5.099	5.072	5.209	pp

6a	5	5.642	5.310	5.435	5.378	pr
6c	1	4.443	4.463	4.413	3.796	pp
6c	2	4.999	5.020	4.946	4.135	pp
6c	3	5.629	5.640	N/A	N/A	pp
7a	1	4.306	4.327	4.306	4.281	pp
7a	2	4.990	5.000	5.000	5.340	pp
7a	3	5.896	5.889	5.785	5.575	pr
7a	4	6.072	6.180	6.043	5.540	np
7c	1	4.355	4.375	4.389	4.276	pp
7c	2	5.055	5.030	5.057	5.342	pp
7c	3	5.841	5.886	5.860	5.546	np
9a	1	4.961	4.989	4.943	4.691	np
9a	2	5.517	5.514	5.525	5.621	pp
9a	3	5.610	5.605	5.619	5.668	pp
9a	4	6.880	6.887	6.870	N/A	pr
9a	5	7.105	7.113	7.096	N/A	pr

D. SUPPLEMENTARY MATERIAL FOR CHAPTER 5

This appendix contains the supplementary information for Chapter 5, evaluation of dispersion term for triplet excited states.

D.1 Coordinates (Å) of water-methane dimer.

Scaling - .90

O -1.57766819 0.05726659 -0.00003997

H -1.80123997 -0.88324541 0.00031394

H -0.61093307 0.04706857 0.00019749

C 1.72374558 -0.00505311 -0.00003082

H 2.78083992 0.30834845 0.00494945

H 1.23170149 0.40694600 -0.89783549

H 1.67068732 -1.10696781 -0.01722498

H 1.23127115 0.37895763 0.91060150

Scaling - .95

O -1.66412973 0.05700478 -0.00003299

H -1.88664448 -0.88375783 0.00023408

H -0.69738382 0.04789315 0.00020742

C 1.82076848 -0.00481076 -0.00002762

H 2.87741804 0.31008402 0.00516324

H 1.32819927 0.40689889 -0.89767694

H 1.76927102 -1.10679102 -0.01772497

H 1.32774520 0.37804869 0.91065013

Scaling - 1.00

O -1.75059032 -0.05677243 0.00000487

H -1.97218037 0.88420844 0.00022552

H -0.78383601 -0.04861080 -0.00040341

C 1.91778767 0.00458588 0.00002286

H 2.97401381 -0.31151435 -0.01263722

H 1.42519534 -0.42582676 0.88884330

H 1.86776686 1.10599089 0.04162298

H 1.42395604 -0.35763156 -0.91800082

Scaling - 1.05

O -1.83704209 0.05655847 0.00000160

H -2.05775476 -0.88462847 -0.00018087

H -0.87028050 0.04929779 0.00024482

C 2.01481128 -0.00438854 -0.00000649

H 3.07069063 0.31306916 0.00571466

H 1.52150142 0.40676147 -0.89750576

H 1.96599698 -1.10647774 -0.01850188

H 1.52087808 0.37640673 0.91028106

Scaling - 1.10

O -1.92347789 0.05636247 -0.00003409

H -2.14344215 -0.88499963 0.00025326

H -0.95671082 0.04987035 0.00021021

C 2.11184716 -0.00422110 -0.00002957

H 3.16745353 0.31415299 0.00521386

H 1.61792803 0.40599686 -0.89762020

H 2.06398129 -1.10636246 -0.01789141

H 1.61754680 0.37688681 0.91072792

Scaling - 1.25

O -2.18279338 0.05587576 -0.00003915

H -2.40085626 -0.88592851 0.00032278

H -1.21601510 0.05133590 0.00020723

C 2.40293193 -0.00377465 -0.00003435

H 3.45777845 0.31711033 0.00520922

H 1.90800869 0.40536496 -0.89756376

H 2.35768890 -1.10602510 -0.01801516

H 1.90770829 0.37609327 0.91087055

Scaling - 1.50

O -2.61494374 -0.05528614 0.00004038

H -2.83078241 0.88703018 -0.00021022

H -1.64815712 -0.05302815 -0.00037230

C 2.88808179 0.00322696 0.00004874

H 3.94201803 -0.32044566 -0.01222738

H 2.39220285 -0.42328200 0.88892287

H 2.84595227 1.10497928 0.04119268

H 2.39157319 -0.35603735 -0.91852754

Scaling - 2.00

O -3.58503582 -0.05677243 0.00000487

H -3.80662587 0.88420844 0.00022552

H -2.61828151 -0.04861080 -0.00040341

C 3.75223317 0.00458588 0.00002286

H 4.80845931 -0.31151435 -0.01263722

H 3.25964084 -0.42582676 0.88884330

H 3.70221236 1.10599089 0.04162298

H 3.25840150 -0.35763156 -0.91800082